

22nd Associação Brasileira de
Cristalografia (ABCr) meeting
&
1st Latin American Crystallographic
Association (LACA) regional meeting

09 – 11 September, 2015

Physics Institute
University of São Paulo - Brazil

Sponsors & Supporters





International Advisory Committee:

Iris C.L. Torriani – Chair	Brazil
Diego G. Lamas	Argentina
Mauricio Fuentealba	Chile
José Antonio Henao Martínez	Colombia
José Roberto Vega-Baudrit	Costa Rica
Graciela D. Delgado	Venezuela
Lauro Bucio Galindo	Mexico
Alejandro Buschiazzo	Uruguay

Local Committee:

Aldo F. Craievich	USP
Rosangela Itri	USP
Sérgio L. Morelhão	USP
Paulo A. Suzuki	USP
Nivaldo L. Speziali	UFMG
Luis Gallego Martinez	IPEN
Jose Ricardo Sabino	UFGO

Organising Committee:

Márcia C. A. Fantini	– president <i>ABCr</i>	USP
Íris C. L. Torriani	– treasurer <i>ABCr</i>	UNICAMP
Nivaldo L. Speziali	– secretary <i>ABCr</i>	UFMG

P r e s e n t a t i o n

It is an honor and a great privilege to present on this occasion the **Joint Meeting of the 22nd Brazilian Crystallographic Association and the 1st Regional Meeting of the Latin American Crystallographic Association**.

In 2015 the Brazilian Crystallographic Association (**ABCr**) will be 43 years old. Founded in 1972 by a group of 52 crystallographers the **ABCr** has nowadays around 300 members and has become a major contributor to scientific research in Brazil.

The interdisciplinary nature of crystallography has been the main factor in the development of theoretical and applied research groups in several areas of knowledge. A recent web search on research groups acting in areas like Exact Sciences (Mathematics, Physics and Chemistry), Biological and Earth Sciences, Health Sciences, as well as Engineering and Material Sciences, reported 88 groups and laboratories working in different branches of crystallography (Source: Brazilian National Research Council-CNPq -registered research groups).

As is usual in our meetings, we programmed three Keynote plenary lectures for this three-day meeting, which will be delivered by Profs. Santiago Garcia-Granda, Miguel Yacamán and Mike Zaworotko. The Directors of two large experimental facilities will make presentations: Prof. Antonio José Roque da Silva from the Brazilian Synchrotron Radiation Facility and Miguel Garcia Aranda from the ALBA Synchrotron Light Source (Spain). Several speakers from Brazil and from most of **LACA** countries have been invited for oral communications. In addition, some oral presentations were chosen from the submitted abstracts, and we expect to have a record number of poster presentations in the three programmed poster sessions.

The **ABCr** General Assembly as well as the **LACA** General Assembly will take place at the end of the first and second days of the meeting.

At a Summit Meeting held in September 22-24, 2014 in Campinas as part of the International Year of Crystallography, senior researchers from Latin American countries and younger scientists gathered with renowned world scientists, such as Ada Yonath (2009 Nobel Prize in Chemistry) and Marvin Hackert (President of the International Union of Crystallography - IUCr). During this meeting, the advances in the last decades in the field of structural crystallography were evaluated. Some of the important points discussed were the existing financial barriers that so much affect the development of competitive scientific research in the Latin American region.

It is expected that during this First Latin American Meeting of the **LACA** as an IUCr Associate member, the participants will have the opportunity to discuss the ways to implement the creation of the UNESCO/IUCr Cooperation Fund for the promotion of crystallography in the LA region. The proposal, as stated in a letter of intention during the IYCr2014-LA Summit, will be to support student exchange activities and scientific events, and also finance the common use of large experimental facilities.

The organization of this **ABCr/LACA** Meeting was sponsored by the Brazilian funding agencies FAPESP, CNPq and CAPES, as well as IF-USP and SBF. IUCr contribution to finance Early Career Research Scientists is gratefully acknowledged. Commercial sponsors were: Bruker, Rigaku/Dairix, PANalytical, XENOCs/Instrutécnica and NanoTemper Technologies.

Iris L. Torriani
Organizing Committee of the
22nd ABCr and 1st LACA Meeting

Program

Wednesday September 09		Thursday September 10	Friday September 11
08:30	Reception/Registration	Invited Talk (chair Graciela Delgado) Alexander Briceño Venezuela (Assoc.Ven.Crist)	Invited Talk (chair Javier Ellena) Mauricio Fuentealba Chile
09:00	Opening (chair Iris Torriani) Márcia C. de Abreu Fantini President of the ABCr	Invited Talk: (chair Graciela Delgado) José Antonio Henao Colombia	Invited Talk (chair Javier Ellena) Alejandro Buschiazzi Uruguay (RUCr)
09:30	Plenary Lecture (I) (chair Iris Torriani) Santiago García Granda Spain / IUCr-LACA Liaison Representative	Plenary Lecture (II) (chair Graciela Delgado) Abel Moreno Cárcamo México (SMCr)	Plenary Lecture (III) (chair Javier Ellena) Mike Zaworotko University of Limerick, Ireland
10:15	Invited Talk (chair Iris Torriani) Beatriz Gomes Guimarães Brazil (ABCr)	Invited Talk (chair Graciela Delgado) Sebastián Klinke Argentina (AACr)	Invited Talk (chair Javier Ellena) Graciela Díaz de Delgado Venezuela
10:45	<u>OFICIAL PHOTO</u> <u>COFFEE BREAK</u>	<u>COFFEE BREAK</u>	<u>COFFEE BREAK</u>
	11:15-Danilo Bittar Bruker's Commercial presentation (chair Iris Torriani)	11:15-Jenny S. Komatsu Rigaku's Commercial presentation (chair Graciela Delgado)	11:15-Leandro Almeida Panalytical's Commercial presentation (chair Javier Ellena)
11:30	Posters A (chair Cristina Nonato) Molecular Structures and Physical/Chemical Properties	Posters B (chair Martin Saleta) Materials; Polycrystals	Posters C (chair Rosangela Itri) Complementary and other methods; Education in Crystallography; Small Molecules and Biological Macromolecules
12:45	<u>LUNCH</u>		
14:00	Invited Talk (chair Lauro Bucio) Eduardo Granado Brazil	Oral Communications (chair Diego Lamas) 14:00 - Andrea M. Araya-Sibaja Costa Rica 14:15 - W. Fabiola Sanjuan Szklarza Poland	Invited Talk (chair Nivaldo Speziali) Ernesto Estevez-Rams Cuba
14:30	Invited Talk (chair Lauro Bucio) José Luis Solís Peru	Bruker's Technical Communication-Danilo Bittar (chair Diego Lamas)	Invited Talk (chair Nivaldo Speziali) Antonio José Roque da Silva CNPEM-LNLS, Brazil
15:00	Oral Communications (chair Lauro Bucio) 15:00 Diego Germán Lamas (Argentina) 15:15 Leopoldo Suescun (Uruguay) 15:30 Miguel Delgado (Venezuela)	Oral Communications (chair Diego Lamas) 15:00 Lauro Bucio (Mexico) 15:15 Griselda E. Narda (Argentina) 15:30 Martín E. Saleta (Brazil)	Invited Talk (chair Nivaldo Speziali) Miguel Ángel García Aranda Sincrotron ALBA Spain
	Invited Talk (chair Lauro Bucio) Glaucius Oliva, Brazil	Rigaku's Technical Communication-Daniel Baker (chair Diego Lamas)	Wrap-up session About LACA 's Next elections
	16:15	<u>COFFEE BREAK</u>	<u>COFFEE BREAK</u>
16:45	<u>ABCr GENERAL ASSEMBLY</u>	<u>LACA GENERAL ASSEMBLY</u>	Closing Ceremony
19:00	<u>Welcome Party</u>		

List of abstracts

Plenary sessions

- A controlled pressure/temperature set-up for synchrotron in situ studies of solid-gas processes and reactions: Case of the structural deformation of ZIF-8*
Santiago García-Granda **Plen01**
- Advances in electron diffraction determination of nano materials*
Miguel Jose Yacaman **Plen02**
- Crystal engineering of task-specific materials*
Michael J. Zaworotko **Plen03**

Invited talks

- Additive manufacturing from a material science perspective*
Rainer Christoph **Invit12**
- Applied crystallography at ALBA Synchrotron Light Source*
Miguel A. G. Aranda **Invit14**
- Caracterización de materiales de interés farmacéutico en formulaciones comerciales y obtenidos bajo diferentes condiciones de cristalización y tratamientos en el estado sólido*
Graciela Díaz de Delgado **Invit11**
- Crystal structure of the bacteriophytochrome from Xanthomonas campestris pv. campestris: insights into pathogenicity in a light-dependent manner.*
Sebastián Klinke **Invit07**
- Estudio estructural de complejos de hierro con potenciales aplicaciones de entrecruzamiento de spin*
Mauricio Fuentealba **Invit09**
- Exploiting the use of multivalent hydrogen bonding templates to direct [2+2] photochemical reactivity of olefins. from molecules to nano/microtemplates.*
Alexander Briceño **Invit05**
- Fighting neglected diseases with structural biology and medicinal chemistry*
Glaucius Oliva **Invit04**
- Laboratory X-ray of Universidad Industrial de Santander and support services: teaching, research and national and international industry.*
J. A. Henao **Invit06**
- Models and Diffraction study of polytypes and planar disorder*
Ernesto Estévez Rams **Invit08**
- Neutron scattering as a crystallographic tool*
Eduardo Granado M da Silva **Invit15**
- Sirius, the new Brazilian Synchrotron Light Source*
Antonio José Roque da Silva **Invit13**
- Structural Biology Initiative at Instituto Carlos Chagas-FIOCRUZ*
Beatriz G. Guimarães beatriz.guimaraes@synchrotron-soleil.fr **Invit01**
- Synthesis of Functional Nanomaterials*
Jose Solis **Invit03**
- The Influence of Electric and Magnetic Fields on the 3D Structure of Proteins*
Abel Moreno **Invit02**
- The crystal structure of the native capsid from bovine leukemia Virus: retroviral capsids are plastic*
Alejandro Buschiazzo **Invit10**

Oral presentations

- A 100 años de la Ecuación de Dispersión de Debye. Una breve revisión desde el mundo actual de los nanomateriales*
Miguel Delgado **Oral03**
- Crystal structure and dynamic forces in hydroxyapatite*
Lauro Bucio **Oral04**
- Focusing on the structure-property relationships in lanthanide-organic frameworks*
Griselda Narda **Oral05**
- Hetero and isovalent substitution on doped $A_yBa_{1-y}Zr_xTi_{1-x}O_3$ ferroelectric material*
Martín Eduardo Saleta **Oral06**
- Nanotecnología en Costa Rica y su vinculación con la UCCr*
Andrea M. Araya-Sibaja **Oral07**
- Powder & single crystal structure determination of divainillin 2H, mono- and di-acetate*
Leopoldo Suescun **Oral02**
- Synthesis and characterization of $La_{0.6}Sr_{0.4}Co_{1-y}Fe_yO_3$ nanorods*
Diego Germán Lamas **Oral01**

Commercial

Bruker's Commercial Communication

News in SCD and Powder XRD instrumentation

Danilo Bittar

Bruker's Technical Communication

Fast and Efficient: Experiments with Modern X-ray Sources and CMOS APS Detectors

Michael Ruf

Rigaku's Commercial Presentation

The latest advances in hardware and software within Rigaku Oxford Diffraction

Jenny Sayaka Komatsu

Rigaku's Technical Communication

Matching sources to samples – A guide to collecting good data with Cu, Mo, & Ag

Daniel Baker

Panalytical's Commercial Presentation

Difratometria Multifuncional

Leandro Almeida

Posters: Complementary and other methods (session C, 11 sept)

Better quality structures from routine X-Ray data collections using different electron density modeling approaches.

Wieslawa Fabiola Sanjuan Szklarz

COMs01

Computer simulation tools for improving X-ray analysis of materials

Sergio L. Morelhao

COMs05

Designing, mounting and testing a conical slit for diffraction contrast x-ray imaging

Maycon Fioreze

COMs02

Nanopartículas de Ag y Cu en KCl doblemente impurificado

Ricardo Rodriguez Mijangos

COMs03

Relevance of Geometrical Crystallography in the study of pharmaceutical substances

Lauro Bucio

COMs04

Poster: Education in crystallography (session C, 11 sept)

Concurso Interescolar de Crecimiento de Cristales Una Experiencia de Divulgación

Gonzalo Arancibia Rojas

EdCr01

Posters: Materials (session B, 10 sept)

Crystal engineering approach in the study of irbesartan crystal forms

Andrea Araya

MAT02

Dielectric properties of $BaTi_{0.9}Zr_{0.1}O_3$ from a mixture of $BaTiO_3$ and $BaZrO_3$

André Luis Boaventura

MAT18

Efeito da temperatura de calcinação na síntese de estruturas do tipo $Ca_3Co_4O_9$

Sara Silveira Vieira Bertoli

MAT10

Estudio por técnicas de difracción de rayos-X de derivados de cobalto y manganeso de la Gabapentina, un principio activo utilizado como anticonvulsivo

Robert Antonio Toro Hernández

MAT14

Evaluation of the synthesis conditions for obtaining nano-crystals of the MOFs series

$[Ln_2Cu_3(oda)6(H_2O)_6].xH_2O$

Guzmán Peinado

MAT07

Hollow Crystals pharmaceutical drugs: Berg Effect

Renata Guimarães

MAT06

Influence of hydrogen and austenization on the martensite start strain in the austenitic stainless steel 316

John Jairo Hoyos Quintero

MAT17

Investigação comparativa entre as fases cerâmicas presentes nas partículas recicladas e virgens de alumina

Alexandre D. Golanda

MAT08

Investigação da formação de quase-cristais nas ligas do sistema Ti-Zr-Ni

Fernando Froes

MAT19

Ordered mesoporous silica synthesized with a new triol copolymer

Marcia Carvalho de Abreu Fantini

MAT09

Síntesis y caracterización de un polímero de coordinación 2D interpenetrado paralelamente inclinado a partir de Cu(II) y anhídrido maleico

Edward E. Ávila

MAT15

Synthesis and structural characterization of a composite material based on powdered magnetite and high density polyethylene

David Arsenio Landinez Tellez

MAT11

<i>Structural and magnetic investigation of Sr₂CrReO₆</i>	Marcos Tadeu D'Azeredo Orlando	MAT01
<i>Structural characterization of a new zn-fluconazole complex</i>	Analió Dugarte	MAT04
<i>Structural studies in single-crystal manganites of Yb_(1-x)Tb_xMnO₃</i>	Mónica Esperanza Bolívar Guarín	MAT03
<i>Structure Characterization of Nevirapine co-crystals prepared using slurry ball milling and temperature annealing process</i>	Rogeria Nunes Costa	MAT05
<i>Synthesis and characterization of La_{0,6}Sr_{0,4}Fe_{0,8}Cu_{0,2}O_{3-δ} oxide as cathode for Intermediate Temperature Solid Oxide Fuel Cells</i>	Sebastian Davyt	MAT16
<i>Synthesis and characterization of structural and microstructural properties of (K_{1-x}Ba_x)(Nb_{1-y}ni_y)O_{3-δ} Ceramics</i>	Ronaldo Crosio Gennari	MAT20
<i>X-ray absorption studies and f-level occupancy in Ce₂Rh_(1-x)Ir_xIn₈</i>	Robert Prudêncio Amaral	MAT13
<i>Zircônia-Céria Mesoporosa para Células a Combustível e Catalisadores</i>	Vinicius Roberto de Sylos Cassimiro	MAT12

Posters: Molecular structure and physical / chemical properties (session A, 09 sept)

<i>Análisis de las interacciones intermoleculares no-covalentes en Trans-1,4-dicarboxamidaciclohexano (DCA) y Trans-1,4-Dibromo-1,4-DCA</i>	Fernando Garcia Reyes	MSPCP10
<i>Analisis of polymorphic contamination in Meloxicam: raw materials and tablets</i>	Jennifer Tavares Jacon Freitas	MSPCP04
<i>Association between cationic liposomes and low molecular weight hyaluronic acid</i>	Leide P. Cavalcanti	MSPCP32
<i>Bergenin isolated from a new source Peltophorum dubium (Spreng.) Taub plants</i>	Larissa Fernandes Batista	MSPCP09
<i>Caracterización química mineralógica estructural de dos arcillas bolivianas utilizadas en medicina tradicional</i>	Wilma Ticona Chambi	MSPCO33
<i>Caracterización química, mineralógica y estructural de arcillas de Viacha y Quellani (La Paz- Bolivia), utilizadas para su aplicación industrial como material cerámico</i>	Julian Ticona Chambi	MSPCO34
<i>Complejos de Fe^{III} conteniendo ligandos imínicos organometálicos del tipo N₂O, con potenciales aplicaciones magnéticas.</i>	Deborah Gonzalez Miranda	MSPCP14
<i>Controlled synthesis of 5-Fluorocytosine salts and cocrystals - a supramolecular análisis</i>	Cecilia Carolina Pinheiro da Silva	MSPCP01
<i>Cristal structure of bimetalic cobalt complexes: looking for new valence tautomers</i>	João Otávio de Sousa Mendes	MSPCP22
<i>Crystallization and preliminary X-ray diffraction analysis of a xylose isomerase from Bifidobacterium adolescentis</i>	Caio Vinicius Dos Reis	MSPCP17
<i>Determinação estrutural do complexo n,n'-(etano-1,2-diil)bis(1-(1h-imidazol-2-il)metanimina)cobre(II) perclorato.</i>	Sinara de Fátima Freire Dos Santos	MSPCP21
<i>Development of a solid solution of the antiretroviral drugs lamivudine and emtricitabine</i>	Jessica de Castro Fonseca	MSPCP13
<i>Estructura cristalina del polimorfo ortorrómbico del metil éster del diclofenaco, un fármaco antiinflamatorio no-esteroido</i>	Estefany Nathaly Hernandez Bastidas	MSPCP30
<i>Estrutura Cristalina da 2-hidroxi-4-o-(3,3-dimetil)-alilbenzofenona</i>	Cristiane Batista Gonçalves	MSPCP07
<i>Estrutura Cristalina do composto 3-[2(3-metilfenil)-2-oxoetil] isobenzofuran-1(3H)-ona</i>	Rafael Aparecido Carvalho Souza	MSPCP03
<i>Estrutura e interações moleculares de derivados da diaminometileno tiouréia</i>	Genivaldo Julio Perpetuo	MSPCP31
<i>Estudio de la microestructura de chapas de aluminio 1050 laminadas a partir de datos de XRD de alta energía de Petra III, Desy</i>	Emanuel Benatti	MSPCP08

<i>Estudio estructural de complejos de Fe(III) conteniendo ligandos hexadentados base de schiff n4o2.</i>	David Villaman Figueroa	MSPCP15
<i>Estudio estructural por DRX de los procesos de absorción de gases en materiales nanomateriales, hexacianometalatos</i>	Christian Isai Rodriguez Martinez	MSPCP12
<i>Estudo cristalográfico de minerais da região de Volta Grande (MG).</i>	Alfredo Antonio Alencar Exposito de Queiroz	MSPCP11
<i>Estudo e caracterização de compósito de matriz polimérica e pó de pneu para utilização na indústria automobilística</i>	Kelly Cristina de Lira Lixandrão	MSPCP28
<i>Exploring lanthanide/succinate system in the formation metal-organic frameworks.</i>	Richard D'Vries	MSPCP06
<i>Ion transport through Supramolecular Channels in Single</i>	Yvens Chérémond	MSPCP18
<i>Obtaining and characterization of crystal structure of Ricobendazole</i>	Keilla Façanha Silva	MSPCP29
<i>Self-assembly of discrete metallocycles versus coordination polymers based on d^{10} ions and flexible ligands: structural diversification and luminescent properties</i>	Ivan Brito Bobadilla	MSPCP23
<i>Síntesis, caracterización y estudio estructural de complejos de Fe(III) derivados de ligandos iminas entre 2-picolilamina y salicilaldehídos para-sustituídos.</i>	Vania Artigas Salinas	MSPCP27
<i>Solid state technologies in the development of new medicines</i>	Javier Alcides Ellena	MSPCP02
<i>Structural determination of the prototype drug lassbio-1755</i>	Isadora Tairinne de Sena Bastos	MSPCP25
<i>Structural transitions induced by gas pressure and temperature in flexible framework nanoporous materials</i>	Rene Salvador Lopez Cabrera	MSPCP20
<i>Synthesis, structural characterization and isomorphism in the coordination polymer catena-(m2-fumarate)-[bis(dimethylsulfoxide)-diaqua-metal(II)] with metal=coii or znii</i>	Iara Maria Landre Rosa	MSPCP05
<i>The Pectin Methylesterase structure from the sugar cane Weevil, Sphenophorus levis.</i>	Danilo Elton Evangelista	MSPCP16
<i>Thermal stability of the ceftazidime pentahydrate</i>	Maria Silmara Alves de Santana	MSPCP24
<i>Transiciones de fases cúbicas en sistemas lípido/agua</i>	Eucarys Jimenez	MSPCP19
<i>X-ray scattering studies of water-nafion systems</i>	Anastasia Burimova	MSPCP26

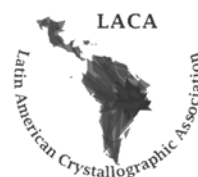
Posters: Polycrystals (session B, 10 sept)

<i>A influência da prensagem a quente na microestrutura do sistema Fe-Cu-Nb</i>	Hellen Cristine Prata de Oliveira	POLY07
<i>An alternative to Rietveld method for phase determination of Ce-TiO₂ materials</i>	Anabela Noel Gravina	POLY08
<i>Análise estrutural do candidato a fármaco antineoplásico LASSBio-1735</i>	Fabio Furlan Ferreira	POLY18
<i>Anisotropic microstructure developed on ARB IF steel using synchrotron X-Ray diffraction data processed by Rietveld analysis.</i>	Raúl Bolmaro	POLY09
<i>Avaliação estrutural do candidato a fármaco hipoglicemiante lassbio-1773</i>	Fabio Furlan Ferreira	POLY19
<i>Caracterização estrutural de candidatos a fármacos para doenças negligenciadas</i>	Vânia Mendes do Prado	POLY17
<i>Caracterização estrutural dos cristais da série L-Arginina.HBr_{1-x}.HCl_x</i>	Adriano Bezerra Pereira	POLY11
<i>Crescimento e caracterização de cristais mistos de K com Ni e Co da família do Sal de Tutton</i>	Tiago de Sousa Pacheco	POLY13
<i>Crystal structure determination of Ciprofibrate using X-ray powder diffraction</i>	Fanny Nascimento Costa	POLY15
<i>Estudo da composição de gessos a partir da difração de raios X aliada ao refinamento de Rietveld</i>	Heloísa Cristina Fernandes Cordon	POLY16

<i>Generalized Pole Figures analysis of an ARB deformed IF steel using synchrotron X-Ray diffraction</i>	Natalia De Vincentis	POLY02
<i>Investigação da ação de diferentes solventes na produção de polimorfos do Efavirenz</i>	Marcelo Monteiro Marques	POLY06
<i>Morphology and size study of (Gd,Er,Yb)-doped naph4 nanoparticles through the X-ray Line Profile Analysis</i>	Raimundo Lora Serrano	POLY12
<i>O uso da Difração de raios X na determinação dos níveis de tensão residual em arames de aço SAE1008 trefilados sob diferentes velocidades</i>	Adriano Corrêa Batista	POLY01
<i>Pigmentos del Sitio Arqueológico Tambo Colorado analizados por difracción de rayos X sincrotrón y refinamiento Rietveld</i>	Elvira Leticia Zeballos Velásquez	POLY04
<i>Quantification of phases of WC-10%Co composite sintered at 1350°C using the Rietveld method</i>	Adriano Corrêa Batista	POLY05
<i>Self-assembly of new chiral L-Aspartic Acid derivatives into hierarchical nanoporous microspheres</i>	olga carolina sanchez montilva	POLY03
<i>The effect of building blocks on the design and construction of four extended networks based on a rigid acetylenic ligand</i>	Vinícius Martins dos Santos	POLY10
<i>Utilização do método de Rietveld para identificação e quantificação de diferentes formas polimórficas da Losartana Potássica.</i>	Juliana Alves Pereira Sato	POLY14

Posters: Small molecules and biological macromolecules (session C, 11 sept)

<i>A new binding site for snake venom C-type lectins?</i>	Maria Cristina Nonato	SMBM14
<i>Caracterização estrutural do sal de tutton misto (co e ni)</i>	Rodolfo Rocha Vieira Leocádio	SMBM02
<i>Crystallization and preliminary X-ray diffraction analysis of a GH74 xyloglucanase from Xantomonas campestris pv.campestris</i>	Evandro Ares de Araújo	SMBM13
<i>Efecto de extractos de hojas de J. Frutescens sobre eritrocitos humanos y modelos moleculares.</i>	Karla A Petit A	SMBM07
<i>Efecto del extracto de Pilocarpus goudotianus sobre eritrocitos humanos y modelos moleculares de membrana celular</i>	Jose Rodolfo Colina	SMBM11
<i>Estrutura cristalina do composto butilsulfonilditiocarbimato bis(trifenilfosfina) níquel(II)</i>	Silvana Guilardi	SMBM06
<i>Estudio de la interacción del fármaco propranolol con membranas celulares in vitro y modelos moleculares</i>	Pablo Andrés Zambrano Lobos	SMBM01
<i>Mononuclear Cu(II) complex of 1-phenyl-1H-1,2,3-triazol-4-carboxylic acid and changes of sequential products due coordination through experimental electron density point of view.</i>	Maria Clara Ramalho Freitas	SMBM05
<i>Motilidad de Espiroquetas: estudios estructurales del flagelo de Leptospira</i>	Fabiana San Martín	SMBM10
<i>Picrato de lamivudina, 3TCH.pic: em busca de novos síntons moleculares, para a modulação de propriedades de estado sólido e farmacêuticas.</i>	Juan Carlos Tenorio	SMBM08
<i>Solid-state investigation of two novel cocrystals of the anti-tuberculosis drug Ethionamide</i>	Cristiane Cabral de Melo	SMBM04
<i>Solubility analysis of carvedilol salts</i>	Olimpia Maria Martins Santos Vianaolimpia_martins@yahoo.com.br	SMBM16
<i>Structural characterization of Imidazole Alkaloids from Pilocarpus microphyllus leaves</i>	Ana Carolina Mafud	SMBM17
<i>Structure of full-length human galectin-4</i>	Joane Kathelen Rustiguel Bonalumi	SMBM12
<i>Study of the structural effect of the addition of a nitro group in Copper(II)-dipeptide-phenanthroline complexes and its consequence on their cytotoxic activity.</i>	Natalia Alvarez Failache	SMBM09
<i>Supramolecular study of 6-((2-(pyridin-2-yl)hydrazono)methyl)pyridin-2-yl)methanol</i>	Mónica Soto Monsalve	SMBM03
<i>The structure of the extended DNA-binding active domains of the E2 bovine papillomavirus type 1 protein</i>	Ludmila Maria Diniz Leroy	SMBM15



Plenary sessions

(Plen)

A controlled pressure/temperature set-up for synchrotron in situ studies of solid-gas processes and reactions: Case of the structural deformation of ZIF-8

Santiago García-Granda¹, Jose Montejó-Bernardo¹, Germán Castro², Conchi O. Ania³

¹ Dept. Química Física y Analítica, Universidad de Oviedo, Oviedo, Spain;

² Spanish CRG BM25, SpLine, Beamline at the ESRF, 38043-Grenoble, France;

^c National Coal Institute (INCAR, CSIC) 33080-Oviedo, Spain.

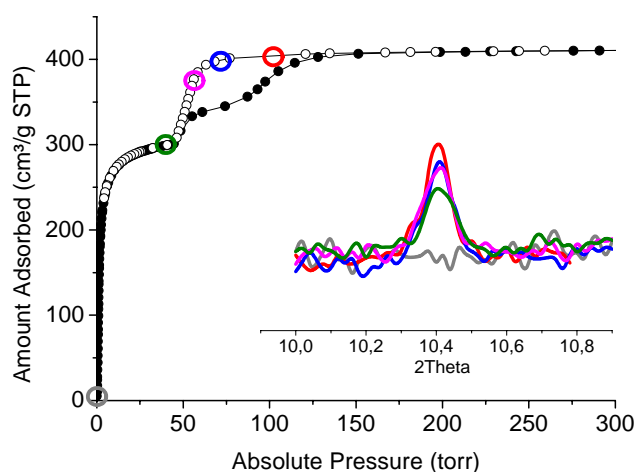
A novel set-up has been designed and used for synchrotron radiation X-ray high-resolution powder diffraction (SR-HRPD) in transmission geometry for in situ solid-gas reactions and processes in an isobaric and isothermal environment. The pressure and temperature of the sample are controlled from 10^{-3} to 1000 mbar and from 80 to 1000 K, respectively. To test the capacities of this novel experimental set-up, structure deformation in the porous material zeolitic imidazole framework (ZIF-8) by gas adsorption at cryogenic temperature.

The adsorption properties of ZIF-8 for a variety of strategic gases, shows unusual multi-stepped adsorption features for the adsorption of various gas probes (i.e., N₂, CO, Ar, O₂) [1-3]. There seems yet to be a dearth in the understanding of the gas adsorption properties of flexible materials [3,4].

X-ray diffraction experiments were conducted at the Spanish CRG BM25 SpLine at ESRF in a controlled environment chamber with fine control of the gas dosage, sample outgassing under vacuum, temperature control and simultaneous SR-HRPD recording [4].

Figure 1 shows the nitrogen adsorption/desorption isotherm of ZIF-8 at 85K and the SR-HRPD diffractograms (inset) corresponding to various gas loadings. Measurements were fast enough to observe the evolution of the crystallographic phases of the material, making possible to determine structural changes in the solid at in operando conditions [4].

Figure 1: Equilibrium N₂ adsorption/desorption isotherm 85 K of ZIF-8 and (inset) real time SR-HRPD during gas release (desorption branch).



The real time monitoring of the SR-HRPD patterns of ZIF-8 indicate that the gas-induced structural flexibility is linked to the organization of the adsorbed gas molecules in the adsorption sites, as well as the polarizability and molecular size and shape of the gases.

- [1] D. Fairen-Jimenez, SA. Moggach, MT. Wharmby, PA. Wright, S. Parsons, T. Duren, *J. Am. Chem. Soc.* **133** (2011) 8900.
- [2] SA. Moggach, TD. Bennett, AK. Cheetham *Angew. Chem., Int. Ed.* **48** (2009) 7087.
- [3] CO. Ania, E. García-Pérez, M. Haro, JJ. Gutiérrez-Sevillano, T. Valdés-Solís, JB. Parra, S. Calero, *J. Phys. Chem. Lett.* **3** (2012) 1159.
- [4] Salas-Colera E, Muñoz-Noval A, Heyman C, Ania CO, Parra JB, García-Granda S, Calero S, Rubio-Zuazo J, Castro GR, *J. Synchr. Rad.* **22** (2015) 1.

Acknowledgments: We thank financial support from Spanish MINECO (MAT2013-40950-R) and ERDF.

Keywords: XRPD; isobaric/isothermal environment, ZIF-8, adsorption, solid-gas reactions.

Advances in Electron diffraction Determination of Nano Materials

Miguel Jose Yacaman

Physics Department University of Texas at San Antonio Texas USA

Electron diffraction (ED) can be a powerful tool to determine the crystal structure of materials. Unlike X-ray or neutron diffraction, ED requires only small amounts of matter to produce a significant pattern. Therefore it is ideal for to apply to nanotechnology and other fields such as protein structure determination. Not all proteins can be crystallized in amounts necessary for X-ray diffraction. However most of proteins can be easily crystallized has Nano crystals.

However two main problems have held back the application of ED: Radiation Damage and the fact that strong dynamical effects on the scattering complete the interpretation.

In this talk we will discuss the advances in our group at the University of Texas at San Antonio to overcome these limitations .We will present as example the application to the determination of noble metals clusters structure determination.

Crystal Engineering of Task-Specific Materials

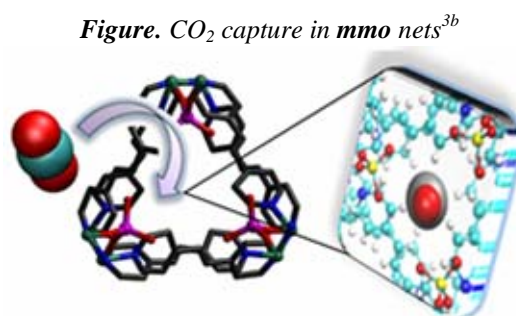
Michael J. Zaworotko

University of Limerick, Limerick, Ireland, E-mail: xtal@ul.ie

That composition and structure profoundly impact the properties of crystalline solids has provided impetus for exponential growth in the field of *crystal engineering* [1] over the past 25 years. This lecture will address how crystal engineering has evolved from structure design (form) to control over bulk properties (function). Strategies for the generation of two classes of functional crystalline materials will be addressed:

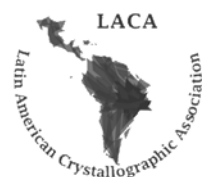
Multicomponent pharmaceutical materials, MPMs, such as cocrystals [2] have emerged at the preformulation stage of drug development. This results from their modular and designable nature which facilitates the discovery of new crystal forms of active pharmaceutical ingredients, APIs, with changed physicochemical properties. The concepts of “supramolecular heterosynthons” and “ionic cocrystals” will be explained and a case study addressing brain bioavailability of lithium will be presented.

Hybrid Ultramicroporous Materials, HUMs, are built from metal or metal cluster “nodes” and combinations of organic and inorganic “linkers”. Two families of HUMs that afford exceptional control over pore chemistry, pore size and binding energy [3], will be detailed. Benchmark selectivity for CO₂ capture in these HUMs with **pcu** or **mmo** (see Figure) topology has been observed thanks to the strong electrostatics associated with pores lined by the inorganic components of these nets. However, they remain understudied because of the synthetic challenges associated with self-assembly of multiple nodes. Interpenetrated 3D nets, another understudied class of material, also afford control over pore size and will also be addressed.



In summary, this lecture will emphasize how crystal engineering coupled with molecular modeling can offer a paradigm shift from the more random, high-throughput methods that have traditionally been utilized in materials discovery and development. In short, how to make the right material for the right application.

- [1] (a) Desiraju, G.R. *Crystal engineering: The design of organic solids* Elsevier, 1989; (b) Moulton, B.; Zaworotko, M.J. *Chemical Reviews* **101**, 1629-1658; 2001.
- [2] Vishweshwar, P.; McMahon, J.A.; Bis, J.A.; Zaworotko, M.J. *J. Pharm. Sci.* 2006, **95**, 499-516, 2006.
- [3] Smith, A.J.; Kim, S.-H.; Duggirala, N.K.; Jin, J.; Wojtas, L.; Ehrhart, J.; Giunta, B.; Tan, J.; Zaworotko, M.J.; Shytle, R.D. *Molecular Pharmaceutics*, **10**, 4728-4738; 2013.
- [3] (a) Burd, S.D.; Ma, S.; Perman, J.A.; Sikora, B.J.; Snurr, R.Q.; Thallapally, P.K.; Tian, J.; Wojtas, L.; Zaworotko, M.J. *J. Amer. Chem. Soc.*, **134**, 3663-3666; 2012. (b) Mohamed, M.; Elsaidi, S.; Wojtas, L.; Pham, T.; Forrest, K.A.; Tudor, B.; Space, B.; Zaworotko, M.J. *J. Amer. Chem. Soc.*, **134**, 19556-19559; 2012. (c) Nugent, P.; Belmabkhout, Y.; Burd, S.D.; Cairns, A.J.; Luebke, R.; Forrest, K.; Pham, T.; Ma, S.; Space, B.; Wojtas, L.; Eddaoudi, M.; Zaworotko, M.J. *Nature*, **495**, 80-84, 2013.



Invited talks

(Invit)

Structural Biology Initiative at Instituto Carlos Chagas-FIOCRUZ

Beatriz G. Guimarães

*Instituto Carlos Chagas, Fundação Oswaldo Cruz
Curitiba, Paraná*

The Oswaldo Cruz Foundation (FIOCRUZ) is a science and technology institution belonging to the Brazilian Ministry of Health which comprises sixteen technical-scientific units over the country. FIOCRUZ is responsible for a range of activities including research and development; highly-regarded hospital and ambulatory care services; production of vaccines, drugs, reagents, and diagnostic kits and implementation of social programs. In 2013, Instituto Carlos Chagas (ICC/FIOCRUZ-Paraná) started an initiative to found a new structural biology group aiming at the production and biophysical characterization of proteins of medical and biotechnological interests. This group is now expanding to include macromolecular crystallography techniques. In this talk, the structural biology initiative at ICC will be presented, along with the ongoing projects that will benefit from structure determination of proteins for medical and biotechnological applications. This includes characterization of proteins from pathogenic organisms that are potential targets of inhibitors and designing of new antibodies for immunodiagnosis

The Influence of Electric and Magnetic Fields on the 3D Structure of Proteins

Abel Moreno

*Instituto de Química, Universidad Nacional Autónoma de México (UNAM). Av. Universidad 3000.
Colonia UNAM. Mexico D.F. 04510, MEXICO.*

A new strategy is proposed for protein crystallization methods in solution-growth or gel-growth by using different crystal growth devices applying electric (in the range of micro-Amperes) and magnetic fields (from 7 to 12 Tesla). The effect of combining both electric and magnetic fields is shown and is reviewed. Proteins with different contents of α -helices and β -sheets, and crystallized in different crystallographic space groups are studied. The crystal quality is improved by using an electric field to electro-migrate ions to the ITO electrodes, and to orientate protein molecules by using a strong magnetic field in either solution or gel-growth to control the transport phenomena. Some advantages to increase the crystal quality for crystals from marginal conditions for X-ray diffraction are discussed. Finally, in order to separate the nucleation and the crystal growth processes (by using these electromagnetic fields), the obtainment of either large amount of small crystals for Powder X-ray Diffraction or big single crystals for the classic X-ray Crystallography (or Neutron Diffraction Crystallography) is also evaluated.

Acknowledgements: The author (A.M.) gratefully acknowledges financial support from Soft Condensed Matter Network (RMCB) from CONACYT for sponsoring the travelling expenses.

Synthesis of Functional Nanomaterials

Jose Solis

Facultad de Ciencias, Universidad Nacional de Ingeniería, Lima, Perú

In the last decade, there has been an increasing interest in the study of nanocrystalline materials owing to their electrical, optical, mechanical and magnetic properties being superior to those of conventional coarse-grained structures. The surface-to-bulk ratio for a nanocrystalline material is much greater than for a material with large grains, which yields a large interface between the solid and a gaseous or liquid medium. For example, a chemical species on a ceramic semiconductor surface yields a signal that is transduced through the microstructure of the sintered ceramic to form a conductance change; this is enhanced if the material has a nanometer size.

We have developed a novel, simple sonochemical one-step process using metallic salts precursors, and obtaining the corresponding nanosized metal oxides (TiO₂, ZnO₂, CuO, ZnO, SnO₂, and NiO) as products. We have studied various proprieties like gas sensing, bactericidal, photocatalytic etc. We have characterized the nanopowders using X ray Diffraction, and Scanning Electron microscopy. The crystallite size of the materials was determined fitting the obtained diffractogram. We have studied the gas sensing properties of NiO, the bactericidal properties of ZnO₂ and CuO, and the photocatalysis of TiO₂.

Fighting neglected diseases with structural biology and medicinal chemistry

Glaucius Oliva

Institute of Physics of São Carlos, University of São Paulo.

Science as the major means for development, social inclusion and the promotion of a better life, is one of the pillars of modern science and technology in many countries, Brazil included. This is the case related to parasitic diseases, which are still a major global cause of illness, morbidity, long-term disability, and death, with severe medical and psychological consequences for millions of men, women and children, specially for the poor. Despite the high prevalence of parasitic diseases worldwide, in most cases their treatment is inadequate, generating an urgent demand for new antiparasitic drugs. However, in addition to the traditional challenges involved in the complex process of drug discovery and development, there is the hurdle of the lack of investments in this field. This situation is especially problematic in *de novo* drug discovery, regarded as a high risk and costly process. Therefore, strategies that allow high quality hit identification rate as well as reduction in drug discovery costs are extremely useful in this field. The biology of parasitic organisms has been continuously studied in detail, providing a solid base for the selection of relevant molecular targets for drug discovery, many of which with structures elucidated by protein crystallography. Virtual screening strategies, including the use of both ligand- and structure-based methods, have been employed in the search for new inhibitors of relevant therapeutic targets related to parasitic diseases. More recently, the combination of computational and experimental techniques has been explored as a useful approach for the identification of high quality hits. This lecture outlines our progresses and applications of *in silico* screening strategies for the discovery of innovative chemotherapy agents for a variety of parasitic diseases, including Chagas disease, leishmaniasis and schistosomiasis.

Exploiting the use of multivalent hydrogen bonding templates to direct [2+2] photochemical reactivity of olefins. From molecules to nano/microtemplates.

Alexander Briceño and Gabriela Ortega

Instituto Venezolano de Investigaciones Científicas (IVIC), Apartado 21827, Caracas 1020-A, Venezuela. E-mail: abriceno@ivic.gob.ve

New supramolecular strategies based on the use of multivalent hydrogen bonding templates is exploited in order to drive [2+2] photocycloaddition either in the solid state or in solution. In this contribution, we describe the potential of the tetratopic 1,2,4,5-benzenetetracarboxylic acid (**bta**) as a hydrogen-bonding supramolecular switch which have been exploited to design a series of novel ionic photoactive self-assemblies based on asymmetrical olefins (stilbazole derivatives). Crystal structure analyses revealed the formation of self-assembly built-up of bta^{2-} anions linked by two kinds of charge-assisted hydrogen bonds between carboxylic and carboxylate groups and carboxylate–pyridinium supramolecular moieties. The bta^{2-} anion displays an interesting ability as template, as a consequence of the proton transfer between carboxylic acid and pyridyl derivatives, which can adopt either intramolecular or intermolecular charge-assisted hydrogen bonds between carboxylic and carboxylate groups. This ability is very useful to accommodate different pyridyl targets with different functional groups as substituents on aryl ring. Other structural features found in those compounds is the organisation in a parallel fashion of all the pyridinium cations with *head-to-tail* stacking assisted *via* charge-assisted hydrogen bonding and reinforced by cation $\cdots\pi$ interactions. Inspired in these assemblies, we also show the ability of hydrophilic nano/micro carbon materials as multivalent H-bonding templates for [2+2] photoreactions in solution. The potential of such templates is evaluated in the photoreaction either of pyridyl or carboxylic compounds in solution to yield a single dimer.

**Laboratory X-ray of Universidad Industrial de Santander and support services:
teaching, research and national and international industry.**

J. A. Henao.

Escuela de Química, Grupo de Investigación en Química Estructural (GIQUE), Vicerrectoría de Investigación y Extensión, Universidad Industrial de Santander, Bucaramanga, Colombia

The X-ray Laboratory (XRL) of the Universidad Industrial de Santander-Parque Tecnológico Guatiguará (UIS-PTG) is supported by specialized staff in different areas which includes the technique of X-rays: Powder Diffraction, Single Crystal and Fluorescence. Additionally, XRL has different crystallographic Database updated (PDF-2 and PDF-4 of the *International Centre for Diffraction Data-ICDD*; *Inorganic Crystal Structure Database-ICSD* and *Cambridge Structural Database-CSD*). Since 1989, the UIS bought the first RIGAKU brand X-ray powder diffractometer and from that year, the X-ray Laboratory started providing internal (UIS) and external services (outside the UIS, national and international level). Currently, the XRL provides support in powder diffraction techniques: qualitative analysis and quantitative Rietveld analysis, *transmission, high temperatures* in inert, oxidizing and reducing atmospheres; *capillarity, Grazing Incidence Diffraction, Reflectometry, High Resolution, Texture Analysis and Microdiffraction*; Single Crystal technique: study of *Small Molecules* and *Macromolecules* and the elemental analysis by Fluorescence technique: qualitative analysis (from beryllium to uranium) and quantitative analysis (from sodium to uranium, except noble gases) of minerals, inorganic compounds, paraffin and fuel (diesel, naphtha, gasoline) samples. During the conference some examples and results obtained in the laboratory will be illustrated.

Crystal structure of the bacteriophytochrome from *Xanthomonas campestris* pv. *campestris*: insights into pathogenicity in a light-dependent manner.

Sebastián Klinke, Lisandro H. Otero, Jimena J. Rinaldi, Fernando A. Goldbaum & Hernán R. Bonomi
Fundación Instituto Leloir (IIBBA-CONICET), and Platform for Structural Biology and Metabolomics PLABEM, Av. Patricias Argentinas 435, Buenos Aires, Argentina.

Phytochromes give rise to the largest photosensor family known to date. However, they are underrepresented in the Protein Data Bank. Plant, cyanobacterial, fungal and bacterial phytochromes share a canonical architecture consisting of an N-terminal photosensory module (PAS2-GAF-PHY domains) and a C-terminal variable output module. The bacterium *Xanthomonas campestris* pv. *campestris*, a worldwide agricultural pathogen, codes for a single bacteriophytochrome (XccBphP) that has this canonical architecture, bearing a C-terminal PAS9 domain as the output module. In this talk, we will present the three-dimensional structure of XccBphP determined at 3.25 Å resolution, together with experimental evidence that confirms the participation of this protein in the infectious process and in the modulation of virulence factors.

Models and Diffraction study of polytypes and planar disorder

Ernesto Estévez Rams

Facultad de Física-IMRE. - Universidad de la Habana

Different approaches used to analyze stacking disorder by powder diffraction are reviewed. Some early treatments although general in the mathematical formulation were forced to adopt strong simplifying assumptions to be used without computer resources. In the classical, most used, approaches, a model of layer interaction is assumed and approximate analytical expressions are sought. This has been further developed by building deterministic state machines describing the stacking process, which allows treating more general cases than the early models. Other developments include the use of Monte Carlo procedures where crystals are “grown” in the computer and diffraction patterns simulated. Other recent approaches return to the general equations of diffraction for a layer structure as a starting point for computer simulations. Finally, other authors have explored the possibility of extracting the stacking information directly from the diffraction data by using the fact that, in reciprocal space, the diffraction pattern can be described by a Fourier series whose coefficients have a direct physical interpretation.

Estudio estructural de complejos de hierro con potenciales aplicaciones de entrecruzamiento de espín

Mauricio Fuentealba

Laboratorio de Cristalografía, Pontificia Universidad Católica de Valparaíso, Chile

Materiales con entrecruzamiento de espín (SCO, por sus siglas en inglés) son compuestos moleculares los cuales pueden conmutar su configuración electrónica entre dos estados en competición termodinámica, un estado de bajo-espín y un estado de alto-espín los cuales son estables a bajas y altas temperaturas, respectivamente. Estos dos estados no sólo tienen propiedades magnéticas diferentes sino también diferentes propiedades estructurales y ópticas. Aún más importante es notar que el cambio entre los dos estados es reversible, detectable y ocurre en respuesta a un estímulo externo que puede ser controlado, generalmente un cambio de temperatura, de presión o de irradiación con luz [1]. En general, el proceso de intercambio en el estado sólido es controlado por interacciones cooperativas intermoleculares. Por lo que, dilucidar la correlación de la estructura con las propiedades físicas es fundamental para la identificación de estas interacciones y para una mayor comprensión de los procesos que controlan el SCO [2].

Por este motivo, en este trabajo se desarrolla el estudio de una serie de complejos de hierro con el propósito de obtener información acerca de las interacciones intermoleculares responsables de los efectos cooperativos entre los complejos, el contraión y/o las moléculas de solvente de cristalización. Se exhibirá que los efectos de cooperatividad intermolecular del tipo $\pi \cdots \pi$ y/o $X \cdots X$ están estrechamente relacionados con el comportamiento magnético en los complejos de hierro estudiados.

[1] P. Gütllich, A. Hauser and H. Spiering, *Angew. Chem., Int. Ed.* **33**, 2024 (1994); P. Gütllich, Y. Garcia and H. A. Goodwin, *Chem. Soc. Rev.*, **29**, 419 (2000); P. Gütllich, *Struct. Bonding.*, **44**, 83 (1981); E. König, *Prog. Inorg. Chem.*, **35**, 527 (1987); A. Hauser, J. Jeftić, H. Romstedt, R. Hinek and H. Spiering, *Coord. Chem. Rev.*, **190-192**, 471 (1999).

[2] A. Tissot, R. Bertoni, E. Collet, L. Toupet, M.-L. Boillot, *J. Mater. Chem.* **21**, 18347 (2011).

**The crystal structure of the native capsid from bovine leukemia
Virus: retroviral capsids are plastic**

Obal, G.^a; Trajtenberg, F.^b; Carrión, F.^a; Tomé, L.^a; Larrieux, N.^b; Zhang, X.^c; Pritsch, O.^a;
Buschiazzo, A.^b

^aProtein Biophysics Unit, and ^bUnit of Protein Crystallography, Institut Pasteur de Montevideo,
Montevideo, Uruguay; ^cUnit of Structural Virology, Institut Pasteur, Paris, France

Retroviruses undergo an obligatory maturation step in the formation of infectious particles. The cleavage of Gag generates several mature proteins, including capsid (CA), which self-assembles into a fullerene-like core, enclosing the RNA genome. Revealing the molecular features of the retroviral mature core and its assembly mechanism is important for understanding retrovirus biology and developing novel antiretroviral drugs. Despite the essential role of the retroviral core, its high polymorphism has hindered high-resolution structural analyses. We now report the crystal structure of the native, mature CA protein from bovine leukemia virus (BLV) at 2.75 Å resolution [1]. The structures of the individual NTD and CTD subdomains of BLV CA were determined, respectively to 1.44 and 2.45 Å resolution, which was instrumental in the structure determination process. This structure represents the first X-ray structure of a native retroviral capsid protein (i.e. containing no mutations). BLV is a tumorigenic B-lymphotropic delta-retrovirus that infects cattle worldwide, closely related to human T-lymphotropic viruses (HTLV). The BLV CA crystals contain one CA hexamer in the asymmetric unit, which pack laterally forming planar layers. CA hexamers deviate significantly from 6-fold symmetry, yet adjust to make two-dimensional pseudohexagonal arrays that mimic mature retroviral cores. Intra- and inter-hexameric quasiequivalent contacts are uncovered, with flexible trimeric lateral contacts among hexamers, yet preserving very similar dimeric interfaces making the lattice. The conformation of each capsid subunit in the hexamer is therefore dictated by long-range interactions, revealing how the hexamers can also assemble into closed core particles, a relevant feature of retrovirus biology. This model of capsid plasticity contributes with a novel framework to develop more accurate hypotheses of capsid self-assembly and uncoating. Implications of this mechanism seem relevant for the discovery of allosteric effectors with novel antiretroviral properties.

[1] Obal G et al., (2015) Science, in press. DOI: 10.1126/science.aaa5182

Caracterización de materiales de interés farmacéutico en formulaciones comerciales y obtenidos bajo diferentes condiciones de cristalización y tratamientos en el estado sólido

Graciela Díaz de Delgado

Laboratorio de Cristalografía-LNDRX, Departamento de Química, Facultad de Ciencias,
Universidad de Los Andes, Mérida 5101, Venezuela.

El estudio del comportamiento de Principios Farmacéuticamente Activos (APIs por sus siglas en inglés) bajo diferentes condiciones de cristalización, presión, humedad, temperatura, entre otras condiciones, es de vital importancia para asegurar la calidad de los medicamentos que se expenden en el mercado. Ligeros cambios en estas condiciones pueden producir diferentes polimorfos, solvatos, o nuevos compuestos de esos APIs lo cual puede influir significativamente en el desempeño del principio activo. Como parte de las actividades que se realizan en nuestro laboratorio, se ha estudiado una variedad de antihistamínicos, broncodilatadores, anticonvulsivos, antifúngicos, suplementos minerales y excipientes, entre otros, tanto en materia prima como en formulaciones comerciales disponibles en el mercado venezolano. Estudios en muestras Policristalinas y Monocristal (tanto con rayos X convencionales como con radiación de sincrotrón) han permitido identificar nuevas formas cristalinas del Clenbuterol (hemihidrato y acetato), Tiocolchicósido (dihidrato, anhidro), derivados metálicos de Gabapentina y Fluconazol, un nuevo polimorfo del metil éster del diclofenaco, entre otros. Estos resultados se presentarán en detalle.

La estructura de algunos materiales, para los cuales no ha sido posible obtener cristales de calidad apropiada para estudios en monocristal, se ha determinado utilizando difracción de rayos X en polvo. Se presentarán los modelos estructurales preliminares para el derivado multicomponente Mirtazapina:Ácido Itacónico y para el Gluconato de Calcio monohidratado (Figura 1).

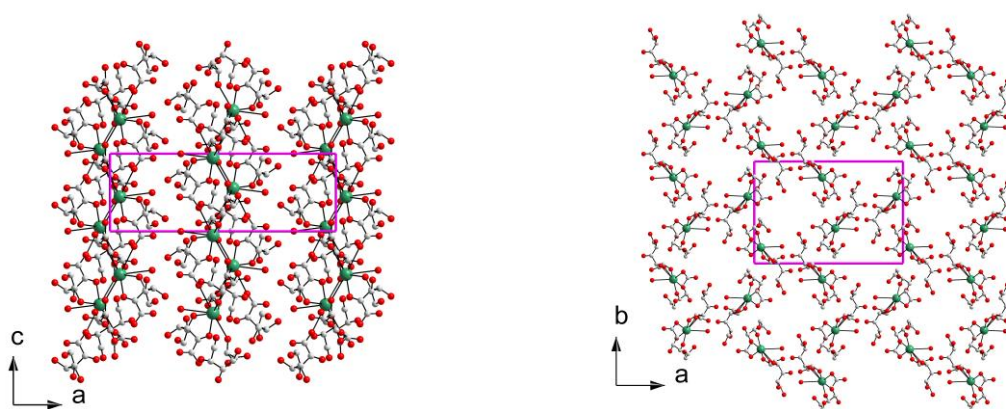


Figura 1: Empaquetamiento del Gluconato de Calcio monohidratado visto a lo largo de los ejes **b** y **c**.

Agradecimientos: Este trabajo es parte de las Tesis de Lic. de G. Borges, A. Dugarte, Y.W. Escalante, A. Guillén, E. Hernández, R.C. López, J. Trejo y Tesis Doctoral de R.A. Toro. Se agradece la colaboración del Prof. J.M. Delgado y M.Sc. J.E. Contreras (ULA), Prof. J.A. Henao, Dr. H. Camargo y M.Sc. J.L. Pinto (UIS, Bucaramanga, Colombia), Dr. A. Briceño, M.Sc. T. González y Dra. J. Bruno-Colmenárez (IVIC) y Drs. M. Pink y C-H. Chen (IUMSC, USA). El financiamiento proviene del proyecto LAB-97000821 del FONACIT (Laboratorio Nacional de Difracción de Rayos-X) y CDCHTA-ULA Proyecto C-1676-09-08-A.

Additive manufacturing from a material science perspectiveRainer Christoph^{a,b}

*^aLaboratorio de Nanotecnología e Impresión 3D, Instituto de Ciencia, Tecnología e Innovación,
Universidad Francisco Gavidia, El Salvador*

^bHead of Nanotecnia, www.nanotecnia.net

The recent emergence and proliferation of additive digital manufacturing techniques (3D printing), such as Fused Deposition Modeling (FDM), Selective Adhesive Deposition, Selective Laser Sintering (SLS), or Continuous Liquid Interface Production Technology (CLIP), bears many new and very promising potentials, not only for industrialized nations, but also for local industries Latin America. FDM provides the capability of locally defining, designing and producing manifold objects for a wide range of applications, and at affordable costs. It allows societies to produce locally, to self-supply specific local demands. This is especially important for small-sized developing societies, where a vast majority of special technological goods is currently being imported. For these countries, new accessible production techniques such as FDM foster local production, innovation and reduce the present strong dependence on imports.

Additive manufacturing however still bears many challenges. On the material side, present material solutions for practical applications like e.g. the production of special spares, rely on synthetic polymers, like ABS. The chemical nature of such materials – which are still being widely deployed in industry - implies a significant environmental impact of the produced goods, and also bears significant health risks during the FDM production process. In other words, most of today's material solutions for additive manufacturing fall quite short from being sustainable. Additive manufacturing is not yet fit for the future. Apart from their “printability”, i.e. their chemical and mechanical behavior during the production process, sustainable material solutions for additive manufacturing must show a combination of sufficient mechanical strength, reasonable lifetime, biodegradability, and non-toxic behavior before, during and after production. Furthermore, such materials must be locally available, at affordable costs. The presentation will document different material solution approaches from own and external work and call for enhanced interdisciplinary collaboration in this field.

Sirius, the new Brazilian Synchrotron Light Source

Antonio José Roque da Silva

CNPEM, LNLS, Campinas, SP, Brazil

The application of synchrotron radiation in a great variety of fields has increased steadily worldwide. This, to a large extent, is a result of the availability of the much brighter third-generation light sources, which opened up new experimental techniques. Recently, new developments in accelerator technology are paving the way for even brighter sources, which are being named fourth-generation light sources. Sirius, the future new Brazilian synchrotron, is one of the first two such equipments being currently constructed in the world. Its first light is expected by 2018. It is being planned to be a state of the art machine, providing tools for cutting edge research that are non existent today in Brazil. It is a project designed and executed by the Laboratório Nacional de Luz Síncrotron – LNLS, which was also responsible for the construction of the current second generation Brazilian light source, the first synchrotron in the southern hemisphere, still the only one in Latin America. In this talk an overview of the status of Sirius will be provided.

Applied crystallography at ALBA Synchrotron Light Source

Miguel A. G. Aranda

ALBA-CELLS synchrotron. Carretera BP 1413, Km. 3,3 - 08290 Cerdanyola del Vallès, Barcelona

e-mail: g.aranda@cells.es

ALBA synchrotron light source (www.cells.es) is the largest Spanish research infrastructure that started full operation of its first 7 beamlines on February 2013. I will divide the talk in two parts: i) the general description of the facility; and ii) a summary of the applied crystallographic studies that are being carried out at our synchrotron.

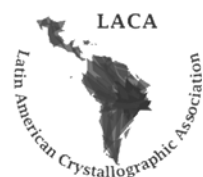
I will start with a very brief description of the facility including the staff structure, general parameters, and our accelerator complex: LINAC, booster and the store ring. Then, I will comment a summary of our seven operating beamlines, the two beamlines (phase-II) which are under construction, and the proposal for new beamlines (phase-III).

Secondly, I will concisely describe some of the applied crystallographic works that are being carried out on our beamlines. These works span from single crystal studies of macromolecules at BL13-XALOC to powder diffraction studies of the hydration of cements at BL04-MSPD. High-pressure powder diffraction studies in diamond-anvil-cells will also be discussed as well as microdiffraction for structural analysis and bio-SAXS (small angle X-ray scattering).

Neutron Scattering as a Crystallography Tool

Eduardo Granado Monteiro da Silva
Instituto de Física Gleb Wataghin-UNICAMP, Brazil

Free neutrons are unstable particles with lifetime of ~ 15 min, spin $\frac{1}{2}$ and no electric charge. High-flux neutron beams for use in scientific research are produced in a number of research-grade nuclear reactors as well as dedicated spallation neutron sources around the world. These particles are liberated in an energy scale of MeV, thermalized to the energy scale of meV, corresponding to wavelengths of the order of 0.1 nm, and guided towards instruments where scientific experiments are performed that probe the structure and dynamics of condensed matter. Neutron techniques, including diffraction, small angle scattering, inelastic scattering, radiography, reflectivity, among others, have been able to give insights into some of the most serious challenges society is facing, such as agriculture, earth sciences, energy, environment, heritage, information technology, medicine and nanotechnology. In particular, neutron powder diffraction can be very useful to crystal structure determination and refinement of transition-metal or rare-earth oxides, as well as of materials where hydrogen atoms positions are to be determined with confidence. In the regional setting, the ongoing RMB (Reator Multipropósito Brasileiro) and RA-10 enterprises to build new research reactors in Brazil and Argentina open a window of opportunities for the development of a robust neutron users community in the region. In this talk, the overall neutron properties and some techniques of relevance will be reviewed, and a few examples of applications of neutron powder diffraction will be presented.



Oral presentations

(Oral)

Synthesis and characterization of La_{0.6}Sr_{0.4}Co_{1-y}Fe_yO₃ nanorods

A. E. Mejía Gómez ^{a,b}, J. Sacanell ^a, A. L. Soldati ^c, C. Ramos ^a, S. J. A. Figueroa ^d, M. C. A. Fantini ^e,
A. F. Craievich ^e and D. G. Lamas ^f

^a CONICET - Departamento Física de la Materia Condensada, Centro Atómico Constituyentes,
Comisión Nacional de Energía Atómica, San Martín, Pcia. de Buenos Aires, Argentina.

^b CINSO (Centro de Investigaciones en Sólidos), UNIDEF-CITEDEF-CONICET, Villa Martelli, Pcia.
de Buenos Aires, Argentina.

^c CONICET - Centro Atómico Bariloche, Comisión Nacional de Energía Atómica, S.C. de Bariloche,
Pcia. de Río Negro, Argentina.

^d CNPEM, Laboratório Nacional de Luz Síncrotron, Campinas, SP, Brazil.

^e Laboratório de Cristalografia, Instituto de Física, Universidade de São Paulo, São Paulo, SP, Brazil.

^f CONICET - Escuela de Ciencia y Tecnología, Universidad Nacional de Gral. San Martín, San
Martín, Pcia. de Buenos Aires, Argentina.

Fuel cells are one of the most promising devices for environmentally clean energy production by directly converting chemical energy into electricity. Among them, solid oxide fuel cells (SOFCs) have the unique capability to use different fuels such as hydrocarbons or hydrogen. However, several issues have to be solved in order to improve their efficiency and reduce their costs. The reduction of their working temperature, which is typically around 900-1000°C, is one of the most important issues. For this reason, extensive research has been devoted to develop novel materials for intermediate temperature SOFCs (IT-SOFCs). In the case of the cathode, one step in this direction is the use of mixed ionic and electronic conductors (MIECs), which exhibit higher performance than conventional electronic conductors. In particular, La_{0.6}Sr_{0.4}Co_{1-y}Fe_yO₃ perovskites have shown excellent electrocatalytic properties for the oxygen reduction reaction.

In the last years, extensive research has been devoted to study the structural and electrochemical properties of nanostructured MIECs as cathodes for IT-SOFCs [1–3]. Nanomaterials are not employed in conventional SOFCs since grain growth is expected to occur at the high operation temperatures of these devices. However, their use in IT-SOFCs is currently under evaluation. Cathodes based on nanostructured MIECs are very interesting because the number of active sites for the oxygen reduction reaction is expected to increase dramatically.

In this work, we report the synthesis and characterization of La_{0.6}Sr_{0.4}Co_{1-y}Fe_yO₃ nanorods (y = 0.2; 0.5 and 0.8). These nanomaterials were synthesized by a pore-wetting technique starting from a nitrate solution of the desired cations and using polycarbonate porous membranes of average pore size of 200 nm as templates [4,5]. The characterization was performed by synchrotron X-ray powder diffraction (SXPD), scanning electron microscopy, X-ray absorption near edge structure (XANES) spectroscopy and Mössbauer spectroscopy. SXPD analysis confirmed that single-phase samples exhibiting the rhombohedral phase ($R\bar{3}c$ space group) can be obtained after calcination at 1000°C for 1 h. The average crystallite size was about 30 nm for all compositions. SEM observations confirmed the rod-like nanostructure of the samples. The rods exhibited typical lengths of about 0.8-1 μm and were formed by nanoparticles with diameters of about 140-150 nm. Finally, XANES and Mössbauer spectroscopies allowed the study of the oxidation states of Co and Fe in the series.

[1] M.G. Bellino *et al.*, *J. Am. Chem. Soc.*, **129**, 3066 (2007)

[2] J. Sacanell *et al.*, *J. Power Sour.*, **195**, 1786 (2010)

[3] L. M. Acuña *et al.*, *J. Power Sour.*, **196**, 9276 (2011)

[4] P. Levy *et al.*, *Appl. Phys. Lett.*, **83**, 5247 (2003)

[5] A. G. Leyva *et al.*, *J. Solid State Chem.*, **177**, 3949 (2004)

Acknowledgments: ANPCyT (Argentina, PICT 2011 No. 1948), LNLS (Brazil) and MinCyT-CAPES (Argentina-Brazil) cooperation agreement.

Powder & single crystal structure determination of divainillin 2H, mono- and di-acetate.L. Suescun^a, N. Estefan^a, V. Aldabalde^b, P. Sáenz^c, D. Gamenara^b, G. Seoane^b.^a *Cryssmat-Lab/DETEMA/Cátedra de Física*; ^b *Departamento de Química Orgánica y*^c *CCBG/DETEMA; Facultad de Química, Universidad de la República, Montevideo, Uruguay.*

The synthesis of a model of lignin, with 5-5' and β -O-4 bonds (present in different native lignins) can be achieved starting from vainillin (1) using horseradish enzyme (HRPO) to connect C5-C5' and form divainillin (2) (Figure 2) and later connect the third monomer in a β -O-4 bond. During the first 5 minutes of the enzymatic reaction a white-gray powder soluble in DMSO corresponding to (2) is obtained, but after 15 minutes of reaction, part of the solid remains insoluble in all tested solvents. Due to the impossibility to dissolve the powder it was impossible to determine its structure by nuclear magnetic resonance (NMR) or re-crystallize it for single crystal structure determination. The structure of the soluble dimer was confirmed by NMR as divainillin-2H and was acetylated to obtain single crystals of vainillin mono and diacetate (3) that allowed to reconfirm the structure of the dimer, using single-crystal X-ray diffraction (XRD) with a Bruker D8 Venture diffractometer. The insoluble solid was studied by powder XRD using the Rigaku ULTIMA IV diffractometer. The conventional powder diffraction pattern obtained, allowed to solve the structure of the compound using EXPO2014 [1] package. The structure was later refined from high-resolution powder diffraction data collected at APS-11BM beamline, (GSAS/EXPGUI [2,3]) using bond distances and angle restraints to favor convergence of the refinement. The final model shows that divainillin crystallizes in an orthorhombic unit cell, Space Group *Pba2* with $a=12.264(1)$ Å, $b=13.954(1)$ Å and $c=3.9436(5)$ Å with $R_p=6.49\%$, $R_{wp}=7.97$, $\chi^2=1.586$ and $R(F^2)=9.93\%$. Packing of the molecules in a polar group is directed by π -stacking of slightly twisted divainillin molecules along c that connect through strong C=O...H-O hydrogen bonds formed by the aldehyde oxygen and alcohol hydrogen of neighbouring molecules. Six divainillin molecules form rings that are interlaced with two other equivalent rings in a complex topology that is thought to stabilize the solid and make it resistant to dissolution after crystal growth during synthesis. The soluble part of divainillin was used to grow single crystals that could not be achieved in sufficient size for a structure determination by single crystal XRD but were sufficient to confirm the unit cell obtained from the powder, therefore validate the structure determined using the powder. In this work we will show the results of structure determination of the three mentioned molecules and compare the three structures and packing emphasizing on the importance of approaching structural chemistry problems through a variety of techniques.

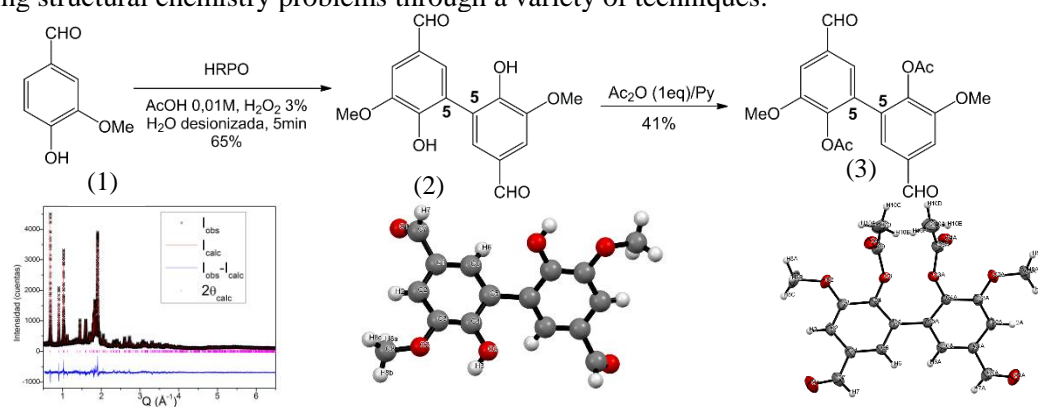


Figure 1. Formation, Rietveld fit and molecular structures of divainillin and its diacetate.

[1] A. Altomare et al., *J. Appl. Cryst.* (2013). 46, 1231-1235. [2] A.C. Larson and R.B. Von Dreele, "General Structure Analysis System (GSAS)", Los Alamos National Laboratory Report LAUR 86-748 (2000). [3] B. H. Toby, 'EXPGUI', a graphical user interface for GSAS, *J. Appl. Cryst.* 34, 210-213 (2001).

Agradecimientos: PEDECIBA-Química, ANII, Prof. F. Rabuffetti, APS-11BM beamline.

**A 100 años de la Ecuación de Dispersión de Debye.
Una breve revisión desde el mundo actual de los nanomateriales**

J. M. Delgado

*Laboratorio de Cristalografía-LNDRX, Departamento de Química, Facultad de Ciencias,
Universidad de Los Andes, Mérida 5101, Venezuela.*

Hace 100 años Peter J.W. Debye, uno de los más eminentes científicos del siglo XX, derivó una ecuación que permite calcular la dispersión generada por un conjunto de átomos de cualquier material [1], en función de las distancias interatómicas de dicho conjunto, cuando se le hace incidir un haz de radiación con una longitud de onda del orden del espaciamiento interatómico presente.

Es bien conocido en el campo de la Cristalografía que cuando el mencionado conjunto de átomos está dispuesto ordenadamente, de una manera regular y periódica, se puede definir una celda unidad que se repite traslacionalmente, cuya forma, tamaño y contenido define la estructura cristalina 3D del material. En tales situaciones, la dispersión registrada ("patrón de difracción"), que exhibe máximos discretos sobre un fondo relativamente insignificante, se analiza por metodologías desarrolladas sobre fundamentaciones teóricas bien conocidas. Por otra parte, cuando la disposición atómica tiene un orden de corto alcance, como en los materiales amorfos y en los materiales nanocristalinos, se debe modelar todo el patrón de difracción registrado considerando simultáneamente los máximos observados (si existiesen) y la llamada dispersión difusa. El modelado se realiza sobre la base de la distribución de las distancias interatómicas, sin que medie necesariamente en ello ningún elemento de orden, simetría o periodicidad. A pesar de las enormes dificultades de cálculo, desde los trabajos pioneros de Warren [2], se ha utilizado la transformada de Fourier del patrón registrado para precisar, usando la ecuación de Debye, las separaciones interatómicas en la estructura local en los materiales amorfos cuya representación es la denominada función de distribución de pares.

El creciente interés en el estudio de los nanomateriales y el cada vez mayor poder computacional, con mejores algoritmos, disponible a los científicos del estado sólido han hecho posible la caracterización de agregados atómicos "con orden a corto alcance" de cierto tamaño, revitalizando a la Ecuación de Dispersión de Debye [3]. En los últimos años, se han implementado programas de computación que permiten realizar tales caracterizaciones [4].

En esta contribución se presentará una breve revisión histórica-conceptual de la Ecuación de Dispersión de Debye y su utilización en la caracterización estructural de nanomateriales.

[1] Debye, P. *Ann. der Phys.*, **351** (6) 809–823 (1915)

[2] Warren, B.E. *Phys. Rev.*, **45**, 657-661 (1934).

[3] Beyerlein, K.R. *Powder Diff.* **28**, S2-S10 (2013).

[4] Cervellino, A., Giannini, C., Guagliardi, A. *J. Appl. Cryst.*, **43**, 1543-1547 (2010).

Agradecimiento: Este trabajo ha sido posible gracias al proyecto LAB-97000821 del FONACIT (Laboratorio Nacional de Difracción de Rayos-X).

Crystal structure and dynamic forces in hydroxyapatiteY. A. Moreno-Vargas^a, C. Thions^b, E. Orozco^c, I.A. Belío-Reyes^d, L. Bucio^c

^a*Programa de Doctorado en Nanociencias y Nanotecnología; Departamento de Biología Celular, Centro de Investigación y de Estudios Avanzados del Instituto Politécnico Nacional, 07360 México, D.F., México.*

^b*Departamento de Física Teórica, Instituto de Física, Universidad Nacional Autónoma de México, 04510 México, D.F., México.*

^c*Laboratorio de Cristalofísica y Materiales Naturales, Instituto de Física, Universidad Nacional Autónoma de México, 04510 México, D.F., México.*

^d*Facultad de Odontología, Universidad Autónoma de Sinaloa. Blvd. de las Américas y Universitarios, 80010 Culiacán, Sinaloa, Mexico.*

Stability and possible phase transformations for hydroxyapatite (HAp) under dynamic pressures produced by shock waves transmitted during the impact of a projectile was studied. For the experiments, synthetic hydroxyapatite was impacted by a projectile at speed of 564 m/s producing an estimated peak pressure of 6.6 GPa at the sample-holder. The original and recovered samples were characterized by X-ray diffraction (XRD) and scanning electron microscopy (SEM). A decrease in the sample lattice parameters after impact were observed by XRD analysis, indicating a slightly increase on the HAp crystal density. No phase transformations were detected. The HAp structure presents high stability under the dynamic pressures used in our experiment, which are higher than those reported for bite forces in humans and in some recent and ancient animals. It has been reported that polycrystalline HAp is stable at static pressures up to 11–13 GPa at temperature of 1300–1800 K. Above this conditions, the decomposition of apatite to tricalcium phosphate is observed [1]. The results were interpreted on the light of the magnitudes of the bite forces reported in humans and in some recent and ancient animals as well.

[1] J.K. Murayama, S. Makai, M. Kato and M. Kumazawa. *Phys. Earth Planet Inter.* **44**, 293 (1986).

Acknowledgments: Projects CONACYT CB-2011/167624 and DGAPA-PAPIIT IN105810. Y. A. Moreno-Vargas acknowledges the fellowship of Consejo Nacional de Ciencia y Tecnología (CONACYT).

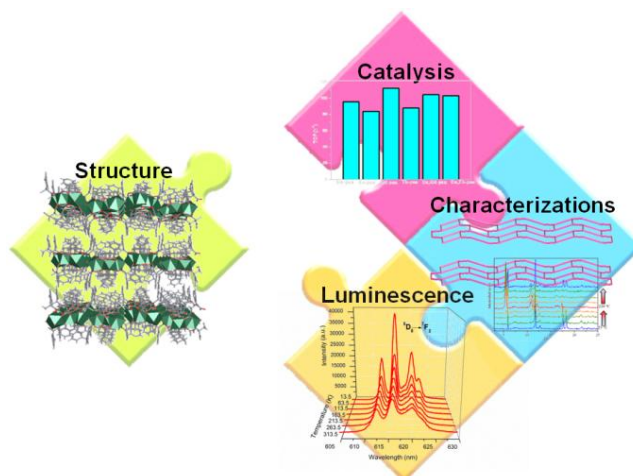
FOCUSING ON THE STRUCTURE-PROPERTY RELATIONSHIPS IN LANTHANIDE-ORGANIC FRAMEWORKS

G.E.Gómez, M.C.Bernini, E.V.Brusau, G.E.Narda

Area de Química General e Inorgánica "Dr. G. F. Puelles", Facultad de Química, Bioquímica y Farmacia, Chacabuco y Pedernera, Universidad Nacional de San Luis. Instituto de Investigaciones en Tecnología Química (INTEQUI-CONICET). 5700, San Luis, Argentina. gnarda@unsl.edu.ar.

Ln-MOFs (Lanthanide Metal – Organic Frameworks) offer a unique platform and methodology for the development of materials with potential applications in several fields and particularly, their luminescent [1] and catalytic [2] properties have received increasing attention. Selecting the appropriate building blocks and experimental conditions is possible to obtain architectures with diverse dimensionalities accompanied with specific and attracting properties [3].

Two sets of 3D compounds based on 2,3-dimethylsuccinate anion and lanthanides with formula $[\text{Ln}_2(\text{C}_6\text{H}_8\text{O}_4)_3(\text{H}_2\text{O})_2]$ (with Ln= Pr, Nd, Sm, Eu) and $[\text{Ln}_2(\text{C}_6\text{H}_8\text{O}_4)_3]$ (with Ln= Tb, Dy, Ho, Er and Yb) [4a] were synthesized and fully characterized. Moreover, to explore the influence of the substituent of the succinate ligand on the structure and properties, phenylsuccinic acid was employed as linker, giving rise to a new type of 2D Ln-MOFs with formula $[\text{Ln}_2(\text{C}_{10}\text{H}_8\text{O}_4)_3(\text{H}_2\text{O})]$ (with Ln= Pr, Nd, Sm, Gd, Eu, Tb, Eu/Gd, Eu/Tb) [4b]. Focusing on the optical properties of these materials, the emission peaks correspond to 4f-4f transitions in most cases. Here we present the strong relationship between the energy levels of the building blocks involved in the radiative and non-radiative processes along with their structural features found in these compounds. Besides, the series exhibit an excellent catalytic activity when it analyzed in the context of other alkyl-substituted succinates Ln-MOFs toward the widely studied reaction of cyanosilylation of benzaldehyde [5].



- [1] Allendorf, M. D., Bauer, C. A., Bhakta, R. K., Houk, R. J., *Chem. Soc. Rev.*, **38**, 1330-1352 (2009).
 [2] Czaja, A. U., Trukhanb, N., Müller, U., *Chem. Soc. Rev.*, **38**, 1284-1293 (2009).
 [3] Janiak, C., *Dalton Trans.*, 2781-2804 (2003).
 [4] (a) Gomez, G.E., Bernini, M.C., Brusau, E.V., Narda, G.E., Massad, W.A., Labrador, A., *Cryst. Growth Des.*, **13**, 5249-5260 (2013). (b) Gomez, G.E., Bernini, M.C., Brusau, E.V., Narda, G.E., Vega, D., Kaczmarek, A.M., Van Deun, R., Nazzarro, M., *Dalton Trans.*, **44**, 3417-3429 (2015).
 [5] D’Vries, R.F. , Snejko, N., Iglesias, M., Gutiérrez-Puebla, E., Monge, M.A., *Cryst. Growth Des.*, **14**, 2516-2521 (2014).

Acknowledgments: PICT 2012-1994, PROICO 2-1612 CyT-UNSL

Hetero and isovalent substitution on doped $A_yBa_{1-y}Zr_xTi_{1-x}O_3$ ferroelectric material

M.E. Saleta ^{a,b}, E. Granado ^a, M.I.B. Bernardi ^c, A. Mesquita ^c, R. C. da Costa ^d, P.S. Pizani ^d, W. Santa Rosa ^c, V.R. Mastelaro ^c.

^a Instituto de Física “Gleb Wataghin”, UNICAMP, Campinas, SP, Brazil,

^b Laboratorio Nacional de Luz Síncrotron, Campinas, SP, Brazil.

^c Instituto de Física de São Carlos, USP, São Carlos, SP, Brazil

^d Universidade Federal de São Carlos, São Carlos, SP, Brazil

One of the most studied lead-free ferroelectric ceramic materials is the BaTiO₃ (BTO). The ferroelectric nature, the structural and dielectric phase transition temperatures of BTO can be significantly modified via partial substitution of either Ba ions (A-site) or Ti ions (B-site). [1] It was observed that the simultaneous substitution on A and B-sites induces a relaxor state at lower amounts of B-site substitution depending if the A-site substitution is isovalent or heterovalent. On the case of heterovalent substitution on BTO system, it was argued that the development of the relaxor state is due to the introduced charge disorder, like in lead-containing relaxors. On the other hand, on the case of isovalent substitution like the substitution of Ti⁴⁺ by Zr⁴⁺ atoms, which have differ only slightly in their ionic radii, the exact structural mechanism involved in the formation of PNR in BTO-based relaxors have not yet been conclusively elucidated.

In this work we characterized **pure and A-doped BaZr_xTi_{1-x}O₃ (BZTO) ferroelectric**. We studied the sample by Raman spectroscopy (RS) and conventional X-ray diffraction at different temperatures. XRD experimental data were fitted by the Rietveld method. With the aim of studying the local order of the samples we analyzed our data using the **Atomic Pair Distribution Function (PDF)**. PDF method is an attractive alternative to the X-ray absorption and diffraction methods for studying the local and medium-range atomic arrangements in material science. [2] This technique can identify local atomic order much beyond the nearest neighbor atoms. By PDF we observed that although the Rietveld refinement reveals non-polar cubic structure at higher T, PDF indicates that the rhombohedral model shows a lower residual R_w than the fits with the cubic model. These results are consistent with the existence of PNR, even at temperatures where the long-range order, fitted by Rietveld method, reveals a cubic structure (non-polar). These results were confirmed by Raman spectroscopy where, for example, the mode 116 cm⁻¹ remains unchanged, even at temperatures well above the structural phase transition (cubic region). This mode been considered as an indicator of the presence of nanoclusters with a local structure of the rhombohedral type. [3]

[1] G. Singh, et al., *Appl. Phys. Lett.*, **102**, 162905 (2013).

[2] T. Egami & S.J.L. Billinge, “*Underneath the Bragg Peaks*”, 2nd Edition, Pergamon Materials Series 7 (2003).

[3] V. Buscaglia, et al., *J. Phys.: Condens. Matter*, **26** 065901 (2014).

Acknowledgments: The authors acknowledge the LNLS for the beamtime, and the staff of the XDS Beamline, especially Marcos Eleoterio, for providing assistance during the experiment. MES acknowledge FAPESP for their postdoctoral fellowships.

Nanotecnología en Costa Rica y su vinculación con la UCCr

José Roberto Vega Baudrit

Director, Laboratorio Nacional de Nanotecnología LANOTEC-CeNAT
San José, Costa Rica

Resumen

El año 2014 se da la creación de la UNION COSTARRICENSE DE CRISTALOGRAFIA – UCCr, y ese mismo año se da el establecimiento de los ESTATUTOS DE LA – UCCr. Este grupo es fuertemente impulsado por el Laboratorio Nacional de Nanotecnología LANOTEC del CeNAT-CONARE.

En 2014 se da la incorporación de COSTA RICA a LACA y a la IUCr y se imparte la I Escuela de Cristalografía en Costa Rica, organizada por la Universidad de Costa Rica. Asimismo, en agosto de 2014 se da un curso de Cristalografía, TEM y XRd entre la Universidad Nacional, la Red de NanoaUNA y el LANOTEC. .

La Universidad de Costa Rica y el LANOTEC, participaron en el evento internacional en Canadá denominado IUCr-2014 con el tema “Stability of progesterone: structural of form 2 and comparison of chemical and thermal stability between both polymorphs under solid-state stress conditions”. En la actualidad la UCCr está conformada por cerca de 30 miembros.

Apresentado por Andrea M. Araya-Sibaja



Complementary and other methods (COMs)

Better quality structures from routine X-Ray data collections using different electron density modelling approaches

W. Fabiola Sanjuan Szklarz^a, Magdalena Wońska^a, Sławomir Domagała^a, Paulina Dominiak^a,
Krzysztof Woźniak^a, Matthias Guttman^b, Jerzy Karpiuk^c

^a*Biological and Chemical Research Centre, University of Warsaw, Warsaw, Poland.*

^b*Rutherford Appleton Laboratory, ISIS Facility, Chilton Didcot, OX11 0QX Oxfordshire, UK.*

^c*Institute of Physics, Polish Academy of Science, Warsaw, Poland.*

Over 1.1 million structures have been solved and refined so far. Although everything seems to be already well known in the field of routine structural single crystal X-ray analysis, even commonly used approaches and models should be critically reevaluated.

The Independent Atom Model (IAM) of electron density introduced a century ago is still the most common model of electron density used in structural analysis. However, within the past century there is an overwhelming progress in design and production of X-ray hardware which is made for needs of both small laboratories and large scale facilities. This progress in sophisticated X-ray hardware should also accelerate progress in the quality and complexity of models of electron density used to interpret experimental results. In my presentation, I will discuss the main ideas of experimental charge density studies within the Hansen-Coppens Multipolar Model (MM) [1], Hirshfeld Atom Refinement (HAR) [2] and Transferable Aspherical Atom Model (TAAM) [3]. I will present a detailed comparison of structural, thermal and electronic parameters obtained for the same diffraction data sets when different models of electron density (IAM, TAAM, HAR, MM) are refined against collected intensities of reflections to different resolutions. Accuracy and precision of structural data obtained from routine and charge density studies going beyond IAM will be discussed and compared to structural data obtained from neutron diffraction data. Some practical suggestions will be presented how to estimate and improve the quality of single crystal X-ray diffraction structural results. In the last part and as an example of the capabilities of the high resolution charge density studies, I will present the results of the Multipolar Model refinement against X-Ray data for malachite green lactone (MGL) and the calculated quantitative electron density properties using the Bader's Quantum Theory of Atoms in Molecules (QTAIM), such as critical points parameters (ρ_{CP} , $\Delta\rho_{CP}$, bond paths), atomic basins or integrated electron density parameters (integrated charges, atomic multipoles and volumes, etc) for the best model of the electron density distribution obtained.

[1] Hansen, N. K. & Coppens, P. *Acta Crystallogr. Sect. A Cryst. Physics, Diffraction, Theor. Gen. Crystallogr.* 34, 909–921. (1978)

[2] Jayatilaka, D. & Dittrich, B. *Acta Cryst. A* 64, 383–393. (2008)

[3] Pichon-Pesme, V., Lecomte, C., & Lachekar, H. *J. Phys. Chem.* 99, 6242–6250. (1995).

Acknowledgments: Polish NCN Council MAESTRO grant decision number DEC2012/04/A/ST5/00609

Designing, mounting and testing a conical slit for diffraction contrast X-ray imagingMaycon Fioreze^a, Cesar Cusatis^b, Jeffrey W. Keister^c, Marcelo G. Hönnicke^a^a*Universidade Federal da Integração Latino Americana, 85867-970 Foz do Iguacu-PR, Brazil*^b*Universidade Federal do Paraná, 81531-980 Curitiba-PR, Brazil*^c*Brookhaven National Laboratory, 11973 Upton-NY, USA*

The major part of breast cancer can be correlated to clusters of microcalcifications which has as basic components calcium oxalate and or hydroxyapatite [1]. Then, detect microcalcifications in earlier stages is an important issue. The commercial mammography equipment offer a spatial resolution ranging from 50 μm to 100 μm and the images are taken just by attenuation projection (radiography). Since calcium oxalate and hydroxyapatite can be found in human body in both, crystalline and non-crystalline forms, we can try to combine the radiography with other contrast imaging techniques such as diffraction contrast imaging [2]. In this technique the microcalcification can be detected simultaneously, by diffraction (by scanning the sample until find a diffraction peak) and by the attenuation projection. In this way, in the present work, we designed and tested conical slits [3] in order to implement a diffraction contrast imaging technique with the aim to detect microcalcifications. The conical slits were designed to collect the most intense powder diffraction cones of hydroxyapatite and calcium oxalate at 17.4 keV ($\text{MoK}\alpha$). Also the conical slits apertures were calculated in order to maximize the diffracted intensity, however, with enough angular resolution to enable indexation of the powder components. For these first tests, hydroxyapatite and calcium oxalate powders were prepared in a plastic (polypropylene) container for transmission powder diffraction measurements. For each test, the conical slit was set just after the powder for measurement of the diffraction cone. The detection was done by a scintillation detector or diodes and by films. The alignment of the conical slits is straight forward. The next step is to build a human body equivalent sample (phantom) in order to certify the applicability of the proposed method.

[1] L. Frappart, M. Boudeulle, J. Boumendil, H. C. Lin, I. Martinon, C. Palayer, Y. Malletguy, D. Raudrant, A. Bremond, Y. Rochet, J. Feroldi, *Human Patology* 15, 880-889 (1984).

[2] G. Harding, J. Kosanetzky, U. Neitzel, *Med. Phys.* 14, 515-525 (1987).

[3] S. F. Nielsen, A. Wolf, H. F. Poulsen, M. Ohler, U. Lienert, R. A. Owen, *J. Synchr. Rad.* 7, 103-109 (2000).

Acknowledgments: This work was supported by Fluxo Continuo/Fundacao Araucaria (302/2013) and CNPq/UNIVERSAL (479404/2013-5). MGH and CC gratefully acknowledges CNPq/PQ (309109/2013-2 and 309614/2013-9) for their research fellow. MF acknowledges PIBIC/CNPq for his research fellow. JK was supported by the U.S. Department of Energy, Office of Science, Office of Basic Energy Sciences, under Contract No. DE-AC-02-98CH10886.

Nanopartículas de Ag y Cu en KCl doblemente impurificadoR. R. Mijangos^a, A. Perez-Rodriguez.^a, R. Perez-Salas^a, M. A. Velarde^b.^a*Departamento de Investigacion em Fisica, Universidad de Sonora, México.*^b*Posgrado del Centro de Investigacion en Materiales Avanzados, Chihuahua, México.*

Se describe el crecimiento por la técnica de Czochralski de monocristales de KCl impurificados con Ag y Cu en concentraciones del orden del 1 %. Utilizando difracción de polvos se constata la cristalinidad del halogenuro alcalino crecido. Se utilizan técnicas de caracterización óptica obteniendo los espectros de absorción óptica y fotoluminiscencia correspondientes. Estas se utilizan para detectar la formación de nanoestructuras de Ag o de Cu, dentro de la matriz de KCl doblemente impurificada. Anteriormente se ha realizado el estudio de KCl impurificado únicamente con Cu [1]

Se investiga la posibilidad de la mezcla de agregados de Ag-Cu. En este trabajo se reportan bandas de absorción y emisión entre otros resultados experimentales, los que nos permitirán conocer la posibilidad de obtener agregados de Ag-Cu.



Figure 1: Crisol de carbono ultrapuro con monocristal de KCl:Ag:Cu recién crecido

[1] A. Perez-Rodríguez, M. Flores, R. R. Mijangos, R. Perez-Salas en Rev. Mex. Fis. 52, 151-154 (2006).

Agradecimiento: Se agradece el apoyo del programa PIFI a través de la División de Ciencias Exactas y Naturales de la Universidad de Sonora.

Relevance of Geometrical Crystallography in the study of pharmaceutical substancesI.A. Belío-Reyes^a, B. A. Ramírez-Almaguer^b, L. Bucio^b^a *Facultad de Odontología, Universidad Autónoma de Sinaloa. Blvd. de las Américas y Universitarios, 80010 Culiacán, Sinaloa, Mexico.*^b *Laboratorio de Cristalofísica y Materiales Naturales, Instituto de Física, Universidad Nacional Autónoma de México, 04510 México, D.F., México.*

At standard conditions of pressure and temperature, some given Active Pharmaceutical Ingredient or excipients are thermodynamically stable and appear as specific polymorph. In such case, the understanding of the basic interactions between the active pharmaceutical ingredient (API) with excipients, is a critical step to know the effect that a given involved crystal morphology could affect, and possibly control, the release of active compounds by influencing the corresponding desorption and/or dissolution rates [1]. With the valuable information of crystal morphology, the API-excipient interactions can be modeled selecting the observed specific planes of the family {hkl} exhibited by the API or some excipient crystals, and the corresponding interacting molecule closer to the interacting plane. The organic molecules are then placed in variable positions with respect to the crystalline generated plane. The geometry of the latter is keeping frozen. Full geometry optimization is then performed using some given procedure (i.e. MM+ force field, Polak-Ribiere conjugate gradient algorithm). Molecular dynamics relaxing of the optimized structures is employed to look for different possible local minima (constant simulation temperature of 300 K). We have performed this methodology for the study of interactions between calcite crystals and alpha chitin in brown shrimp [2]. In order to apply this kind of analysis for studying the interactions between APIs and excipients relevant in Mexico, we have started the research analyzing morphologies of some APIs and excipients available in the Mexican market applying geometrical crystallography. To do this, the generated morphologies using the KrystalShaper software [3] were compared with the images obtained by scanning electron microscopy (SEM). These morphologies will be discussed in the presentation.

[1] M. Ukrainczyk, M. Gredicak, I. Jeric and D. Kralj. *Cryst. Growth Des.* **14**, 4335-4346 (2014).

[2] A. Heredia, M. Aguilar-Franco, C. Magaña, C. Flores, C. Piña, R. Velázquez, T.E. Schäffer, L. Bucio y V.A. Basiuk. Structure and interactions of calcite spherulites with alpha-chitin in the brown shrimp (*Penaeus aztecus*) shell. *Mat. Sci. and Eng. C* **27**, 8-13 (2007).

[3] KrystalShaper. <http://www.jcrystal.com>

Acknowledgments: Projects CONACYT CB-2011/167624.

Computer simulation tools for improving X-ray analysis of materials

S. L. Morelhão

Instituto de Física, Universidade de São Paulo, São Paulo, Brazil.

Coherent scattering of X-rays by electrons is one of the most useful physical process by which we gain knowledge on atomic structure of the materials, as it is widely acknowledged [1]. With exception of a few cases, such as lattice parameters of crystalline structures that are directly extracted from intensity data, detailed structural information can only be achieved by simulation of the scattering process. It is a fact to all kinds of materials, ranging from low to high ordered systems. Lower is the order of a system, more complex are the methods of creating accurate model structures, and higher are the required X-ray power and energy to probe its atomic structure. Powerful sources of broad spectrum covering hard X-ray regions are available. Computational limitations impose simplified models in simulating the scattering by complex systems, leading to low resolution of the systems. Although, data processing have been improved tremendously in the last decades, simulated X-ray scattering by extended complex systems can be exactly simulated in a few cases only [2]. In this work, we present the frontiers in computer simulation for studying several systems of increasing complexity: single molecules by free electron lasers, disperse systems of biological molecules, polymer chains, liquids, amorphous clusters, and macromolecular crystals. Phase measurement for improving resolution of protein crystals is a new frontier in X-ray crystallography which also requires accurate model structures [3].

- [1] Crystallography at 100. *Science* **343**, special issue, 1091-1116 (2014).
- [2] S. L. Morelhão. "Computer Simulation Tools for X-ray Analysis: Scattering and Diffraction Methods". Springer (2015). ISBN: 978-3-319-19553-7
- [3] S. L. Morelhão, Z. G. Amirkhanyan, C. M. R. Remédios. Absolute refinement of crystal structures by X-ray phase measurements. *Acta Cryst. A* **71**, 291-296 (2015). doi: 10.1107/S2053273315002508

Acknowledgments: FAPESP, CNPq, and Leybold



Education in crystallography (EdCr)

CONCURSO INTERESCOLAR DE CRECIMIENTO DE CRISTALES

Una experiencia de divulgación

G. Arancibia^a, R. Jara^a, M. Fuentealba^a, A. Galdamez^b, J. Camacho^c.

^a Instituto de Química, Facultad de Ciencias, Pontificia Universidad Católica de Valparaíso. Valparaíso, Chile.

^b Laboratorio de Química de Sólidos. Facultad de Ciencias. Universidad de Chile. Santiago, Chile

^c Departamento de Estudios Pedagógicos. Facultad de Filosofía y Humanidades. Universidad de Chile. Santiago, Chile.

E-mail: gonzalo.arancibia.rojas@gmail.com; mauricio.fuentealba@ucv.cl

Resumen

Considerando la importancia que ha tenido el estudio de los cristales en nuestra vida cotidiana, en el desarrollo de la nanotecnología y la biotecnología y, el campo fructífero de conocimiento científico que ha sido para comprender la estructura, organización y simetría de la materia, la Asamblea General de las Naciones Unidas proclamó el 2014 como el Año Internacional de la Cristalografía¹. En este marco de celebración y con el patrocinio de la Asociación Chilena de Cristalografía (AChCr) se realizó el “Concurso Interescolar de Crecimiento de Cristales”, en el cual participaron estudiantes de educación media de 14 colegios y liceos de Santiago y Valparaíso.



Figura 1. Banner del concurso.

Las modalidades del concurso fueron: crecimiento de monocristal o de conglomerado. En conjunto con el desarrollo de este propósito, se realizaron diferentes actividades en los liceos y en la universidad, como exposiciones de cristales, exhibiciones de películas, mini-cursos de cristalografía y una feria científica para mostrar sus resultados. Dentro de los resultados, se aprecia que fue posible integrar conocimientos químicos teóricos y prácticos; trabajar con los profesores diseñando diferentes estrategias para estudiar los cristales en el aula de química y fortalecer lazos entre la universidad y los establecimientos participantes.

Para este año 2015, se realizará la segunda versión de este concurso, en donde esperamos volver a tener una gratificante experiencia y además poder sumar más establecimientos que gusten de incentivar a sus alumnos, con esta práctica de indagación experimental.

[1] Naciones Unidas (2012). Resolución aprobada por la Asamblea General el 3 de Julio de 2012. 66/284. Año Internacional de la Cristalografía. Recuperado 10 Julio de 2015 desde: <http://bit.ly/14mKvZF>

Agradecimientos: Los autores agradecen al proyecto FONDECYT N° 1130640. Además, se agradece a la Dirección General de Vinculación con el Medio de la Pontificia Universidad Católica de Valparaíso por el financiamiento otorgado.



Figura 2. Feria Científica realizada en Instituto de Química PUCV, Valparaíso.



Materials (MATS)

Structural and magnetic investigation of Sr₂CrReO₆M. T. D. Orlando^a, J. B. Depianti^a, A. S. Cavichini^a, and J. L. Passamai Jr^a.^a*Universidade Federal do Espírito Santo, Vitória, Brasil.*

Sr₂CrReO₆ and Sr₂CrOsO₆ are compounds that have this type of structure and exhibit the largest values of the Curie temperature (TC) with about 610 K [1] and 720 K [2], respectively. These compounds are stable and they have been used to made high-quality thin films and they can be grown by a widely synthesis technics [3], opening the possibility of creating Spin Electronic devices (e.g. electrodes for magnetic tunnel junctions) based on this material [4].

We have been studied the properties magnetic and structural properties of Sr₂CrReO₆ double perovskite since 2013. This compound was prepared by a solid-vapor reaction in sealed quartz tube. The compound produced shows a single structural phase (cubic cell with *Fm3m* space group). Crystal size, lattice parameters and disorder were evaluated from Rietveld refinement of X-ray diffraction pattern. Measurements of magnetic moment indicated 620 K as a Curie temperature.

References

- [1] J. Longo, R. Ward, *J. Am. Chem. Soc.* **83**, 8, 2816 (1961).
- [2] Kato, H., et al. *Applied Physics Letters* **81**,328 (2002).
- [3] Krockenberger, Y., et al. *Physical Review B* **75**, 020404 (2007).
- [4] Chakraverty, S., A. Ohtomo, and M. Kawasaki. *Applied Physics Letters* **97**, 243107 (2010).

Acknowledgments: FAPES; CAPES, CNPq and LNLS

Crystal engineering approach in the study of irbesartan crystal forms

A. M. Araya-Sibaja^{a,b}, P. Santamaría-Benavides^{a,b}, J. R. Vega-Baudrit^b, T. Guillén Girón^c, M. Navarro Hoyos^a and S. L. Cuffini^d

^a Escuela de Química, Universidad de Costa Rica, Costa Rica

^b Laboratorio Nacional de Nanotecnología LANOTEC-CeNAT-CONARE, Costa Rica

^c Área Académica de Doctorado en Ingeniería, Instituto Tecnológico de Costa Rica, Costa Rica

^d Instituto de Ciência e Técnica, Universidade Federal de São Paulo, Brasil.

Irbesartan is a polymorphic drug that exhibits a particular case of desmotropy in which its individual tautomers can be isolated in the solid state. Previous studies reported two crystal forms corresponding with its tautomers, known as A and B [1]. There are some patents reported irbesartan form C, pseudopolymorphs and other crystalline salts of this drug. However, in the Cambridge Structural Data Base only crystallographic data NOZWII: form B is reported [1]. In addition, physicochemical characterization, thermodynamic stability between them and intrinsic dissolution rate are scarce. Hence, the choice of an irbesartan crystal form in the development and formulation of pharmaceutical products is quite ambiguous.

In order to obtain, identify and characterize irbesartan crystal forms, several crystallization methods were applied in this work. Antisolvent crystallization in an ethanol/water system allowed obtaining Form B (figure 1). Here, it was developed a novel method which is easier than the previously reported [1].

An unidentified crystal form was obtained from slurry in an acidic solution and maintained for 8 h without stirring. Then, the solid was washed with distilled water and recrystallized from acetone at ambient conditions. The diffractogram obtained did not coincide with the reported data.

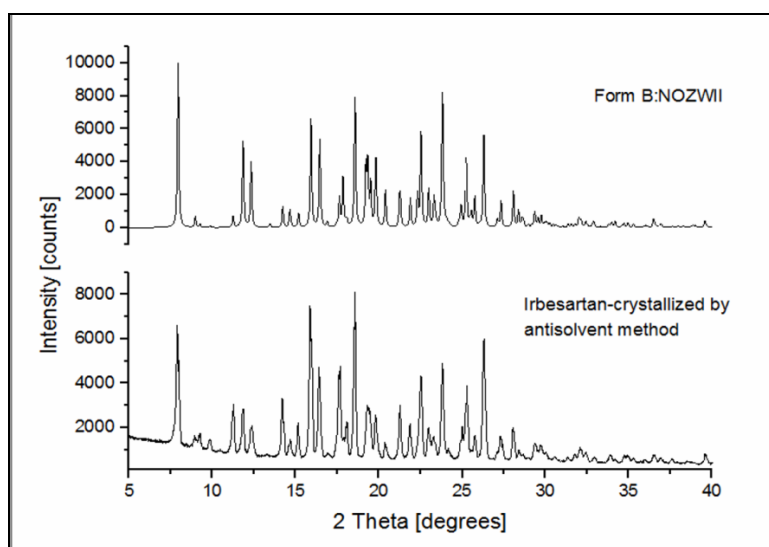


Figure 1: X-ray powder diffractograms of irbesartan crystallized by using antisolvent method

This study aimed to characterize this novel crystal by using X-ray diffraction techniques for powder and single crystals, infrared and Raman spectroscopies, microscopy and thermal analysis.

Reference

- [1] Z. Böcskei, K. Simon, R. Rao, A. Caron, C. A. Rodger, and M. Bauer, "Irbesartan Crystal Form B," *Acta Crystallogr. Sect. C Cryst. Struct. Commun.*, vol. 54, no. 6, pp. 808–810, Jun. 1998.

Acknowledgments: Fondo Especial para la Educación Superior, Consejo Nacional de Rectores (FEES-CONARE), Costa Rica for financial support.

Structural studies in single-crystal manganites of $Yb_{(1-x)}Tb_xMnO_3$ M. Bolívar Guarín^a, N.L. Speziali^a, M. Andreetta^b.^a Federal University of Minas Gerais, Department of Physics, Belo Horizonte, Brazil^b Institute Federal University of São Carlos, Department of Materials Engineer, São Carlos, Brazil

Rare-earth manganites, $RMnO_3$, have been object of intense theoretical and experimental research; mainly focused on the exotic properties observed in these materials. Ferroelectricity, ferromagnetism, superconductivity and multiferroicity are some of the properties observed in $RMnO_3$, been the multiferroicity the most important phenomena of the parent manganites $YbMnO_3$ and $TbMnO_3$ [1]. The focus of the present work is to look for correlations between structural characteristics and the physical properties of some type of ferroic materials. Single crystals of $Yb_{1-x}Tb_xMnO_3$ ($x = 0, 0.25, 0.50, 0.75$ and 1) were produced by LHPG (Laser Heated Pedestal Growth) [2]. In the present work structural studies at room temperature will be reported. Samples with $x = 0$ and 1 crystallizes in the $P6_3cm$ and $Pnma$ space groups, respectively. In the case of mixed compounds attention was paid to the study of the phase coexistence as well as to the site occupancy shared between rare-earth Tb and Yb [3].

[1] T. Kimura, T. Goto, H. Shintani, *et al.*, *Nature*, **426**, 55-58 (2003).

[2] M.R.B. Andreetta, A.C. Hernandez, S.L. Cuffini, *et al.*, *J. Crystal Growth*, **200**, 621-624 (1999).

[3] M.E. Bolívar, A de M. Moreira, N.L. Speziali, *J. Appl. Cryst.* **46**, 644-648 (2013).

Acknowledgments: FAPEMIG, CNPq.

Structural characterization of a new Zn-Fluconazole complex

Analio J. Dugarte⁽¹⁾, J.A. Henao⁽²⁾, Chun-Hsing Chen⁽³⁾, G. Díaz de Delgado⁽¹⁾, J.M. Delgado⁽¹⁾

⁽¹⁾ *Laboratorio de Cristalografía-LNDRX, Facultad de Ciencias, Universidad de Los Andes, Mérida, Venezuela.*

⁽²⁾ *Laboratorio de Rayos X, Universidad Industrial de Santander, Bucaramanga, Colombia.*

⁽³⁾ *Indiana University Molecular Structure Center, Bloomington, IN, USA.*

As part of the work being carried out in our laboratory to explore the possible formation of polymorphs of some highly used drugs and some of their metal complexes, we have synthesized a new zinc complex of fluconazole. Fluconazole is a well-known antifungal belonging to the azole family of compounds. It is administered topically, orally, and intravenously to treat common infections such as *tinea pedis* (athlete's foot) and *tinea cruris* (jock itch). Reaction of fluconazole and ZnSO₄·7H₂O in a 1:1 molar ratio in water produced over a period of three months crystalline colorless material. The powder diffraction pattern was recorded on a Bruker D8 Advance diffractometer working in the Bragg-Brentano geometry, using CuK α radiation, operating at 40 kV and 30 mA. The data were collected in steps of 0.01526° (2 θ), from 5° to 70° at 1.5 s step⁻¹. The diffractometer is equipped with primary and secondary Soller slits of 2.5°, a divergence slit of 0.2 mm, Ni filter of 0.02 mm, and a LynxEye detector. After the peak positions were established with FullProf, the indexing of the pattern was successfully performed with Dicvol06 in a triclinic unit cell. The analysis of the 89 diffraction maxima registered, carried out with NBS*AIDS83, led to the following parameters: $a=10.955(2)$, $b=13.693(1)$, $c=17.113(2)$ Å, $\alpha=104.31(1)^\circ$, $\beta=90.17(1)^\circ$, $\gamma=90.28(2)^\circ$ with $V=2487.5(4)$ Å³. The figure of merits were $M_{20}=34.4$ and $F_{30}=90.3$ (0.0050; 67). The single crystal structure determination confirmed that the unit cell was correct. A search in the Cambridge Structural Database (CSD) indicated that this was a new compound. The intensity data were collected at the APS (Argonne National Laboratory) line 15-ID assigned to the ChemMatCARS as part of the SCrAPS program, through the Indiana University Molecular Structure Center (IUMSC). The frames were collected using ϕ -scans in a Huber 4-circle goniometer equipped with a SMART 6000 detector ($\lambda=0.41328$ Å), an undulator beam, and a diamond [111] crystal and two mirrors (to exclude higher harmonics), in the beam path. Exposure time was 1 s per frame. SHELXS and SHELXL were used to determine and refine the structure. The refinement converged to: $R_I=0.1094$, $wR2=0.3101$ and $S=0.99$. The Zn atoms are octahedrally coordinated to 5 fluconazole and one water molecule. The structure is stabilized by several hydrogen bonds, and π - π and C-F $\cdots\pi$ interactions. In this contribution, the most relevant features of the structure of new Zn-fluconazole complex prepared will be discussed in the context of the other Zn-fluconazole derivatives reported.

Acknowledgments: This work has been supported by a grant (LAB-97000821) from FONACIT-Venezuela for Laboratorio de Cristalografía-LNDRX and a grant for Laboratorio de Difracción de Rayos X, PTG, Universidad Industrial de Santander, Bucaramanga, Colombia. The authors thank M.Sc. José Luis Pinto for technical assistance with the powder diffractometer.

Structure Characterization of Nevirapine Co-crystals prepared using slurry ball milling and temperature annealing process

R. N. Costa^a, M. P. de Oliveira^a, S. Siedler^b, C. E. M. de Campos^c, S. G. Cardoso^b, H. V. A. Rocha^d, S. L. Cuffini^a

^aInstituto de Ciência e Tecnologia, Universidade Federal de São Paulo, São José dos Campos, Brasil.

^bLaboratório de Controle de Fármacos, Universidade Federal de Santa Catarina, Florianópolis, Brasil.

^cDepartamento de Física, Universidade Federal de Santa Catarina, Florianópolis, Brasil.

^dLaboratório de Sistemas Farmacêuticos Avançados, Farmanguinhos/Fiocruz, Rio de Janeiro, Brasil.

Nevirapine (11-Cyclo-propyl-5,11-dihydro-4-methyl-6H-dipyrido[3,2-b:2',3'-e][1,4]diazepin-6-one) (NVP) is an antiretroviral drug, belonging to the class of non-nucleoside reverse transcriptase inhibitors, used in treatment of HIV-1 infection. According to the Biopharmaceutics Classification System (BCS) [1], NVP is a class II drug, having high permeability and poor solubility. The second characteristic leads to formulation problems and low bioavailability. To improve the drug dissolution profile and, consequently, increase its bioavailability, different preparation methods to obtain crystalline structure modifications have been studied [2,3]. Among different possible modifications, there is a special interest in co-crystal formation. Co-crystals are multicomponent solids that have in its structure different drug molecules or molecules of a drug and a non-volatile substance [4]. NVP

(figure 1) has a conformational rigid amide group in their structure. It allows the formation of hydrogen bonds with carboxylic and amide groups. Therefore, it is possible to form co-crystals using soluble co-formers that have these groups in their molecular structure [2]. The co-formers used in the present work are saccharin (SAC), salicylic acid (AS), caffeine (CAF) and theophylline (TEO) (figure 2). Two preparation methods have been tested: 1) slurry ball milling and 2) temperature annealing.

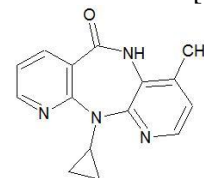


Figure 1: Structural formula of Nevirapine.

The first consists in a physical mixture of NVP and co-former in different stoichiometric ratios and in the presence of a solvent (methanol or chloroform). The thermal annealing consisted in applying a temperature controlled treatment to a physical mixture of NVP and co-former. The materials were characterized by Powder X-Ray Diffraction (PXRD), using conventional and synchrotron sources, and thermal analysis – Differential Scanning Calorimetry (DSC) and Thermogravimetry (TG). Diffraction patterns were collected in different temperatures to evaluate changes in crystalline structure as function of temperature. DSC and TG results show thermodynamic events and indicate the possible formation of co-crystals. Co-crystals, NVP-SAC and NVP-AS, were obtained in a pure form and in a higher proportion than by other chemical and/or grinding methods.

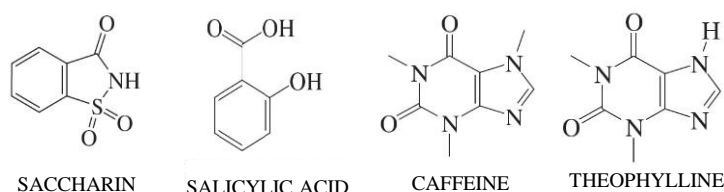


Figure 2: Structural formula of co-formers

[1] Lindenberg, M., Kopp, S., Dressman, J. B. *Eur. J. Pharm. Biopharm.*, **58**, 2, 265-278 (2004).

[2] Caira, M. R., et al. *CrystEngComm*, **14**, 7, 2541–2551 (2012).

[3] Pereira, B. G., et al. *Cryst. Growth&Des.*, **7**, 10, 2016–2023 (2007).

[4] Cuffini, S. L., Pitaluga Jr. A., Tombari, D., in: *Ciências Farmacêuticas Biofarmacotécnica*, Guanabara, Rio de Janeiro, 21–31 (2009).

Acknowledgments: UNIFESP, CAPES, FIOCRUZ and UFSC.

Hollow Crystals pharmaceutical drugs: Berg Effect

R. Guimarães^a, R. N. Costa^a, S. Siedler^b, A. S. Paulino^b, Simone G. Cardoso^b, A. M. E. Santo^a, C. Fandaruff^b, H. V. A. Rocha^c, S. L. Cuffini^a.

^a Instituto de Ciência e Tecnologia, Universidade Federal de São Paulo (UNIFESP), São José do Campos, Brasil.

^b Laboratório de Controle de Qualidade, Universidade Federal de Santa Catarina, Florianópolis, Santa Catarina, Brasil; Farmanguinhos (FIOCRUZ), Rio de Janeiro, Brasil.

A critical problem associated with poorly soluble drugs is their low and variable bioavailability derived from their slow dissolution and erratic absorption [1]. Crystallization is an important process employed to produce a wide variety of materials in the pharmaceutical industry. The control of the crystal size and shape and polymorphism is crucial as these factors can influence the physical and chemical properties of the solid including the dissolution rate and bioavailability [1]. Although some cases of hollow crystals have been reported in the literature [2] with increase of dissolution [1,3], there is no study about the crystal growth mechanism which explains this morphology.

In crystal growth from solution, one of the most important equilibrium consideration is the solute behavior in the solution. The solute concentration close to the growing interface is different for solid and liquid phases, giving rise to a solute gradient at the interface. Usually, there will be a buildup of the components that tend to be rejected from the solid close to the growing crystal interface. The concentration at the growing interface is greater than the concentration in the bulk of the liquid, which is greater than the concentration in the solid. This solute gradient at the interface provides the required condition to the boundary for Berger effect.

Hence the aim of this work is study the crystal growth mechanism of hollow crystals applying the Berg Effect in pharmaceutical drugs such as Deflazacort (DFZ), Nevirapine (anhydrate and hydrate) and Carbamazepine. Samples were characterized by XRPD and SEM. SEM images show hollow crystal morphology (Figure 1) and dissolution studies proved that hollow crystals exhibit better dissolution profile than the crystalline raw material (Figure 2).

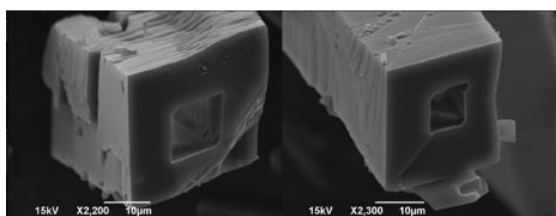


Figure 1: SEM of hollow crystals of DFZ.

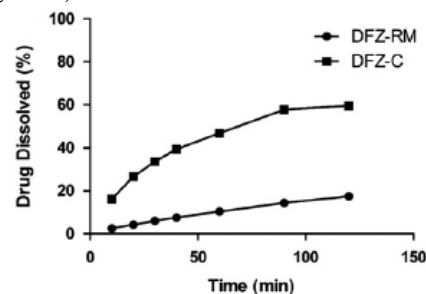


Figure 2: Dissolution profile of raw material (DFZ-RW) and hollow crystal (DFZ-C).

The dissolution performance and dissolution efficiency significantly increased using hollow crystals in comparison with the initial raw materials. These results demonstrated the relevance of the design and control the polymorphism and also the morphology of APIs during the crystallization process. The anti-solvent crystallization process with specific operational conditions is a promising strategy for solid APIs preparation in order to improve the dissolution properties and, as a consequence, the bioavailability of poorly soluble drugs. Therefore the importance of studying the crystal growth mechanism.

References:

- [1] Paulino, A. S., Cuffini, S.L., *et. al.*, *European Journal of Pharmaceutical Sciences*, **49**, 294-301 (2013).
- [2] Paulino, A. S., Cardoso, S. G., *et. al.*, *Jornal of Crystal Growth*, **366**, 76-81 (2013).
- [3] Martins, D., Coquerel, G., *et. al.*, *Crystal Growth & Design*, **11**, 3020-3026 (2011).

Acknowledgments: CNPq, FIOCRUZ and UNIFESP.

**Evaluation of the synthesis conditions for obtaining
nano-crystals of the MOFs series $[\text{Ln}_2\text{Cu}_3(\text{oda})_6(\text{H}_2\text{O})_6] \cdot x\text{H}_2\text{O}$.**

Guzmán Peinado ^{a,b}, Leopoldo Suescun ^a, Julia Torres ^b, Carlos Kremer ^b

^a*CRYSSMAT-LAB, DETEMA, Facultad de Química (UdelaR), Montevideo, Uruguay*

^b*Cátedra de Química Inorgánica, DEC, Facultad de Química (UdelaR), Montevideo, Uruguay*

In recent years, a number of metal-heteropolynuclear complexes constituting metal-organic frameworks (MOF) with interesting properties, which could lead to numerous applications, have been studied. This is a series of compounds of general formulae $[\text{Ln}_2\text{Cu}_3(\text{oda})_6(\text{H}_2\text{O})_6] \cdot x\text{H}_2\text{O}$ ($\text{Ln} = \text{Y}, \text{La}, \text{Ce}, \text{Pr}, \text{Nd}, \text{Sm}, \text{Eu}, \text{Gd}, \text{Tb}, \text{Dy}, \text{Ho}, \text{Er}, \text{Yb}$) [1-3]. The structural resolution of such compounds has shown an isostructural series of compounds varying the ion Ln (except for $\text{Ln} = \text{La}$), crystallizing all in the hexagonal system $P6/mcc$ space group. The most interesting feature about these structures is the formation of a three dimensional network containing hexagonal channels with diameter close to 10-11 Å, where H_2O crystallization molecules are stored (Figure 1). Replacing the lanthanide ion, the diameter of this hexagonal channel can be adjusted, which is very important for potential applications as catalysts or gas storage. Very recently, we have sought to synthesize nano-MOFs, meaning MOFs with nano-scaled particles. In this way, multiple structural properties of these materials could be used for further technological applications.

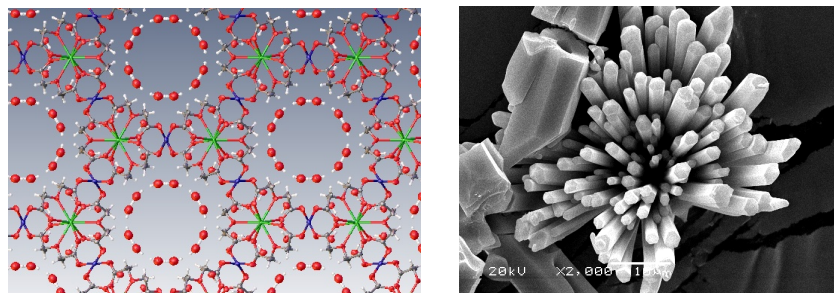


Figure 1: Extended structural packing with H_2O molecules in hexagonal channels (left) and screening electron microscopy images for hexagonal crystals of $[\text{Nd}_2\text{Cu}_3(\text{oda})_6]$ (right).

In this work, two compounds of this isostructural MOF series (with $\text{Ln} = \text{Nd}, \text{Eu}$) have been synthesized and completely characterized by several techniques (elemental analysis, Fourier transform infrared spectroscopy, X-ray powder and single crystal diffraction, thermo gravimetric analysis and screening electron microscopy), so as to evaluate which conditions for synthesis may decrease the size of the crystals obtained, if possible down to nano-crystals. Different synthesis factors were taken into account to assess trends that suggest focusing synthesis in a certain direction: reagent mass weighed (m_L), initial pH adjustment (pH_i), stirring time (t_s) and temperature (T). In all synthetic processes, single crystals were obtained as well as sub-microscaled powder for $[\text{Nd}_2\text{Cu}_3(\text{oda})_6(\text{H}_2\text{O})_6] \cdot 11\text{H}_2\text{O}$ and $[\text{Eu}_2\text{Cu}_3(\text{oda})_6(\text{H}_2\text{O})_6] \cdot 12\text{H}_2\text{O}$. Furthermore, an ethanol-water mix was used as solvent for additional synthesis and it showed that other small molecules besides H_2O can probably be stored in the hexagonal channels of these solids. Thermal stability was determined, as well as luminescent and adsorption properties were studied preliminarily.

[1] Kremer, C., Torres, J., Domínguez, S., *J. Mol. Struct.*, **879**, pp. 130-149 (2008).

[2] Baggio, R., Garland, M.T., Moreno, Y., Peña, O., Perec, M., Spodine, E., *J. Chem. Soc. Dalton Trans.*, pp. 2061-2066 (2000).

[3] Rizzi, A., Calvo, R., Baggio, R., Garland, M.T., Peña, O., Perec, M., *Inorg. Chem.*, **41**, pp. 5609-5614 (2002).

Acknowledgments: CAPES/UdelaR; PEDECIBA; CSIC; ANIL.

Investigação comparativa entre as fases cerâmicas presentes nas partículas recicladas e virgens de alumina

A. D. Golanda, K. C. G. Candioto, C. Y. Shigue.

Escola de Engenharia de Lorena, Universidade de São Paulo, Lorena, Brasil.

As ferramentas abrasivas representam um importante segmento industrial de aplicação de materiais cerâmicos duros, que são ancorados mecanicamente por ligante orgânico (abrasivos resinoides) ou inorgânico (abrasivos vitrificados) [1,2]. As ferramentas abrasivas resinoides são constituídas por partículas abrasivas, principalmente alumina [3,4], ancoradas por um ligante orgânico, geralmente uma mistura de resinas fenólicas resol e novolaca.

A reciclagem de partículas abrasivas representa uma oportunidade de estudo científico com viés tecnológico, por meio do qual se promoverá o reaproveitamento econômico desse insumo industrial, com apoio técnico e logístico de uma empresa que atua neste ramo, visando a valorização desse insumo.

Este trabalho tem o objetivo de realizar uma investigação das fases presentes nas partículas recicladas de rebolos de alumina e comparação com as fases presentes nas partículas de alumina virgem (branca e marrom) visando determinar a influência do processo de reciclagem sobre as características estruturais de partículas de alumina. Os materiais estudados foram partículas cerâmicas de alumina recicladas a partir de ferramentas abrasivas resinóides (RR), vitrificadas (RV), sendo ambas incineradas ao fogo, e partículas de alumina oriundas de ferramentas abrasivas vitrificadas somente cominuídas mecanicamente (BR). Para comparação foram utilizadas partículas de alumina precipitada branca (BV) e alumina marrom eletrofundidas (MV), sendo que a primeira trata-se de alumina usada para fabricação de cerâmicas refratárias.

A Tabela 1 ilustra análise realizada por espectroscopia por energia dispersiva de raios X (EDS). Nela observa-se que a composição em óxidos presents nas diversas amostras estudadas apresentam variações estatisticamente significativas, indicando assim que o processo de reciclagem modifica não apenas a estrutura mas a própria composição por causa da contaminação por elementos presents no processo de reciclagem térmica.

Tabela 1: Composição percentual dos óxidos presentes nas amostras de partículas abrasivas.

Amostra	% massa									
	Al ₂ O ₃	SiO ₂	Na ₂ O	K ₂ O	CaO	TiO ₂	FeO	MgO	SrO	SO ₃
ALO BV	100,00									
ALO MV 46	97,28					2,72				
ALO BR 60	65,47	29,90	2,95	0,86	0,81	-	-	-	-	-
ALO RR 60	18,12	12,61	0,71	1,82	3,21	0,61	3,40	0,37	-	2,12
ALO RV 60	39,62	31,04	1,51	1,37	1,16	1,20	0,72	-	5,55	-

Referências

- [1] Nussbaum, G., Rebolos e Abrasivos. Tecnologia Básica, Ícone Editora, São Paulo (1988).
- [2] Malkin, S., Guo, C. Grinding Technology: Theory and Application of Machining with Abrasives, Industrial Press Inc., New York (2008).
- [3] Ratterman, E., Cassidy, R. Abrasives. In: ASM International, Engineered Materials Handbook, vol. 4: Ceramics and Glasses, ASM International, Materials Park, Ohio (2000).
- [4] Gitzen, W. H., Alumina as a Ceramic Material, The American Ceramic Society, Westerville, Ohio (1970).

Agradecimentos: Os autores agradecem à Capes e à Fapesp pelo suporte financeiro.

Ordered mesoporous silica synthesized with a new triol copolymer

G. P. Perl, M.C.A. Fantini.

Departamento de Física Aplicada, Instituto de Física, Universidade de São Paulo, São Paulo, Brazil.

Ordered mesoporous silica (OMS), having mean pore diameter around 10 nm, demonstrated unusual adjuvant properties in oral immunization procedures [1-3]. The synthesis of new OMS, based on the use of polymeric templates, is a very important material science issue, since the pore sizes must be tailored to encapsulate antigens, molecules and proteins of different mass.

In this work we tested a new Dow Triol-copolymer, PEO₂₁PPO₈₆PEO₂₁, in a synthesis process similar to that described with Basf Pluronic P123, PEO₂₀PPO₇₀PEO₂₀ [4], aiming to obtain a large pore diameter, because the triol has a higher mass of the hydrophobic component. The three leg triol molecular arrangement is depicted in Figure 1. The samples were prepared with different triol mass, keeping constant the amount of the silicon precursor, tetraethoxysilane (TEOS) and two temperatures were checked, 21°C and 40°C. The amount of triol in the synthesis process varied from 0.83 g up to 2.0 g. In order to increase the pore diameter, a swelling agent, triisopropylbenzene (TIPB) was used in the synthesis of samples prepared with the optimized polymer mass. The optimization was based on the analysis of the ordered porous network, surface area, pore diameter and volume.

The structural characterization of the powders was performed by Small Angle X-ray Scattering (SAXS) and Nitrogen Adsorption Isotherm (NAI). Figure 2 shows the SAXS results of the first tested synthesis parameters. The results indicate that a larger polymer mass should be tested. The best synthesis temperature was found to be 40°C.

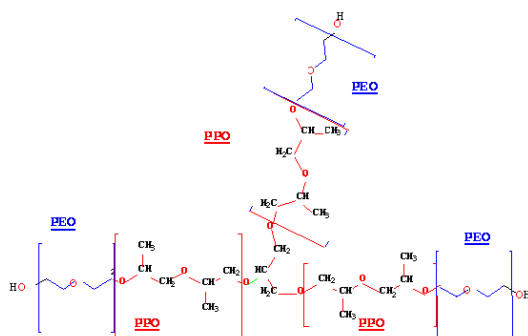


Figure 1: PEO₂₁PPO₈₆PEO₂₁ molecular arrangement.

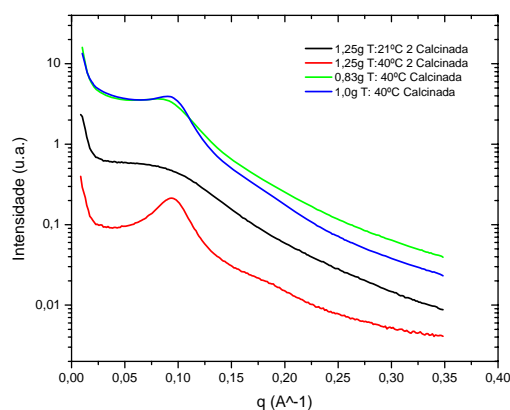


Figure 2: SAXS curves of sample prepared with different template mass and temperature.

Testing larger polymer masses the SAXS and NAI results revealed that the best polymer mass was 1.5 g, presenting an ordered porous matrix, BET surface area of 918 m²/g, pore volume of 1.22 cm³/g and mean pore diameter of 6.7 nm. Non ordered porous networks were produced with larger mass and TIPB. The presence of TIPB lead to a decrease of surface area, but increased the mean pore diameter to values up to 10.6 nm. This new OMS will be tested to encapsulated molecules with sizes smaller than 6 nm.

- [1] Mercuri, L.P. et al., *Small*, **2**, 254-256 (2006).
- [2] Carvalho, L.V., et al., *Vaccine*, **28**, 7829-7836 (2010).
- [3] Mariano-Neto, F., et al., *J. Phys. D: Appl. Phys.*, **47**, 425402-425412 (2014).
- [4] Zhao, D. et al, *Science*, **279**, 548-552 (1998).

Acknowledgments: FAPESP; CNPq; Dow do Brasil, Santander.

Efeito da temperatura de calcinação na síntese de estruturas do tipo $\text{Ca}_3\text{Co}_4\text{O}_9$

S. S. Vieira^a, G. S. Rizzi^a, A. C. Doriguetto^a, H. B. Carvalho^a, P. P. Neves^a.

^aUniversidade Federal de Alfenas – UNIFAL-MG

Sistema do tipo Ca-Co-O tem atraído muito interesse nos últimos tempos devido às suas propriedades elétricas e magnéticas, os quais podem ser em grande parte, atribuídas à menor dimensionalidade das suas estruturas cristalinas [1]. Vários métodos de síntese, tais como; co-precipitação, sol-gel, hidrotérmico têm sido usados para sintetizar este tipo de material. O método sol-gel tem atraído muito atenção devido às suas vantagens, tais como; baixa temperatura de processamento, distribuição homogênea do reagente e a enorme flexibilidade para sintetizar pós com estrutura nanocristalina [2]. Assim, o presente trabalho teve por objetivo investigar a influência da temperatura de calcinação na síntese de $\text{Ca}_3\text{Co}_4\text{O}_9$ (CCO) obtido a partir do método Pechini. Para o preparo do CCO foram usados como reagentes de partida os nitratos de cálcio e cobalto, ácido cítrico e etilenoglicol. Na síntese foram usadas razões otimizadas de ácido cítrico/metálico e ácido cítrico/etilenoglicol. A temperatura de calcinação foi variada entre 380 e 980 °C. A Figura 1 mostra os DRXs dos pós calcinados nas diferentes temperaturas e o TG/DTA do “puff”.

Pelo TG/DTA apresentado do “puff”, pó obtido através de tratamento térmico à 300 °C, foi observado que o CCO se forma entre 700 °C e 950 °C. Através dos dados de DRX apresentados é possível perceber que entre 380-550 °C apenas fases de CaCO_3 e Co_3O_4 foram detectadas. Com o aumento da temperatura de calcinação para 750 °C é possível perceber que as fases de $\text{Ca}_3\text{Co}_4\text{O}_9$ ficam mais evidentes. Em 850 °C a fase pura de $\text{Ca}_3\text{Co}_4\text{O}_9$ é obtida. Com o aumento da temperatura para 980 °C o $\text{Ca}_3\text{Co}_4\text{O}_9$ começa a se decompor em $\text{Ca}_3\text{Co}_2\text{O}_6$. Algumas fases de $\text{Ca}_3\text{Co}_4\text{O}_9$ ainda são percebidas nesta temperatura. Como este material ainda é relativamente novo, pouca informação cristalográfica é encontrada na literatura. As fichas cristalográficas para o CCO ainda são escassas e, o melhor encontrado foi a JCPDS 21-0139. O CCO possui uma estrutura laminar composta por dois diferentes tipos de camadas que se alternam. Em uma das camadas, Ca, Co e O formam o composto $\text{Ca}_2\text{CoO}_{3+\delta}$ em uma estrutura cúbica de face centrada. Na outra camada, átomos de Co são cercados por seis átomos de O em um sítio octaedro, formando o composto de CoO_2 [3]. Pelos dados apresentados foi possível perceber que o aumento da temperatura favorece a formação de fase pura de CCO, no entanto esta fase só é observada a temperaturas inferiores a 980 °C. A partir dessa temperatura CCO não é mais observado.

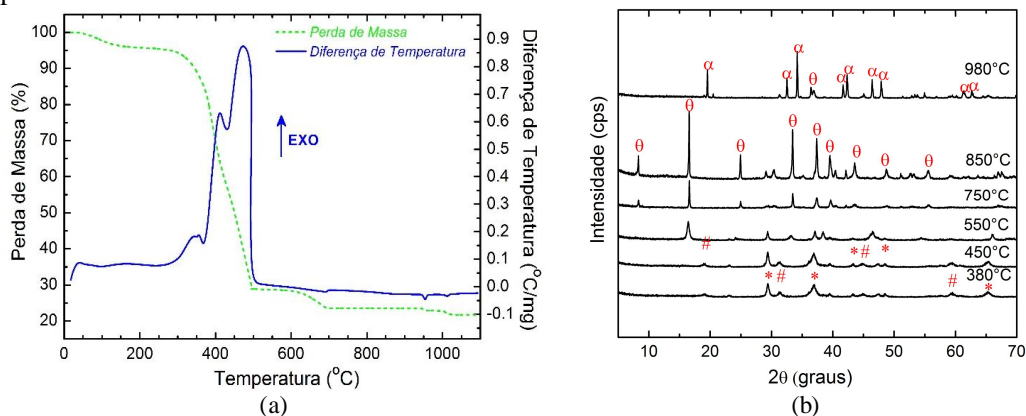


Figura 1. (a) TG/DTA do “puff”. (b) DRX dos pós calcinados nas diferentes temperaturas (B) (*- CaCO_3 ; #- Co_3O_4 ; α - $\text{Ca}_3\text{Co}_2\text{O}_6$; θ - $\text{Ca}_3\text{Co}_4\text{O}_9$).

[1] Tran, H., Mehta, T., Zeller, M., Jarman, R. H., Materials Research Bulletin **48** 2450–2456 (2013).

[2] Pechini, M.P., Method of Preparing Lead and Alkaline Earth Titanates and Niobates and Coating Method Using the Same to Form a Capacitor, U.S.P. Office, Editor (1967).

[3] Zhang, Y. F., Zhang, J. X., Lu, Q. M., Zhang, Q. Y. Materials Letters **60** 2443–2446, (2006).

Acknowledgments: FAPEMIG, FINEP, CAPES, CNPq, PPGQ-UNIFAL-MG e a RQ-MG. Ao Laboratório de Cristalografia da Unifal-MG pelas medidas de DRX

SYNTHESIS, ELECTRICAL AND STRUCTURAL CHARACTERIZATION OF A COMPOSITE MATERIAL BASED ON POWDERED MAGNETITE AND HIGH DENSITY POLYETHYLENE .

David A. Landinez Tellez,^a A. O. Garzon Posada,^a J. Roa Rojas,^a

^a Grupo de Física de Nuevos Materiales, Departamento de Física, Universidad Nacional de Colombia, AA 5997, Bogotá DC, Colombia E-mail: dalandinezt@unal.edu.co

This work describes the synthesis and characterization of a composite material based on magnetite filled HDPE, which is commonly known for its magnetic properties. Composites of this kind are used in different applications such as magnetic and microwave absorption, transducers manufacturing, and biomedical applications like targeted drug delivery, organs tagging, etc. The samples were produced according to different volume ratios of magnetite and HDPE. The samples structure was analyzed through X-ray diffraction tests and the crystallinity degree was calculated. Then, the samples were electrically characterized through volume resistivity measurements. The results showed that for ratios less than the 20% of magnetite there is not a substantial reduction in the resistivity of the composite compared to the unfilled HDPE. For magnetite ratios above the 30% the composite shows a substantial reduction of six orders of magnitude in its electrical resistivity.

Keywords: X-ray diffraction in Magnetite, volumetric resistivity.

ZIRCÔNIA-CÉRIA MESOPOROSA PARA CÉLULAS A COMBUSTÍVEL E CATALISADORES

M. C. A. Fantini^a, R. Bacani^a, V. R. S. Cassimiro^a

^aInstituto de Física, Universidade de São Paulo, Brasil

Materiais mesoporosos a base de céria (CeO_2) e zircônia (ZrO_2) estão presentes em diversas aplicações tecnológicas destacando-se especialmente como catalisadores para a produção de H_2 ^[1] e automotivos^[2] (Three-Way Catalysis) e como anodos de células a combustível de óxido sólido^[3]. A solução sólida ($\text{Ce}_x\text{Zr}_{1-x}\text{O}_2$) é de especial interesse pois apresenta melhor estabilidade térmica e capacidade de armazenamento de oxigênio (OSC) quando comparada com os óxidos não dopados^[4]. A síntese da zircônia-céria mesoporosa já foi estudada em diversos trabalhos. Uma das estratégias de sucesso, é a utilização do copolímero tribloco P123 ($\text{PEO}_{20}\text{PPO}_{70}\text{PEO}_{20}$) como direcionador de estrutura no processo de autoformação das micelas com as espécies metálicas, resultando no material poroso após a remoção do copolímero por calcinação^[5-6]. Neste trabalho, $\text{Zr}_{0,1}\text{Ce}_{0,9}\text{O}_2$ foi sintetizada com P123, adicionando o dilatador de estrutura Triisopropilbenzeno (TIPB) com o objetivo obter materiais com poros de tamanhos maiores. Os precursores ZrCl_4 e $\text{CeCl}_3 \cdot 7\text{H}_2\text{O}$ foram utilizados na síntese. Após tratamento térmico por 48h a 80°C em autoclave, o material foi calcinado com lenta rampa de aquecimento até o patamar de 400°C por 4h. Amostras foram produzidas com diferentes razões em massa TIPB/P123 (0, 1, 2, 4). As amostras, analisadas por SAXS, não apresentaram poros ordenados. Resultados de difração de raios X foram analisados por refinamento Rietveld, mostrando a presença majoritária da fase cúbica (fig. 1). Medidas de adsorção de N_2 (fig.2) indicaram que a adição do TIPB foi capaz de dilatar os poros de ~ 29 para 38 nm (ramo de adsorção). Imagens de microscopia eletrônica de varredura (SEM), mostraram uma morfologia similar para todas as amostras, com poros em forma de fenda e dimensões compatíveis com os resultados de adsorção (fig. 3).

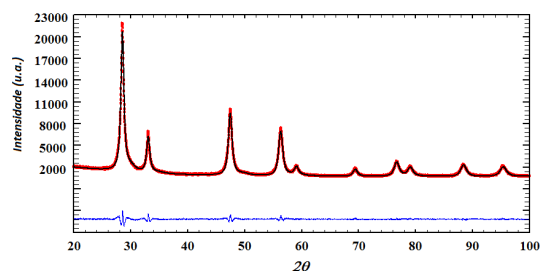


Figura 1: Refinamento Rietveld do padrão de difração da mostra ZrCe-1 (TIPB/P123=1).

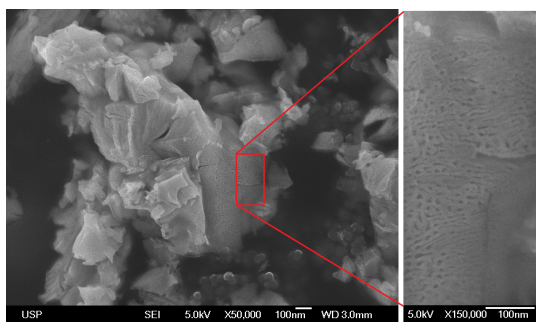


Figura 3: Imagens de SEM da amostra ZrCe-4 (TIPB/P123=4) onde observa-se os mesoporos.

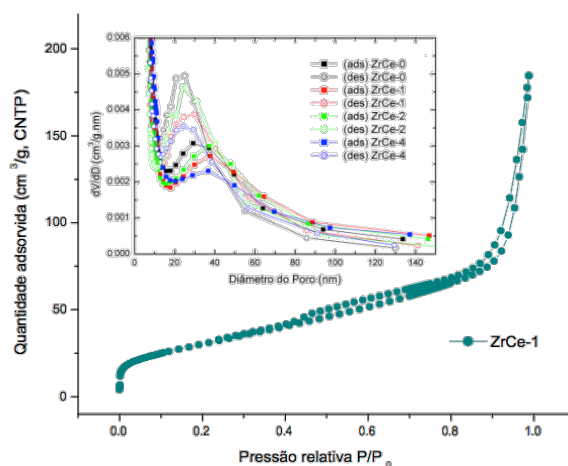


Figura 2: Isotherma de adsorção de N_2 para a amostra ZrCe-1 (TIPB/P123=1) e distribuição do diâmetro dos poros (BJH) calculada para as quatro amostras com os ramos de adsorção (ads) e dessorção (des).

- [1] Nahar, G., Dupont, V., *Renew. Sust. Energ. Rev.*, **32**, 777-796 (2014).
- [2] Kašpar, J., Fornasiero, P., Graziani, M., *Catal. Today.*, **50**, 285-298 (1999)
- [3] Sun, C., Stimming, U., *J. Power. Sources.*, **171**, 247-260 (2007).
- [4] Monte, R. D., Kašpar, J., *J. Mater. Chem.*, **15**, 633-648 (2005).
- [5] Yuan, Q., Li, L., Lu, S., Duan, H. Li, Z., Zhu, Y., Yan, C., *J. Phys. Chem. C*, **113**, 4117-4124 (2009)
- [6] Bacani, R., *Tese de Doutorado* (2014)

X-ray absorption studies and f-level occupancy in Ce₂Rh_(1-x)Ir_xIn₈.R. Prudêncio Amaral^a, N. S. Camilo^a, C. Adriano^b, L. Bufaiçal^c, P. G. Pagliuso^b, R. Lora-Serrano^a.^a*Instituto de Física, Universidade Federal de Uberlândia, 38400-902, Uberlândia, MG, Brazil.*^b*Instituto de Física "Gleb Wataghin", UNICAMP, 13083-970, Campinas, SP, Brazil.*^c*Instituto de Física, Universidade Federal de Goiás, 74001-970, Goiânia, GO, Brazil.*

Within the series of heavy fermions Ce₂Rh_(1-x)Ir_xIn₈ (Ce218) intermetallic compounds it has been observed the occurrence of two low-temperature superconducting (SC) phases as a function of temperature both at ambient and applied pressure for intermediate Ir-content ($x \sim 0.25-0.70$). Remarkable different behaviour of both states were observed [1] which seems to be reminiscent of the SC phases found in the CeRh(1-x)Ir_xIn₅ system [2]. The SC phases in the title compounds appear for smaller x ranges, which has been associated to its higher dimensionality and structural disorder. In this work, we have performed EXAFS (X-ray Absorption Fine Structure) and XANES (X-ray Absorption Near Edge Structure) measurements in the series Ce₂Rh_(1-x)Ir_xIn₈ ($x = 0.00, 0.25, 0.50, 0.75$). We aim at shading light into the relationship between the local atomic order and the interesting ground states previously observed. The experimental data were obtained for the Ir (L3), Rh (K) and Ce (L3) absorption edges at the Brazilian Synchrotron Light Source (LNLS). Our results have been analysed by using FEFF and IFEFFIT codes and they suggest that there is no evidence for the presence of local structural disorder until the lowest temperature measured (10K). This is contrary to what has been suggested, however sample inhomogeneities (Rh clustering) and changes in the Rh/Ir stoichiometry could be responsible for the smaller doping range where SC were observed. XANES data reveals that Ce valence is 3+ over the entire studied T interval. Preliminary results of EXAFS data under pressure of up to 20 kbar will be presented and compared to the ambient pressure EXAFS data.

Acknowledgments: we thanks to CAPES.

[1] Hering, E. N. et al. Phys. Rev. B, **82**, p. 184517, 2010.

[2] Nicklas, M. et al. Phys. Rev. B, **70**, 2004. 020505.

Estudio por Técnicas de Difracción de Rayos-X de Derivados de Cobalto y Manganeso de la Gabapentina, un Principio Activo Utilizado como Anticonvulsivo

R. Toro¹, G. Borges¹, G. Díaz de Delgado¹, J. M. Delgado¹

⁽¹⁾Laboratorio de Cristalografía-LNDRX, Departamento de Química, Facultad de Ciencias, Universidad de Los Andes, Mérida 5101, Venezuela.

La gabapentina (GBP, figura 1) es un Principio Farmacéuticamente Activo (PFA) utilizado como agente anticonvulsivo, y en el tratamiento del dolor neuropático y de diversas afecciones del sistema nervioso. La gabapentina, siendo un aminoácido, tiene la potencialidad de coordinar con átomos metálicos. La presencia de un átomo metálico en la estructura de este principio activo podría tener un efecto en su eficacia terapéutica [1]. Como parte del trabajo realizado en el Laboratorio de Cristalografía de la Universidad de Los Andes, con el objetivo de caracterizar PFAs para examinar la posible formación de polimorfos bajo diferentes condiciones de cristalización y formación de complejos metálicos, se llevó a cabo un estudio por técnicas de difracción de rayos-X de complejos metálicos de la gabapentina con metales que desempeñan alguna función biológica en el organismo humano. Los derivados de Cobalto-GBP se prepararon utilizando cantidades estequiométricas de dos sales de cobalto (acetato de cobalto y cloruro de cobalto) y gabapentina. En la síntesis del derivado de cobalto usando cloruro de cobalto se obtiene un polvo cristalino de color azul (Co-GBP01). El indexado del patrón de polvo produce una celda unidad monoclinica $P2_1/a$ con parámetros $a=16,870(5)$ Å, $b=10,460(2)$ Å, $c=13,239(2)$ Å, $\beta=109,10(2)$ ° y $V=2207,50$ Å³ ($M_{20}=34,1$, $F_{20}=94,2(0,0042; 50)$). Estos parámetros son similares a los reportados en el *CSD* (*REFCODE*: DOBBIG) para un derivado de Zinc de la gabapentina. El patrón de polvo experimental es similar al patrón de polvo calculado utilizando los datos cristalográficos de DOBBIG, indicando que el derivado Cobalto-GBP es isoestructural al derivado de Zn. Por otro lado, cuando se utiliza acetato de cobalto para la síntesis, se obtiene un polvo de color rosa (Co-GBP02) cuyo patrón de polvo es diferente al obtenido para Co-GBP01 y diferente a los reportados en las bases de datos *PDF-4/Organics* y *CSD*. En la síntesis del derivado de Zn, con $ZnCl_2$, se obtienen cristales incoloros en formas de aguja. Estudios llevados a cabo mediante métodos térmicos indican que esta fase es una forma monohidratada. El estudio por difracción de rayos X de cristal único de este material indica que cristaliza con una celda unidad monoclinica $C2/c$ con parámetros $a=36,713(7)$ Å, $b=6,397(1)$ Å, $c=20,742(4)$ Å y $\beta=93,253(3)$ °. Estos parámetros son similares a los contenidos en el *CSD* bajo el *REFCODE*: VIXCIQ. El patrón obtenido para este material luego de ser sometido a calentamiento a 60°C por 2 horas, es diferente a los mencionados previamente. Todos los patrones de difracción fueron analizados usando programas de determinación estructural (TALP [2], EXPO2013 [3] y FOX [4]). En esta contribución se presentan comparativamente los resultados.

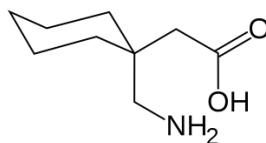


Figura 1. Diagrama molecular de la Gabapentina, GBP.

- [1] Zhang, G. G. Z., Law, D., Schmitt, E. A., and Qiu, Y. *Advanced Drug Delivery Reviews*, **56**, 371-390 (2004).
- [2] Vallcorba, O., Rius, J., C. Frontera, C., Miravittles, C. *J. Appl. Cryst.* **45**, 1270-1277 (2012).
- [3] Altomare, A., Cuocci, C., Giacobozzo, C., Moliterni, A., Rizzi, R., Corriero, N., Falcicchio, A. *J. Appl. Cryst.* **46**, 1231-1235, (2013).
- [4] Cerny, R., Favre-Nicolin, V. *Z. Kristallogr.* **222**, 105-113, (2007).

Agradecimientos: Este trabajo ha sido posible gracias al proyecto LAB-97000821 del FONACIT (Laboratorio Nacional de Difracción de Rayos-X) y al CDCHTA-ULA. Los autores agradecen a M. Pink y C-H. Chen (IUMSC) por la toma de datos de monocristal.

Síntesis y caracterización de un polímero de coordinación 2D interpenetrado paralelamente inclinado a partir de Cu(II) y anhídrido maleico

E. E. Ávila^a, M. E. Quintero^{a,b}, A. Mora^b, A. Briceño^a

^aCentro de Química, Instituto Venezolano de Investigaciones Científicas, San Antonio de Los Altos, Miranda, Venezuela.

^bLaboratorio de Cristalografía, Departamento de Química, Universidad de Los Andes, Mérida, Venezuela.

En las últimas décadas el gran número de estudios publicados sobre la preparación de estructuras metal-orgánicas (por sus siglas en inglés Metal-Organic Framework, MOF) se ha incrementado por aplicación de diferentes métodos de síntesis que van desde condiciones hidrotérmicas, sonoquímica, síntesis asistida por microondas y mecanoquímica [1]. Todos estos métodos resultan altamente eficiente en la preparación de estos materiales; sin embargo, la mecanoquímica ha derivado en un método de fácil implementación y amigable con el ambiente; debido a dos razones en particulares: 1) no requiere solvente, y sí lo quiere éste es en pequeñas cantidades [2]. Dado a esta particularidad, en este trabajo se estudia la formación de especies polinucleares de compuestos de coordinación, en el estado sólido, con estructuras infinitas construidas a partir de los iones metálicos y ligandos orgánicos como el Cu(II) y el anhídrido maléico, respectivamente.

La preparación de CP-1 se llevó a cabo por vía mecanoquímica asistida con solvente, en este caso metanol. Donde se procedió como se nombra a continuación: en un mortero de ágata se colocó un 1 mmol de Cu[(NO₃)₂].4H₂O (241,1 mg), 1 mmol de 4,4'-bipiridilo, *bpy*, (156,19 mg) y 2 mmol anhídrido maleíco, *amal*, (98,06 mg). El tiempo total de molienda fue de 40 min; dividido en períodos de 20 min. En el primer período, como se muestra en la figura 1, el sólido presenta una coloración azul verdosa (ver Fig. 1b) y luego, transcurrido los últimos 20 min, pasa a un azul celeste como se muestra en la Fig. 1c.

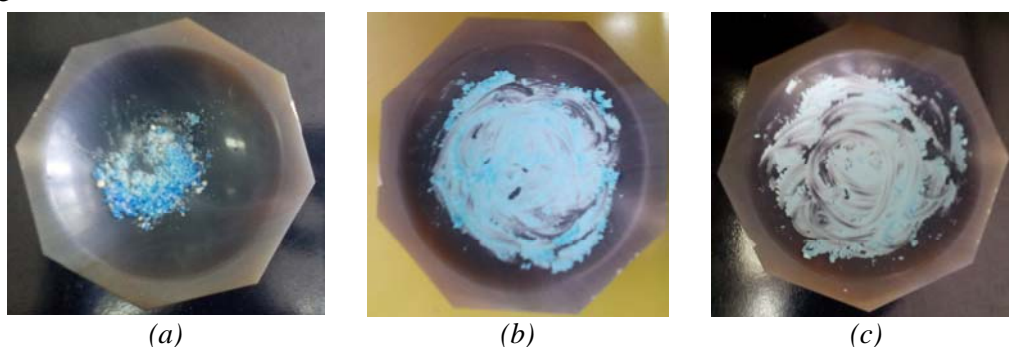


Figura 1. Fotografías ópticas para la evolución de la reacción mecanoquímica asistida con metanol del CP-1. (a) Tomada a 0 min de molienda, (b) 20 min de molienda con tres gotas de metanol y (c) 40 min de reacción.

A continuación, el sólido formado a los 40 min de reacción se llevó a un vial y se le adicionó metanol y se recristalizó mediante evaporación lenta de solvente. Durante un período de una semana se obtuvo un material cristalino de color azul celeste. El sólido resultante, se filtró y lavó repetidas veces con metanol, finalmente se dejó secar a temperatura ambiente. La caracterización preliminar de CP-1 se realizó mediante difracción de rayos-X de cristal único, utilizando un difractómetro Rigaku AFC7S con radiación de MoK α ($\lambda=0,71073\text{\AA}$), equipado con un detector de área Mercury. El tratamiento de los datos de difracción arrojó que CP-1 cristaliza en un sistema ortorrómbico, con grupo espacial *Cccm* (N^o 66), $Z = 16$, y parámetros de celda $a = 11,792(8)\text{\AA}$, $b = 19,533(14)\text{\AA}$, $c = 7,426(5)\text{\AA}$. La determinación de la estructura cristalina se realizó con el Superflip [3] y el refinamiento se hizo utilizando el programa SHLEXL-2013 [4], el cual arrojó los siguientes parámetros de confiabilidad: $R(F^2) = 8,0\%$; $wR(F^2) = 23,1\%$ y $S = 1,10$.

The abstract was not suitable for template. The text had to be cut

MAT15

Synthesis and characterization of $\text{La}_{0.6}\text{Sr}_{0.4}\text{Fe}_{0.8}\text{Cu}_{0.2}\text{O}_{3-\delta}$ oxide as cathode for Intermediate Temperature Solid Oxide Fuel Cells

Authors Davyt, S.^a; Vázquez, S.^a; Basbus, J. F.^b; Soldati, A. L.^b; Amaya, A.^c; Serquis, A.^b; Faccio, R.^a; Suescun, L.^a.

^aLaboratorio de Cristalografía, Estado Sólido y Materiales, DETEMA, Facultad de Química, UdelaR, Montevideo, Uruguay

^bGrupo Caracterización de Materiales, CAB-CNEA, Bariloche, Argentina

^cLaboratorio de Fisicoquímica de Superficies, DETEMA, Facultad de Química, UdelaR, Montevideo, Uruguay

Nanocrystalline $\text{La}_{0.6}\text{Sr}_{0.4}\text{Fe}_{0.8}\text{Cu}_{0.2}\text{O}_{3-\delta}$ (LSFCu) material was synthesized by combustion method using EDTA as fuel/chelating agent and NH_4NO_3 as combustion promoter. Structural characterization using thermodiffraction data allowed to determine a reversible phase transition at 425 °C from a low temperature R-3c phase to a high temperature Pm-3m phase and to calculate the thermal expansion coefficient (TEC) of both phases [1]. Important characteristics for cathode application as electronic conductivity and chemical compatibility with $\text{Ce}_{0.9}\text{Gd}_{0.1}\text{O}_{2-\delta}$ (CGO) electrolyte were evaluated. LSFCu presented a p-type conductor behavior with maximum conductivity of $135 \text{ S}\cdot\text{cm}^{-1}$ at 275 °C and showed a good stability with CGO electrolyte at high temperatures. This work confirmed that as prepared LSFCu has excellent microstructural characteristics and an electrical conductivity between 100 and $60 \text{ S}\cdot\text{cm}^{-1}$ in the 500–700 °C range which is sufficiently high to work as intermediate temperature Solid Oxide Fuel Cells (IT-SOFCs) cathode [2]. However a change in the thermal expansion coefficient consistent with a small oxygen loss process may affect the electrode-electrolyte interface during fabrication and operation of a SOFC.

[1] Santiago Vázquez et al., Journal of Solid State Chemistry 228, 208–213(2015).

[2] Brian C.H.Steele, Angelika Heinzl, Nature 414, 345–352(2001).

Influence of hydrogen and austenitization on the martensite start strain in the austenitic stainless steel 316

J. J. Hoyos^a, J. Rodríguez^a, P. Craidy^b, M. T. Piza^b, A. J. Ramírez^{a,c}.

^a*Metals Characterization and Processing Laboratory (CPM), Brazilian Nanotechnology National Laboratory (LNNano), National Research Center for Energy and Materials (CNPEM). Rua Giuseppe Máximo Scolfaro 10000, Campinas, SP 13083970, Brazil.*

^b*Petrobras, Av. Horácio Macedo 950, Ríó de Janeiro, RJ 21941915, Brazil.*

^c*Department of Materials Science and Engineering, Ohio State University, U.S.*

Austenitic Stainless Steel (ASS) 316 is known to transform to martensite α' or martensite ϵ during deformation or hydrogenation. This steel is widely employed for structural and high-pressure applications. However, it can undergo several forms of embrittlement, depending of the hydrogen charging or heat treatment. Therefore, it is necessary a better understanding of the kinetics of the phase transformations during deformation, and the role of the martensitic transformation on the embrittlement under several conditions. In this work, the martensite start strain is determined for as-received, hydrogenated, and austenitized states. The hydrogenation was made during 7 days in a solution of 0,1M H₂SO₄ + 10mg/L As₂O₃, at room temperature, with an intensity current of 20 mA/cm². The sensitization was made heating at 1100 °C for 10 minutes. Simultaneous measurements of X-ray diffraction were made during tensile test at strain rate of $2.5 \times 10^{-3} \text{ s}^{-1}$. Hydrogen charge increases the content of martensite α' and martensite ϵ . While the heat treatment generates precipitates and reduces the strain necessary to the start of the martensitic transformation.

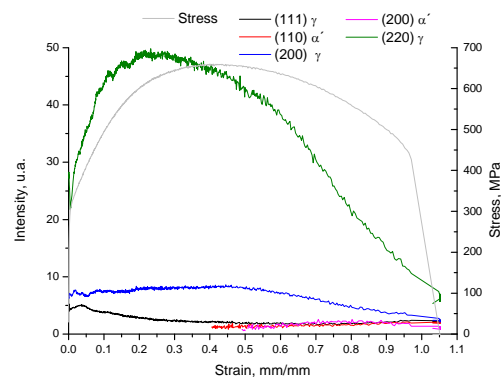


Figure 1: Intensity of the diffraction peaks in function of the strain for the as-received state.

References

- [1] Sugiyama, S., Ohkubo, H., Takenaka, M., Ohsawa, K., Ansari, M.I., Tsukuda, N., Kuramoto, E., *Journal of Nuclear Materials*, **283-287**, 863-867 (2000).
- [2] Touseef Nauman, M., Rasool Mohideen, S. Kaleem, N., *International Journal of Mechanical and Industrial Engineering (IJMIE)*, **2, 1**, 44-48 (2012).
- [3] San Marchi, C., Somerday, B.P., Tang, X., Schiroky, G.H., *International Journal of Hydrogen Energy*, **33**, 889-904 (2008).

Acknowledgments: The authors are grateful to the LNNano/CNPEM for the technical support during the usage of the XTMS installation and LNLS/CNPEM for the infrastructure present in the XRD1 beamline. The authors J. J. Hoyos, J. Rodríguez and A. J. Ramírez are grateful to CAPES (Project Inomat) and CNPq for financial support.

DIELECTRIC PROPERTIES OF BaTi_{0.9}Zr_{0.1}O₃ FROM A MIXTURE OF BaTiO₃ AND BaZrO₃A. L. Boaventura^a, E. Antonelli^a.^a *Instituto de Ciências e Tecnologia, Universidade Federal de São Paulo, São José dos Campos, SP, Brasil*

Lead-free ceramic materials with high dielectric performance are widely used in electronic industry for applications in devices as capacitors and actuators [1]. Thus, the main studies in ceramic materials are focused in to design ceramics compositions and to prepare homogeneous and single-phase materials.

Here, we proposed a different methodology in which new properties are obtained in composites of pseudo-binary compositions. The structural, microstructural and dielectric properties of (0.90)BaTiO₃ – (0.10)BaZrO₃ (90BT-10BZ) ceramic composites are correlated with the processing parameters.

The ceramic materials were prepared by conventional solid state reaction. Initially, were prepared the compounds BaTiO₃ (BT), BaZrO₃ (BZ) and BaTi_{0.90}Zr_{0.10}O₃ (BZT10). Thereafter, the calcined powders of BT and BZ were mixed in the proportions (0.90)BaTiO₃ – (0.10)BaZrO₃ (90BT-10BZ) to form the ceramic composites.

According to x-ray diffractions the calcined powders (1200°C/2h) presented single-phase. As expected, the BT, BZ and BZT10 were identified as tetragonal, cubic and orthorhombic-like, respectively. The milling process for the 90BT-10BZ do not results in reactions between the compositions and the initial compositions can be identified in the x ray diffraction. Otherwise, sintering of the 90BT-10BZ compounds (1350°C/2h) results in an apparently single-phase material. Nevertheless, the 90BT-10BZ pattern is shifted in relation to BZT10.

Besides, the electrical properties and nature of the ferroelectric-to-paraelectric phase transition are changed by processing methodology.

Finally, the overall phase development is discussed in terms of the processing methodology and the nature of BT-BZ diffusion, and appears to mainly or, at least, partially also involve a presence of local *inhomogeneities*.

[1] Lee, S. G. & Kang, D. S. Dielectric properties of ZrO₂-doped (Ba,Sr,Ca)TiO₃ ceramics for tunable microwave device applications. *Mater. Lett.* **57**, 1629–1634 (2003).

Acknowledgments: CAPES.

Investigação da formação de quase-cristais nas ligas do sistema Ti-Zr-Ni

Fernando Froes, André Luiz Carvalho de Rezende Silva, Paulo Atsushi Suzuki

*Departamento de Engenharia de Materiais, Escola de Engenharia de Lorena,
Universidade de São Paulo, Lorena, SP, Brazil*

Os quasecristais são sólidos que apresentam arranjo atômico cuja simetria é proibida em cristais periódicos [1]. D. Schechtman observou a existência destes compostos pela primeira vez em ligas de Mn-Al em 1984 [2]. Desde então, centenas de quase-cristais foram descobertos até hoje [1].

O grupo liderado por K. F. Kelton descobriu a formação de quase-cristais em ligas do sistema Ti-Zr-Ni em 1997 [3]. Esta fase, identificada como sendo do tipo Franck-Kasper, cristaliza em uma estrutura icosaédrica e foi denominado i-TiZrNi [4]. A estrutura cristalina é próxima da fase W-TiZrNi, cuja estrutura é cúbica, grupo espacial $Im-3m$ com 162 átomos por célula unitária e parâmetro de rede $a = 14,30 \text{ \AA}$ [4]. O grupo tem desenvolvido a aplicação destes materiais em armazenamento de hidrogênio [5]. Eles observaram a formação monofásica dos quase-cristais em condições específicas, mas o diagrama ternário é complexo, onde aparecem diversas fases cristalinas [6].

No presente trabalho, objetivou-se a investigação da formação e estabilidade das fases e o estudo da estrutura cristalina das fases presentes nas ligas do sistema Ti-Zr-Ni. Lingotes com massa de aproximadamente 5 g foram produzidas por fusão a arco a partir de chapas de elementos puros. Tratamentos térmicos a $570 \text{ }^\circ\text{C}$ por 24 h em argônio foram feitas em algumas amostras. As medidas de difratometria de raios X (DRX) foram conduzidas pulverizando-se o material na forma de pó em um difratômetro de marca Panalytical, modelo Empyrean, com radiação $\text{MoK}\alpha$. Uma parte das amostras foi embutida em baquelite e a superfície passou por preparação metalográfica. As imagens de microscopia eletrônica de varredura (MEV) foram obtidas em um microscópio Hitachi Tabletop3000 com detector de elétrons retroespalhados. Medidas de composição elementar foram obtidas por espectrometria de energia dispersiva (EDS).

Nas imagens de MEV observou-se a formação de microestruturas multifásicas finas. A combinação de DRX e EDS mostram a formação de uma solução sólida β -(Ti,Zr), fase Laves C14 de composição ternária [7] e picos que foram associadas à fase icosaédrica. A fase Laves cristaliza numa estrutura cúbica com parâmetro de rede a de aproximadamente $5,2 \text{ \AA}$ e varia com a composição das amostras. A fase icosaédrica foi associada à uma região eutética ultrafina presente na imagem de MEV. Os resultados observados estão em acordo com a literatura [8].

Concluiu-se, portanto, que a obtenção da fase icosaédrica monofásica é mais difícil que a descrita na literatura, mas houve eventualmente a formação no interior da região eutética ultrafina. Pequenas variações na composição produzem alterações significativas na microestrutura do material.

- [1] Louzguine-Luzgin, D. V., Inoue, A., *Annu. Rev. Mater. Res.*, **38**, 403 (2008).
- [2] Shechtman, D., Blech, I. Gratias, D., Cahn, J. W., *Phys. Rev. Lett.*, **53**, 1951 (1984).
- [3] Kelton, K. F., Kim, W. J., Stroud, R. M., *Appl. Phys. Lett.*, **70**, 3230 (1997).
- [4] Hennig, R. G., Kelton, K. F., Carlsson, A. E., Henley, C. L., *Phys. Rev. B*, **67**, 134202 (2003).
- [5] Takasaki, A., Kelton, K.F., *Int. J. Hydrogen Energy*, **31**, 183 (2006).
- [6] Lee, G. W., Gangopadhyay, A. K., Kelton, K. F., *Acta Materialia*, **59**, 4964 (2011).
- [7] Waterstrat, R. M., *J. Alloys and Comp.*, **179**, L33 (1992).
- [8] Park, G. H., Hong, S. H., Kima, J. T., et al., *J. Non-Cryst. Sol.*, **392–393**, 6 (2014).

Agradecimentos: F.F. agradece à Pró-reitoria de Graduação da USP pela bolsa concedida no Programa Ensinar com Pesquisa. A.L.C.R.S. agradece à Pró-reitoria de Pesquisa da USP pela bolsa de iniciação científica.

Synthesis and characterization of structural and microstructural properties of $(K_{1-x}Ba_x)(Nb_{1-y}Ni_y)O_{3-\delta}$ ceramics

R. C. Gennari^a, J. A. Eiras^b, R. Lang^a, M. H. Lente^a.

^aUniversidade Federal de São Paulo, Instituto de Ciência e Tecnologia, SJC, SP, Brazil.

^bUniversidade Federal de São Carlos, Departamento de Física, São Carlos, SP, Brazil.

Perovskite ferroelectric ceramics have recently attracted much attention for possible applications in photovoltaic devices^{1,2}. The challenge in this use is to reduce their typical wide band-gap, allowing absorbs light in the visible wavelength, without losing the useful ferroelectricity. Recent work³ have shown the viability of using lead-free ferroelectric ceramics for solar energy conversion by suitable doping.

In this work, solid solution $(K_{1-x}Ba_x)(Nb_{1-y}Ni_y)O_{3-\delta}$ were synthesized by conventional solid-state route using niobium pentoxide (99.9%), nickel oxide (99%), barium carbonate (99.8%) and potassium carbonate (99%) as precursors. The XRD pattern measured at room temperature showed perovskite phase for different sintering temperature. Dielectric measurements performed from 400 to 15 K for all samples revealed no dielectric anomalies at cryogenic temperatures, suggesting that the formed phase persists up to 15 K, that shows the suppression of the ferroelectric-ferroelectric phase transition observed in the $KNbO_3$ system. The FTIR absorbance spectra of KBNN ceramics showed a strong dependence on the sintering temperature. The IR absorption spectra around 950 cm^{-1} , assigned to Nb/Ni-O bond, revealed to be more active for samples sintered at higher temperatures, in which the light absorption present a strong anomaly in the visible range.

[1] Grinberg, I., et al. *Nature* **503**, 509 (2013).

[2] Choi, T., et al. *Science* **324**, 63-66 (2009).

[3] Zhou, W., et al. *Applied Physics Letters*, **105**, 111904 (2014).

Acknowledgments: UNIFESP, CAPES, FAPESP e FINEP.



Molecular structure and physical / chemical
properties
(MSPCP)

Controlled synthesis of 5-Fluorocytosine salts and cocrystals – a supramolecular analysis

Cecilia C. P. da Silva¹, Rebeka de O. Pepino¹, Cristiane C. de Melo¹, Juan C. Tenorio¹, Sara B. Honorato², Alejandro P. Ayala², Javier Ellena¹
¹ Instituto de Física de São Carlos, Universidade de São Paulo, São Carlos, SP, Brazil. ² Departamento de Física, Universidade Federal do Ceará, Fortaleza, CE, Brazil E-mail: javiere@ifsc.usp.br

5-Fluorocytosine (5-FC) was investigated towards the controlled synthesis of crystalline structures according to the ΔpK_a rule¹⁻³. Six co-crystals⁴ and three salts⁵ were obtained and studied by X-ray diffraction, having their synthons compared with other reported structures. All salts crystallize in the monoclinic space group $P2_1/c$. In the 5-FC oxalate and fumarate ones, the acid molecules are placed on an inversion center, in a fashion that each half molecule exhibits one terminal donor-acceptor site leading to the constitution of a 5-FC–acid–5-FC heterodimer. Such a heterodimer is observed in only one donor-acceptor site of the maleate of 5-FC, whose acid molecule exhibits a closed chain architecture. On the other hand, for the co-crystals of 5-FC with succinic, adipic, benzoic and terephthalic acids it is observed the formation of 5-FC homodimers, where each 5-FC molecule performs two  motifs assembled via complementary N-H...O and N-H...N hydrogen bonds. Also, each 5-FC molecule is linked to two acid molecules by single N-H...O and O-H...O hydrogen bonds. These intermolecular interactions result in similar synthons for these co-crystals. The co-crystal of 5-FC with malic acid exhibits a ΔpK_a of -0.1 and its supramolecular structure was found to be an intermediate among salts and co-crystals, preserving the heterodimer formed among the 5-FC and the acid molecule (as the salts) and exhibiting one 5-FC homodimer (as the co-crystals). A comparison with neutral 5-FC structures reported indicates a tendency of 5-FC to form planar and/or tubular cavities where the 5-FC molecules exhibit homodimeric supramolecular synthons. The reported 5-FC salts, until the present, just show heterodimeric synthons. It was believed that due to this quite predictable behavior of the 5-FC molecule should enable the application of crystal engineering techniques to design new solid forms with 5-FC exhibiting specific improvements in the physical and chemical properties of this and other drugs when crystallized together. As the first step toward the application of 5-FC as a suitable co-former candidate for the design of new tailor-made drugs, we synthesized a multi-API co-crystal of 5-FC with the antineoplastic drug 5-fluorouracil.

[1] A. Vermes, H.-J. Guchelaar, J. Dankert, J. Antimicrob. Chemother. 2000, 46, 171–179.

[2] S.L. Childs, G.P. Stahly, A. Park, Mol. Pharm. 2007, 4(3), 323–338.

[3] B.R. Bhogala, S. Basavoju, A. Nangia, CrystEngComm. 2005, 7, 551–562.

[4] C.C.P. da Silva, R.O. Pepino, J.C. Tenorio, S. Honorato, A.P. Ayala, J. Ellena *Cryst. Growth Des.*, 2013, 13(10), 4315–4322.

[5] C.C.P. da Silva, R.O. Pepino, C.C. de Melo, J.C. Tenorio, J. Ellena *Cryst. Growth Des.*, 2014, 14(9), 4383–4393.

Abstract not suitable for defined template.

MSPCP01

Solid State Technologies in the Development of new MedicinesJ. Ellena^a, C. C. de Melo^a, C.C.P. da Silva^a, J.C. Tenorio Clavijo^a, P. de S. Carvalho-Jr^a^a*Instituto de Física de São Carlos, Universidade de São Paulo, CP 369, 13560-970, São Carlos, SP, Brazil.*

Active pharmaceutical ingredients (APIs) are frequently delivered to the patient in the solid state as part of an approved dosage form (e.g., tablets, capsules, etc.). Solids provide a convenient, compact and generally stable format to store an API or a drug product. Understanding and controlling the solid-state chemistry of APIs, both as pure drug substances and in formulated products, is therefore an important aspect of the drug development process. Pharmaceuticals may exist in numerous solid forms, which may feature different physical and chemical properties.

The different structural arrangements of the API are followed by changes in physical and chemical properties such as the thermodynamic, spectroscopic, kinetic, interfacial, and mechanical and bioavailability. Typically the most stable form is chosen for development into the final dosage product but, more recently, metastable forms have been also used owing to enhanced dissolution or bioavailability profiles[1]. As a consequence, the understanding of the physical and chemical properties of the API substances is of fundamental importance to the successful development of final pharmaceutical formulations [2,3].

One of the major problems facing developing countries is the influence of the high cost of medicines in government public health policies. Added to this, other problems are also important such as quality control of medicines and problems related to international intellectual property litigation involving active pharmaceutical inputs have led some Latin American governments to take extreme measures like breaking the international intellectual property laws to reduce the cost of medicines production.

Within this framework, we present here the application of crystal engineering methods to the design, development and supramolecular synthesis of new solid forms of active pharmaceutical ingredients with improved pharmacokinetic, physical, chemical or production properties of antiretroviral-type reverse transcriptase inhibitors as well as drugs used in the treatment of Aids, the Lymphatic filariasis disease, depression and Cancer. Thus the application of solid state physicochemical tools currently allows us to get better, cheaper and safer medicines solving old problems of quality control and industrial production. The fact that new solid multicomponent forms drug could be considered as a "new chemical entities" both by international Pharmaceutical Federations and international intellectual property offices open a whole new era where appropriate relatively low-cost investments could allow to developing countries to sustain and enhance their national pharmaceutical industries.

[1] Hancock, B. C. & Parks, M. *Pharmaceutical Research* **17**, 397-404 (2000).

[2] Almarsson, O. & Zaworotko, M. J *Chemical Communications*, 1889-1896 (2004).

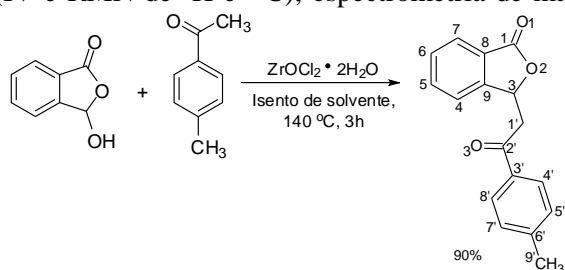
[3] Datta, S. & Grant, D. J. W. *Nature Reviews Drug Discovery* **3**, 42-57 (2004).

Acknowledgments: We thank CNPq, CAPES and FAPESP for the financial support.

Estrutura Cristalina do composto 3-[2(3-metilfenil)-2-oxoetil] isobenzofuran-1(3H)-onaR. A. C. Souza^a, S. Guilardi^a, R. R. Teixeira^b, A. F. S. Maia^b^aInstituto de Química, Universidade Federal de Uberlândia, Uberlândia, Brasil.^bDepartamento de Química, Universidade Federal de Viçosa, Viçosa, Brasil.

Durante as últimas décadas, vários produtos naturais contendo o núcleo isobenzofuran-1(3H)-ona foram isolados e apresentam importantes atividades biológicas. Em particular, isobenzofuran-1(3H)-onas (ftalidas) funcionalizadas na posição C-3 exibem propriedades medicinais úteis. Dentro deste contexto, dezenove 3-(2-aryl-2-oxoetil) isobenzofuran-1(3H)-onas foram sintetizadas, caracterizadas e avaliadas quanto à sua atividade citotóxica frente às linhagens de células cancerosas HL-60 (leucemia mielóide aguda), K562 (leucemia granulocítica crônica) e NALM6 (leucemia linfoblástica de células-B) [1]. No presente trabalho, a estrutura cristalina de um dos compostos que apresentou significativa citotoxicidade foi elucidada por difração de raios X.

O composto em estudo foi sintetizado (Esquema 1) e caracterizado por técnicas espectroscópicas (IV e RMN de ¹H e ¹³C), espectrometria de massas e difração de raios X. Monocristais apropriados foram obtidos por recristalização lenta em etanol:água (2:1 v/v). Os dados de raios X foram coletados em difratômetro Enraf-Nonius Kappa CCD a 100 K, usando radiação MoK α (0,71073 Å), e corrigidas pelos fatores de Lorentz e polarização. A estrutura foi resolvida por métodos diretos e refinada por mínimos quadrados (F²), utilizando matriz completa.



Esquema 1. Síntese da 3-[2(3-metilfenil)-2-oxoetil] isobenzofuran-1(3H)-ona.

O composto cristaliza no sistema monoclinico, grupo espacial C2/c.

As duplas ligações C1-O1 e C2'-O3 são de 1,205(3) Å e 1,228(3) Å, respectivamente. A ligação C1-O2 [1,364(3) Å] tem caráter de dupla ligação e a distância C3-O2 [1,464(3) Å] é consistente com o valor esperado para uma ligação simples, como observado em outros derivados de ftalidas [2]. No substituinte 2-aryl-2-oxoetil, todos os comprimentos e ângulos de ligação são normais e comparáveis com os observados em compostos correlatos [3]. O ângulo diedro entre os planos traçados pelos dez átomos do núcleo isobenzofuran-1(3H)-ona (rms de 0,0335 Å) e pelos átomos do substituinte 2-(3-metilfenil)-2-oxoetil (rms de 0,0533 Å) é de 60,17(5) °.

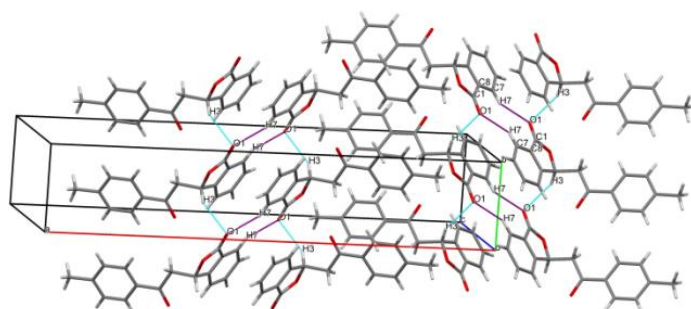


Figura 1. Empacotamento cristalino do composto em estudo.

No empacotamento cristalino, além da interação intramolecular C4-H4...O3, interações C7-H7...O1 entre moléculas relacionadas por inversão formam dímeros gerando motivos estruturais R₂²(10). Interações C3-H3...O1 conectam os dímeros ao longo do eixo *b* e interações C-H... π formam uma rede supramolecular tridimensional.

[1] A. F. S. Maia. *Síntese e avaliação das potenciais atividades fitotóxica e citotóxica de 3-(2-aryl-2-oxoetil) isobenzofuran-1(3H)-onas*, Dissertação de mestrado, UFV, Viçosa (2014).

[2] R. R. Teixeira, J. L. Pereira, S. F. Da Silva, S. Guilardi, D. A. Paixão, C. P. A. Anconi, W. B. De Almeida, J. Helena, G. Forlani. *J. Molec. Struct.* **1061**, 61-68 (2014).

[3] F. Bian, Y. Jin, S. Chi, G. Shi, S. Xu. *Acta Cryst.* **E68**, o3243 (2012).

Agradecimentos: Rede Mineira de Química; FAPEMIG; CAPES; CNPq; Prof. Dr. Javier Ellena.

Analisis of polymorphic contamination in Meloxicam: raw materials and tablets

J.T. Jacon Freitas^a, O.M. M. Santos Viana^b, R. Bonfilio^c, M. B. Araújo^a, A.C. Doriguetto^{a,b}

^a Faculty of Pharmaceutical Sciences, Federal University of Alfenas, Alfenas-MG, Brazil;

^b Institute of Chemistry, Federal University of Alfenas, Alfenas-MG, Brazil;

^c Institute of Health Sciences, Federal University of Mato Grosso State, Sinop University Campus, Sinop-MT, Brazil.

Meloxicam (MLX), a nonsteroidal anti-inflammatory and analgesic drug, is a class II drug according to the Biopharmaceutical Classification System, *i.e.*, possessing low solubility and high permeability. Four MLX polymorphs (forms I, II, III, V) and a monohydrate (form IV) are known.[1,2] Identifying, understanding and anticipating the occurrence of polymorphism is of fundamental importance and concern to the pharmaceutical industry, since different polymorphs of an active pharmaceutical ingredient (API) in its solid form may differ substantially in their physicochemical properties such as refractive index, solubility, dissolution rate, melting point and mechanical properties. Thus, this study evaluated the occurrence of polymorphic contamination in on five batches of MLX APIs and its effect on the solubility and dissolution profiles of APIs and tablets (at a dosage of 15 milligrams), respectively. These are essential properties for predicting the bioavailability of a drug *in vitro*. All samples were characterized by powder X-ray diffraction (PXRD), infrared spectrophotometry (IR-ATR) and differential scanning calorimetry (DSC). The PXRD results (Figure 1) show that MLX L04 is a mixture of polymorphs I and III of MLX, which was corroborated by IR-ATR and DSC analysis. Thus, evaluation of influence of polymorphism was performed by API solubility studies and dissolution profile using the MLX L01 (form I only) and the contaminated MLX L04 (forms I and III) batches. Our results show that presence of a small amount of form III (a metastable more soluble polymorph) in the MLX L04 increases significantly its solubility and rate of dissolution of the meloxicam tablets prepared from it (Figure 2). For these reasons, we recommend solid state characterization techniques such as powder X-ray diffraction to control the polymorphic quality of MLX APIs and tablets containing MLX. This control is mandatory to guarantee the therapeutic effects of this drug.[3]

References:

- [1] Luger, P., Daneck, K., Engel, W., Trummlitz, G., Wagner, K. *Eur. J. Pharm. Sci.*, **4**, 175-187 (1996).
- [2] Coppi, L., Sanmarti, M.B., Clavo, M.C. United States patent US 6967248 B2, 21p, 22 Nov (2005).
- [3] Jacon Freitas, J.T., Viana, O.M.M.S., Vilaca, J.L.J., Bonfilio, R., Doriguetto, A.C., Araújo, M.B., *J. Pharm. and Biomed. Anal.*, submitted article (2015).

Acknowledgments: CAPES; FAPEMIG; CNPq, FINEP

MSPCP04

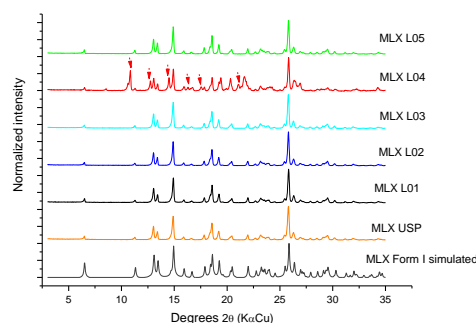


Figure 1: Comparison of XRPD patterns of APIs studied MLX L01 to L05 compared to reference API MLX USP and simulated Form I. Arrows in red on the lot API MLX L04 indicates the degree of diffraction of Form III of MLX reported in literature.

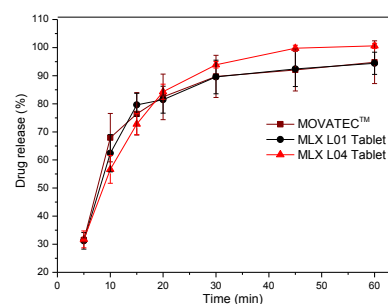


Figure 2: Comparison of dissolution profiles of the tablets formulated with reference MLX and APIs MLX L01 and L04 meloxicam. Sampling conditions: dissolution medium phosphate buffer pH 7.5; paddle apparatus; stirring speed of 75 rpm at 37°C.

Synthesis, structural characterization and isomorphism in the coordination polymer catena-(μ 2-fumarate)-[bis(dimethylsulfoxide)-diaqua-M(II)] where M=Co^{II} or Zn^{II}

I. M. L. Rosa^a, M. C. da Costa^a, C. B. Pinheiro^b and A. C. Doriguetto^a

^aLaboratório de Cristalografia, Instituto de Química, Universidade Federal de Alfenas, Alfenas-MG.

^bLaboratório de Cristalografia, Departamento de Física, Universidade Federal de Minas Gerais, Belo Horizonte-MG.

Coordination polymers based on transition metals and multifunctional organic ligands are potentially important due to their catalytic, electrical, magnetic and gas sorption properties.¹ Rigid dicarboxylate ligands have been explored to generate a variety of coordination polymers with open frameworks.² The fumarate dianion is a useful linker, since its use as a ligand results in linear, rigid, metal-fumarate-metal bridges.³ In this work we report two new 1D coordination polymers obtained by synthesis from Co(NO₃)₂·6H₂O (0.20 mmol) / Zn(NO₃)₂·6H₂O and fumaric acid (0.10 mmol), through the base diffusion method (DMSO and water as solvents). Pale pink pyramidal crystals and colourless cubic crystals were obtained *in situ* and evaluated by single-crystal X-ray diffraction experiments. The measurements were performed using a Gemini-Oxford diffractometer at 150K equipped with MoK α radiation. The main crystallographic data are shown in Table 1.

Table 1. Main crystallographic data for the products.

	<i>trans</i> -[Co(C ₄ H ₂ O ₄)(DMSO) ₂ (H ₂ O) ₂]	<i>trans</i> -[Zn(C ₄ H ₂ O ₄)(DMSO) ₂ (H ₂ O) ₂]
Space Group	P21/n	P21/n
Cell parameters	a=7.7340(4)Å, b=8.9892(4)Å, c=10.7320(5)Å $\alpha=90^\circ$, $\beta=102.108(5)^\circ$, $\gamma=90^\circ$	a=7.7905(4)Å, b=8.9725(4)Å, c=10.7445(6)Å $\alpha=90^\circ$, $\beta=102.379(5)^\circ$, $\gamma=90^\circ$
R1 / wR2 / S	0.0243 / 0.0554 / 1.115	0.0305 / 0.0793 / 1.204

The single-crystal X-ray diffraction data suggested that the complexes are isostructural. The crystal structure is related to [*trans*-M^{II}(C₄H₂O₄)(DMSO)₂(H₂O)₂]_n, with M=Co (**1a**) or Zn (**1b**), and the asymmetric unit contains one metal ion, one DMSO molecule, one water molecule and half fumarate molecule. The metal ions are six-coordinated by two oxygen atoms from water and two oxygen atoms from fumarate ions, in equatorial positions, and two oxygen atoms from the DMSO molecules in axial positions, resulting in an octahedral geometry. The M–O distances range from 2.060 to 2.115 Å for **1a** and from 2.047 to 2.132 Å for **1b**, and O–M–O angles close to 90° for both. The fumarate dianions bridges the neighbouring metal atoms generating a 1D linear chain along [010] direction. The coordination environments of metal ion and a view of the chain structure are depicted in Fig. 1. Inside each chain, the uncoordinated oxygen atom from fumarate anion atom performs a strong intramolecular H-bond with the coordinated water molecule and, between the chains, the same system performs a strong intermolecular H-bond generating a 2D supramolecular framework parallel to (001).

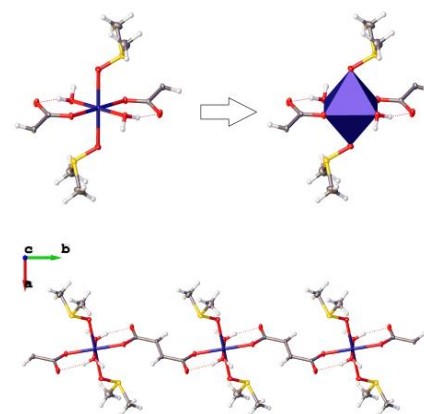


Fig. 1. Octahedral environment of metal center and formation of a linear 1D structure along [010] direction.

[1] (a) A. Facchetti, *Angew. Chem. Int. Ed. Engl.* **50**, 6001 (2011); (b) W. L. Leong, J. J. Vittal, *Chem. Rev.* **111**, 688 (2011).

[2] (a) H. Li, M. Eddaoudi, M. O'Keeffe, O. M. Yaghi, *Nature* **402**, 276 (1999); (b) S. S. -Y. Chui, S. M. -F. Lo, J. P. H. Charmant, A. G. Orpen, I. D. William, *Science* **283**, 1148 (1999).

[3] S. L. Bekö, J. W. Bats, M. U. Schmidt, *J. Coord. Chem.* (2014) doi: 10.1080/00958972.2014.978765

Acknowledgments: FAPEMIG, CNPq, CAPES e FINEP, RQ-MG,

Exploring Lanthanide/Succinate System in the Formation Metal-Organic Frameworks.

R. F. D’Vries^a, I. Camps^b, J. Ellena^a.

^a Instituto de Física de São Carlos, Universidade de São Paulo, CP 369, 13560-970, São Carlos - SP, Brasil.

^b Instituto de Ciências Exatas, Universidade Federal de Alfenas—Unifal-MG, CEP 37130-000 Alfenas, Minas Gerais, Brazil.

Since the appearance of Metal-Organic Frameworks (MOFs), several types of connectors (metallic centers) and linkers (organic ligands) have been used in their design, in search of new compounds with new architectures, topologies and interesting properties.[1-2] Lanthanide metals exhibit properties that make them excellent candidates for the synthesis of new MOFs.[3-4] In this work we present a study of the Ln/succinate system and the template effect in hydrothermal synthesis (Figure 1). It was possible to obtain the compounds $[\text{La}_2(\text{Succ})_3(\text{H}_2\text{O})_3]\cdot 2\text{H}_2\text{O}$ and $[\text{Ln}_2(\text{Succ})_3(\text{H}_2\text{O})_2]$ where Ln = La, Pr, Nd, Sm, Eu, Gd and Tb. The first case is a 2D network with a **sql** plane net topology. The 3D supramolecular network is formed by strong hydrogen bonds, which give rise to a **pcu** network. In the second case, could be synthesized a family of 3D compounds with a **bnn** topology. Both compounds can be obtained in the presence of 5-sulfosalicylate (5-SSA³⁻) as a template agent and only for $[\text{Ln}_2(\text{Succ})_3(\text{H}_2\text{O})_2]$ compounds the presence of toluene in the reaction enables its formation. Also we addresses a systematic synthetic and theoretical study of the formation equilibrium of the molecules reported. The influence of the template agent on the formation of porous MOFs and the luminescent behaviour.

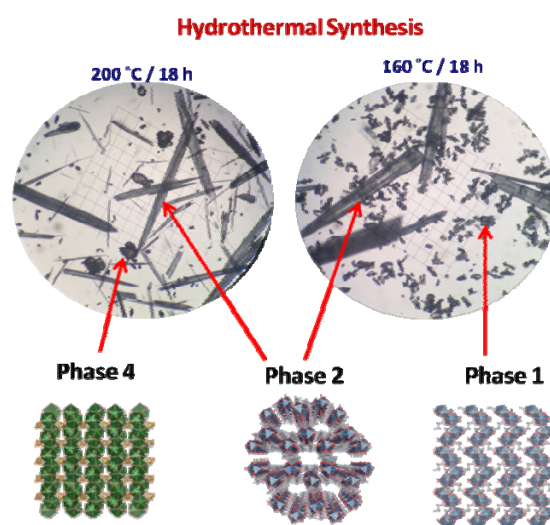


Figure 1: Hydrothermal synthesis crystalline products.

[1] Horike., S.; Kitawa., S. In *Metal-Organic Frameworks: Applications from Catalysis to Gas Storage*; Farrusseng, D., Ed.; Wiley-VCH.: 2011, p 1.

[2] Coronado, E.; Minguez Espallargas, G. *Chem. Soc. Rev.* **42**, 1525, 2013.

[3] Allendorf, M. D.; Bauer, C. A.; Bhakta, R. K.; Houk, R. J. T. *Chem. Soc. Rev.* **38**, 1330, 2009.

[4] D’Vries, R. F.; Camps, I.; Ellena, J. *Cryst. Growth Des.* **15** (6), pp 3015–3023, 2015.

Acknowledgments: R. D. Acknowledges Coordenação de Aperfeiçoamento de Pessoal de Nível Superior for the CAPES/PNPD scholarship from the Brazilian Ministry of Education

ESTRUTURA CRISTALINA DA 2-HIDROXI-4-O-(3,3-DIMETIL)-ALILBENZOFENONA

Gonçalves, C. B.^a, Rosa, I. M. L.^a, dos Santos, M. H.^b Dias D. F.^a, Doriguetto, A. C.^a

^aInstituto de Química, Universidade Federal de Alfenas, Alfenas, Brasil. ^bDepartamento de Química, Universidade Federal de Viçosa, Viçosa, Brasil.

Hidroxibenzenonas têm atraído particular atenção, nos últimos anos, por serem compostos de grande potencial biológico [1-2]. Com o intuito de correlacionar atividade com a estrutura molecular e supramolecular das moléculas, é importante conhecer a estrutura cristalina. Neste sentido determinou-se a estrutura cristalina da 2-hidroxi-4-O-(3,3-dimetil)-alilbenzofenona (C₁₈H₁₈O₃), massa molar 282,32g.mol⁻¹, nomeada LFQM-117 (Figura 1).

Cristais incolores foram obtidos a partir da lenta evaporação do solvente (metanol). As medidas de difração de raios X de monocristal foram realizadas no Laboratório de Cristalografia (LabCri) da UFMG, utilizando radiação Mo-K_α do difratômetro Gemini-Oxford à 150 K. Os principais dados cristalográficos são: Grupo espacial Pbc_a (ortorrômbico), *a* = 13,1235(4) Å, *b* = 6,7511(1) Å, *c* = 32,865(1) Å, *V* = 2911,78(16) Å³, *R*₁ = 0,0513, *wR*₂ = 0,1175 e *Z* = 8.

Os comprimentos e ângulos de ligações observados apresentam valores no intervalo previsto para estruturas similares. Enfatiza-se que, como esperado, devido a repulsão entre as posições 6 e 6' (C6-H e C8-H), o plano passando pelos dois anéis benzofenônicos não são coplanares (ângulo de 54,04°). A Figura 1 mostra a representação da estrutura intramolecular da LFQM-117. Embora tenha átomos capazes (O1, O2 e O3) de atuarem como aceptores de ligações de hidrogênio intermoleculares, o único hidrogênio ligado a átomo eletronegativo está envolvido apenas na ligação de hidrogênio intramolecular (O2-H...O1). Portanto, nenhuma ligação de hidrogênio clássica participa da estabilização do empacotamento cristalino da estrutura, o qual é representado na Figura 2.

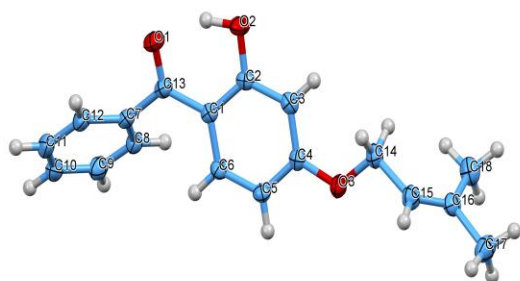


Figura 1: Representação da estrutura cristalina da LFQM-117. Elipsóides a 50% de probabilidade e átomos de H mostrados como esferas de raio arbitrário.

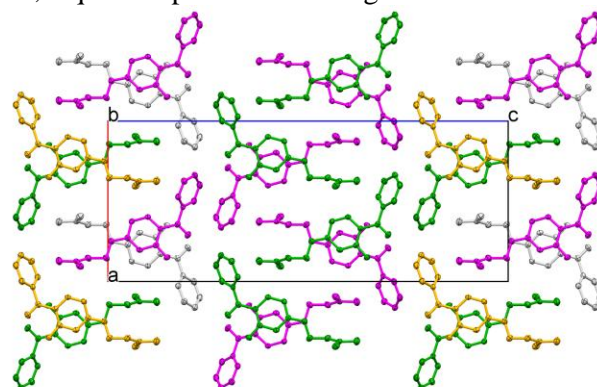


Figura 2: Representação do empacotamento cristalino da LFQM-117 visto no plano ac. O esquema de cores diferencia as 4 moléculas geradas pelas operações de simetria do grupo de espaço Pbc_a.

[1] Dávalos, J. Z.; Guerrero, A.; *et al.* *Journal Org. Chemistry*, **75**, 2564–2571 (2010).

[2] Sancho, M. I.; *et al.* *The Journal Physical Chemistry B*, **119**, 5918–5925 (2015).

Agradecimentos: CAPES; CNPq; FAPEMIG; UNIFAL-MG; LabCri.

Estudio de la microestructura de chapas de aluminio 1050 laminadas a partir de datos de XRD de alta energía de Petra III, Desy

Emanuel A. Benatti*^a, Raúl E. Bolmaro^a, Natalia S. De Vincentis^a, Martina C. Avalos^a, Sangbong Yi^b, Heinz-Günter Brokmeier^b

^a Laboratorio de Ciencia de los Materiales, Instituto de Física Rosario CONICET-UNR, Rosario, Argentina.

^b Clausthal University of Technology-Helmholtz Zentrum Geesthacht, Germany.

La acumulación de defectos microestructurales en materiales sujetos a deformación plástica es fuertemente dependiente de la orientación de los granos además de la cristalografía, el tipo de aleación considerada, el proceso de deformación, etc.. La literatura ofrece algunos ejemplos de esa acumulación anisotrópica^[1, 2], aunque la evaluación cuantitativa de tal almacenamiento de energía en materiales sometidos a deformación plástica severa (SPD) dista mucho de contar con modelos universalmente aceptados. Los experimentos de difracción de rayos X (XRD) constituyen una de las herramientas estándar para estudiar la microestructura de los materiales y los llevados a cabo con luz de sincrotrón son especialmente eficaces en la generación de gran cantidad de datos de los que es posible extraer información de varios parámetros microestructurales.

En la actualidad existen varios modelos que permiten extraer información cuantitativa a partir del ensanchamiento de los picos de un patrón de XRD, siendo dos de los más importantes el método de Williamson-Hall con sus modificaciones^[3-4] y el Convolutional Multi Whole Profile (CMWP), desarrollado por Ungár et al^[4-6], siendo el método CMWP uno de los más confiables para obtener datos cuantitativos sobre parámetros microestructurales como el tamaño de dominio y densidad de dislocaciones.

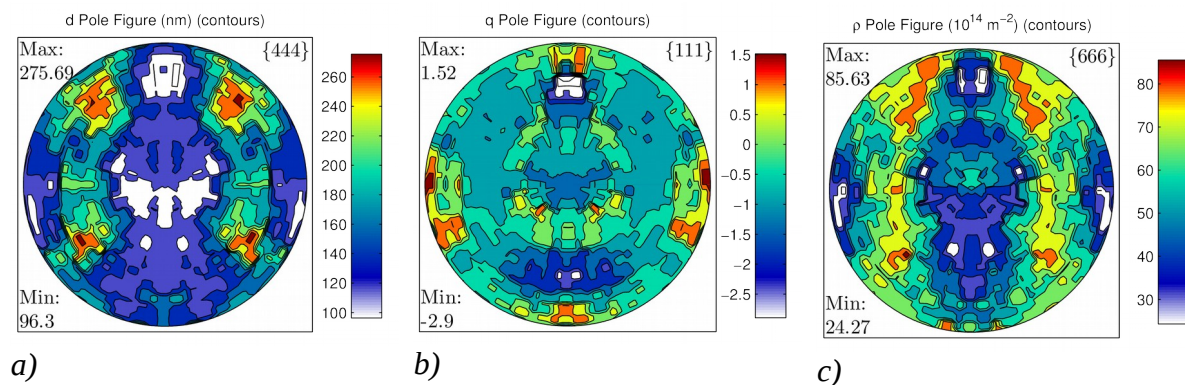


Figura 1: Figuras de polos generalizadas de diferentes parámetros microestructurales:
a) Tamaño de dominio b) Carácter de las dislocaciones (hélice o borde) c) Densidad de dislocaciones

En este trabajo se presentan análisis microestructurales sobre chapas de aluminio 1050 obtenido comercialmente, laminadas al 70 %. Utilizando el método CMWP, se comparan los resultados obtenidos de procesar patrones de difracción completos con los obtenidos al hacer un análisis individual de cada pico del difractograma. A través de la generación de figuras de polos generalizadas se buscó separar la influencia de la cristalografía de la de la orientación de la muestra en la acumulación de defectos.

- [1] S. Diligent, E. Gautier, X. Lemoine, M. Berveiller, Acta mater., **49** 4079-4088 (2001)
- [2] A. Godfrey, N. Hansen, D. Juul Jensen, Metal. Mater. Trans. A, **38** 2329-2339 (2007)
- [3] Williamson, G. K., Hall, W. H., Acta Metall, **1**, 22 (1953)
- [4] Ungár, T., Gubicza, J., Hanák, P., Alexandrov, I., Mat. Sci. and Eng., **A319-321**, 274-278 (2001)
- [5] Ribárik, G., PhD Thesis (2008)
- [6] Ungár, T., Dragomir, I. C., Révész, Á., Borbély, A., J. Appl. Cryst., **32**, 992-1002 (1999)

Bergenin isolated from a new source *Peltophorum dubium* (Spreng.) Taub plants

L. F. Batista¹; E. S. Sanches²; Y. P. Mascarenhas¹; A. C. Mafud^{1*}.

¹ São Carlos Physics Institute, University of São Paulo, São Carlos, Brazil. ² Federal University of Amazonas (UFAM), Department of Physics, Manaus, Brazil. *mafud@usp.br

Bergenin (BERG), a C-glucoside of 4-O-methyl gallic acid, biologically active [1-4], has been isolated for the first time from the *Peltophorum dubium* (Spreng.) Taub plants [to be published]. The purified product was crystallized in solvent, which it was slowly evaporated at room temperature. PXRD pattern was collected to assess the purity of crystalline sample and to obtain the cell dimensions through the Rietveld method [5], with MAUD package (Fig.1A). ($a = 7.79\text{Å}$, $b = 13.93\text{Å}$, $c = 14.29\text{Å}$, orthorhombic system). Orange prism suitable single crystal was selected and measured with $\text{MoK}\alpha = 0.71073\text{Å}$ at 290 K, in a orthorhombic system, space group $P2_12_12_1$, with cell parameters $a = 7.496(5)\text{Å}$, $b = 13.928(5)\text{Å}$, $c = 14.289(5)\text{Å}$ and four units per cell. The difference between the obtained cell parameter 'a' is due to the water molecule in the structure. FT-IR spectra (Fig.1B) shows characteristics bands for the aromatic rings (1467 cm^{-1}), alcohol (1089 and 1378 cm^{-1}), ether (1130 cm^{-1}), phenol (1232 and 1332 cm^{-1}) and ketones (1710 cm^{-1}) group. In addition, a spectra band between 3000 and 3600 cm^{-1} is observed due to the water molecule in the structure.

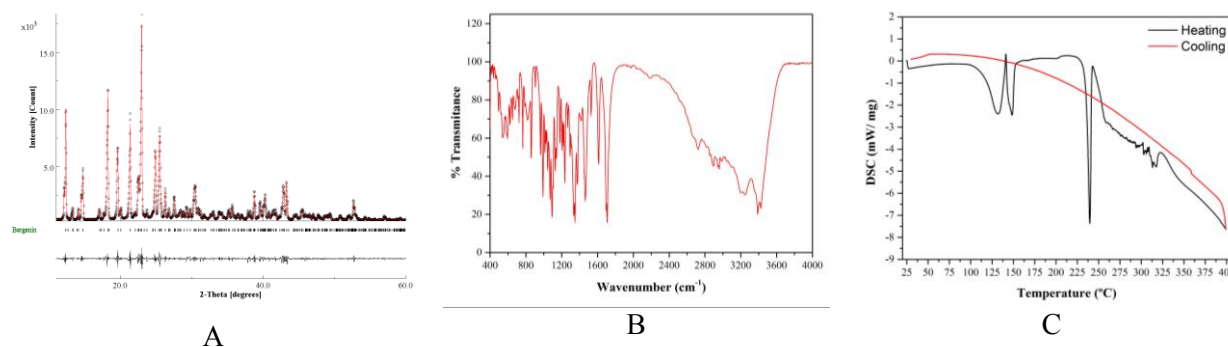


Figure 1: Obtained results of Bergenin: (A) Rietveld plot: experimental, calculated and difference curve data; (B) FT-IR spectra and (C) DSC curve.

The heating curve in the DSC thermogram (Fig.1C) shows two peaks: between 132 and 148°C due to the crystallization, and other, at 240°C is observed a sharp peak related to the phase transition solid-liquid. By the cooling curve, it is noticed that BERG undergoes an irreversible transformation. NMR spectra of ^1H $\{^{13}\text{C}\}$ and $^{13}\text{C}\{^1\text{H}\}$ were performed on a Bruker AC-200 spectrometer (200 MHz). The chemical shifts of the salt obtained by spectrometry ^{13}C (D_2O) was $\delta(\text{ppm})$ 165,7 (C-O-C) 111.0; 117.3; 119.4; 142.2; 149.3; 152.3 (aromatic); 83.0-62.6 (C-glucoside) and ^1H (D_2O) $\delta(\text{ppm})$ 3.35-4.09 (C=O); 7.07 (aromatic); 4.94 (C-glucoside); 3.90 (OCH_3).

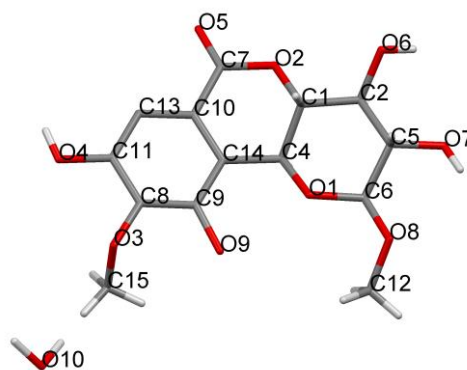


Figure 2: Perspective view of Bergenin, with annotated atoms.

[1] Patel, D. K., et al., Asian Pacific Journal of Tropical Disease, 2, 163-167 (2012). [2] Singh, U., Barik, A., Priyadarsini, K.I., Bioorganic & Medicinal Chemistry, 17, 6008-6014 (2009). [3] Chen, J., et al., Talanta, 72, 1805-1810 (2007). [4] Nazir, N., et al., European Journal of Medicinal Chemistry, 46, 2415-2420 (2011) [5] Rietveld, H.M., Acta Crystallographica, 22,151-152 (1967).

Acknowledgments: FAPESP (Grant 2014/02282-6). CNPq (Grant 302674/2010-1). "Facility for advanced studies of materials/FAMa" (FAPESP Project No.2009/540354).

Análisis de las interacciones intermoleculares no-covalentes en *Trans*-1,4-dicarboxamidaciclohexano (DCA) y *Trans*-1,4-Dibromo-1,4-DCAF. García Reyes^a, G. A. Echeverría^{a,b}, A. C. Fantoni^a, G. M. Punte^a.^a*IFLP (CCT-La Plata), Departamento de Física, Facultad de Ciencias Exactas-UNLP, CC 67-1900, La Plata, Argentina.*^b*Departamento de Ciencias Básicas, Facultad de Ingeniería Universidad Nacional de La Plata 115 y 49, 1900, La Plata, Argentina.*

Las propiedades de las interacciones puente de hidrógeno (PH) resultan de gran importancia en la formación de arreglos estructurales característicos con implicancias en biología, química y ciencia de los materiales [1]. Las interacciones N-H···O=C establecidas entre amidas primarias, como en el caso del grupo carboxamida (CONH₂), presenta interés por ser parte integrante de numerosos sistemas biológicos (principalmente proteínas) y de algunas fibras sintéticas, como en el caso del nylon. Las interacciones N-H···O=C imponen restricciones en la forma que las amidas primarias interactúan, y por ende en la disposición molecular resultante, originando motivos estructurales característicos, dímeros cíclicos del tipo R₂²(8) y cadenas infinitas C(4) [2]. Al respecto, una faceta particularmente interesante de estudiar, es el rol de las interacciones formadas por éste grupo en presencia de otras importantes interacciones no-covalentes como los puentes de hidrógeno débiles o los de halógeno [3, 4] en la determinación de la estructura cristalina. Por este motivo, continuando con una serie de estudios previos, sobre los factores que rigen la conformación molecular y la agregación de ciclohexanos simétricamente sustituidos, en el presente trabajo analizamos la sinergia de las distintas interacciones no-covalentes en los sistemas *Trans*-1,4-dicarboxamidaciclohexano y *Trans*-1,4-dibromo-1,4-dicarboxamidaciclohexano (N-H···O, C-H···O, Br···O) a partir de: datos de rayos X de monocristales, la información estructural disponible en la base de datos *Cambridge Crystallographic Data Base*, el análisis topológico de la densidad de carga electrónica [5] y la energía de interacción o empaquetamiento (según corresponda) [6] calculada en agregados moleculares de distinto número de átomos y en el cristal.

[1] Desiraju, G. R., Steiner, T., *The Weak Hydrogen Bond: In Structural Chemistry and Biology*, IUCr, Oxford (1999r).

[2] Berstein, J., Etter, M.C., Leiserowitz, L., *The Role of Hydrogen Bond in Molecular Assembly en Structure Correlation*, VCH Weinheim, New York (1994).

[3] Cavallo, G., Metrangolo, P., Pilati, T., Resnati, G., Terraneo, G., *Topics in Current Chemistry*, **358**, 1-17 (2014)

[4] Metrangolo, P., Resnati, G., *Halogen Bonding: Fundamentals and Applications*, Springer-Verlag Berlin Heidelberg, New York (2008).

[5] Bader, R. F. W., *Atoms in Molecules: A Quantum Theory*, Clarendon Press, Oxford Science Publications: Oxford (1990).

[6] Boys, S. F., Bernardi, F., *Mol. Phys.* **19**, 553 (1970).

Agradecimientos: UNLP: Proyectos X-577 y X-709, CONICET: PIP 0985, SNRX MINCyT Proyecto RX-AC7. GAE, ACF y GMP son miembros de la CIC del CONICET,

Estudo Cristalográfico de Minerais da região de Volta Grande(MG)A. A. A. E. Queiroz^a, M. B. Andrade^a, J. A. Ellena^a.^a*Instituto de Física de São Carlos, Universidade de São Paulo, São Carlos, Brasil.*

Os minerais apresentam características tecnológicas atrativas a exemplo dos minérios de ferro e cobre, fundamentais para a fabricação de diferentes tipos de aço e fiações; respectivamente. O conhecimento da estrutura cristalina, pode servir de modelo para a obtenção de um análogo sintético, como no caso da menezesita, que é isoestrutural com o composto sintético $Mg_7[MgW_{12}O_{42}](OH)_4 \cdot 8H_2O$.

O Brasil possui uma grande variedade de ambientes geológicos nos quais foram encontrados importantes minerais-gema, como o crisoberilo (na região norte de Minas Gerais, São Paulo e Espírito Santo) e a fluor-elbaíta (em São José da Safira, Minas Gerais), além dos minerais importantes tecnologicamente: a menezesita ($Ba_3MgZr_4Nb_{12}O_{42} \cdot 12H_2O$, no carbonatito de Jacupiranga, São Paulo) e coutinhoíta ($Th_xBa_{1-2x}(UO_2)_2Si_5O_{13} \cdot 3H_2O$, no pegmatito do Córrego do Urucum, Minas Gerais).

Comparada com a diversidade de espécies, há poucas ocorrências brasileiras completamente caracterizadas, sendo apenas 67 aprovadas pela Associação Mineralógica Internacional (IMA). O objetivo deste trabalho é contribuir para a caracterização de espécies minerais raras realizando estudos de amostras provenientes da região de Volta Grande, Minas Gerais.

As amostras foram caracterizadas utilizando um difratômetro de monocristal Kappa-CCD (Enraf-Nonius) com anodo de molibdênio emitindo radiação $MoK\alpha$ ($\lambda = 0.71703 \text{ \AA}$) monocromatizada com cristal de grafite.

Os resultados indicaram que as estruturas cristalográficas das amostras estão relacionadas com a fluorcalciomicrolita ($(Ca,Na)_2(Ta,Nb)_2O_6F$) e rutilo (TiO_2) da região Volta Grande, Minas Gerais (MG). Os parâmetros cristalográficos na difração de raios-X para fluorcalciomicrolita foram: sistema cúbico, $a = 10.39(90) \text{ \AA}$, Volume = $1121,62(2) \text{ \AA}^3$ com grupo espacial Fd-3m. Com relação ao rutilo, se obteve os seguintes parâmetros para a célula reduzida: $a = 4.7027(3) \text{ \AA}$, $b = 4.7102(3)$, $c = 3.1634(2)$, Volume = $69,95(2) \text{ \AA}^3$ e sistema tetragonal com grupo espacial $P4_2/mnm$.

[1] Atencio, D., Coutinho, J. M. V., Doriguetto, A. C., Mascarechas, Y. P., Ellena, J., Ferrari, V. C., *American Mineralogist*, 93, 81-87(2008)

[2] Atencio, D., *Brazilian Journal of Geology*, 45, 143-158 (2015).

[3] Atencio D., *Memória da Mineralogia Brasileira*, Universidade de São Paulo, São Paulo (1999).

Acknowledgments: os autores agradecem ao CNPq e a FAPESP pelo financiamento parcial deste trabalho.

Estudio Estructural por DRX de los Procesos de Absorción de gases en Materiales Nanoporosos, Hexacianometalatos

C. I. Rodríguez^a, Rene Cabrera^a, M. Ávila^a y E. Reguera^a

^aCentro de Investigación en Ciencia Aplicada y Tecnología Avanzada del Instituto Politécnico Nacional, D.F. México.

Resumen

En los últimos años, un número de compuestos interesantes conocidos como MOF's de enrejado flexible, muestran transiciones estructurales reversibles entre baja porosidad y alta porosidad durante la fase adsorción y desorción de las especies huéspedes. En la búsqueda de nuevas estructuras y aplicaciones este trabajo busca obtener nuevos materiales con una estructura 2D con Metales de Transición y ligantes Ciano e Imidazolato.

Introducción

Los MOF's, debido a sus potenciales aplicaciones, han demostrado un enorme potencial para el almacenamiento de los gases, como el CO₂, N₂, CH₄, CO y O, poseen muchas características excepcionales, gran superficie, alta cristalinidad, poros bien definidos, estructuras fácilmente ajustable y funcionalidad química[1].

Nuevas arquitecturas revelan topologías de enrejados porosos y, aportan información muy valiosa para la comprensión de las propiedades de los materiales moleculares. El desarrollo de nuevos materiales absorbentes sólidos podría proporcionar una manera costo-efectiva para la capturar gases.

Los hexacianometalatos de los metales de transición constituyen una familia de materiales moleculares microporosos, cuyas estructuras se basan en un arreglo tridimensional de cadenas Ti-C≡N-Te. El metal Ti, enlazado al átomo de carbono, se encuentra siempre formando bloques moleculares octaédricos [Tiⁿ⁺(CN)₆]⁶⁻ⁿ; en tanto el metal Te, actúa como elemento ensamblador de los bloques octaédricos, y puede tener coordinación octaédrica o tetraédrica. Formando una red porosa con cavidades esféricas de 8.5 Å de diámetro Figura 1, las cuales se comunican por ventanas de aproximadamente 4.5 Å[2].

Se sabe de la coordinación en la estructura del N Piridinico del imidazol con el metal Te, existiendo interacción de fuerzas de Van der Waals entre los anillos del imidazol, dando estructuras 2D. La existencia de acoplamiento π-π entre moléculas vecinas se hace evidente por la presencia de una interacción ferromagnético de baja temperatura para los metales T involucrados de capas vecinas. Si se somete a altas presiones estas estructuras el ligante imidazol puede rotar permitiendo el paso al poros de la estructura, permitiendo almacenar moléculas de gases, tales como, H₂, CO₂, N₂, etc, y existiendo transiciones estructurales[3].

Conclusiones. Existe una necesidad de comprender la respuesta estructural de materiales nanoporosos de cuando son sometidos bajo gas a presión y cambios de temperatura. Sin embargo, hasta la fecha hay muy pocas investigaciones publicadas dedicadas a determinar el comportamiento de los materiales nanoporosos en estas condiciones, para la aplicación en energías renovables.

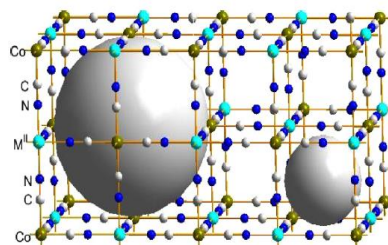


Figura 1: Estructura de Hexaciano cobaltato.

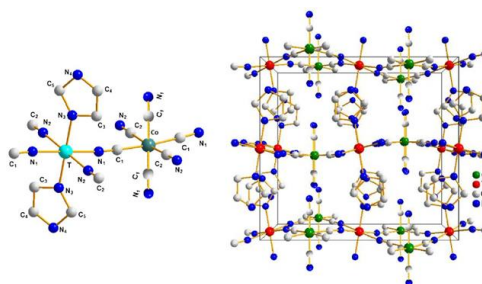


Figura 2: Boceto de estructura esperada

[1]A.A. Lemus-Santana, M. González, M. Knobel, E. Reguera, J. Phys. Chem. A 117 (2013).

[2]J. Roque, Microporous and Mesoporous Materials 103 (2007).

[3] M. González, A.A. Lemus-Santana, J. Rodríguez-Hernández, M. Knobel, E. Reguera, J. Solid State Chem. 197 (2013) 317.

Development of a solid solution of the antiretroviral drugs lamivudine and emtricitabine

Fonseca, JC¹; Tenorio, JC²; Ellena, J²; Alvarez, N³; Ayala, AP⁴

¹Departamento de Farmácia, UFC, Fortaleza-CE, Brazil

²Departamento de Física, IFSC, São Carlos-SP, Brazil

³Facultad de Química, Universidad de la República, Montevideo, Uruguay

⁴Departamento de Física, UFC, Fortaleza-CE, Brazil

Solid solutions could represent a viable alternative to better understanding and controlling structure-property relationships of drugs, in order to optimize their properties for practical applications. These phases consist of different molecular constituents randomly occupying equivalent crystallographic sites, more importantly, the stoichiometry of the solid solutions is not limited to integer values. To some extent, their composition can be controlled by simply varying the relative amount of the active ingredients to afford continuous changes in the structural parameters and properties such as density, solubility, reactivity, etc. [1]. Lamivudine (3TC) and emtricitabine (FTC) are nucleoside analogues reverse transcriptase inhibitor antiretroviral drugs. 3TC exists in two main crystalline forms, being form I a lamivudine hydrate, whose asymmetric unit contains one water and five 3TC molecules [2]. FTC has an extremely similar molecular structure compared to 3TC, differing by a single fluorine atom, which is only present in the FTC molecule [3]. Due to the similarities in structure and molecular size of these drugs, 3TC and FTC are good candidates for the obtainment of a solid solution, resulting in a new compound with completely different properties [4]. This work reports the development and characterization of a solid solution containing 3TC and FTC. The solution was obtained by slow evaporation and solvent assisted mechanical activation. The stability concentration range of solvent/solute solid solution was also investigated by solvent assisted mechanical activation. The process was monitored and characterized by scanning electron microscopy, infrared and Raman spectroscopies, powder and single crystal X-ray diffraction, and thermal analysis, using thermogravimetry, differential scanning calorimetry and hot-stage polarized microscopy. Thus, crystal engineering contributed to the rational design of a solid-solution comprising 3TC and FTC in a wide range of concentrations, which had its crystalline structure elucidated. Multicomponent crystals are a vast land for the development of new materials with different physical and chemical properties, which can be rationally tailored by varying the crystal composition. A new solid solution of organic compounds was obtained using simple execution techniques, supported with the possibility of modulating the concentration of drug inside the crystalline structure.

[1] Lusi, M; Vitorica-Yrezabal, I; Zaworotko, M. *Cryst. Growth Des*, ASAP, (2015)

[2] Harris, R; Yeung, R; Lamont, B; Lancaster, R; Lynn, S; Staniforth, S. *J Chem Soc, Perkin Trans. 2*, 2653 – 2659 (1997)

[3] Roey, P; Pangborn, W; Schinazi, R; Painter, G; Liotta, D. *Antiviral Chem & Chemo* 4(6), 369-375 (1993)

[4] Schur, E.; Nauha, E.; Lusi, M.; Bernstein, J. *Chem.—Eur. J.*, 21 (2015)

Acknowledgments: Financial Support FUNCAP; CAPES; CNPq

Complejos de Fe^{III} conteniendo ligandos iminicos organometálicos del tipo N₂O, con potenciales aplicaciones magnéticas.

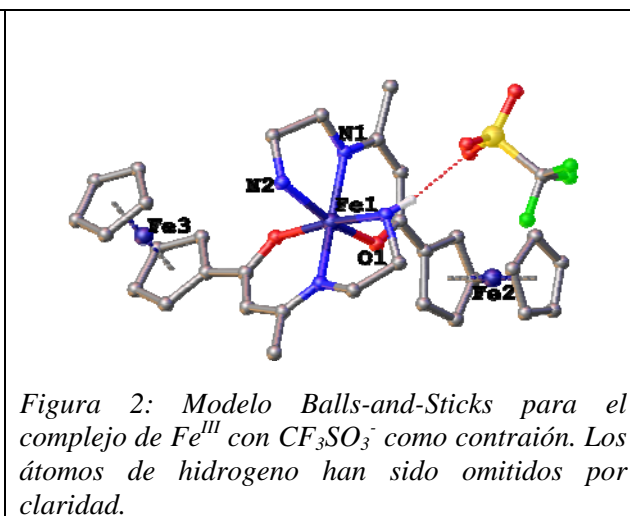
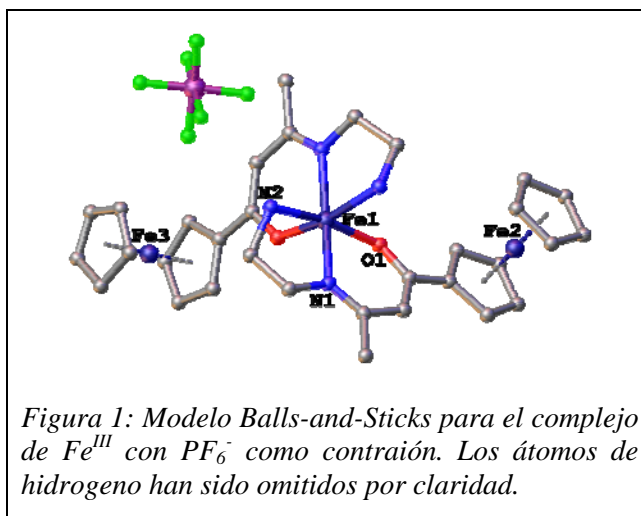
D. González^a, V. Artigas^a, M. Fuentealba^{*a},

^aInstituto de Química, Pontificia Universidad Católica de Valparaíso.

Campus Curauma, Avenida Universidad 330, Valparaíso, Chile

E-mail: mauricio.fuentealba@ucv.cl

Con el objetivo de desarrollar nuevos compuestos de coordinación con potencial respuesta *spin crossover* (SCO) [1], hemos realizado la preparación de siete nuevos complejos octaédricos de Fe^{III} conteniendo ligandos organometálicos tipo base de Schiff N₂O. Estos ligandos han sido sintetizados mediante una reacción de condensación entre la 1-(ferrocenil)-1,3-butanodiona, la etilendiamina [2] o la 2-picolilamina [3]. Los respectivos complejos de Fe^{III} han sido sintetizados mediante la técnica de reflujo o difusión lenta, empleando diferentes solventes, contraiones y precursores de Hierro(III) con el fin de modular las propiedades magnéticas en función de estas variables.



La estructura cristalina y molecular de algunos de estos complejos ha sido determinada mediante la técnica de difracción de rayos-X de monocristal (ver fig.1 y 2), además del estudio de las interacciones intermoleculares mediante las superficies de Hirshfeld utilizando el software CrystalExplorer[4]. A través de estos resultados cristalográficos es posible conocer la influencia de la naturaleza del ligando en las distancias Fe-N y Fe-O en la obtención de complejos de alto espín (*HS*) y bajo espín (*LS*) y la variación de estos estados en función de los distintos contraiones.

[1] Tissot, R Berton, E. Collet, L. Toupet, M-L Boillot *J. Mater. Chem.*, **21**, 18347-18353 (2011).

[2] Trujillo, A., Sinbandhit, S., Toupet, L., Carrillo, D., Manzur, C., Hamon, J.-R. *J. Inorg. Organomet. Polym.*, **18**, 81-99 (2008) .

[3] De-Suo, Yang, *Journal of Chemical Crystallography*, **37**, 6 (2007).

[4] Snackman. M. A.. Javatilaka. D.. *Crvst. Eng. Comm.* **11**. 19(2009).

Agradecimientos:

Los autores agradecen al proyecto FONDECYT N° 1130640 por el financiamiento otorgado.

Además se agradece al proyecto FONDEQUIP EQM120095 por el financiamiento para el difractómetro de Rayos-X de monocristal BRUKER D8 QUEST.

V. Artigas agradece a BECA CONICYT N° 21130944.

ESTUDIO ESTRUCTURAL DE COMPLEJOS DE Fe(III) CONTENIENDO LIGANDOS HEXADENTADOS BASE DE SCHIFF N₄O₂.

D.Villaman^a, V. Artigas^a, M. Fuentealba^{*a}.

^a Facultad de Ciencias, Instituto de Química, Pontificia Universidad Católica Valparaíso, Chile
Email: david.villaman.f@gmail.com, Mauricio.fuentealba@ucv.cl

Desde la pasada década diversos grupos de investigación [1a] han estudiado las propiedades ópticas, magnéticas y estructurales de complejos con esfera de coordinación del tipo [FeN₄O₂] y [FeN₄O₂]⁺ conteniendo ligandos base de Schiff. Estos complejos han presentado estados de *High-Spin* (HS), *Low-spin* (LS) y Spin-Crossover (SCO). Este último estado permite el desarrollo de nuevos materiales moleculares biestables [1b].

Con estos antecedentes en mente se propuso estudiar las propiedades estructurales en complejos de Fe(III), por consiguiente se efectuó la síntesis con ligandos hexadentados base Schiff del tipo N₄O₂ [2]. La síntesis *template* se realizó mezclando salicilaldehído sustituidos (Br [1]⁺, Cl [2]⁺) en posición 5, con 1,2-Bis(3-aminopropylamino)ethane. La obtención de monocristales se realizó por difusión lenta de éter dietílico sobre una solución saturada del complejo en metanol o por evaporación lenta de una solución saturada del complejo en metanol.

El análisis de las estructuras cristalinas se realizó por difracción de rayos X de monocristal, para los complejos mostrando grupos espaciales quirales P2₁, en donde se observa el enantiomero Λ (lambda) para cada estructura. Por otro lado, para el complejo con solvente, se reveló el grupo espacial centro simétrico C2/c. Con el fin de recopilar información sobre las interacciones intermoleculares, se realizaron las superficies de Hirshfeld, mostrando los efectos cooperativos intermoleculares entre los complejos de Fe(III), el contraíón y/o la molécula de solvente, para ello se utilizó el software Cristalexplorer [3]. Actualmente se están realizando estudios de dicroísmo circular para mostrar la quiralidad de estos complejos.

Referencias:

[1] a) Zhang, L.; Xu, G.-C.; Xu, H.-B.; Zhang, T.; Wang, Z.-M.; Yuan, M.; Gao, S. *Chemical communications* (Cambridge, England) 2010, 46, 2554–2556 b) Gamez, P.; Costa, J. S.; Quesada, M.; Aromí, G. *Dalton transactions* (Cambridge, England: 2003) 2009, 7845–7853.

[2] R.Pritchard, S.A.Barrett, C.A.Kilner, M.A.Halcrow (2008) *Dalton Trans.*, 3159.

[3] M. A. Spackman, D. Jayatilaka, (2009) *CrystEngcomm* 11, 19.

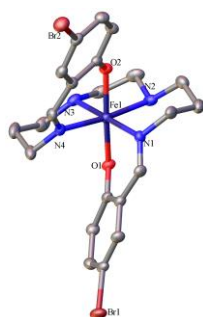


Figura 1: Ortep para los complejos Fe(III) [1]⁺, omitiendo hidrógenos, contraíón.

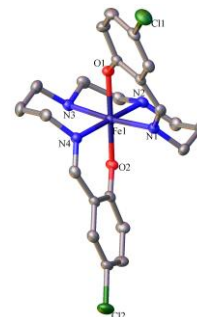


Figura 2: Ortep para complejo Fe(III) [2]⁺, omitiendo hidrógenos, contraíón y solvente.

Tabla 1: Distancia de enlace y parámetro de distorsión octaédrico de los complejos [1]⁺ y [2]⁺.

Grupo Espacial	[1] ⁺ PF ₆	[2] ⁺ PF ₆	[2] ⁺ PF ₆ ·Et ₂ O	Ref. 2
	Monoclínico P2 ₁	Monoclínico P2 ₁	Monoclínico C2/c	Ortorrómico Pccn
T (K)	293	293	293	293
Fe-O1	1,890(3)	1,877(2)	1,876(3)	1,894(10)
Fe-O2	1,879(3)	1,885(2)		
Fe-N1	1,955(3)	1,956(3)	1,955(3)	2,090(13)
Fe-N2	2,012(3)	1,958(3)	2,016(3)	2,183(13)
Fe-N3	2,017(3)	2,007(3)		
Fe-N4	1,966(3)	2,011(3)		
Σ/°	25,71	25,23	28,92	43,8

$${}^1_1-x, +y, 1/2-z; {}^2_2-x, +y, 1/2-z \quad \sum_{hkl} |F_{hkl}|^2 \quad \text{--- Low-Spin (LS)} \quad \text{--- High-Spin (HS)}$$

Agradecimientos:

M. Fuentealba agradece a Proyecto Fondecyt N° 1130640 y a Fondecip EQM120095.

V. Artigas y D. Villaman agradecen a Becas Conicyt.

The Pectin Methyltransferase Structure from the Sugar Cane Weevil, *Sphenophorus levis*.Danilo Elton Evangelista^a, Andre Godoy Schutzer^a, Igor Polikarpov^a.^aSão Carlos Institute of Physics, University of São Paulo, São Carlos, Brazil.

Pectin is the major component of the middle lamella, contributing to the structure support and protection of plant tissues. Pectin is mainly composed of galacturonic acid units linked by α -1,4 glycosidic bonds, which is partially esterified by methyl groups (1). This polysaccharide is naturally degraded by pectinases, such as the Pectin-methyltransferase (PME), which removes methyl-ester groups (1). Pectinases are involved in the plant cell wall development, micro-organisms enzymatic arsenal used to attack plants and have also a wide range of application in the industrial sector (1). Recently, studies of a cDNA library from *Sphenophorus levis*, the "Sugar Cane Weevil", indicate the presence of one PME gene, which we named SI-PME (2). Considering the importance of this enzyme in biological studies and their several industrial applications, we promote X-rays diffraction studies of this recombinant enzyme. The ORF was linked into the pPICZUB expression vector and used to transform competent *Pichia pastoris*. The recombinant clones produced a large amount of the recombinant enzyme, which was purified by affinity chromatography in a nickel column. The recombinant enzyme activity was confirmed by halos of modified substrate by the enzyme incubated in a matrix gel containing 1% esterified-polygalacturonic acid. The sitting-drop vapour-diffusion method was used to crystallization screens with commercial kits. After 10 days, crystals were observed in the Index kit (Hampton) with 25% (w/v) PEG 3,350, 0.1 M citric acid pH 3.5 as a crystallization solution and (1:1 v/v) protein-to-crystallization solution ratio. Data were collected at Bruker APEX DUO single-crystal diffractometer system equipped with KAPPA goniometer and APEX II CCD detector. The exposure time was set to 20 seconds for data collection. The point group determination and data collection strategy were performed with PROTEUM2 software. Data was integrated to 2.1 Å with SAINT and scaled with SADABS. Data statistics collection and space group determination were obtained with XPREP. The solvent content was calculated using Matthews coefficient, as implemented in phenix.xtriage. Protein was solved with Phaser through an ensemble of models generated with phenix.ensemble and phenix.sculptor (3). The data set was indexed in the monoclinic C2space group. After integration, reflections were scaled and merged 22,383 total reflections, with a total R_{merge} of 5.2%: the completeness of data set was 96.6%. Based on the systematic absences, the space group was found has C121, with unit-cell parameters $a=122.181$, $b=82.213$, $c=41.176$ and $\beta=97.48$. Assuming one protein molecule in the asymmetric unit cell, the Matthews coefficient was calculated as $2.71 \text{ \AA}^3 \text{ Da}^{-1}$. This corresponds to 54.7% of solvent content in the crystal (4). The protein was solved with Phaser using an ensemble of models based on the structures with PDB ids: 3GRH, 1XG2, 1GQ8 and 3UW0 all selected by HHpred. This process resulted in a unique solution, with satisfactory statistics in the given space group. The SI-PME structure presents the right-handed parallel β -helix fold, already described for the others pectin methyltransferases. A detailed comparative analysis between the PME structures from different phylogenetic origins is in progress.

[1] Kashyap, D., R., et al., *J. Bioresource Technology*, **77**, 215-227 (2001).

[2] Evangelista, D., E., et al., *J. Insect Science*, **0**, 1-8 (2015).

[3] Adams, P., D., et al., *J. Acta Crystallographica Section D*, **66**, 213-221 (2010).

[4] Matthews, B., W., *J. Molecular Biology*, **33**, 491-497 (1968).

Acknowledgments: This work was supported by FAPESP and CAPES.

Abstract printed as received, without corrections.

Crystallization and preliminary X-ray diffraction analysis of a xylose isomerase from *Bifidobacterium adolescentis*

C. V. dos Reis ^a, A. Bernardes ^a and I. Polikarpov^a

^a Instituto de Física de São Carlos, Universidade de São Paulo, 400, Trabalhador Saocarlense, São Carlos, São Paulo, 13566-590, Brasil.

Xylose isomerase (EC 5.3.1.5) is a key enzyme in xylose metabolism, which is industrially important for transformation of glucose and xylose into fructose and xylulose, respectively. The *Bifidobacterium adolescentis* *xylA* gene (NC_008618.1), encoding for xylose isomerase (XI), was cloned and the enzyme was overexpressed in *Escherichia coli*. Purified recombinant XI was crystallized using sitting-drop vapor diffusion method with polyethyleneglycol 3350 as precipitating agent. A complete native data set to 1.7 Å resolution was collected using synchrotron radiation source. The crystals belong to the orthorhombic space group P2₁2₁2 and have unit cell parameters a= 88.78 Å, b= 123.98 Å and 78.63 Å. The initial modeling and refinements are in course. Firstly, we confirm the usual folding for enzymes set in this xylose isomerase group: TIM barrel.

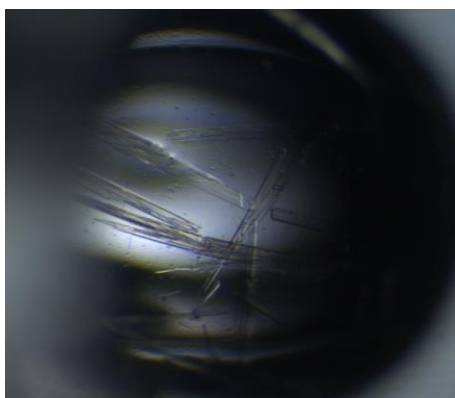


Figure 1: Crystals of *B. adolescentis* xylose isomerase obtained during initial screening

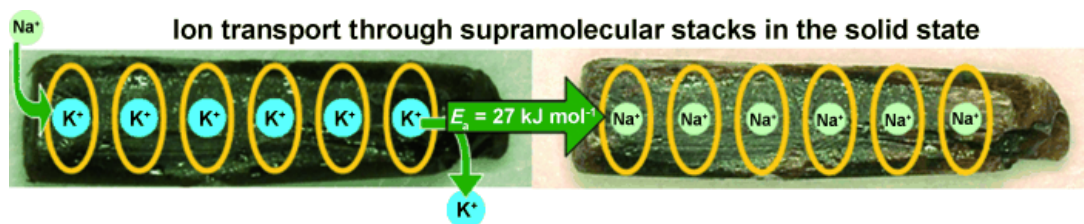
Acknowledgments: Brazilian National Synchrotron Light Source (LNLS) and Laboratório Nacional de Biociências (LNBio, CNPEM). This work was supported by Fundação de Amparo a Pesquisa do Estado de São Paulo (FAPESP) and Conselho Nacional de Desenvolvimento Científico e Tecnológico (CNPq).

Abstract for 2015 LACA Meeting

Ion Transport through Supramolecular Channels in Single Crystals

Cyrille D. Assouma, Aurlien Crochet, Yvens Chérémond*, Bernd Giese, and Katharina M. Fromm
Environment Research Unit, Faculty of Science, State University of Haiti., Port-au-Prince
yvens.cheremond@fds.edu.ht

Reactions in single crystals of supramolecular assemblies are most often associated with the breaking of the crystals into polycrystalline or amorphous materials, induced by the major transformations and related strain during the reaction.¹ Single-crystal to single-crystal transformations are possible by ion-exchange and transport reactions through supramolecular channels that are composed of crown ether molecules and use trihalide ions as scaffolds. In this study we used trihalide anions of the type X^{3-} , X_2Y^- , and XY_2^- ($X=I$ and $Y=Br$) as structural pillars, which induce the stacking of dibenzo[18]crown-6 molecules.



Kinetic measurements² of ion transport at different temperatures provide activation energy data (See figure above) and show that a very fast exchange of K^+ ions with Na^+ ions occurs. In this purpose, the synthesis, crystal structures, measurements methodologies and the kinetic results will be presented.

Abstract printed as received, without corrections.

MSPCP18

References

- ¹ a) S. Takahashi, H. Miura, H. Kasai, S. Okada, H. Oikawa, H. Nakanishi, *J. Am. Chem. Soc.* 2002, 124, 10944–10945.
b) G. J. Halder, C. J. Kepert, *Aust. J. Chem.* 2006, 59, 597–604.
- ² C. D. Assouma, A. Crochet, Y. Chérémond, B. Giese, K.M. Fromm, *Angew. Chem. Int. Ed.*, 2013, 52: 4682–4685.

TRANSICIONES DE FASES CÚBICAS EN SISTEMAS LÍPIDO/AGUA

Eucarys JIMÉNEZ, Tomás BONILLO, Elisamelis MARTÍNEZ, Rodolfo VARGAS.

Unidad de Estructura Molecular. Instituto de Estudios Avanzados (IDEA). Caracas, Venezuela.

ejimenez@idea.gob.ve

Resumen: Los sistemas lípido/agua presentan una amplia variedad de fases cristalinas periódicas a 1, 2 y 3 dimensiones. Tales fases corresponden a estructuras laminares, hexagonales y cúbicas respectivamente; y han sido establecidas, en su gran mayoría, por técnicas de difracción de rayos X, observándose transiciones y relaciones epitaxiales entre fases. Esas transiciones de fase en sistemas lípido/agua dependen usualmente de cambios liotrópicos y/o termotrópicos (fenómeno conocido como Polimorfismo Lipídico).

En los sistemas lípido-agua, se han encontrado siete estructuras cúbicas: Q^{230} (grupo espacial $Ia3d$), Q^{212} (g.e. $P4332$), Q^{223} (g.e. $Pm3n$), Q^{224} (g.e. $Pn3m$), Q^{227} (g.e. $Fd3m$), Q^{229} (g.e. $Im3m$) y Q^{225} (g.e. $Fm3m$). Estas fases cúbicas pueden ser de dos tipos principalmente: 'bicontinuas' y 'micelares'. Sólo las fases Q^{224} (bicontinua) y Q^{227} (micelar) son estables en exceso de agua, tal como ocurre en las membranas biológicas.

Las fases cúbicas de lípidos Q^{224} (g.e. $Pn3m$) y Q^{227} (g.e. $Fd3m$) son de tipo II (agua en aceite) [1,2]. La Q^{224} es abierta (bicontinua) y descrita por dos laberintos disjuntos de cilindros de agua en una matriz de grasa, unidos 4x4 en juntas tetraédricas. Por su lado, la Q^{227} es cerrada (micelar) descrita por dos tipos de esferas de agua en una matriz de grasa, dispuestas en arreglos tetraédricos unas con respecto a otras.

En este trabajo estudiamos posibles mecanismos de transición de Q^{224} a Q^{227} , a través de la evolución de cilindros de agua a esferas y viceversa, transición que ha sido observada por Nieva *et al* [3] en dispersiones de fosfolípidos:colesterol:diacilglicerol, y comentadas por otros autores [4,5].

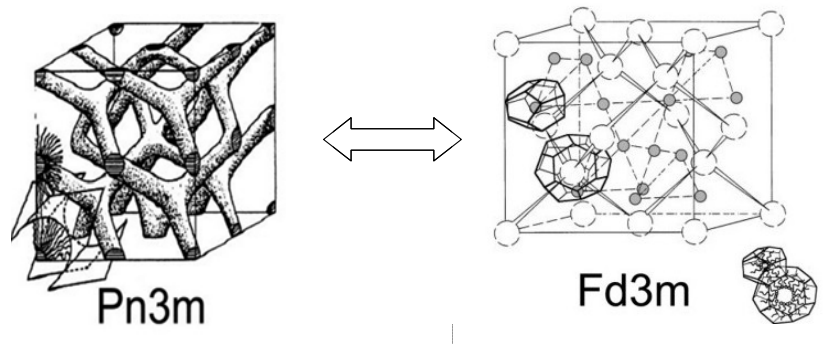


Figura 1. Estructuras con simetría cúbica de Q^{224} y Q^{227}

El estudio de las estructuras cúbicas se ha incrementado en el tiempo, debido a la variedad de estructuras y utilidad en diversas áreas como: técnica de cristalización de proteínas, encapsulación de drogas y entregas terapéuticas; además de las vinculaciones con los procesos biológicos.

Palabras clave: Fases Cúbicas, Difracción de rayos X, Mecanismos de transición.

- 1) Mariani P., Luzzati V., Delacroix H. 204, 165-189. (1988).
- 2) Luzzati V., Vargas R., Gulik A., Mariani P., Seddon J., Rivas E. Biochemistry. 31 (1): 279-285. (1992).
- 3) Nieva J., Alonso A., Basáñez G., Goñi F., Gulik A., Vargas R., Luzzati V. FEBS Letters 368: 143-147. (1995).
- 4) Luzzati V., Vargas R., Mariani P., Gulik A., and Delacroix H. Journal Molecular Biology. 229: 540-551. (1993).
- 5) Luzzati V., Delacroix H., Gulik-Krzywicki A., Mariani P., Vargas R. Studies in surface science and catalysis. ELSEVIER. Terasaki O (Ed). Amsterdam. 17-39.(2004)

MSPCP19

MSPCP19

Structural Transitions Induced by Gas Pressure and Temperature in Flexible Framework Nanoporous Materials

René Cabrera^a, C. I. Rodríguez^a, M. Ávila^a y E. Reguera^a

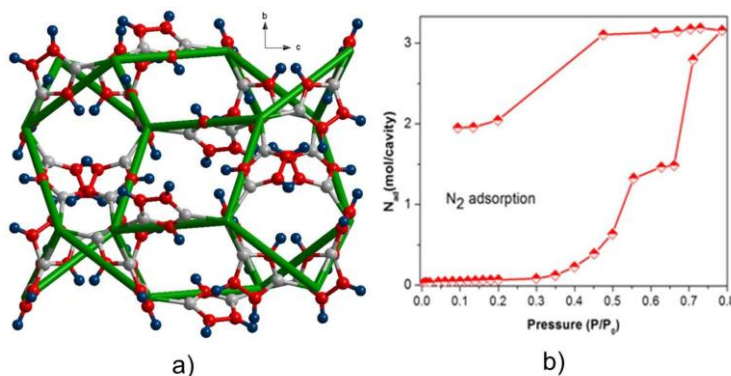
^aCICATA - IPN, D.F. México.

Abstract. The most of nanoporous materials reported to date have been found to exhibit little structural changes during guest exchange. In recent years, however, a number of interesting compounds known as flexible framework nanoporous materials have been discovered, which show reversible structural transitions between low porosity and high porosity phases during the adsorption and desorption of guests. The functional properties of these materials are closely related to their crystal structure and, particularly, to the structural transitions induced by thermal energy and pressure. Nevertheless, until now there are very few published investigations dedicated to determining this behavior. So, in this project, the possible structural transitions for a series of flexible framework nanoporous materials as consequence of gas pressure in the porous framework and changes in the temperature will be studied.

The structural information to be obtained and its correlation with the materials adsorption, thermal and spectroscopic properties for the considered series of materials have no precedent in the available scientific literature. Such information is relevant for the potential applications of these porous solids, such as gases storage, smart membranes and others.

Introduction. Open framework materials, often called nanoporous materials have attracted considerable attention because of their structural functions and physical properties. Their frameworks are extended by coordination linkages involving metal ions, multidentate bridging ligands, and co-ligands, which allow high regularity, flexibility, and diversity in rationally combining a wide range of components [1]. The scope for new open framework materials has recently been expanded through the developments in the field of hybrid metal organic frameworks (MOFs), attracting considerable interest due to their spectacular properties and applications in luminescence, ionic conduction, and biomedical uses [2, 3]. MOFs are, in fact, coordination polymers, that can be built using molecular blocks linked by metal ions. Due to their structure, MOFs present flexible frameworks [4], which favor temperature and/or pressure driven structural transitions.

Structural Transitions in Flexible Framework Materials. Flexible framework solids typically exhibit bonds with sufficient flexibility to adopt diverse ligand conformations as well as varied framework topologies. In porous materials of molecular nature, the lateral substituent groups, not participating in the coordination bonds, serve as bond directing agents to produce different porous framework topologies, with tunable cavity shape and volume [3, 4]. These substituent groups are naturally found oriented toward the center of the cavity in order to minimize the material free space. Under the pressure of guest species or as a thermal energy effect, these substituent groups can be moved out of the cavity, increasing its available volume. In the recorded gas adsorption curves this effect is observed as a series of steps in the adsorption process combined with a pronounced hysteresis with a step-like behavior. Figure 3a shows the cavity for cobalt imidazolate where the imidazole rings occupy the cavity volume. We have shown [4] that an increase of N₂ pressure leads to the ligand rotation, liberating the cavity volume and allowing the entrance of nitrogen molecules to the available free space (Figure 3b).



[1] L. Q. Ma, J. M. Falkowski, C. Abney & W. B. Lin, *Nature Chem.* (2010), 2, 838-846.

[2] P. Horcajada et al., *Nature Mat.* (2010), 9, 172-178.

[3] J. T. Culp, C. Madden, K. Kauffman, F. Shi & C. Matranga, *Inorg. Chem.* (2013), 52, 4205.

[4] C. Vargas, M. Ávila, J. Roque, J. Hernández & E. Reguera, *Micropor. Mesopor. Mater.* (2011)

DETERMINAÇÃO ESTRUTURAL DO COMPLEXO N,N'-(etano-1,2-diil)bis(1-(1H-imidazol-2-il)metanimina)cobre(II) perclorato.

S.F.F.Santos^a, D.Pereira^b, A.M.C.Ferreira^b, R.H.A. Santos^a.

^aInstituto de Química de São Carlos, Universidade de São Paulo, São Carlos, Brasil.

^bInstituto de Química, Universidade de São Paulo, São Paulo, Brasil.

Aplicações de nanomateriais em biossensores têm recebido muito interesse nos últimos anos. Entre os vários tipos de biossensores estudados, sensores de glicose têm recebido destaque devido a sua importância em diagnósticos clínicos¹. Este trabalho tem como objetivo apresentar a determinação da estrutura do complexo N,N'-(etano-1,2-diil)bis(1-(1H-imidazol-2-il)metanimina)cobre(II) perclorato, que será utilizado na produção de filmes para obtenção de sensores de glicose.

Para a escolha de monocristais, foi usado um microscópio de luz polarizada e para a obtenção dos dados das intensidades dos feixes difratados, utilizou-se o difratômetro Enraf-Nonius Kappa CCD monocromatizada por grafite, à temperatura ambiente. A resolução da estrutura foi realizada pelos métodos diretos utilizando o sistema WingX², e o modelo foi refinado (usando SHELX97³) por mínimos quadrados usando matriz completa em F².

Os dados de difração de raios X do composto, com fórmula química [Cu₂(C₁₀H₁₂N₆)₂](ClO₄)₄, foram obtidos à temperatura de 293K, com monocristal de dimensões 0,13 x 0,17 x 0,34 mm³. Para a coleta das intensidades utilizou-se a radiação MoK α ($\lambda = 0,71073\text{\AA}$). Os parâmetros cristalográficos obtidos foram: sistema cristalino triclinico, grupo espacial P $\bar{1}$. Os parâmetros cristalográficos são: a = 8,5992(5), b = 13,1647(8), c = 15,5461(10)\AA, Z = 2 moléculas/célula unitária, V = 1715,71(18)\AA³ e F(000) = 964. Foram coletadas 6283 reflexões sendo 5002 consideradas observadas [I > 2.0 σ (I)].

A representação da molécula com os átomos identificados está apresentada na Figura 1.

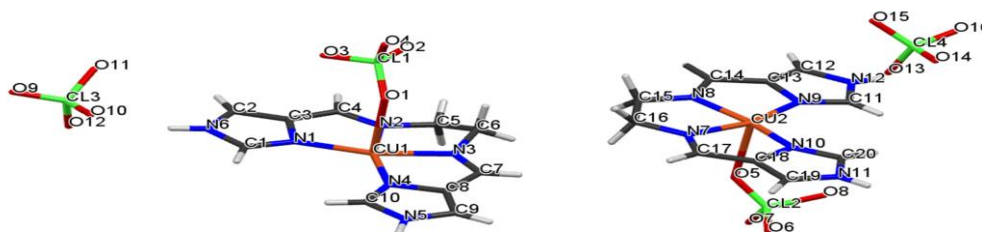


Figure 1: Representação da unidade assimétrica do N,N'-(etano-1,2-diil)bis(1-(1H-imidazol-2-il)metanimina)cobre(II) perclorato. com os átomos de identificados.

A estrutura do [Cu₂(C₁₀H₁₂N₆)₂](ClO₄)₄, consiste de 2 moléculas independentes por unidade assimétrica gerando 4 por cela unitária, num arranjo molecular feito por unidades discretas. O final do refinamento foi considerado quando o deslocamento/ erro tornou-se $\leq 0,01$, e com as densidades eletrônicas residuais mínima e máxima de -0,63 e 1,59 e/\AA³ respectivamente, próximas do átomo de Cu, confirmando que todos os átomos foram identificados. O modelo final mostrou um índice de discordância de R₁ = 0,0696, R_w = 0,2341 e S = 1,06. Os resultados das distâncias e dos ângulos interatômicos das ligações obtido pelo PLATON⁴ estão de acordo com os valores normais e esperados.

¹ SANTOS, J. C. C. **Imobilização da enzima glicose oxidase em filmes nanoestruturados para aplicação em biossensores.** 94p. Dissertação. Universidade de São Paulo, São Carlos, 2012.

²FARRUGIA, L,J, **WinGX-Version 2013,3**, J, Appl, Cryst, 45, 849-854, 2012,

³SHELDRICK, G,M,, **SHELX97 Program for the Solution and Refinement of Crystal Structures**, University of Göttingen, Germany, 2012

⁴ SPEK, A,L, (2009) Acta Cryst, D65, 148-155, **PLATON – A Multipurpose Crystallographic Tool** Utrecht University, Utrecht, The Netherlands, A,L,Spek (2011).

Agradecimento: FAPEMA e CNPq.

Cristal structure of bimetallic cobalt complexes: looking for new valence tautomers

J. O. S. Mendes^a, M. A. Ribeiro^b, C. B. Pinheiro^a.

^aDepartamento de Física, Universidade Federal de Minas Gerais, Belo Horizonte, Brazil.

^bDepartamento de Química, Universidade Estadual de Campinas, Campinas, Brazil.

Electronic labile molecules have distinct electronic states accessible under a given set of thermodynamic conditions, which allow switching between one or other state by applying an external perturbation (*e.g.* temperature change, pressure or light irradiation).^[1] Inorganic complexes that show valence tautomerism (VT) are a subclass of electronic labile materials. Examples of these materials are complexes of cobalt and semiquinones (SQ^{•-}). In these complexes, external perturbation induces an equilibrium of the type $ls\text{-Co}^{3+}(\text{SQ}^{\bullet-})(\text{Cat}^{2-}) \rightleftharpoons hs\text{-Co}^{2+}(\text{SQ}^{\bullet-})_2$, where Cat^{2-} = catecholate, with electronic transition between ligand and metal.^[2] Aiming to achieve new valence tautomers, dinuclear complexes of cobalt and naphthoquinones were synthesised and characterized by X-ray diffraction techniques. Naphthoquinones and quinones show similar structural and electronic properties; nonetheless, naphthoquinones have an extra aromatic ring that allows π -stacking interactions between neighbouring molecules.^[3] Two new bimetallic cobalt and bisnaphthoquinones complexes [Co(BiLaw)₂(Phen)] and [Co₂(MBHN)₂(Phen)₂], where BiLaw = Bis(2-hydroxy-1,4-naphthoquinone) and MBHN = 2,2'-Methylenobis(2-hydroxy-1,4-naphthoquinone), were synthesized and analyzed by X-ray diffraction techniques at different temperatures, their crystal structures are shown in *Figure 1*.

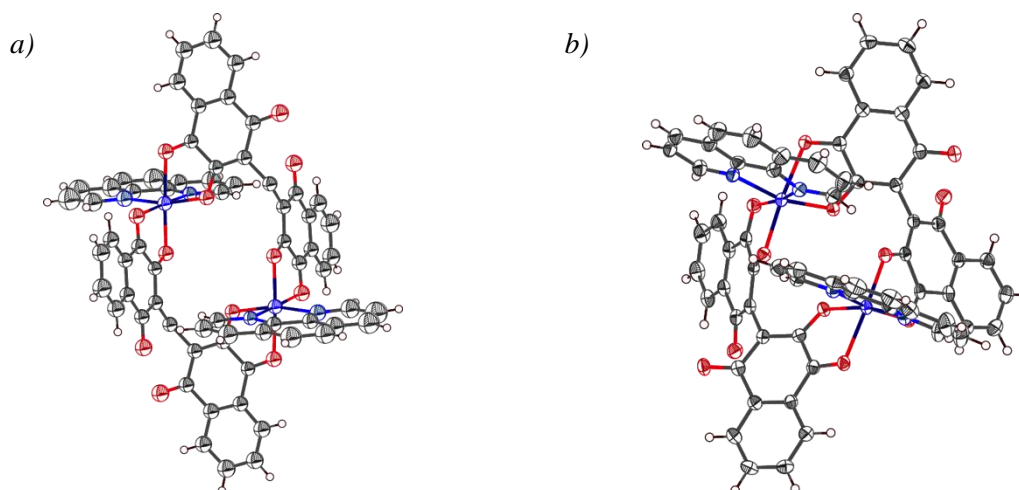


Figure 1: a) [Co(BiLaw)₂(Phen)] and b) [Co₂(MBHN)₂(Phen)₂].

The average distances between cobalt and ligands found at 120 K for both complexes are about 2.1 Å, this bond length value is typical of the form $hs\text{-Co}^{2+}\text{-L}$. Typical distances between the cobalt ion and ligands in the $ls\text{-Co}^{3+}\text{-L}$ form shall be around 1.9 Å, due to the occupation of an antibonding orbital and decreasing of metal-ligand bond order. Therefore, no evidence of a valence tautomeric transition was found until 120 K. Attempts of synthesizing new complexes with different radical forms of bisnaphthoquinones and cobalt ions are been done in order to try to achieve new valence tautomers.

[1] Sato, O.; Cui, A.; Matsuda, R.; Tao, J. *Acc. Chem. Res.*, **40**, 361-369 (2007).

[2] SATO, O. *et al. Chem. Let.*, **30**, 874-875 (2001).

[3] Ribeiro, M. A. *et al. Dalton Trans.*, **42**, 5462–5470 (2013).

Acknowledgments: FAPEMIG e CNPq.

Self-Assembly of Discrete Metallocycles versus Coordination Polymers Based on d¹⁰ Ions and Flexible Ligands: Structural Diversification and Luminescent Properties

Iván Brito ^{a*}, Alejandro Cárdenas ^b, Pere Alemany ^c and Jaime Llanos ^d

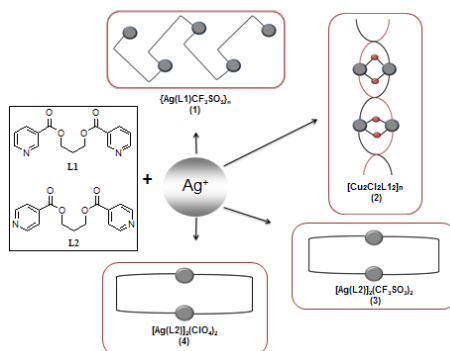
^bDepartamento de Física, Universidad de Antofagasta, Av. Angamos 601, Antofagasta-Chile.

^cDepartament de Química Física and Institut de Química Teòrica i Computacional (IQTCUB),
Universitat de Barcelona, Martí i Franqués 1, Barcelona 08028, Spain.

^dDepartamento de Química, Universidad Católica del Norte, Av. Angamos 0610, Antofagasta, Chile.

^aDepartamento de Química, Universidad de Antofagasta, Av. Angamos 601, Antofagasta-Chile.

Three new Ag(I) and one Cu(I) coordination compounds with two different positional isomers, L1 and L2, of a bis-(pyridyl-carboxylate) ligand have been synthesized. X-ray diffraction analysis revealed that the self-assembly of L1 with AgCF₃SO₃ and CuCl salts results in 1-D zig-zag chain coordination polymers {Ag(L1)CF₃SO₃}_n (**1**) and 1-D double stranded helical chain {Cu₂Cl₂(L1)₂}_n (**2**) respectively. However, self-assembly of the other ligand, L2, with AgCF₃SO₃ and AgClO₄ salts leads to the formation of discrete binuclear metallocycles {Ag(L2)CF₃SO₃}₂ (**3**) and {Ag(L2)ClO₄}₂ (**4**) respectively. Solid emission spectra recorded at room temperature of (**1**)-(4) show interesting luminescence properties for all four compounds in the range from 438 to 550 nm.



Scheme 1. Graphic description of the compounds included in this work.

[1] Brito, I.; Vallejos, J.; Cárdenas, A.; López-Rodríguez, M.; Bolte, M.; Llanos, J. *Inorg. Chem. Commun.*, **14**, 897-901 (2011)

[2] Vallejos, J.; Brito, I.; Cárdenas, A.; López-Rodríguez, M.; Bolte, M.; Llanos, J. *Inorg. Chem. Commun.* **24**, 59-62 (2012)

[3] Brito, I.; Vallejos, J.; Bolte, M.; López-Rodríguez, M.; Cárdenas, A. *Acta Crystallogr.* **E66**, o1015 (2010)

[4] Brito, I.; Vallejos, J.; López-Rodríguez, M.; Cárdenas, A.; Bolte, M. *Acta Crystallogr.*, **E67**, o2423 (2011)

[5] Brito, I.; Vallejos, J.; López-Rodríguez, M.; Cárdenas, A.; Bolte, M. *Acta Crystallogr.*, **E67**, o278 (2011)

Acknowledgments I.B & AC gratefully acknowledges Facultad de Ciencias Básicas, Universidad de Antofagasta for financial support.

Thermal stability of the ceftazidime pentahydrate

Santana, MSA¹; Fonseca, JC²; Ayala, AP¹

¹Departamento de Física, UFC, Fortaleza-CE, Brazil

²Departamento de Farmácia, UFC, Fortaleza-CE, Brazil

Ceftazidime is a third generation antibiotic of the of the cephalosporin family with activity against gram negative bacteria, especially *P. aeruginosa*, being used in hospitals to treat serious infections [1][2]. Solvation/desolvation phenonema are widely reported in literature, as this structural transitions can occur during processing, handling and storage, and may influence the bioavailability and solubility of the drug. It is essential to understand the mechanism and kinetics of this process. In the case where the solvent stabilizes the lattice, the desolvation process may produce a change in the crystalline lattice, resulting in the formation of either a new crystal form or an amorphous form [3]. Considering that processes involving temperature variations and the use of vacuum are common practices in pharmaceutical manufacturing, it is important to notice that they may alter the physicochemical properties of a solvate. The aim of this work is to investigate the stability of ceftazidime pentahydrate under thermal and vacuum stresses. Raw materials were studied by temperature dependent X-ray powder diffraction and thermal analysis techniques, using thermogravimetric analysis (TG) and differential scanning calorimetry (DSC) coupled to an infrared equipment for the analysis of the evolved gases. The temperature dependent powder diffraction measurements have shown intensity changes, shift and the appearance of new peaks, which indicates changes in the crystalline structure of the original material. During analysis of the thermal behavior of ceftazidime pentahydrate it was possible to check a thermal event related to the water release, confirmed by infrared spectrum of the evolved gases, with onset temperature about 78,4°C linked to a mass loss of 12.45%. It was also found the decomposition temperature of the drug in approximately 179,2°C. It was possible to verify the existence of an anhydrous ceftazidime form, easily obtained when the sample is subjected to temperatures above 78° C or to vacuumThe high decomposition temperature is an indicative of the good stability of the product. Therefore, the ceftazidime pentahydrate is a drug that requires care during handling and production, considering that higher temperatures or the use of vacuum in production may affect product characteristics.

[1] RIETHMUELLER et al, Fundamentals of Antimicrobial Pharmacokinetics and Pharmacodynamics, 2009

[2] Robert J. Fass, MD: Arch Intern Med 1983 Sep;143(9):1743-5.

[3] Van Gyseghem e et al: European Journal of Pharmaceutical Sciences, ELSEVIER, Amsterdam, NL, vol. 38, no. 5, 8 December 2009, 489-497

Financial Support: FUNCAP, CAPES, CNPq

Structural determination of the prototype drug LASSBio-1755

I.T.S. Bastosa^a, F.N. Costa^b, T.F. Silva^c, E.J. Barreiro^c, L.M. Lima^c, F.F. Ferreira^b, D. Braz^d, R.C. Barroso^a.

^aInstituto de Física, Universidade do Estado do Rio de Janeiro, Rio de Janeiro, Brasil

^bCentro de Ciências Naturais e Humanas (CCNH), Universidade Federal do ABC, Santo André, SP, Brasil

^cLaboratório de Avaliação e Síntese de Substâncias Bioativas (LASSBio), Faculdade de Farmácia, Universidade Federal do Rio de Janeiro, Rio de Janeiro, RJ, Brazil

^dLaboratório de Instrumentação Nuclear/COPPE; Universidade Federal do Rio de Janeiro, Rio de Janeiro, RJ, Brasil

The use of X-ray diffraction has been very important in the structural determination of new synthesized compounds. As important as the design and synthesis of new drugs is their structural characterization, since the structure (conformation) can be directly related to the therapeutic action [1]. In this work we determined the crystal structure of LASSBio-1755 with X-ray powder diffraction data.

This compound was synthesized in the Laboratory of Evaluation and Synthesis of Bioactive Substances (LASSBio[®]) of the Federal University do Rio de Janeiro. The compound LASSBio-1755 belongs to a new class of cycloalkyl-*N*-acylhydrazone compounds planned for the development of derivatives with antinociceptive and anti-inflammatory activities [2].

This compound crystallized in a triclinic system (P-1), with unit cell parameters $a = 4,86647(9)$ Å, $b = 9,3108(2)$ Å, $c = 11,3402(2)$ Å, $\alpha = 106,649(1)^\circ$, $\beta = 101,958(1)^\circ$, $\gamma = 82,629(2)^\circ$ and $V = 480,30(2)$ Å³.

The crystal structure of LASSBio-1755 consists of two formula units per unit cell ($Z = 2$), thus accommodating one molecule in the asymmetric unit ($Z' = 1$). The Rietveld method [3] was used to refine the crystal structure and the goodness-of-fit indicator as well as R-factors were $\chi^2 = 1.131$, $R_{Bragg} = 0,856\%$, $R_{wp} = 4,174\%$ and $R_{exp} = 3,692\%$.

The crystal structure of LASSBio-1755 allowed us to show structural aspects of the composite solid phase allowing the characterization of the relative configuration *E* of the imine double bond. We also saw that the *s*-cis conformation of the amide function of the *N*-acylhydrazone compound (see Fig. 1).

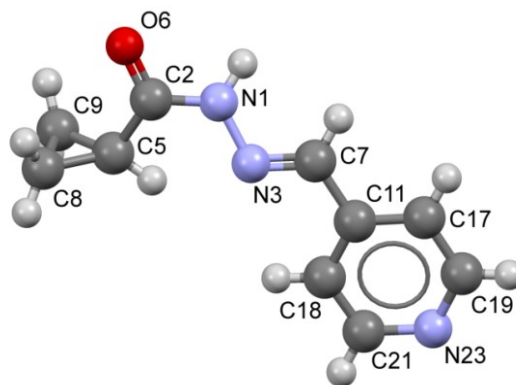


Figure 1: Crystal structure of LASSBio-1755. The relative configuration *E* of the imine double bond and *s*-cis conformation of the amide function of the *N*-acylhydrazone compound.

[1] BARREIRO, E. J.; FRAGA, C. A. M. *Química medicinal as bases moleculares da ação dos fármacos*. 2. ed., Artmed, Porto Alegre, 536p. (2008).

[2] SILVA, T. F., *Planejamento, síntese e avaliação farmacológica de uma nova série de derivados cicloalquil-*N*-acilidrazônicos: análogos de LASSBio-294*, (Dissertação de M.Sc)-Programa de Pós-graduação em Química/LASSBio/UFRJ, Rio de Janeiro, 194 f. (2012).

[3] RIETVELD, H. M. A Profile Refinement Method for Nuclear and Magnetic Structures. *J. Appl. Cryst.*, v. 2, n. 65, p. 65-71 (1969).

Acknowledgments: CAPES, CNPq and FAPERJ.

X-ray Scattering Studies of Water-Nafion Systems

S. L. Morelhão^a, A. Burimova^a

^a*Department of Applied Physics, University of São Paulo*

Recent works on liquid water confined in carbon nanotubes and ionomer membranes [1,2], water polymorphism [3] and possible structuring [4] are the best evidence of new wave of interest to the peculiarities of water behavior.

The effects that were observed by J. Zheng and H. Pollack in [5] demonstrate how significantly the properties of $\sim 200\mu m$ thick water layer near the Nafion® surface, termed "the exclusion zone" (EZ), differ from that of bulk water. The existence of similar effect near lipid bilayers was earlier mentioned in [6], however, the size of EZ was claimed to be only $\propto 10nm$.

Understanding the process of EZ formation at Nafion/water interface may be a key to building a model of the behavior of fluids near biological cell membranes. Moreover, the conductivity of proton exchange membranes depends strongly on the degree of hydration, which makes crucial the interpretation of the mechanism of water confinement in Nafion.

Using SAXS and WAXS techniques we performed a series of experiments aimed at studying water-Nafion interaction complex. Particularly, SAXS analysis of Nafion-IPA solution with different concentration of solvent was carried out. Measurements were repeated after adding 10% of liquid water to the solution. Further, SAXS and WAXS patterns were collected for two mutually orthogonal configurations of Nafion membrane immersed in water, namely, parallel and perpendicular to incident beam.

[1] Reiter, G. F. et al, *Phys. Rev. Lett.*, 111, (036803)1-5 (2013)

[2] Reiter, G. F. et al, *arXiv:1101.4994v1 [cond-mat.mes-hall]* (2011)

[3] Mallamace, F. P., *Natl. Acad. Sci. USA*, 106, 15097-15098 (2009)

[4] Gudkov, S. V. et al, *Entropy*, 16, 6166-6185 (2014)

[5] Zheng, J., Pollack, G. H., *Phys. Rev. E*, 68, (031408)1-7 (2003)

[6] Vogler, E. A., *Adv. Colloid Interface Sci.*, 74, 69-117 (1998)

Síntesis, caracterización y estudio estructural de complejos de Fe(III) derivados de ligandos iminas entre 2-picolilamina y salicilaldehídos *para*-sustituídos.

V. Artigas^a, G. Arancibia^a, M. Fuentealba^{*a}.

^aFacultad de Ciencias, Instituto de Química, Pontificia Universidad Católica Valparaíso, Chile
mail: vanial19@gmail.com, Mauricio.fuentealba@ucv.cl

Con el objetivo de desarrollar nuevos materiales con potenciales propiedades *Spin-Crossover* (SCO)^[1], se llevó a cabo la síntesis, caracterización y el análisis de la estructura cristalina de cuatro complejos de Fe(III). La estructuras cristalinas revelan que el centro metálico de Fe(III) hexacoordinado [FeN₄O₂]X y la esfera de coordinación puede ser descrita como un octaedro distorsionado formado por 4 átomos de N del fragmento 2-aminopicolina y 2 átomos de O hidroxílico del fragmento salicilato, esta distorsión fue evaluada a 100 y 298 K (La figura 1).

La tabla 1 exhibe los resultados estructurales obtenidos para dos de los complejos Fe(III) estudiados. La mayor distorsión fue observada en los complejos [1]⁺CF₃SO₃⁻ EtOH y [2]⁺CF₃SO₃⁻ EtOH, característico del estado *High-Spin* (HS), mientras que el complejo [1]⁺NO₃⁻ reportado anteriormente por De-Suo Yang^[2] mostró una menor distorsión, propia del estado de *Low-Spin* (LS).

Tabla 1: Distancia de enlace y parámetro de distorsión octaédrico de los complejos [1]⁺ y [2]⁺.

	[1] ⁺ CF ₃ SO ₃ ⁻ EtOH	[2] ⁺ CF ₃ SO ₃ ⁻ EtOH	[1] ⁺ NO ₃ ⁻
Grupo Espacial	Triclínico P-1	Triclínico P-1	Tetragonal P4 ₂ /n
T (K)	100	100	298
Fe-O1	1,920(4)	1,908(5)	1,899(3)
Fe-O2	1,923 (4)	1,906(5)	1,881(3)
Fe-N1	2,111(4)	2,098(5)	1,893(3)
Fe-N2	2,173(4)	2,177(6)	1,955(3)
Fe-N3	2,102(4)	2,173(5)	1,892(3)
Fe-N4	2,184(4)	2,011(6)	1,952(3)
Σ ^o	71,2	72,8	43,3

¹1-x,y,1/2-z; ²-x,y,1/2-z $\sum = \sum_{i=0}^{10} i - 4i$ — Low-Spin (LS) — High-Spin (HS)

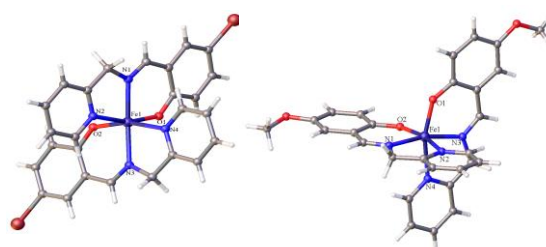


Figura 1. Figura 1: ORTEP para los complejos Fe(III) [1]⁺ (izq) y [2]⁺ (der), contraión y solvente fueron omitidos para mayor claridad de la molécula.

Finalmente, con el propósito de tener información acerca de las interacciones intermoleculares responsables de los efectos cooperativos entre los complejos de Fe(III), el contraión y/o la molécula de solvente, utilizamos el software Crystalexplorer^[3].

Referencias:

- [1] P. Guionneau (2014) Dalton Trans, 43, 382.
- [2] D. Yang, (2007) J. Chem. Crystallogr. 37, 429.
- [3] M. A. Spackman, D. Jayatilaka, (2009)

Agradecimientos:

M. Fuentealba agradece a Proyecto Fondecyt N° 1130640 y a Fondecip EQM120095. V. Artigas agradece a la becas Conicyt y de gastos operacionales N° 21130944.

ESTUDO E CARACTERIZAÇÃO DE COMPÓSITO DE MATRIZ POLIMÉRICA E PÓ DE PNEU PARA UTILIZAÇÃO NA INDÚSTRIA AUTOMOBILÍSTICA

K. C. Lira^a, F. F. Ferreira^a

^a*Centro de Ciências Naturais e Humanas, UFABC, Santo André, SP, Brazil.*

O constante aumento da população quanto da produção de veículos ao longo dos anos, fez com que a quantidade de resíduos sólidos gerados e depositados no meio ambiente crescesse de forma considerável. A fim de minimizar os impactos oriundos desta deposição, alguns órgãos ambientais (IBAMA - Instituto Brasileiro do Meio Ambiente e dos Recursos Naturais Renováveis e CONAMA - Conselho Nacional do Meio Ambiente) criaram resoluções para assegurar o adequado descarte dos materiais inservíveis.

O pneu, que é um destes materiais, é constituído por uma mistura de elastômeros, de cargas, de aditivos e de uma estrutura de aço. [1] Na sua produção utiliza-se a borracha vulcanizada, cujo processo gera a formação de ligações cruzadas, tornando o material com alta resistência química e física.

No final de sua vida útil, os pneus inservíveis, sem condições de rodagem ou reformas, apresentam difícil reciclagem, pois a vulcanização torna o material infusível e de difícil processabilidade. E, quando são abandonados em locais inadequados podem servir como meio para o desenvolvimento de vetores de doenças, podem representar risco de incêndio, contaminando o ar com uma fumaça tóxica, contendo poluentes como carbono e enxofre, além da liberação de óleo que pode contaminar o lençol freático. [2]

No intuito de diminuir sua quantidade enviada ao meio-ambiente e de gerar um ciclo produtivo mais adequado, o resíduo de pneu foi utilizado como reforço em matriz polimérica para ser aplicado no encapsulamento do motor de veículos comerciais. A sua utilização visa assegurar uma redução do peso da peça e, conseqüentemente, do veículo, otimizando seu consumo de combustível e diminuindo a emissão de poluentes; além de garantir uma minimização da poluição sonora, através da atenuação do ruído pelo compósito.

Análises acústicas de perda de transmissão e de ruído externo foram realizadas para verificar se o material atende aos limites especificados pelas resoluções. Análise térmica, mecânica e de difração de raios X foram realizadas no material para determinar as suas propriedades.

[1] Associação Nacional das Indústrias de Pneumáticos - ANIP. – “Produção na Indústria Brasileira e Reciclagem de Pneus”, ANIP, São Paulo, 2010. Disponível em: <<http://www.anip.com.br>>. Acesso em: 10 de julho de 2015.

[2] Laganinhos, C. A.; Tenório, J. A. S. Tecnologias utilizadas para a reutilização, reciclagem e valorização energética de pneus no Brasil. *Polímeros: Ciência e Tecnologia*, v. 18, p. 106-118, 2008.

Agradecimentos: CNPq e PPG-Nano/UFABC.

Obtaining and characterization of Crystal Structure of Ricobendazole

K. F. Silva^a, J. C. Fonseca^b, Y. S. Oliveira^b, Claudio J. Salomón^c, María C. Lamas^c, A. P. Ayala^a

^a*Departamento de Física, Universidade Federal do Ceará, Fortaleza, Brasil.*

^b*Departamento de Ciências Farmacêuticas, Universidade Federal do Ceará, Fortaleza, Brasil.*

^c*Departamento Farmacia, Facultad de Ciencias Bioquímicas y Farmacéuticas, Universidad Nacional de Rosario, Rosario, Argentina*

Ricobendazole (RBZ) or albendazole sulphoxide is an active metabolite of albendazole. This compound is a benzimidazole, drug widely used in veterinary medicine for the prevention and treatment of parasitic diseases [1]. Ricobendazole, as a benzimidazole anthelmintic, is a compound of broad spectrum, becoming, in this way, one of the main agents capable of inhibit a high number of parasites [1,2]. Drugs in the solid state can present diverse crystalline forms. These arrangements are associated with physicochemical properties that are of fundamental importance for the effect of the drug. In this context, the objective of this work is to determine the crystal structure of ricobendazole, as well as, relevant physicochemical properties.

Single crystals were obtained from the recrystallization of ricobendazole in methanol. These crystals were collected and characterized by several techniques. The crystal structure determination was realized based in single-crystal X-ray diffraction measurements. The additional characterization was realized by infrared spectroscopy, powder X-ray diffraction and thermal analysis using thermogravimetry and differential scanning calorimetry.

Ricobendazole crystallizes in monoclinic system belonging to the space group $P2_1/c$ with one molecule in the asymmetric unit (Figure 1). Ricobendazole molecules are arranged as dimers linked by $NH\cdots N$ bonds from the carbamate and benzimidazol moieties. These dimers are connected by another hydrogen bond $NH\cdots O$ between the benzimidazol and the sulfoxide groups. This drug exhibits a quite high melting point (218,5°C) followed by its decomposition, which is consistent with the strong hydrogen bonds stabilizing the crystalline structure. This stability could also be reflected in its poor water solubility.

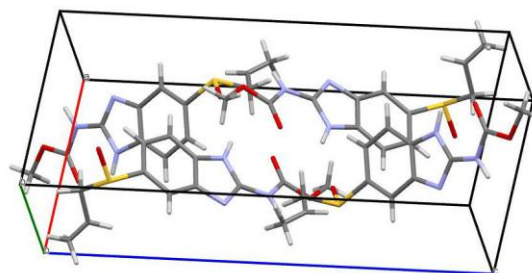


Figure 1: Ricobendazole unity cell.

[1] Mckellar, Q.A., Scott, E.W., *Journal of Veterinary Pharmacology and Therapeutics*, 13, 223-247 (1990).

[2] Zimei, W.U., Majid, Razzar., et al., *Journal of Pharmaceutical Sciences*, 94, 983-993 (2005).

[3] Cristofl, C., G. Virkel., et al., *Journal of Veterinary Pharmaceutical and Therapeutics*. 24, 117-124 (2011).

Acknowledgements: CAPES, CNPq, FUNCAP

Estructura Cristalina del Polimorfo Ortorrómico del Metil Éster del Diclofenaco, un Fármaco Antiinflamatorio No-Esteroideo

E. Hernández¹, R. Toro¹, G. Díaz de Delgado¹, J. M. Delgado¹

⁽¹⁾Laboratorio de Cristalografía-LNDRX, Departamento de Química, Facultad de Ciencias, Universidad de Los Andes, Mérida 5101, Venezuela.

El diclofenaco es un Antiinflamatorio No-Esteroideo (AINE) comúnmente utilizado en forma de sal de sodio o de potasio como analgésico y antipirético. Estas propiedades, aunadas a su bajo costo y fácil disponibilidad por el vencimiento de las patentes de invención, lo hacen uno de los fármacos más vendidos a nivel mundial. Como parte de los estudios relacionados con el control de calidad de materia prima farmacéutica y de medicamentos terminados que se llevan a cabo en nuestro laboratorio, se han realizado diferentes ensayos de preparación de derivados metálicos del ácido libre del diclofenaco (HD, C₁₄H₁₁Cl₂NO₂, figura 1). El diclofenac ácido (HD) se obtuvo en forma de polvo blanco por extracción previa con HCl de una solución acuosa de diclofenac potásico y se recristalizó en metanol caliente. Un cristal en forma de placa se seleccionó para el registro de datos de difracción de rayos X de monocristal. Este material cristaliza en el sistema monoclinico, grupo espacial C2/c, con parámetros $a=20,146(1)$ Å, $b=6,950(5)$ Å, $c=19,989(1)$ Å, $\beta=109,76(1)^\circ$, $V=2634,16(6)$ Å³, $Z=8$. Estos parámetros son similares a los reportados en el *Cambridge Structural Database (CSD)* para uno de los polimorfos del HD (Refcode: SIKLIH01). Posteriormente, en un sistema de reflujo se añadió una solución de 0,0508 g de HD en metanol-agua y CdCO₃ (0,0180 g, 0,0084 mmol) y se mantuvo en reflujo por 48 horas entre 70-80 °C. Cristales traslúcidos de color amarillo en forma de prismas se obtienen de este proceso. Este material cristaliza en una celda unidad ortorrómbica, *Pbcn*, con parámetros $a=17,253(3)$ Å, $b=7,083(1)$ Å, $c=23,618(3)$ Å, $V=2886,0(7)$ Å³, $Z=8$. Estos parámetros son similares a un reporte contenido en el *CSD* para el polimorfo identificado como SIKLIH04 del HD. Sin embargo, en este estudio se reportan altos valores del factor de discrepancia ($R1=0,13$) generando dudas sobre la estructura propuesta. El análisis detallado de la densidad electrónica y de las distancias y ángulos de enlace, indicó la formación del metil éster del diclofenaco (D-Me, C₁₅H₁₄Cl₂NO₂) y no el derivado de Cd esperado. El refinamiento preliminar por mínimos cuadrados convergió a valores de $R1=0,0769$, $wR2=0,2050$, $S=1,038$. Se debe señalar que se ha reportado un polimorfo triclinico (Refcode: XEYZIL) y una fase monoclinica (Refcode: XEYZIL01) del D-Me. Los parámetros de celda del material preparado son diferentes a los previamente reportados para las dos fases del D-Me, lo cual corrobora la existencia de un tercer polimorfo de este material. La Figura 2 muestra una visa del empaquetamiento del D-Me a lo largo del eje **b**.

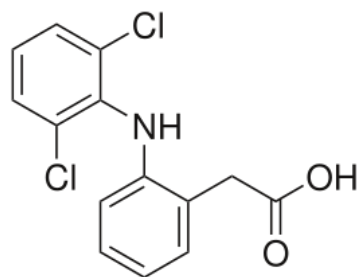


Figura 1. Diagrama molecular del ácido libre del diclofenaco (HD).

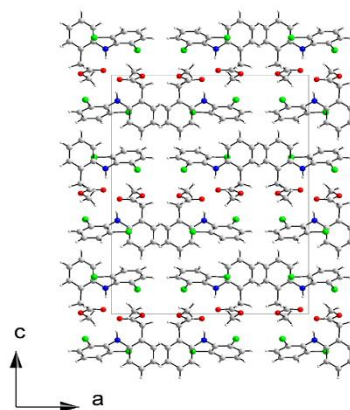


Figura 2. Vista del empaquetamiento del polimorfo ortorrómbico del D-Me a lo largo del eje **b**.

Agradecimientos: Este trabajo ha sido posible gracias al financiamiento a través del proyecto LAB-97000821 del FONACIT (Laboratorio Nacional de Difracción de Rayos-X) y al CDCHTA-ULA, Proyecto C-1676-09-08-A. Los autores agradecen al Dr. J.A. Henao y Dr. H. Camargo (UIS, Bucaramanga, Colombia) por el apoyo en la toma de datos de monocristal.

Estrutura e interações moleculares de derivados da diaminometileno tiouréia

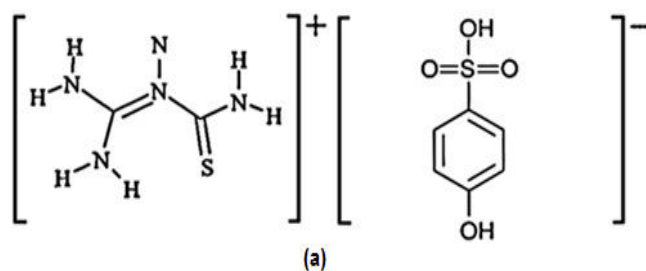
T.Ferreira^a, R.S.Gonçalves^a, J.Janczak^b, G.J.Perpétuo^a

^aDepartamento de Física, Universidade Federal de Ouro Preto

^bPolish Academy of Sciences, Wrocław, Poland

Construir estruturas supramoleculares de moléculas programadas para se envolver em várias interações com os vizinhos é uma estratégia produtiva que pode ser usada em engenharia de cristais para construir cristais moleculares, permitindo o estudo energético das interações intra- e intermoleculares^[1].

A ligação de hidrogênio é uma importante interação para organização estrutural das moléculas em meio cristalino. A observação de múltiplas ligações de hidrogênio em arranjos estendidos é uma estratégia na obtenção de novos materiais^[2].



(b)

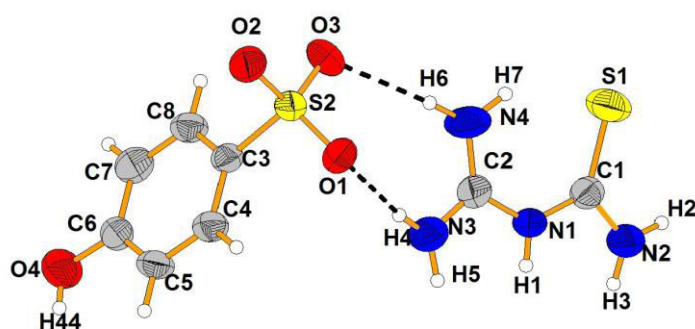


Figure 1: Diaminomethylene thiuron-1-ium 4-hydroxybenzene sulfonate: (a) fórmula estrutural e (b) unidade assimétrica.

Este trabalho consiste em analisar ligações de hidrogênio na formação de sub-arranjos estendidos em cristais contendo a diaminometileno tiouréia. A estrutura do derivado foi analisada através do método de difração de raios X de monocristais. A fim de explorar a conformação deste novo composto com padrão de ligações de hidrogênio estendida em sólidos, outros métodos físicos, além de cálculos *ab initio* foram realizados.

[1] Desiraju, G.R. *Crystal Engineering: The Design of organic solids*. Elsevier, Amsterdam (1990).

[2] Janczak, J., Perpétuo, G.J. *Acta Cryst.* **C64**, p. o114–o116 (2008).

Agradecimentos: FAPEMIG; UFOP; PAsci.

Association between Cationic Liposomes and Low Molecular Weight Hyaluronic Acid

Antonio Gasperini^a, Ximena Puentes-Martinez^a, Tiago Balbino^b, Thais Rigoletto^c, Alexandre Cassago^d, Rodrigo Portugal^d, Lucimara de La Torre^b, Leide P. Cavalcanti^b

^aLNLS, CNPEM, Campinas, BRAZIL

^bSchool of Chemical Engineering, University of Campinas, BRAZIL

^cUNIFAE, S.J. da Boa Vista, BRAZIL

^dLNNano, CNPEM, Campinas, BRAZIL

Low molecular weight hyaluronic acid (16 kDa HA) associates with cationic liposomes composed of EPC-DOPE-DOTAP [1,2]. Small angle X-ray scattering results revealed that neighboring cationic liposomes will aggregate after a partial coating of low concentration HA or disperse completely in excess of HA (> 80% w/w). Cryo-transmission electron microscopy images confirm the existence of large aggregates of unilamellar vesicles and dispersed unilamellar vesicles for low and high HA fractions respectively. High concentrations of HA proved to be efficient for coating extruded liposomes, leading to particle complexes with sizes in the nanoscale range and a negative zeta potential.

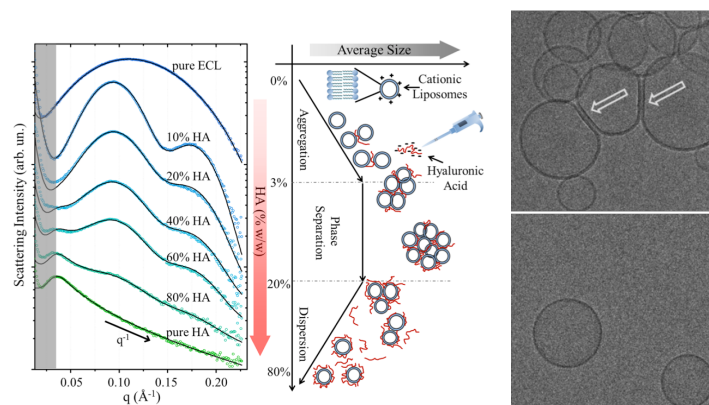


Figure 1: Left: SAXS intensity and fitting curve for cationic liposome systems with different HA fractions; Middle: cartoon highlighting the complexation stages as a function of HA content; Right: two images of cryo-TEM at low and high HA concentrations.

Low molecular weight HA has not been previously investigated in similar systems and this work shows that it favors particles with sizes in the nanoscale range for the complexes with the cationic liposomes. These findings contribute to the understanding of cationic liposomes and HA interactions and to the development of new strategies for gene delivery and vaccine therapy for systems based on the electrostatic association between polymers and vesicles.

[1] Gasperini et al, *Langmuir*, **31**, 3308 (2015)

[2] Balbino et al, *Langmuir*, **28**, 11535 (2012)

Acknowledgments: FAPESP and CAPES.

Caracterización química mineralógica estructural de dos arcillas bolivianas utilizadas en medicina tradicional

Ticona Wilma^a, Blanco Mario^b, Cabrera Saúl^a

^a*Laboratorio Sólidos y Química Teórica, Instituto de Investigaciones Químicas UMSA, Campus Universitario, Cota – Cota. Calle Nro. 27. P. O. Box: 303, La Paz (Bolivia),*

^b*Instituto de Investigaciones Geológicas y del Medio Ambiente (IGEMA), Campus Universitario, Cota – Cota, Calle No. 27, UMSA, La Paz (Bolivia).*

The present article summarizes the chemistry, mineralogical and structural characterization of two “phasas” (clays montmorillonite type) strongly utility in traditional medicine in the “Altiplano” region of Bolivia, one from to Achocalla locality (La Paz) and other Andamarca (Oruro), Bolivia. Both present how phases of interest the clay montmorillonite, but the La Paz clay have more impurity (pheldespat phases), in the other the minor phase impurity is the silice quartz type. The more Sodic – Potasic character of La Paz clay, in front of the calcic character of Oruro clay, this favoured the glycol and water adsorption, hydration end acid neutralization properties in the La Paz clay. In this sense this clay has better properties to your application in traditional medicine.

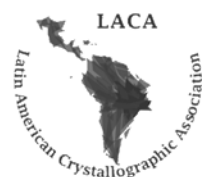
Caracterización química, mineralógica y estructural de arcillas de Viacha y Quellani (La Paz- Bolivia), utilizadas para su aplicación industrial como material cerámico

Wilma Ticona Chambi^a, Mario Blanco^b, Julian Ticona^a, Saul Cabrera^a

^a*Instituto de Investigaciones Químicas (IIQ), UMSA, La Paz, Bolivia.*

^b*Instituto de Investigaciones Geológicas y del Medio Ambiente (IGEMA), UMSA, La Paz, Bolivia*

Se presenta la caracterización química, mineralógica y estructural de dos depósitos de materiales arcillosos del departamento de La Paz, uno ubicado en la localidad de Viacha (VIA-AMA), y el otro en la localidad de Quellani (KEL-PLO y KEL-ROJ), ambos materiales son utilizados como materia prima en la industria de cerámica roja que se ha instalado en el sector, pero también muestra buen potencial de aplicación en cerámica artesanal y artística. Ambas áreas se encuentran en un mismo contexto geológico, no hay más a 10 Km entre ellas. Los depósitos de material arcilloso tienen aspecto similar pero, sus edades son diferentes, Quellani es Pleistoceno antiguo asignada a la Formación de Ulloma, mientras Viacha es Pleistoceno reciente, perteneciendo a los sedimentos lacustres del denominado "Lago Ballivián". Los dos yacimientos presentan características mineralógicas algo similares, el material arcilloso está en el orden de un 55% compuesto por Illita, Clorita y Caolinita o Vermiculita (en Viacha), y el material granular compuesta por feldespato, del tipo albita, y mucho Cuarzo, ambos en una proporción aproximada de 45%. En la muestra de Viacha, además, se reporta presencia de Mn. Los dos depósitos estudiados son clasificados como arcillitas férricas.



Polycrystals (POLY)

O uso da difração de raios X na determinação dos níveis de tensão residual em arames de aço SAE 1008 trefilados sob diferentes velocidades

Daniel Fraga Pinto^a, Adriano Corrêa Batista^a, Maria Aparecida Pinto^b.

^aRede Temática em Engenharia de Materiais – REDEMAT / UFOP, Ouro Preto - MG, Brasil.

^bDep. de Engenharia Metalúrgica e de Materiais – DEMET / UFOP, Ouro Preto - MG, Brasil.

Avaliou-se a influência da velocidade de trefilação nos níveis de tensão residual em amostras de aço SAE 1008 com 3,0mm de diâmetro, trefilado nas velocidades: 1,0m/s; 1,5m/s; 2,0m/s; 2,5m/s e 3,0m/s, fixando a redução em área 12,9% com feira de semiângulo 6° e lubrificante à base de sabão de cálcio, com tempo de trefilação de cinco segundos para cada velocidade. As medidas da tensão residual no arame foram realizadas utilizando a técnica de difração de raios X (DRX).

A importância das tensões residuais reside no fato que elas constituem uma das causas principais para diversos problemas como a formação de trincas e falta de estabilidade dimensional, podendo provocar falhas prematuras e distorções na peça, comprometendo o comportamento e até mesmo diminuindo a vida útil do componente. Contudo, as tensões residuais podem atuar beneficentemente. Em geral tensões residuais compressivas na superfície do material são mais favoráveis, pois podem evitar a nucleação de microtrincas que podem se propagar acarretando falhas em componentes estruturais.

Com relação a análise da tensão residual, atualmente, podemos citar a técnica de alívio de tensão, a técnica do furo cego e a técnica de DRX.

A técnica de DRX aplicada na medida de tensão residual é descrita pela equação 1 [1,2].

$$\sigma_R = -\frac{E}{2(1+\nu)} \cot g \theta_0 \frac{\Delta(2\theta_\Psi)}{\Delta(\text{sen}^2\Psi)} \quad (1)$$

onde, σ_R representa a tensão residual, E é o módulo de elasticidade do material, ν é o coeficiente de Poisson e o termo $2\theta_\Psi$, relacionado ao experimento de DRX, representa o ângulo entre os raios incidentes e refratados. A partir do valor de $2\theta_\Psi$, é possível relacioná-lo em um gráfico ao seu correspondente $\text{sen}^2\Psi$, o que teoricamente fornece uma reta. Assim, a equação 1 pode ser reduzida à equação 2.

$$\sigma_R = KM \quad (2)$$

onde, K é uma constante do material e, para aços ao carbono tem valor igual a 318,128MPa e M representa a inclinação da reta, dada pela equação 3.

$$M = -\frac{E}{2(1+\nu)} \cot g \theta_0 \quad (3)$$

As análises foram realizadas na direção longitudinal, em relação ao eixo do arame, com o ângulo Ψ variando de 0° a 40° no intervalo de 150° a 163°. A Figura 1 apresenta o resultado da análise da tensão residual no arame na condição de partida e trefilado.

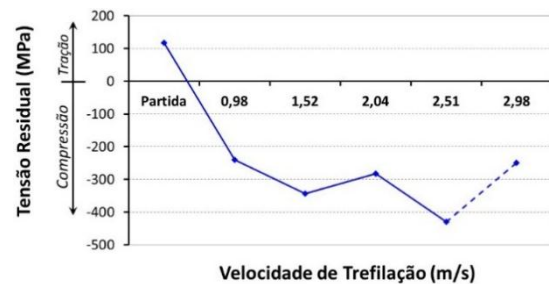


Figura 1 - Tensões residuais no arame em função da velocidade de trefilação. A linha tracejada indica que houve ruptura do arame durante a trefilação na condição de velocidade correspondente a 2,98m/s.

À medida que o arame é trefilado, a condição de tensão trativa é alterada para tensões compressivas.

A partir dos resultados obtidos com a técnica de DRX para a análise de tensões residuais concluir que para todas as velocidades de trefilação ensaiadas, as tensões residuais medidas foram tensões de compressão. O aumento da velocidade de trefilação influenciou no sentido de aumentar os níveis de tensão residual de compressão na superfície do arame trefilado. Existe uma dependência da tensão em função da velocidade de trefilação. Essa dependência não se mostrou linear em função do aumento da velocidade.

[1] FITZPATRICK, M. E.; LODINI, A. Analysis of Residual Stress by Diffraction using Neutron and Synchrotron Radiation. USA: Taylor & Francis, p. 354, 2003.

[2] AMERICAN SOCIETY FOR TESTING AND MATERIALS. E8M-04: Standard Test Methods for Tension Testing of Metallic Materials (Metric). USA: American Society for Testing and Materials, 1999.

Generalized Pole Figures analysis of an ARB deformed IF steel using synchrotron X-Ray diffraction

N. S. De Vincentis^a, E. Benatti^a, A. M. Salcedo Garrido^b, F. Cruz Gandarilla^b, H-G. Brokmeier^c, M. C. Avalos^a, R. E. Bolmaro^a

^a*Instituto de Física Rosario (CONICET-UNR), Rosario, Argentina.*

^b*Instituto Politécnico Nacional, México DF, México.*

^c*Institut für Werkstoffkunde und Werkstofftechnik, TU Clausthal, Clausthal-Zellerfeld. Helmholtz-Zentrum Geesthacht, GEMS Outstation, Hamburg, Germany.*

The mechanical properties of a material are highly influenced by its microstructure, which also depends on the particular thermo-mechanical process undergone by the material. These processes modify the microstructural features mostly by introducing or removing defects, affecting the materials' strength and ductility. Accumulative Roll Bonding (ARB) [1], as one of the so-called Severe Plastic Deformation (SPD) techniques, allows increasing both mentioned mechanical properties by reducing the grain size into the micro-nanometer range. Several techniques can be used to quantify the changes observed in the microstructure with increasing deformation, both at local or global level. For a global microstructural analysis of bulk nanostructured materials, X-Ray diffraction can be used because the microstructure of a material affects its diffraction pattern, mainly through peak broadening. There are several models that correlate the variations in peak breadth and shape with changes in diffraction domain size and dislocation density, such as Williamson-Hall (W-H) [2] and Convolutional Multiple Whole Profile (CMWP) [3].

In severely deformed materials, the microstructure -and in extent, the mechanical properties- are orientation-dependent. Generalized Pole Figures (GPFs) [4], which are similar to the conventional pole figures but showing the dependence of any parameter or variable with orientation, can be used to evaluate anisotropy. The present paper presents the GPFs obtained for an IF steel deformed by ARB up to 5 cycles, by using highly penetrative high-energy synchrotron radiation. The results show a very distinctive evolution of the orientation dependence of the microstructure with increasing deformation, with a continuous diminution of domain sizes and compactness rising arrangements of dislocations.

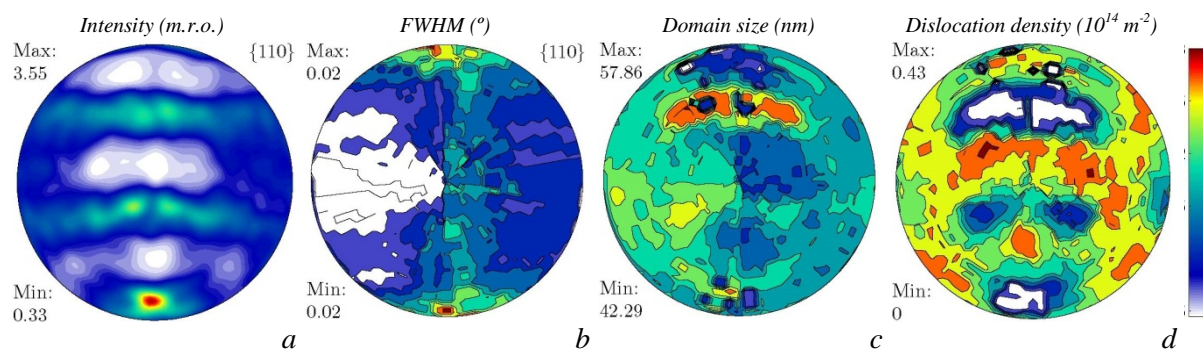


Figure 1: Generalized Pole Figures obtained for a sample deformed in 1 ARB cycle (measured (100) (a) intensity and (b) FWHM and calculated (c) domain size and (d) dislocation density pole figures)

[1] Tsuji, N., Ito, Y., Saito, Y., Minamino, Y., *Scripta Materialia*, **47**, 893-899 (2002).

[2] Williamson, G. Hall, W., *Acta Metallurgica*, **1**, 22-31 (1953).

[3] Ribárik, G., Modelling of diffraction patterns based on microstructural properties, PhD Thesis (2008).

[4] Perlovich, Yu., Isaenkova, M., Fesenko, V., Bunge, H., *Materials Science Forum*, **495-497**, 77-86 (2005).

Acknowledgements: CONICET; MinCyT.

Self-assembly of new chiral L-Aspartic Acid derivatives into hierarchical nanoporous microspheres

O.C. Sánchez, F. Movilla, F. Di Salvo.

DQIAQF/INQUIMAE-CONICET, FCEN, UBA, Buenos Aires, Argentina.

Amino acids and derivatives are able to self-assemble into ordered superstructures when they are subjected to certain crystallization conditions such as, pH, supersaturation level and the use of additives, being the last one the most popular. While different morphologies of crystalline arrangements are known, the greatest interest lies in the obtaining of three-dimensional (3D) self-assemblies with hierarchical architectures that can contribute to the knowledge of the controlled manufacture of nanoscale materials and novel devices. There are several examples in recent literature of inorganic compounds which provide interesting responses to this problem however, only a few organic molecules have been considered as building blocks [1]. Thus, the design and synthesis of 3D supramolecular structures with hierarchical morphologies based on a single kind of organic molecule is an interesting challenge. In this work we present the synthesis of new chiral L-amino acid based molecules which, after protonation using several organic acids give place to different types of hierarchical microspheres when L-aspartic acid is used, and other crystalline material when other L-amino acid are employed. All of them were characterized by polarized optical microscopy (POM), scanning electron microscopy (SEM), XRD, FTIR and NMR, confirming in all cases that the resultant material is built exclusively by the organic compound. We suggest that the formation of such organized structures only for the L-aspartic acid derivative is promoted mainly by the presence and directionality of the hydrogen bonds sustained by the carboxylate. Other aspect to point out is that, in all studied cases the compounds are obtained as a mixture of the two possible geometric isomers with symmetry C_{3h} and C_s respectively. Surprisingly, only the latter give place to mentioned microspheres for the L-aspartic acid derivative. Another variable that influences the morphology of the microstructures is the type of acid (Fig. 1). On the other hand, the analysis of the images obtained by SEM showed nanopores distributed homogeneously in the symmetrical microspheres, making them a potential material for gas sorption application. Based on the obtained results, it is possible to suggest that the molecular symmetry together with the presence and directionality of certain intermolecular interactions are key factors in the mechanism of self-assembly into hierarchical structures.

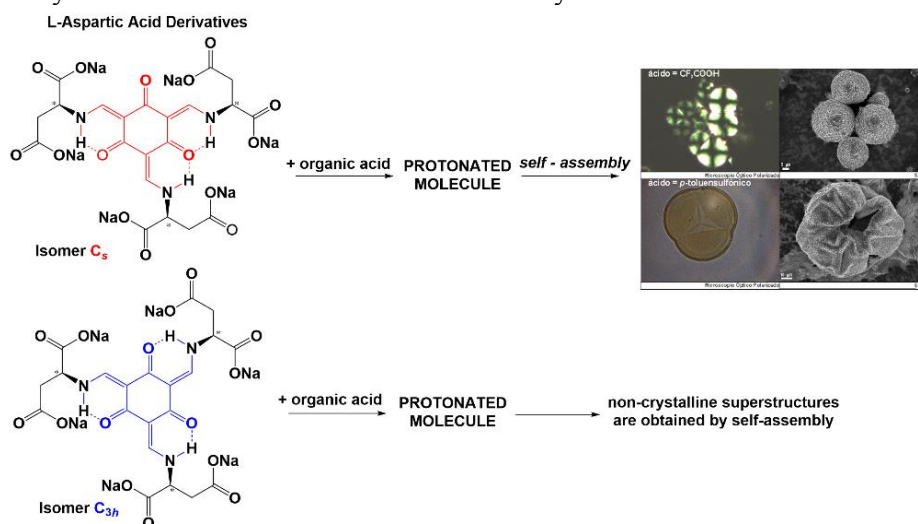


Figure 1: Schematic structures of the L-aspartic acid derivatives involved in the self-assembly microsphere process.

[1] H. Jiang, L. Gower, D. Volkmer, H. Cölfen, *Cryst. Growth Des*, **11**, 3243–3249 (2011). [2] S. Wohlrab, H. Cölfen, M. Antonietti, *Angew. Chem. Int. Ed*, **44**, 4087–4092 (2005). [3] M. Ejgenberg, Y. Mastai, *Cryst. Growth Des*, **12**, 4995–5001 (2012).

Acknowledgments: Financial support from ANPCyT (PICT 2012-1335 and 2011-2013), and CONICET (PIP 112 201001 00125). O.C. Sánchez to CONICET for a PhD scholarship.

Pigmentos del Sitio Arqueológico Tambo Colorado analizados por difracción de rayos X sincrotrón y refinamiento Rietveld

E. L. Zeballos-Velasquez^a, V. Wright^b, M. R. Suchomef^c, L. Suescun^d, P. C. Melero^a

^aFacultad de Ciencias Físicas, Universidad Nacional Mayor de San Marcos, Lima Peru.

^bInstitut Français d'Études Andines, Lima Peru.

^cAdvanced Photon Source, Argonne National Laboratory, Argonne USA.

^dFacultad de Química, Universidad de la República, Montevideo Uruguay.

A pesar de la excepcionalidad arquitectónica y policroma del sitio arqueológico Tambo Colorado (Figura), no se han realizado trabajos de conservación ni en las estructuras arquitectónicas de tierra cruda, ni en las superficies (pintura mural, enlucidos), a pesar de la evidente velocidad de degradación del complejo, justificando una intervención urgente para conservar y proteger este sitio único. Con este propósito, los resultados del estudio que presentamos buscan explicar la naturaleza de los materiales (pigmentos) utilizados en las pinturas murales, así como determinar las fuentes de estos materiales (canteras); esto, a su vez, permitirá reconstituir la cadena operativa de la elaboración de los murales y comprender la tecnología utilizada por los artesanos pintores. Estos resultados complementan los resultados generales del “*Proyecto Tambo Colorado*” [1] jefaturado por el Instituto Francés de Estudios Andinos.

Pigmentos de murales y de cantera fueron investigados aplicando la técnica de Difracción de rayos-X sincrotrón (DRXS) y refinamiento estructural por el método de Rietveld. Fue determinada la composición de los pigmentos, así como el porcentaje de cada uno de sus componentes. Preliminarmente, las muestras fueron medidas por la técnica de Fluorescencia de Rayos-X de Energía Dispersiva, cuyos resultados reportaron la presencia de una serie de elementos, entre ellos Fe, S y Ca en la mayoría de los pigmentos.



Figura: Vista panorámica de Tambo Colorado.

La identificación mineralógica por DRXS determinó la presencia de cuarzo, anorthita, chlorita, yeso, illita, albita, jarosita, ortoclasea y calcita en los pigmentos de mural; en tanto que en los pigmentos de cantera fueron identificadas fases de cuarzo, anorthita, chlorita, yeso, illita y halita. El refinamiento Rietveld confirmó las fases identificadas y determinó su porcentaje en peso.

[1] Wright V. *Proyecto de Investigación Tambo Colorado*. Instituto Francés de Estudios Andinos. Lima (2012).

Agradecimientos: Nuestro agradecimiento a Argonne National Laboratory (USA) por su contribución con las medidas sincrotrón, así como al Vice-Rectorado de Investigación de la Universidad Nacional Mayor de San Marcos por el soporte financiero.

Quantification of phases of WC-10% Co composite sintered at 1350°C using the Rietveld method.

Adriano Corrêa Batista^a, Hellen Cristine Prata de Oliveira^a e Genivaldo Júlio Perpétuo^a.

^aRede Temática em Engenharia de Materiais – REDEMAT/UFOP, Ouro Preto/MG, Brasil.

This paper presents the results obtained in the initial stages of the project "Study of metastable phases of the composite WC10% Co - Hard Metal". Using the Rietveld method aims to monitor the evolution of the microstructure formed during sintering this composite, processed with nanometer WC powder using 10% by weight of Co as a binder, sintered in vacuum at the temperature tectotherm of 1350°C. At this stage of the project, our objective characterize and quantify the metastable phases η ($\text{Co}_3\text{W}_3\text{C}$ and $\text{Co}_6\text{W}_6\text{C}$).

In Figure 01 is shown Rietveld graph where one can observe that y_{cal} is very well adjusted, modeling y_{obs} reaching the value of 51.49% difference between them [1,2,4]. In Table I it can be seen that the parameters obtained from the refinement display the behavior of all phases identified in the hard metal structure after sintering. The metastable phases $\text{Co}_6\text{W}_6\text{C}$ and $\text{Co}_3\text{W}_3\text{C}$ have certain complexity, great contribution throughout the diffractogram with peaks manifesting multiple configurations. The largest amount of $\text{Co}_6\text{W}_6\text{C}$ phase can be justified based on the results given in reference literature, or Co_3W is a stable phase in the temperature range of 1000°C and can be carbureted contributing to the formation of $\text{Co}_6\text{W}_6\text{C}$ phase [3,4].

It can also be explained the formation of $\text{Co}_3\text{W}_3\text{C}$ phase being formed from the $\text{Co}_6\text{W}_6\text{C}$ phase with increasing temperature [3,4].

The sintering promotes relaxation events that will structures, phase transition and residual stress between the phases present. Such events do vary the volume values and density of unit cells, promoting fluctuations in the values of interplanar distances and positions in 2θ hampering the refinement of data from X-ray diffraction.

Table I – Results obtained with the Rietveld method.

<i>Fase WC – GE P6̄m2 (187) hp – {S = 1.49%}</i>			
a (Å)	b (Å)	c (Å)	Fase (%)
2.90512(2)	2.90512(2)	2.83616(3)	63.619 (6)
<i>Fase Co₆W₆C – GE Fd3̄m (227) cfc – {S = 1.49%}</i>			
a (Å)	b (Å)	c (Å)	Fase (%)
10.8994(1)	10.8994(1)	10.8994(1)	24.82 (1)
<i>Fase Co₃W₃C – GE Fd3̄m(227) cfc – {S = 1.49%}</i>			
a (Å)	b (Å)	c (Å)	Fase (%)
11.0690(5)	11.0690(5)	11.0690(5)	9.312 (9)
<i>Fase Co – GE P6₃/mmc (194) hp – {S = 1.49%}</i>			
a (Å)	b (Å)	c (Å)	Fase (%)
2.500 (1)	2.500 (1)	4.092 (3)	2.24 (2)

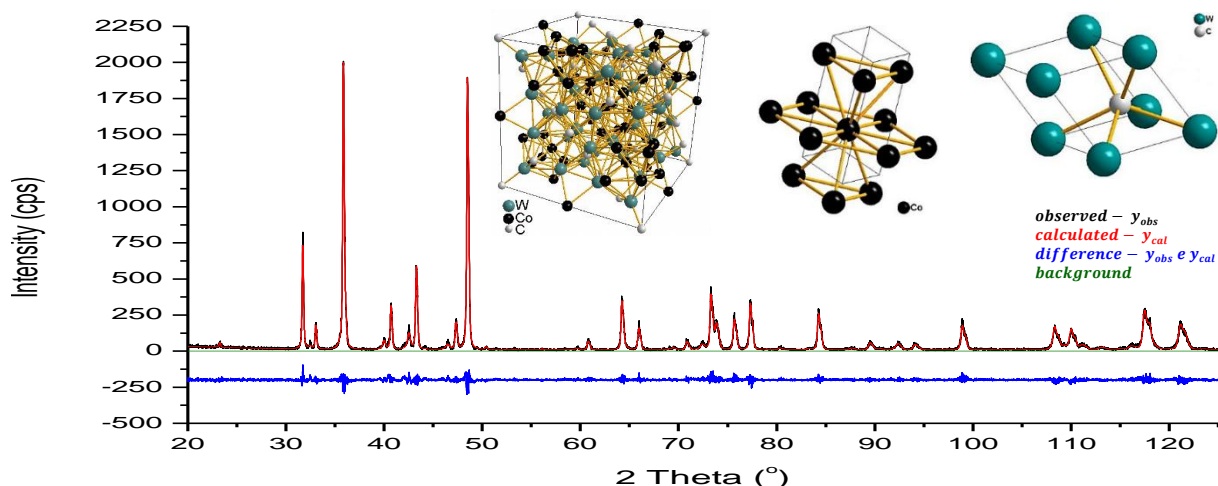


Figure 01 – Rietveld graph of the sample sintered at 1350°C.

- [1] Bragg, W.L., *The Diffraction of Short Electromagnetic Waves by a Crystal*, Proceedings of the Cambridge Philosophical Society, 17, 43-57 (1913).
- [2] Rietveld, H.M., *J. Appl. Crystallogr.*, Vol. 2, p.65-71 (1969).
- [3] Pollock C.B., *The eta carbides in the Fe–W–C and Co–W–C systems*. Metall. Trans. v.1, n°14, p. 767 (1970).
- [4] Batista, A.C., *The use of the Rietveld method as evaluation tool in the stages of production of nanostructured hard metal*. 21° Congresso Brasileiro em Engenharia de Materiais, p 2681-2691 (2014).

Investigação da Ação de Diferentes Solventes na Produção de Polimorfos do Efavirenz

M.M.Marques^a, G.C.Lima^a, A.C.S. Marques^{a,b}, L.D.Prado^{a,b}, H.V.A. Rocha^b, G.B.Ferreira^a, J. A. L. C. Resende^a.

^aDepartamento de Química Inorgânica, Universidade Federal Fluminense, Niterói, Brasil

^bFarmanguinhos, Fiocruz, Rio de Janeiro, Brasil

O efavirenz é um fármaco antiviral da classe dos inibidores não-nucleosídicos da enzima transcriptase reversa, é um dos mais utilizados no tratamento da Síndrome da Imunodeficiência Adquirida (SIDA), é um sólido de cor branca, levemente amarelada que possui ponto de fusão (139-141°C) e pKa de 10,2. O efavirenz é classificado biofarmaceuticamente como um fármaco de classe II, ou seja, apresenta baixa solubilidade e permeabilidade sendo sua solubilidade controlada através da solubilidade ou velocidade de dissolução do medicamento[1]. Essa baixa solubilidade do efavirenz faz com que seja necessário sua admissão em altas doses o que pode causar reações alérgicas.

A literatura relata a existência de diversos polimorfos do efavirenz[2] obtidos das mais diversas maneiras, seja por cristalização, aquecimento/resfriamento ou evaporação de solvente. Assim, o objetivo deste trabalho é demonstrar que com o uso da moagem manual por vias úmidas é possível converter as formas 1 e 2 (mais estáveis) do efavirenz em diferentes polimorfos.

Todo trabalho foi realizado partindo-se da forma 1 do efavirenz. A forma 2 foi obtida através de metanol, conforme descrito na figura 1. A metodologia utilizada foi a de macerar manualmente por 30 minutos as formas 1 e 2 do efavirenz com gotejamento de 5µL de solvente a cada 10 minutos. Os solventes utilizados foram: metanol, etanol, álcool isopropílico, butanol, água, acetonitrila, acetona, acetato de etila, tolueno, éter etílico e pentano. As amostras foram caracterizadas por difração de raios-X, calorimetria diferencial de varredura e espectroscopias infravermelho e Raman. Os resultados foram compilados e estão apresentados nas figuras 1 e 2 abaixo.

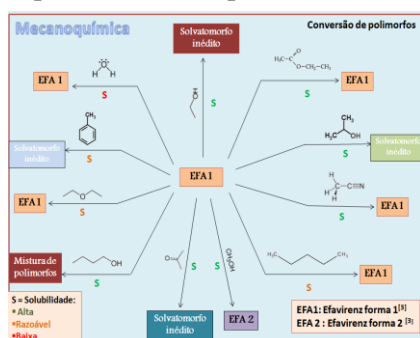


Figura 1: Resultados da conversão da forma 1 do efavirenz com uso dos diversos solventes

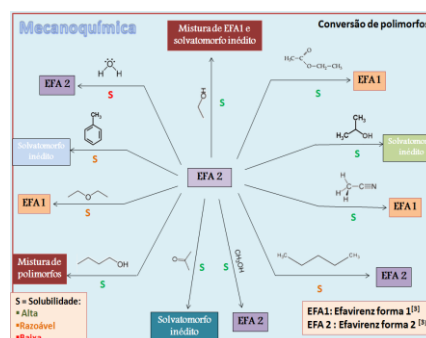


Figura 2: Resultados da conversão da forma 2 do efavirenz com uso dos diversos solventes

Após as análises, pode-se concluir que a forma 1 é mais facilmente obtida com o acetato de etila enquanto que a forma 2 com o metanol. Percebe-se também que os alcoóis são solventes que geram novos polimorfos sejam esses inéditos ou não. Outra observação, é que as formas 2 e os solvatomorfos de tolueno e acetona foram obtidos de maneira simples e menor custo do que descrito na literatura[3], baseando-se em conceitos de Green Chemistry, já que utilizou-se quantidades ínfimas de solvente.

[1] Costa, M.A., Seiceira, R.C., Rodrigues, C.R., Hoffmeister, C.R.D., Cabral, L.M., Rocha, H.V.A., in *Pharmaceutics*, **5**, 1-22 (2013).

[2] Chadha, R., Bala, M., Rani, D., Aora, P., in *Current Topics Medicinal Chemistry*, **13**, 1933-1962 (2013).

[3] Mahapatra, S., Thakur, T., Joseph, S., Varughese, S., Desiraju, G., in *Crystal Growth & Design*, **10**, 3191-3202 (2010).

Agradecimentos: CAPES, FAPERJ e ao laboratório de difração de raios-X.

A influência da prensagem a quente na microestrutura do sistema Fe-Cu-Nb

H. C. P. Oliveira^a, A. C. Batista^a, G. J. Perpétuo^a, P. S. Assis^a

^aRede Temática em Engenharia de Materiais/REDEMAT/UFOP, Ouro Preto/MG, Brasil.

O objetivo deste trabalho foi avaliar o comportamento microestrutural das ligas do sistema Fe-Cu-Nb, variando o teor de nióbio em 15, 25, 35 e 45%Nb em peso. As matrizes metálicas foram obtidas por prensagem a quente usando o parâmetro de sinterização: 35MPa / 800°C / 3min. Para fins comparativos, os pós metálicos de Fe, Cu e Nb e as misturas referentes a cada liga metálica também foram analisadas para acompanhar a influência da prensagem a quente na microestrutura. Todos os materiais foram analisados por difração de raios X.

O processo que antecede à prensagem a quente, corresponde a etapa em que os pós metálicos são pesados individualmente segundo a composição de cada liga desejada e então, são introduzidos em um misturador rotativo por 2hs para ocorrer a homogeneização, formando assim a mistura dos pós metálicos^[1].

A Figura 1 mostra os difratogramas das quatro diferentes misturas dos pós de Fe-Cu-Nb e com seus respectivos pós metálicos de Fe, Cu e Nb, sendo identificado as fases Cu (CFC), Nb (CCC) e Fe (CCC). Os picos 65,110° e 98,920° aparecem no difratograma de Fe, embora não estão aparecendo de forma nítida nos difratogramas das misturas e ligas, pois os mesmos foram identificados junto ao *background*. Após realizar a prensagem a quente, foram identificadas nas ligas metálicas sinterizadas, Figura 2, as fases Cu, Nb e solução sólida Fe. Verifica-se a sobreposição dos picos à medida que a concentração de Nb é aumentada, sendo observado junto ao *background* o possível início da formação das fases secundárias: FeNb; Fe₂Nb; Fe₇Nb₆; Fe_aNb_b; CuFe. Com o aumento de elemento Nb na liga, faz com que a rede CCC da fase Nb fique saturada e se transforme para a rede HCC, formando a fase Laves ϵ (Fe₂Nb) e, conseqüentemente, até mesmo para a rede CFC de fase metaestável, dependendo da quantidade de elemento adicionado, formando soluções sólidas como Fe₇Nb₆ (fase μ) e Fe_aNb_b.

Entretanto, o baixo limite de solubilidade entre os elementos Fe, Cu e Nb, diminui a interação entre estes elementos para a formação de novas fases utilizando o parâmetro de sinterização em questão^[1-3]. De acordo com os estudos termodinâmicos e cinéticos para este intervalo de temperatura e, também, pelo aspecto dos difratogramas, nota-se que o efeito termodinâmico não foi suficientemente intenso para promover em quantidades consideráveis fases metaestáveis oriundas da difusão entre os elementos das ligas.

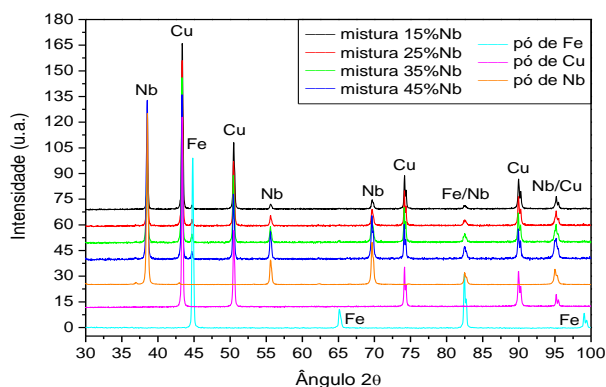


Figura 1: Difratogramas obtidos das misturas de Fe-Cu-Nb e pós de Fe, Cu e Nb.

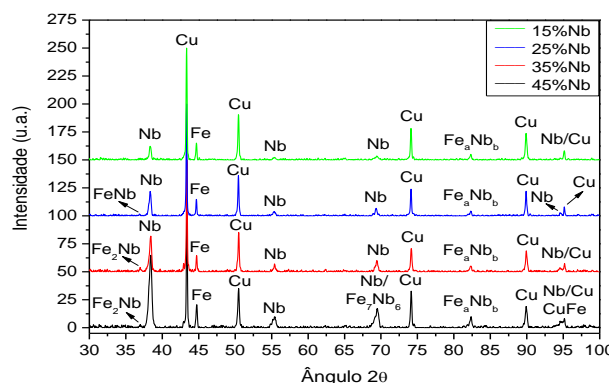


Figura 2: Difratogramas obtidos das matrizes metálicas de Fe-Cu-Nb.

[1] Oliveira, H.C.P. *Influência de Adições de Nióbio no Sistema Ferro-Cobre para Atuar como Matriz Ligante em Ferramentas Diamantadas*. Tese, UENF, Campos dos Goytacazes/RJ, 232p (2010).

[2] Yamaguchi, K.; Takakura, N.; Imatani, S. *Journal Materials Processing Technology*. v.63, p. 364-369 (1997).

[3] Del Villar, M. *et al.*, *Powder Metallurgy*. v.44, n.1, p. 82-90 (2001).

Agradecimentos: UFOP/REDEMAT, CAPES.

An alternative to Rietveld method for phase determination of Ce-TiO₂ materials

A. N. Gravina^a, N. L. D'Elía^a, J. Sartuqui^a, P. V. Messina^a

^aDepartment of Chemistry, Universidad Nacional del Sur, INQUISUR-CONICET, Bahía Blanca, Argentina.

The importance of phase content in Ce-TiO₂ materials is a widely known fact due to its influence in thermal stability, heterogeneous catalytic properties and even in bioactivity. In this work we present a thorough analysis of phase composition that could be used to select the appropriate synthesis conditions in order to obtain the desired properties for a wide range of applications.

A microemulsion mediated route has been chosen to synthesize Ce-TiO₂ materials, using n-heptane/n-butanol/CTAB/water system as a reactor and Titanium Isopropoxide (TTIP) and Cerium Valerate (Ce(Val)₃) as inorganic precursors; final products were obtained after hydrothermal treatment, purification and calcination, according to the procedure described in a previous report [1]. Different Ce(Val)₃/TTIP ratios were used in the range of 6.0×10^{-4} to 0.30 as well as different calcination temperatures: 100, 200, 400, 700, 800, 900 °C. Pure TiO₂ and no calcination were used as control conditions.

Phase determination from XRD data is a relatively complex procedure and full fitting performed using Rietveld Quantitative Analysis (RQA) is often the method of choice, but it requires certain precision in the knowledge of crystal parameters which are rather blurry when dealing with poorly structured materials. Also, the use of an internal standard is needed when trying to quantify the amorphous content that implies further sample processing. In this work we present a phase analysis performed using a less demanding method based on peak deconvolution inspired in the determination of cellulose crystallinity index [2]. Certain assumptions have been made such as Voigt function for the peaks shape and the amorphous content was assigned to the wide peak at 20° and considered responsible of peak broadening. Validation of the method has also been performed by contrast with others such as the widely used method of Spurr and Myers, which gives the Anatase/Rutile ratio, and the Rietveld refinement did by Matějová *et al.* [3] to determine the Amorphous/Anatase/Cerianite ratio in CeO₂-TiO₂ materials. In both cases, the differences were smaller than 1 %.

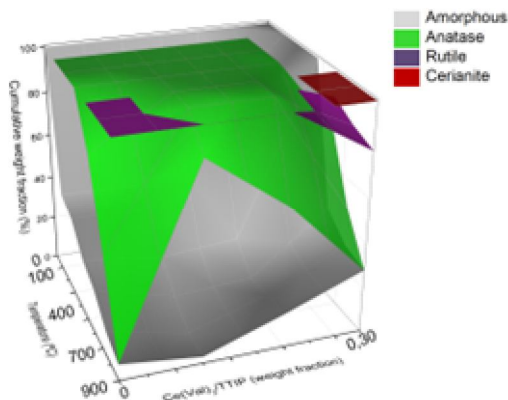


Figure 1: Three-dimensional phase diagram for Ce-TiO₂ materials with different Ce(Val)₃/TTIP weight ratios and temperature processing. Each layer represents the upper limit of the respective phase and weight fractions are showed as cumulative percentages.

Phase content has been determined using peak deconvolution of XRD diffraction patterns collected with a Philips PW1710 diffractometer with Cu K α radiation ($\lambda = 1.5418$ nm) and Graphite monochromator operated at 45 kV, 30 mA and 25 °C.

- [1] Gravina, A.N., Ruso, J.M., Mbeh, D.A., Yahia, L., Merhi, Y., Sartuqui J., and Messina, P.V., *RSC Adv.*, 5, 8077–8087(2014).
- [2] Park, S., Baker, J.O., Himmel, M.E., Parilla, P., and Johnson, D.K., *Biotechnol. Biofuels*, 3, 10 (2010).
- [3] Matějová, L., Valeš, V., Fajgar R., Matěj, Z., Holý, V., and Šolcová O. *J. Solid State Chem.*, 198, 485–495(2013).

Acknowledgments: CONICET, Universidad Nacional del Sur and Drs. Matějová and Matěj for their kind contribution.

Anisotropic Microstructure Developed on ARB IF Steel Using Synchrotron X-Ray Diffraction Data Processed by Rietveld Analysis

R. E. Bolmaro^a, N. S. De Vincentis^a, E. Benatti^a, M. C. Avalos^a, A. M. Salcedo Garrido^b, F. Cruz Gandarilla^b, N. Schell^c, H-G. Brokmeier^c.

^a*Instituto de Física Rosario (CONICET-UNR), Rosario, Argentina.*

^b*Instituto Politécnico Nacional, México DF, México.*

^c*Institut für Werkstoffkunde und Werkstofftechnik, TU Clausthal, Clausthal-Zellerfeld. Helmholtz-Zentrum Geesthacht, GEMS Outstation, Hamburg, Germany.*

Severely deformed materials develop a nano-microstructure, including domain size diminishing and dislocation patterning, simultaneously with characteristic textures. It has been suggested that microstructure is highly anisotropic but we still lack a complete study of the orientation dependence, either sample or crystallographic related, including large variations on strain paths and/or crystal structures. The nano-microstructure is one of the main characteristics influencing mechanical, thermal and electric properties. One of the most promising Severe Plastic Deformation (SPD) techniques for industrial applications is Accumulative Roll Bonding (ARB) [1], which draws high expectation for simultaneously increasing strength and improving ductility by reducing the grain size into the micro-nanometer range. Quantifying changes in the microstructure with increasing deformation, both at local or global levels, has been made possible since very long by X-Ray diffraction. Several models allow the interpretation and/or quantification of diffraction pattern peak broadening. The most common, such as Williamson-Hall (W-H) [2] and Convolutional Multiple Whole Profile (CMWP) [3] have been in use during a long time. We will carry the analysis by using extended Rietveld fitting, including defect accumulation models, as implemented in MAUD software [4, 5].

Experimental data stems from high energy synchrotron light diffraction collected in DESY, HEMS outstation, Petra III, Hamburg. Data is collected in transmission, with an 87 KeV energy beam and an image plate solid state Mar345 detector.

The material is a collection of ARB SPD samples, obtained by 1-5 rolling passes on IF steel. Samples of 1 mm² section x 10 mm length were cut along the rolling direction. Data on a similar size LaB6 powder sample was obtained for instrument broadening evaluation.

[1] Tsuji, N., Ito, Y., Saito, Y., Minamino, Y., *Scripta Materialia*, **47**, 893-899 (2002).

[2] Williamson, G. Hall, W., *Acta Metallurgica*, **1**, 22-31 (1953).

[3] Ribárik, G., Modelling of diffraction patterns based on microstructural properties, PhD Thesis (2008).

[4] Ischia G, Wenk H-R, Lutterotti L and Berberich F. *J. Appl. Cryst.* **38(2)**, 377 (2005).

[5] Lutterotti L and Bortolotti M. *IUCr: Compcomm Newsletter* **1**, 43 (2003).

Acknowledgements: CONICET; MinCyT.

The effect of building blocks on the design and construction of four extended networks based on a rigid acetylenic ligand

V. Martins, J. A. L. C. Resende, C. M. Ronconi.

Instituto de Química, Universidade Federal Fluminense, Niterói, Brazil.

Extended networks are a class of hybrid materials that can be designed through the rational manipulation of the building blocks such as ligand, metal and solvent.¹ However, the predictability of the structures remains one of the main challenges in the design of new functional materials.² This work describes the structural characterization of four new coordination networks obtained by the reaction of the bis carboxylated ligand 4,4'-ethynylenedibenzoic acid (H₂edb) with Co²⁺, Cd²⁺, Er³⁺, and Gd³⁺. The isolated networks are described as [Co(edb)(OH₂)(Py)₂](Py)(DMSO) (1), [Cd(edb)(DMSO)₂](DMSO) (2), [Er₂(edb)₃(DMSO)₂(OH₂)₂].xH₂O (3) and [Gd₂(edb)₃(OH₂)₄].xH₂O (4).

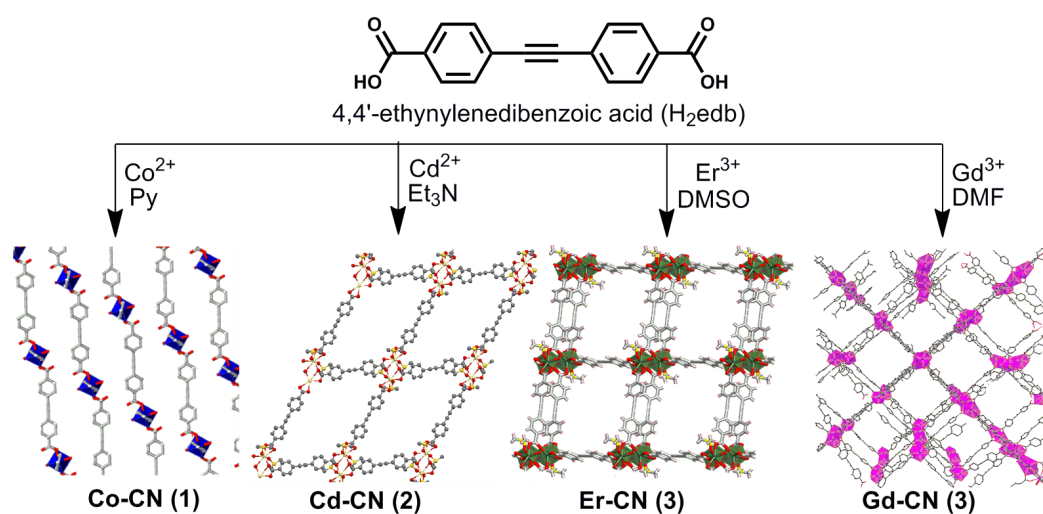


Figure 1. Scheme showing the construction of four extended networks.

The X ray single crystal diffraction analysis reveals that compound **1** is a 1D extended network, which the ligand coordinates to Co²⁺ in the bridging mode. Compounds **2** and **3** are 2D extended networks formed from a secondary unit with four points of extension. The secondary unit is generated by the coordination of the ligand in both chelating and bridging mode to the metal. Coordination network **3** forms a secondary unit with six points of extension that directs the growth of the framework in three dimensions.

The ligand exhibited coordination modes that led to the formation of subunits comprising one (**1**) or two metallic centers (**2**, **3**, **4**). Furthermore, by the variation of the species involved in the reaction, it was possible to build mono, bi, and three-dimensional structures. We conclude that the use of coordinative bases and solvents such as pyridine and DMSO, respectively, yielded networks with low dimensionality. The use of metal cations with higher coordination numbers, e.g. gadolinium in a non-coordinative solvent, allowed for the construction of a compound with higher dimensionality.

[1] Yaghi, et al, *Chem. Rev.*, **112**, 673 (2012).

[2] Kitagawa, S., Kitaura, R., Noro, S.-I., *Angew. Chem. Int.*, **43**, 2334-2375 (2004).

Acknowledgments: FAPERJ; CNPq; Capes

Caracterização estrutural dos cristais da série L-Arginina•HBr_{1-x}HCl_xA. B. Pereira¹, A. C. Pereira¹, P. R. S. Ribeiro¹, A.O. dos Santos¹¹Centro de Ciências Sociais Saúde e Tecnologia (CCSST), Universidade Federal do Maranhão – UFMA

Materiais constituídos por aminoácidos são de grande interesse na aplicação em óptica não-linear (NLO) e estão sendo estudados com maior atenção por apresentarem propriedades (por exemplo: resistência mecânica, limiar de dano) melhores do que os materiais mais utilizados para Geração de Segundo Harmônico (SHG); dihidrogênio fosfato de potássio (KDP). Neste trabalho os cristais de L-arginina hidrobromídrica monohidratada (LAHBr) e L-arginina hidrocloreídrica monohidratada (LAHCl) foram crescidos à temperatura ambiente (25°C), pelo método de evaporação lenta do solvente. Também foram sintetizados cristais de L-arginina hidrocloreobromídrica monohidratada (LAHClBr), a partir da mistura dos compostos, nas proporções equimolares 1:3, 1:1 e 3:1.

Foi realizada a análise da composição química dos materiais por Fluorescência de Raios-X (FRX) e a composição química das amostras das misturas de LAHCl e LAHBr foram obtidas e a estequiometria da amostras são: C₆H₁₄N₄O₂•HCl_{0,14}Br_{0,86}•H₂O (LAHCl_{0,14}Br_{0,86}), C₆H₁₄N₄O₂•HCl_{0,42}Br_{0,58}•H₂O (LAHCl_{0,42}Br_{0,58}), e C₆H₁₄ N₄O₂•HCl_{0,63}Br_{0,37}•H₂O (LAHCl_{0,63}Br_{0,37}), para as amostras de LAHClBr 1:3, LAHClBr 1:1 e LAHClBr 3:1, respectivamente. Os parâmetros estruturais dos cristais foram caracterizados por Difração de Raios-X (DRX) em associação com o refinamento de Rietveld.

As medidas de difração de raios-X foram adquiridas em um difratômetro de raios-X da marca PANalytical modelo Empyrean utilizando a geometria de Bragg-Brentano e um monocromador de grafite pirolítico, com radiação Cu K_α (λ = 1,5418 Å), com passo de 0,02° em 2θ e tempo de aquisição de 2s/passos no intervalo de 10° a 50° em 2θ. Todas as amostras da série apresentam a estrutura cristalina monoclinica (grupo espacial P 2₁ 2₁ 2₁) com 4 moléculas por célula unitária. A partir do refinamento Rietveld observamos que o volume da célula unitária da série LA•HBr_{1-x}HCl_x diminuem conforme há aumento da concentração de Cloro na composição das amostras.

[1] Pal, T.; Kar, T.; Bocelli, G.; Rigi, I. *Crystal growth & design*, **Vol. 4 N. 4**, 743-747 (2004).

[2] Meera, K.; Muralidharan, R.; Dhanasekaran, R.; Manuym, P.; Ramasamy, P. *Journal of Crystal Growth*, **263**, 510–516 (2004).

[3] Mukerji, S.; Kar, T. *Materials Research Bulletin*, **Vol. 33, N. 4**, 619–626 (1998).

Acknowledgments: Agradecemos a empresa PANalytical pela colaboração nas análises de FRX e ao CNPq, a CAPES e a FAPEMA pelo apoio financeiro.

Morphology and size study of (Gd,Er,Yb)-doped NaYF₄ nanoparticles through the X-ray Line Profile Analysis.

R. Lora-Serrano¹, W Iwamoto¹, E. Estevez-Rams², Jeann C. Rodrigues¹, and B. Aragón-Fernandez².

¹Instituto de Física, Universidade Federal de Uberlândia, 38400-902, Uberlândia, MG, Brazil

²Facultad de Física, Universidad de la Habana, San Lázaro y L, CP 10400 La Habana, Cuba

X-ray line profile analysis (XLPA), i.e. the analysis of the broadening, shifting and asymmetries of the Bragg reflections due to microstructure, enables the thorough characterization of the properties of materials, especially those of nanostructured materials. XLPA makes a quantitative analysis of the microstructure in terms of grain and subgrain size, dislocation structure and dislocation densities and planar defects, especially stacking faults and twin boundaries [1]. In this work, we use the XLPA to determine the shape and size of the system of nanoparticles (NPs) Gd-, Er- and Yb-doped NaYF₄. For Yb/Er and Yb/Tm co-doped NaYF₄ samples, the up converting fluorescence effect has been observed [2]. It is known that in nanosystems both, size and shape of the particles can change the physical properties. In particular, the title samples crystallizes in both hexagonal (*h*) and cubic (*c*) nanocrystals depending on the dopant and heat treatment [2,3].

The powder diffraction data were collected at the XPD beamline of the Brazilian synchrotron lightsource. For the deconvolution of the instrumental contribution, standard samples of LaB₆-NIST were used. The evaluation was carried out by using the convolutional multiple whole profile (CMWP) fitting procedures [1]. To obtain the mean size of crystallites and/or their size-distributions, specific functional form of size-distribution has to be assumed. The log-normal size distribution function has been used to describe the size profile of our samples. For *h* NPs, size distribution of about 400 nm were obtained, while less than 100 nm were observed for *c* Nps, depending on the heat treatment. This is in agreement with TEM and HRTEM results [3]. Our results are correlated with the optical and magnetic properties observed.

This work was supported by FAPEMIG and CAPES.

[1] T. Ungár. *J. Mater. Sci.* (2007) **42**:1584–1593.

[2] Holanda *et al.* *Phys. Rev. Lett.* **107**, 026402 (2011)

[3] W. Iwamoto *et al.* *J. Nanosci. Techn.* **10**, 5708 - 5714 (2010).

Crescimento e Caracterização de Cristais Mistos de K com Ni e Co da Família do Sal de Tutton

T. S. Pacheco^a, C. J. Franco^a, G. J. Perpétuo^a.

^a*Departamento de Física, Universidade Federal de Ouro Preto, Ouro Preto, Brasil.*

Uma classe importante de cristais que vem despertando o interesse de muitos pesquisadores são os cristais da família do sal de Tutton, especialmente no estudo de suas propriedades e possíveis transições de fases estruturais. Além disto, propriedades dos cristais mistos são relativamente pouco estudadas.

Os cristais desta família apresentam fórmula química do tipo $A_2^+ B^{2+} (YO_4)_2 \cdot 6H_2O$ onde o íon monovalente $A^+ = K, Rb, Cs$ e NH_4 , e o íon bivalente $B^{2+} = Ni, Co, Fe, Mn, Zn, V, Cu, Cd$ e Mg e $Y = S$ ou Se . Estes cristais possuem estrutura cristalina monoclinica e o grupo espacial P21/c. A combinação das propriedades físicas e químicas dos elementos que formam estes sais permite obter cristais mistos do tipo $A_2^+ B_1^{2+} B_{(1-x)}^{2+} (YO_4)_2 \cdot 6H_2O$, com x variando entre $0 \leq x \leq 1$ em quase todo domínio de composição. Através do método de crescimento de cristais por solução, é possível obter cristais puros e mistos de boa qualidade por evaporação isotérmica da solução. No presente trabalho, apresentamos resultados do crescimento de cristais com composição $K_2 Ni_x Co_{(1-x)} (SO_4)_2 \cdot 6H_2O$, análises termogravimétricas, medidas de espectroscopia Raman e UV-vis, microscopia eletrônica de varredura, análise química por EDS e ICP-OES e difração de raios X.

Resultados preliminares de medidas termogravimétricas mostram que as temperaturas de desidratação destes cristais estão entre 90°C e 100°C. A espectroscopia Raman mostra as bandas associadas aos modos vibracionais de SO_4 , H_2O e do octaedro $Ni(H_2O)_6$ ou $Co(H_2O)_6$. As medidas espectroscopia UV-vis mostram as bandas de absorção nos espectros. Detalhes destes resultados serão apresentados e discutidos.



Figura 1: Amostras cristalinas dos sais de $K_2 Ni_x Co_{(1-x)} (SO_4)_2 \cdot 6H_2O$: puros (vermelho Co, azul Ni) e mistos (verde).

Referências

- [1] HE, Y.; CHEN, J.; SU, G.; ZHUANG, X.; LEE, G.; JIANG, R. Growth of potassium nickel sulfate hexahydrate (KNSH) crystal and its characterization. *Journal of Crystal Growth*, 233. 2001. p. 809-812.
- [2] ZHUANG, X.; SU, G.; HE, Y.; ZHENG, G. Growth and characterization of potassium cobalt nickel sulfate hexahydrate for UV light filters. *Cryst. Res. Technol.*, 41, No.10. 2006. p. 1031-1035.

Agradecimentos: FIMAT/UFOP; LabCri/UFMG; LQN/CDTN; FAPEMIG; CNPq; CAPES.

Utilização do método de Rietveld para identificação e quantificação de diferentes formas polimórficas da Losartana Potássica.

J. A. P. Sato^a, F. F. Ferreira^a

^a*Centro de Ciências Naturais e Humanas, Universidade Federal do ABC, Santo André, Brasil.*

A Losartana Potássica é um medicamento utilizado no tratamento da hipertensão arterial, sendo também utilizado contra insuficiência cardíaca congestiva. Foi o primeiro anti-hipertensivo da classe dos antagonistas receptores da angiotensina disponível no mercado. São reportadas na literatura três diferentes formas cristalinas: ácida, anidra e hidratada, sendo a forma farmacologicamente ativa a anidra [1][2].

O polimorfismo é um fenômeno muito importante a ser considerado pela indústria farmacêutica, pois diferentes polimorfos podem apresentar diferentes propriedades físico-químicas, como solubilidade, taxa de dissolução, reatividade ou ponto de fusão e, portanto, diferentes atividades farmacológicas. Segundo a FDA (*U.S. Food and Drug Administration*), os polimorfos podem ser descritos como "formas cristalinas com diferentes arranjos e/ou conformações das moléculas na rede cristalina". Os princípios ativos podem existir em uma variedade de formas sólidas distintas, incluindo polimorfos, solvatos, hidratos, sais, co-cristais e sólidos amorfos. Cada forma exibe propriedades físico-químicas únicas que podem influenciar profundamente a biodisponibilidade, estabilidade e outras características afetando o desempenho do medicamento[3].

Foram estudadas três amostras do insumo farmacologicamente ativo da Losartana Potássica – duas provenientes de duas farmácias de manipulação da região de Santo André-SP (que serão chamadas de F e S) e uma doada por uma indústria farmacêutica (MX). Foi realizada a caracterização estrutural utilizando as técnicas de difração de raios X por policristais aliada ao método de Rietveld para identificação e quantificação de diferentes formas cristalinas, espectroscopia no infravermelho com transformada de Fourier, microscopia eletrônica de varredura, termogravimetria e calorimetria exploratória diferencial. Além destas amostras, foram objeto de estudo os medicamentos genérico, similar e referência adquiridos em drogarias. Para estas amostras foi realizada a quantificação de fase fármaco-excipiente para identificar qual forma cristalina está presente nos medicamentos.

Para a amostra da farmácia S foi encontrada majoritariamente a fase hidratada com 99,0(3)%. Uma pequena quantidade da forma anidra foi encontrada, correspondendo a 1,0(3)%, porém foi necessário incluir esta fase, mesmo que em pequena proporção, para que alguns picos se ajustem. Para a tentativa de retirada de água da amostra foi realizada uma liofilização a 60 °C por 30 minutos. Após este procedimento, verificamos na amostra 3,6(2,0)% em massa da fase hidratada e 96,4(2,0)% da fase anidra. Já na amostra da farmácia F encontramos 71,1(5)% referente à fase hidratada e 28,9(5)% referente à forma anidra. Por último, a amostra MX apresentou a predominância referente à fase anidra com 97,3(3) %, e uma pequena fração de apenas 2,7(3) % da fase hidratada. A difração de raios X por policristais aliada ao método de Rietveld mostrou-se uma ferramenta eficiente para identificação e quantificação de diferentes polimorfos presentes nas amostras de fármacos bem como na quantificação de excipientes presentes nos medicamentos. Uma vez que a estrutura cristalina do fármaco afeta diretamente a eficácia terapêutica faz-se necessário garantir que a forma cristalina presente nas amostras é a farmacologicamente ativa. As demais técnicas utilizadas neste trabalho corroboraram com as informações obtidas com o uso da difração de raios X por policristais.

[1] Hu, X. R., Wang, Y. W., Gu, J. M., *Acta Crystallographica Section E: Structure Reports*, E61, 1686-1688 (2005).

[2] Do Carmo, W. R., Ferreira, F. F., Diniz, R., *Journal of Pharmaceutical and Biomedical Analysis*, 88, 152-156 (2014).

[3] Elder, D. P., Holm, R., Diego, H. L., *International Journal of Pharmaceutics*, 453, 88-100 (2012).

Agradecimentos: FAPESP; CNPq e UFABC-PPG Nano.

Estudo da composição de gessos a partir da difração de raios X aliada ao refinamento de Rietveld

Heloísa Cristina Fernandes Cordon^a, Fabio Furlan Ferreira^a.

^a*Centro de Ciências Naturais e Humanas, Universidade Federal do ABC, Santo André, Brasil.*

O gesso é um material com larga aplicação. Sua maior utilização se dá na indústria da construção civil, sob a forma de placas, elementos decorativos e pastas para revestimento, embora possa também ser utilizado na confecção de moldes para indústrias cerâmica, metalúrgica e de plásticos; em moldes ortopédicos e dentários, na agricultura e em diversas outras aplicações. A produção de cimento Portland também depende fundamentalmente do gesso, visto que este material é adicionado em teores de 3% a 5% para controle da reação de hidratação do clínquer, que seria imediata sem a sua presença.

Devido ao seu curto tempo útil para utilização após mistura com água, conhecido como tempo de pega, o gesso utilizado como revestimento na construção civil gera um grande desperdício, caracterizando-se como o segundo maior constituinte dos resíduos de construção e demolição (RCD) e a importância de sua reciclagem tem crescido com o aumento da demanda por práticas sustentáveis de construção. Entretanto, a presença de elevado volume de gesso nos RCD pode ser um complicador para a reciclagem destes resíduos se não forem incorporados processos de controle nas Centrais de Reciclagem, uma vez que a reação entre os aluminatos do cimento e o sulfato do gesso, quando em presença de água, leva à formação de etringita, composto cujo volume é maior que dos reagentes originais, gerando tensões expansivas que desagregam as peças de concreto. Por ser um material solúvel em água, a presença de gesso em aterros traz problemas em longo prazo devido à lixiviação, podendo afetar a composição e o pH da água e do solo, ou até mesmo a formação do gás sulfídrico, que é tóxico e inflamável, dependendo de condições específicas de umidade, baixo pH e presença de bactérias redutoras de sulfato.

Uma vez que os resíduos compostos por gesso são facilmente reciclados, bastando calciná-los com baixo consumo energético e reidratá-los para obtenção de novos produtos de gesso, o segmento gesseiro apresenta grande potencial de contribuição para a sustentabilidade da indústria da construção. Apesar das vantagens do processo de reciclagem, acredita-se que o gesso reciclado apresente tempo de pega ainda menor que o gesso natural, talvez devido à redução no tamanho dos cristais, o que provavelmente aumentaria ainda mais o desperdício deste material. Dessa forma, torna-se importante o estudo e caracterização da microestrutura do gesso reciclado para entendimento e controle do fenômeno. O estudo de sua microestrutura, incluindo ensaios de análise térmica (DSC, TG/DTG), difração de raios X, microscopia eletrônica de varredura, é pouco discutido na literatura. Não foi tomado conhecimento de nenhum estudo que se utiliza do refinamento de Rietveld para realizar a análise quantitativa de fases (AQF) presentes no material.

Neste trabalho foram avaliados inicialmente por ensaios de difração de raios X por policristais (DRXP) dois gessos com aplicações diferentes: um de uso odontológico e outro para a construção. Ambos foram estudados em sua forma original e após hidratados, neste caso em duas situações: apenas moídos e moídos e peneirados em peneira com malha de 10 µm de abertura. Os ensaios de DRXP foram conduzidos em um equipamento da marca STOE, modelo STADI-P, com radiação Cu-K α operando a 40 kV e 40 mA, na geometria de transmissão, com as amostras acondicionadas em capilares de vidro especial 14, da marca Hilgenberg, com diâmetro de 0,3 mm e espessura da parede de 0,01 mm, que foram mantidos em rotação durante a aquisição dos dados realizada por um detector com fenda estreita e faixa de 2 θ variando de 10° a 110°. A partir dos difratogramas obtidos fez-se uma determinação da análise quantitativa de fases pelo refinamento de Rietveld, onde observou-se uma grande diferença na composição química dos materiais. O gesso de construção apresentou alto teor de materiais inertes (64,7%), enquanto o gesso odontológico mostrou-se mais puro, com 8,7% de impurezas, ambos na sua forma original. Os materiais hidratados também mostraram-se diferentes entre si. O gesso para construção hidratado e moído apresentou composição diferente do gesso de construção hidratado moído e peneirado, devido à separação de fases ocasionada pelo peneiramento, indicando que a preparação da amostra é um fator importante a ser considerado. A difração de raios X, aliada ao método de refinamento de Rietveld, mostrou-se adequada para a determinação da composição química dos gessos em estudo.

Caracterização Estrutural de Candidatos a Fármacos para doenças negligenciadas.V. M. Prado^a, F. F. Ferreira^a.^a*Centro de Ciências Naturais e Humanas, Universidade Federal do ABC, Santo André, Brasil.*

Sabe-se que a identificação e o estudo das propriedades das diferentes formas cristalinas dos fármacos são de grande importância para avaliar suas possíveis consequências para a manufatura, a segurança e a eficácia dos medicamentos. Sendo assim, o tema polimorfismo tem se destacado cada vez mais na área farmacêutica. Exemplificando, se a formulação farmacêutica será física e quimicamente estável, se o pó irá ou não ser compressível, se o pó será solúvel ou não, são algumas das características que podem estar relacionadas com a escolha da forma cristalina. Neste contexto, o estudo das propriedades estruturais de novos candidatos a fármacos por difração de raios X, entre outras técnicas, permite definir as características conformacionais e configuracionais, úteis aos estudos da relação entre a estrutura química e a afinidade sobre os alvos eleitos [1].

Neste trabalho, algumas novas moléculas, denominadas: LASSBio 1940, LASSBio 1941 (sintetizadas no LASSBio-UFRJ) e MEFAS (sintetizada na FIOCRUZ-Farmanguinhos), potencialmente ativas para algumas doenças negligenciadas como a malária e doença de Chagas foram estudadas e os resultados iniciais obtidos até o momento serão apresentados. Como a obtenção das moléculas aqui estudadas só foi possível na forma de pó, a técnica de difração de raios X por policristais (DRXP) foi considerada. Utilizando os dados de DRXP juntamente com métodos *ab initio* como, por exemplo, o *simulated annealing*, torna-se viável, na grande maioria dos casos, a tentativa da determinação estrutural dessas novas moléculas [2]. Para o posterior refinamento das estruturas será utilizado o método de Rietveld [3]. Outras técnicas complementares como análise térmica – termogravimetria (TG) e calorimetria exploratória diferencial (DSC) – espectroscopia no infravermelho por transformada de Fourier (FTIR), microscopia eletrônica de varredura (MEV) e análise elemental estão sendo utilizadas para complementar e corroborar os resultados obtidos com a DRXP para caracterização estrutural dos compostos. Até o momento, tem-se encontrado dificuldades na indexação dos difratogramas, devido todas as amostras apresentarem difratogramas com muitos picos, sobreposições e regiões pouco definidas. Alguns procedimentos adicionais foram feitos antes das medidas das amostras por DRXP, como liofilização e secagem em estufa. Comparando os dados das análises das amostras como recebida e após os procedimentos citados verificou diferenças nos difratogramas, o que indica que as amostras ainda necessitam de mais procedimentos de purificação, algo que pode encarecer o procedimento de fabricação das mesmas, o que não é muito bom se tratando de possíveis fármacos para doenças negligenciadas. Além disso, indícios que algumas das amostras estão na forma de cloridratos ou solvatos foram encontrados, que serão comprovados com o uso conjunto do DRXP com as técnicas complementares.

[1] G. L. B. Araujo, et al., *Rev. Ciênc. Farm. Básica Apl.*, **33**, 27-36 (2012).

[2] E. H. L. Aarts e J. Korst, *Simulated Annealing and Boltzmann Machines: a Stochastic Approach to Combinatorial Optimization and Neural Computing*, 2 ed. John Wiley & Sons, Chichester (1991).

[3] H. M. Rietveld, *J. Appl. Crystallogr.*, **2**, 65-71 (1969).

Agradecimentos: PPG-Nano-UFABC, CAPES, FIOCRUZ e LASSBio.

Análise estrutural do candidato a fármaco antineoplásico “LASSBio-1735”L. P. de Figueiredo^a, F. F. Ferreira^a.^a*Centro de Ciências Naturais e Humanas, Universidade Federal do ABC, Santo André, Brasil.*

O câncer é uma das doenças que mais causam temor na sociedade por ter se tornado um estigma de mortalidade e dor. Atualmente, é um dos problemas de saúde pública mais complexos que o sistema de saúde brasileiro enfrenta, dada a sua magnitude epidemiológica, social e econômica [1]. Grandes progressos foram feitos nos últimos tempos no entendimento dessa doença e tais progressos têm levado a uma linha de tratamento mais racional do câncer. Entretanto, um dos grandes problemas na quimioterapia do câncer ainda continua sendo a falta de seletividade, ou seja, os antineoplásicos atuam indistintamente nas células neoplásicas e normais, sendo responsáveis por inúmeros efeitos colaterais. Neste contexto, a busca por fármacos antineoplásicos tem aumentado com vistas a se encontrar tratamentos mais efetivos e seletivos, ou que visem à descoberta de novas estratégias que impeçam o avanço da doença. Dentre as substâncias bioativas que atualmente estão em estudos clínicos, a combretastatina A4 (CA-4) tem se destacado quando comparada aos fármacos antineoplásicos disponíveis atualmente para o tratamento do câncer [2].

Neste sentido, recentemente no Laboratório de Avaliação e Síntese de Substâncias Bioativas (LASSBio[®]) da Universidade Federal do Rio de Janeiro (UFRJ), uma série de novos análogos da CA-4 foi sintetizada, destacando-se o composto LASSBio-1586, o qual apresentou resultados promissores quando avaliado seus efeitos citotóxicos frente às linhagens tumorais: HL-60 (leucemia humana), SF-295 (glioblastoma humano), MDA-MB435 (melanoma) e HCT-8 (carcinoma ileocecal – cólon) [2]. Sendo assim, empregando estratégias de modificação molecular características da Química Medicinal, obteve-se a partir do composto LASSBio-1586, o candidato a fármaco antineoplásico denominado “LASSBio-1735”. Dessa forma, o presente trabalho centrou-se na análise estrutural do candidato a fármaco antineoplásico “LASSBio-1735”, mais especificamente, análogo sintético da CA-4. Para tal estudo foi utilizada, principalmente, a técnica de difração de raios X por policristais (DRXP) aliada ao método de Rietveld. Tendo em vista que o candidato a fármaco LASSBio-1735 se trata de uma molécula inédita cuja estrutura cristalina ainda não havia sido reportada, proceder-se com a determinação estrutural utilizando os dados obtidos por DRXP foi de extrema importância. Além disso, pôde-se evidenciar a vantagem de ser executável tal procedimento independentemente de se ter um monocristal, bastando apenas que se tenha uma amostra com um ordenamento cristalino de longo alcance, ou seja, que a amostra seja cristalina. O uso da DRXP aliada ao método de Rietveld também permitiu, de forma inequívoca, identificar e quantificar a mistura de fases presente no composto denominado como “LASSBio-1735-2^o envio” (o qual apresentou diferenças estruturais quando comparado ao LASSBio-1735), mostrando assim, uma das aplicabilidades da referida técnica. A partir destes dados, será possível o LASSBio[®] prover informações para uma melhor compreensão do perfil farmacológico destes compostos sintetizados com diferentes estados de hidratação. Tal fato ressalta a importância de se determinar corretamente a estrutura cristalina dos compostos, pois as eventuais diferenças encontradas entre estes, podem ter importantes implicações farmacológicas.

Vale ressaltar que também estão sendo realizados estudos com nanopartículas poliméricas a fim de promover o encapsulamento do referido candidato a fármaco, visando uma maior acumulação nos tecidos tumorais devido ao efeito EPR, do inglês – *Enhanced Permeability and Retention*, objetivando contornar os conhecidos efeitos colaterais da quimioterapia convencional. Os dados experimentais preliminares demonstraram características promissoras que ainda serão investigadas com maiores detalhes.

[1] INCA, *ABC do câncer: abordagens básicas para o controle do câncer*, Rio de Janeiro:Inca (2012).

[2] Amaral D. N., Planejamento, síntese e avaliação da atividade antitumoral de análogos da combretastatina A4 (CA-4), UFRJ, Rio de Janeiro (2012).

Agradecimentos: FAPESP; CAPES; PPG-Nano-UFABC.

Avaliação estrutural do candidato a fármaco hipoglicemiante “LASSBio-1773”A. L. Ibiapino^a, F. F. Ferreira^b.^a*Centro de Ciências Naturais e Humanas, Universidade Federal do ABC, Santo André, Brasil.*

Diabetes mellitus é um problema de saúde pública com elevado ônus social e econômico, cujo diagnóstico é desconhecido em metade dos indivíduos portadores. O termo diabetes mellitus pode ser definido como uma desordem metabólica de etiologia múltipla, caracterizado pela hiperglicemia crônica resultante de distúrbios no metabolismo de carboidratos, lipídios e proteínas decorrentes de deficiências na secreção de insulina, na ação da insulina, ou ambos. Atualmente, a classificação do diabetes baseia-se na etiologia da doença, o que inclui quatro subtipos: diabetes Tipo 1 (DM1), diabetes Tipo 2 (DM2), diabetes gestacional (DMG) e outros tipos específicos de diabetes. O DM2 é o tipo mais comum de diabetes e está presente em 90% a 95% dos casos. O tratamento farmacológico do DM2 consiste do uso de hipoglicemiantes orais [1]. Hoje, existem diferentes classes de hipoglicemiantes orais sendo comercializados visando o tratamento do DM2, porém, devido aos diversos efeitos adversos que os mesmos ocasionam, muitos deles já foram retirados do mercado, como exemplo, a rosiglitazona[®] e a troglitazona[®]. Baseado nisso, novos candidatos a fármacos hipoglicemiantes com padrão estrutural de ligantes no receptor ativado pelo proliferador de peroxissomo do tipo α (PPAR α) foram planejados e sintetizados no Laboratório de Avaliação e Síntese de Substâncias Bioativas (LASSBio[®]) da Universidade Federal do Rio de Janeiro (UFRJ). Entre os novos candidatos a fármacos sintetizados, merece destaque o LASSBio-1773. O LASSBio-1773 é uma molécula orgânica inédita, que tem apresentado atividade hipoglicemiante quando testada em ratos *Wistar*. O candidato a fármaco LASSBio-1773 foi originado a partir do LASSBio-1471. O LASSBio-1471 é um composto protótipo com atividade hipoglicemiante e anti-inflamatória, o qual também foi desenvolvido no LASSBio[®]. Com a finalidade de otimizar a propriedade hipoglicemiante e anti-inflamatória apresentada pelo LASSBio-1471, foram realizadas no LASSBio[®] algumas modificações estruturais no LASSBio-1471, como: estratégia de abertura de anel e simplificação molecular. Foi com base nessas modificações estruturais que se originou o LASSBio-1773 [2]. Diante desses achados, decidiu-se realizar a caracterização estrutural do LASSBio-1773 baseado na técnica de difração de raios X por policristais (DRXP) aliada ao método de Rietveld, uma vez que, por ser uma molécula inédita não há relatos na literatura relacionados a estrutura cristalina do LASSBio-1773. Assim, através do difratograma experimental foi possível observar que o LASSBio-1773 trata-se uma molécula cristalina e de baixa simetria. Com os dados de DRXP de boa qualidade realizou-se a determinação estrutural do LASSBio-1773 empregando o programa *DASH*. Após a estrutura cristalina do LASSBio-1773 ter sido determinada, prosseguiu ao refinamento de Rietveld utilizando o software *TOPAS Academic v. 5*, e através deste, foi verificado que o LASSBio-1773 se cristaliza em um sistema ortorrômbico, com grupo espacial $P2_12_12_1$. A estrutura cristalina do candidato a fármaco LASSBio-1773 consiste em quatro moléculas por cela unitária ($Z=4$), acomodando uma molécula na unidade assimétrica ($Z'=1$). Outros estudos também estão sendo realizados com o LASSBio-1773, neste caso, o encapsulamento do LASSBio-1773 em nanopartículas de PLGA (ácido poli (D,L-láctico-co-glicólico), objetivando sistema de liberação. Inclui ressaltar que alguns testes preliminares já foram realizados com as nanopartículas de PLGA encapsuladas com o LASSBio-1773, e que por meio destes testes (caracterização físico-química por diferentes técnicas de espalhamento), pôde-se obter partículas coloidais na escala nanométrica, estáveis, monodispersas, e na forma esférica. Tais resultados demonstraram que as nanopartículas de PLGA encapsuladas com LASSBio-1773 apresentam características promissoras para aplicação em sistema de liberação.

[1] IDF *Diabetes Atlas*, Brussels (2013).

[2] da Costa F.P., Novos candidatos a protótipos de fármacos hipoglicemiantes com atividade anti-inflamatória: LASSBio-1773 e LASSBio-1774, UFRJ, Rio de Janeiro (2013).

Agradecimentos: FAPESP; CAPES; PPG-Nano-UFABC.



Small molecules and biological macromolecules (SMBM)

ESTUDIO DE LA INTERACCIÓN DEL FÁRMACO PROPRANOLOL CON MEMBRANAS CELULARES *in vitro* Y MODELOS MOLECULARES

Pablo Zambrano^a, Mario Suwalsky^a, María José Gallardo^b, Strzalka, K.^c

^(a)Facultad de Ciencias Químicas, Universidad de Concepción, ^(b)Centro de Óptica y Fotónica, CEFOP, Facultad de Ciencias Físicas y Matemáticas Universidad de Concepción. ^(c) Department of Plant Physiology and Biochemistry, Faculty of Biochemistry, Biophysics and Biotechnology, Jagiellonian University.

Propranolol (PROP) es un medicamento perteneciente al grupo de los betabloqueadores, ampliamente utilizado en el tratamiento de la hipertensión arterial. Sus principales efectos tóxicos son depresión cardiovascular grave, hipotensión e insuficiencia cardiaca. El objetivo del presente trabajo fue determinar los efectos de propranolol sobre la membrana de eritrocitos humanos y modelos moleculares. Para ello se utilizaron cuatro técnicas experimentales: (a) Se determinó mediante difracción de rayos X los efectos estructurales del fármaco en modelos moleculares de membranas celulares constituidos por bicapas de dimiristoilfosfatidilcolina (DMPC) y dimiristoilfosfatidiletanolamina (DMPE), clases de fosfolípidos que se ubican respectivamente en las monocapas externas e internas de membranas celulares, en particular de glóbulos rojos humanos [1]. Las intensidades relativas de reflexión y espaciados interplanares se obtuvieron a partir de un sistema de MBraun PSD- 50 M lineal sensible a la posición del detector (Garching, Alemania) y el software ASA. Los experimentos se realizaron a 18 ± 1 °C, la cual está por debajo de la temperatura de transición de fase de ambos DMPC (24.3 °C) y DMPE (50.2 °C). (b) Mediante la técnica de calorimetría diferencial de barrido se detectaron los cambios en el comportamiento de fase termotrópico de bicapas de lípidos resultante de la interacción de propranolol con vesículas multilamelares de DMPC y DMPE (c) Mediante microscopía electrónica de barrido (SEM) se evaluaron los efectos de PROP sobre eritrocitos humanos incubando las células en distintas soluciones de la droga en estudio; (d) Finalmente, se utilizó una nueva aplicación de microscopía óptica de desenfoque para cuantificar fluctuaciones de la membrana de glóbulos rojos en tiempo real, estudiando el proceso de “drogado” y “desdrogado” de la célula y su influencia en las propiedades mecánicas en la membrana.

La investigación presenta las siguientes evidencias que demuestran que PROP interacciona con las membranas de glóbulos rojos humanos: (a) Mediante difracción de rayos – X de bicapas fosfolípicas se detecta un aumento en el ancho de bicapa de DMPC desde 55 Å aprox. en su forma cristalina seca hasta 64 Å en su forma hidratada. Esta distancia corresponde a los grupos polares del fosfolípido. Se observa además una fuerte reflexión de 4.2 Å perteneciente a la distancia promedio entre las cadenas acílicas del fosfolípido. El contacto de DMPC con PROP 4 µM genera una fuerte disminución de las intensidades de reflexiones alta y baja. Las reflexiones prácticamente desaparecen con una concentración de PROP 40 µM. Las intensidades de reflexión de DMPE se mantuvieron inalteradas incluso a una concentración de PROP de 7 mM. A partir de estos resultados, se puede concluir que propranolol produce una perturbación estructural significativa de bicapas DMPC; (b) Los resultados de DSC indican que la presencia de propranolol indujo una perturbación más bien leve del comportamiento termotrópico de vesículas de DMPC y DMPE disminuyendo las temperaturas de transición de fase en no más de 1.2 °C; (c) Por medio de microscopía electrónica de barrido (SEM) se comprueba la formación de estomatocitos, debido a la inserción de PROP en la monocapa externa de la membrana de los glóbulos rojos; (d) Microscopía óptica de desenfoque muestra la existencia de cambios biomecánicos en la membrana a concentraciones mucho menores a las concentraciones plasmáticas. Las reconstrucciones tridimensionales de la forma del eritrocito luego de interactuar con propranolol confirman la evolución de la forma discocítica a estomatocítica. Con estos resultados es posible interpretar en términos moleculares los mecanismos tóxicos a nivel celular del propranolol.

[1] Suwalsky M., “Phospholipid Bilayers”, *Polymeric Materials Encyclopedia*, pág. 5073-5075 (1996).

Agradecimientos: El autor agradece al Sr. Fernando Neira por su valiosa asistencia técnica y a FONDECYT (Proyecto 1130043).

CARACTERIZAÇÃO ESTRUTURAL DO SAL DE TUTTON MISTO (Co E Ni)

R. R. V. Leocádio^a, A. C. Batista^a, C. J. Franco^b, G. J. Perpétuo^a

^aRede Temática em Engenharia de Materiais – REDEMAT – Praça Tiradentes nº 20, centro, Ouro Preto/Minas Gerais, 35400-000, Brasil – rodolfoloc@yahoo.com.br

^bUniversidade Federal de Ouro Preto – UFOP / Departamento de Física – Campus Universitário s/n, Morro do Cruzeiro, Ouro Preto/Minas Gerais, Brasil – 35400-000

Estudos dos sais de Tutton de amônia, fórmula geral $(\text{NH}_4)_2\text{M}(\text{SO}_4)_2 \cdot 6\text{H}_2\text{O}$, são amplamente reportados na literatura (M metal bivalente) como compostos isomórficos e isoestruturais que exibem transições de fase. É possível obter também monocristais mistos (M, M') na forma de soluções sólidas, $(\text{NH}_4)_2\text{M}_x\text{M}'_{(1-x)}(\text{SO}_4)_2 \cdot 6\text{H}_2\text{O}$, onde x representa a fração molar. Nesse trabalho propomos o crescimento de cristais

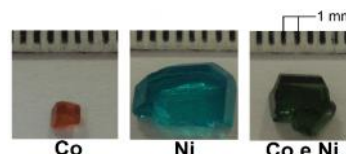


Figura 1: Cristais obtidos.

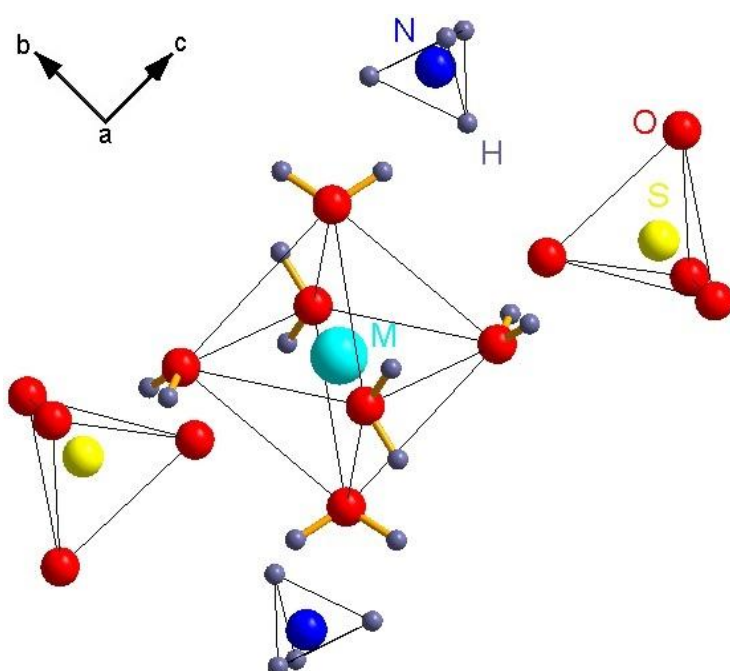


Figura 2: Estrutura cristalina dos sais.

acoplado indutivamente. A difração de raios X por monocristais possibilita confirmar a estrutura (figura 2) dos sais puros para comparação com a literatura, bem como do sal misto, ainda não reportada. Além disto, a análise vibracional por meio da espectroscopia Raman permite o estudo das modificações no espectro (figura 3) com relação à estrutura do sal puro.

mistos $(\text{NH}_4)_2\text{Ni}_{0,5}\text{Co}_{0,5}(\text{SO}_4)_2 \cdot 6\text{H}_2\text{O}$ utilizando o método de evaporação isotérmica da solução em água (figura 1). Espera-se que os cristais obtidos sejam isoestruturais aos sais puros, requerendo métodos de investigação estrutural a fim de analisar as modificações causadas pela formação da solução sólida à temperatura ambiente. Para a caracterização estequiométrica empregamos um espectrômetro de emissão atômica por plasma

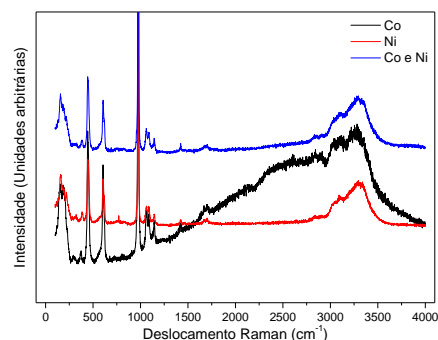


Figura 3: Espectros Raman.

Palavras-chave: Sal de Tutton, Crescimento de cristais, Espectrômetro de emissão, Difração de raios X por monocristais, Espectroscopia Raman.

Agradecimentos: FAPEMIG; UFOP; LabCri/UFMG.

Supramolecular study of 6-((2-(pyridin-2-yl)hydrazono)methyl)pyridin-2-yl)methanol

M. Soto-Monsalve^a, A. Cabrera-Espinoza^b, C. D. Grande^c, R. F. D'Vries^d, M. N. Chaur^b.

^aInstituto de Química de São Carlos, Universidade de São Paulo, São Carlos, Brazil.

^bDepartamento de Química, Universidad del Valle, Cali, Colombia.

^cPrograma de Ingeniería Agroindustrial, Universidad San Buenaventura, Cali, Colombia.

^dInstituto de Física de São Carlos, Universidade de São Paulo, São Carlos, Brazil.

6-((2-(pyridin-2-yl)hydrazono)methyl)pyridin-2-yl)methanol (Figure 1) was synthesized with 82% yield, crystallized in the monoclinic space group $C 2/c$ and presents a configuration E with respect to the $C7=N2$ bond hydrazone framework.

The crystal packing is formed via hydrogen bonds. Weak interactions join the layers stacking.

The 2D supramolecular arrangement was topologically simplified. Each molecule is interconnected by hydrogen bonds acting as 3- connected nodes. This connectivity give rise to 2D network type hcb (Shubnikov hexagonal plane net/(6,3)) with point symbol (6^3) [1].

The analysis of the Hirshfeld surface was studied. The convex blue curvature for the donor groups is observed mainly in the N—H, O—H and C—H region [2, 3]. The finger prints graphic presents a symmetric behavior where the two sharp peaks projecting towards the bottom of the fingerprint plot is due to strong N—H...N interactions and O—H...N [4]. The analysis of overlapping contributions showed that the H...H and C...H interactions contribute in largest value to the Hirshfeld surface with 44.7% and 14.3% respectively. The N...H interactions that corresponding with the homosynthon formation contribute with 10.1%, while the H...N interaction that involve the dimmers connectivity and other interactions contribute with 7.4%. Finally, the strong O...H interaction contribute with the 3.5% of the surface.

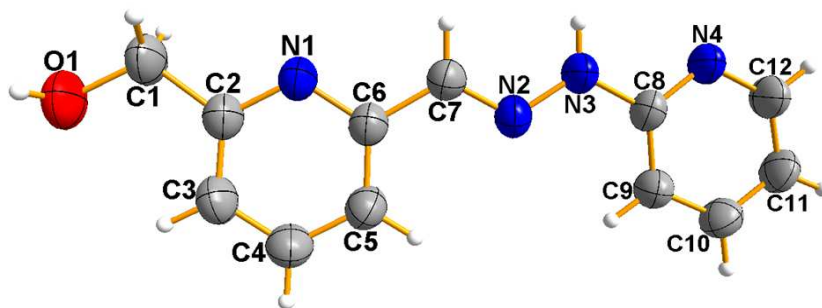


Figure 1: ORTEP representation of the title compound, showing the atom labelling. Displacement ellipsoids are drawn at the 50% probability level.

[1] Blatov, V. A., Shevchenko, A. P. & Proserpio, D. M. *Cryst. Growth & Des*, **14**, 3576-3586 (2014).

[2] McKinnon, J. J., Spackman, M. A. & Mitchell, A. S. *Acta Cryst. B*, **60**, 627-668 (2004).

[3] Hirshfeld, F. L. *Theor. Chim. Acta*, **44**, 129-138 (1977).

[4] Spackman, M. A. & McKinnon, J. J. *CrystEngComm*, **4**, 378-392 (2002).

Solid-state investigation of two novel cocrystals of the anti-tuberculosis drug Ethionamide

C. C. Melo^a and J. Ellena^a

^a*Instituto de Física de São Carlos, Universidade de São Paulo, CP 369, 13560-970, São Carlos-SP, Brazil*

Ethionamide (ETH) is a second-line antituberculosis drug, manufactured as an oral dosage form under the brand name Trecator®, and is in general administered in combination with others antimycobacterium drugs, such as pyrazinamide, rifampicin and ethambutol, in cases where it is observed intolerance or resistance by isoniazid to the *Mycobacterium tuberculosis*[1-2]. As part of ongoing efforts to develop new solid-state forms of ETH, herein we present two cocrystals obtained through the reaction of ethionamide with fumaric and adipic acids. These acids were chosen not only because of their pKa values, but also because they are pharmaceutically accepted, belonging to the GRAS list. Furthermore, in the design of new solid-state forms, it is important to consider the functional groups present in the API and in the co-formers in order to search for a specific synthon. In this case, we used the robust pyridine-carboxylic acid heterosynthon for the designing of these novel solid forms. The cocrystals were investigated by single crystal X-ray diffraction and are both belong to the triclinic centrosymmetric space group $P\bar{1}$. As expected, the crystal structures feature the classical $R_2^2(7)$ heterosynthon involving ETH and the carboxylic acid. Additionally, the crystallographic results have been complemented by thermal analysis (DSC, TGA and Hot-stage microscopy) studies.

[1] Brossier, F., Veziris, N., Truffot-Pernot, C., Jerlier, V., Sougakoff, W., *Antimicrobial Agents Chemotherapy*, **55**(1), 355–360 (2011).

[2] Goldberg, D. E., Siliciano, R. F., Jacobs Jr, W. R., *Cell*, **148**(6), 1271–1283 (2012).

Acknowledgments: CAPES and CNPq.

Mononuclear Cu(II) complex of 1-phenyl-1*H*-1,2,3-triazole-4-carboxylic acid and changes of sequential products due coordination, through experimental electron density point of view

M. C. R. Freitas^{a,b}, W. B. S. Braga^a, L. H. R. Santos^b, K. Krämer^b, C. Fiolka^b, N. A. Rey^c, J. A. L. C. Resende^a, P. Macchi^b.

^aInstituto de Química, Universidade Federal Fluminense, Niterói, Brazil.

^bDepartment of Chemistry and Biochemistry, University of Bern, Bern, Switzerland.

^cDepartamento de Química, Pontifícia Universidade Católica do Rio de Janeiro, RJ, Brazil.

In this work, for the first time experimental electron density and topological analyses are presented for derivative 1,2,3-triazoles compounds – **I** and **II** as well as the corresponding Cu(II) complex - **III** (**Figure 1a**). The charge density maps are obtained from right resolution XRD at T =110 K, applying the multipole refinement [1]. Then we present an analysis of electron density changes (EDC) along the oxidation from **I** to **II**, as well as the coordination process from **II** to **III** (**Figure 1b**). Moreover we could correlate the experimental *d*-orbital population and the magnetic properties. All compounds belong to the monoclinic system, space group P2₁/c. The electron density redistributions are usually small, as represented by the 0.01 e.Å⁻³ isosurface level in **Figure 1b**, and do not show any systematic trend. The $\rho^{\text{compII}} - \rho^{\text{compI}}$ difference present very small redistributions around the nuclei, while the $\rho^{\text{compIII}} - \rho^{\text{compII}}$ difference shows slightly larger charge density redistributions in both nuclei and valence regions. The most striking differences are those concerning the electron density redistributions around the N3 - atom and the carboxylic group, which are the sites directly coordinated to the metallic center. As a consequence of the coordination, the electron density at the C6=O2 bond decreases, whereas there is an accumulation of charge in the O2 lone-pair region. The electrostatic potentials (EP) are present in **Figure 1c**. Nitrogen atoms N2 and N3, oxygens O1 and O2 (for **II** and **III**) as Cl (in **III**- not shown in the figure), have negative electrostatic potentials (drawn as red contours), corresponding to low electron affinity. The *d*-orbital populations reveal an orbital asymmetric filled due differences energie related to the Jahn-Teller effect. A magnetic measurement (MM) was also performed (**Figure 1d**) and the confirmation for an incomplete filled orbital was extracted from the fit to a Brillouin function (red curve - **Figure 1d**), with S = ½ and g = 2.16, as seen from the adjustment (blue curve - **Figure 1d**).

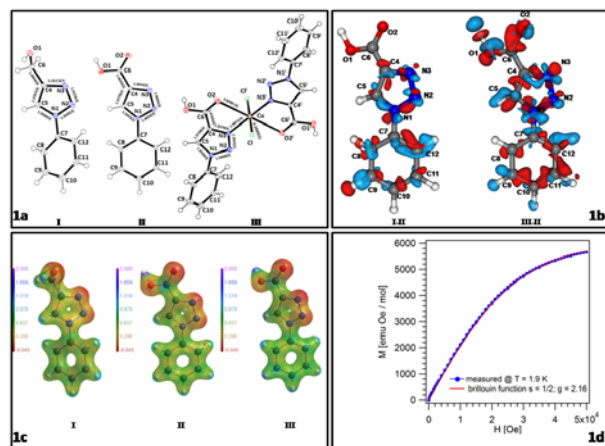


Figure 1: a-Ortep, b-EDC, c- EP and d-MM.

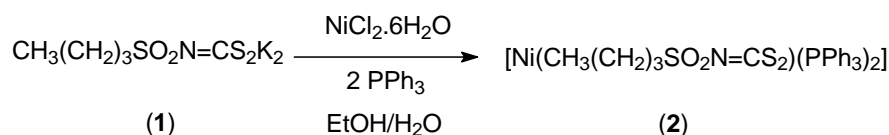
[1] Volkov, A.; Macchi, P.; Farrugia, L.; Gatti, C.; Mallinson, P.; Richter, T.; Koritsanszky, T. XD2006 -

Acknowledgments: CAPES, CNPq, SNSF and UFF.

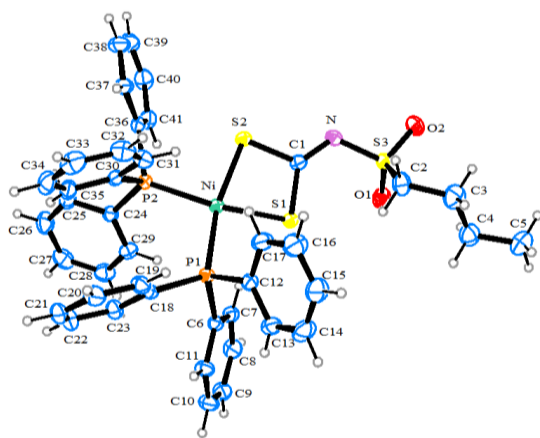
The abstract was not suitable for template. The text had to be cut

Estrutura cristalina do composto butilsulfonilditiocarbimatobis(trifenilfosfina)níquel(II)R. A. C. Souza^a, S. Guilardi^a, A. E. C. Vidigal^b, M. M. M. Rubinger^b, M. R. L. Oliveira^b, J. A. Ellena^c^aInstituto de Química, Universidade Federal de Uberlândia, Uberlândia, Brasil.^bDepartamento de Química, Universidade Federal de Viçosa, Viçosa, Brasil.^cInstituto de Física de São Carlos, Universidade de São Paulo, São Carlos, Brasil.

Ditiocarbamatos ($R_2NCS_2^-$) são utilizados como aceleradores da vulcanização da borracha e fungicidas^[1]. Uma classe de compostos estruturalmente semelhantes e menos estudados, os ditiocarbimatos ($RN=CS_2$)²⁻, apresenta atividade antifúngica. Este trabalho reporta a caracterização estrutural por difração de raios X de um complexo de níquel contendo ditiocarbimato, que apresenta significativa atividade antifúngica contra *Botrytis cinerea*, um fungo que afeta mais de 200 culturas. O complexo em estudo (**2**) foi sintetizado a partir do butilsulfonilditiocarbimato de potássio (**1**) em reação com cloreto de níquel(II) e trifenilfosfina em etanol/água, como ilustrado pelo esquema 1.

Esquema 1. Síntese do butilsulfonilditiocarbimatobis(trifenilfosfina)níquel(II) (**2**)

Os dados de intensidade de raios X do complexo foram coletados em um difratômetro Nonius Kappa CCD, a temperatura de 293(1) K, usando radiação MoK α (0,71073 Å). A estrutura foi resolvida por Métodos Diretos e refinada por mínimos quadrados. O composto cristaliza no sistema triclinico, grupo espacial P $\bar{1}$. A representação ORTEP-3 da unidade assimétrica está ilustrada na Figura 1.



O átomo de níquel está coordenado por dois átomos de enxofre do ânion ditiocarbimato e dois átomos de fósforo dos ligantes trifenilfosfina em uma geometria quadrado planar distorcida. O ângulo S-Ni-S [77,95(3)°] é menor do que o ângulo P-Ni-P [100,67(3)°] devido a quelação bidentada do ligante RSO_2NCS_2 e ao efeito estereoquímico dos ligantes volumosos trifenilfosfina. Os comprimentos de ligação Ni-S [2,194(1) - 2,212(1) Å] e Ni-P [2,211(1) - 2,232(1) Å] não são significativamente diferentes.

Figura 1. Representação ORTEP-3 do complexo em estudo (elipsóides com 30% de probabilidade).

As distâncias de ligação C-S [1,735(2) e 1,753(2) Å] do fragmento NCS_2 são próximas e mais curtas do que uma ligação C-S simples [ca de 1,81 Å]. A dupla ligação C1=N é de 1,283(3) Å. Comportamento similar é observado para compostos de níquel (II) correlatos^[2]. O ângulo de torção C1-N-S3-C2 é de -69,4(1)°. No empacotamento cristalino estão presentes interações intermoleculares do tipo C-H \cdots O.

[1] G. Hogarth. *Prog. Inorg. Chem.*, **53**, 71 (2005).[2] M. R. L. Oliveira; E. F. Franca; C. Novais; S. Guilardi; I. Machado Jr; J. Ellena; J. Amim Jr.; V. M. De Belli; M. M. M. Rubinger. *Inorg. Chim. Acta*, **376**, 238 (2011).

Agradecimentos: Rede Mineira de Química; FAPEMIG; CAPES; CNPq.

Efecto de extractos de hojas de *Jacquinia frutescens* sobre eritrocitos humanos y modelos moleculares.

K. Petit^a, M. Suwalsky^a, J. Colina^a, M. Avello^b

^aFacultad de Ciencias Químicas, Universidad de Concepción, Concepción, Chile.

^bFacultad de Farmacia, Universidad de Concepción, Concepción, Chile.

Jacquinia frutescens, también conocida como "Trompillo", es una planta de la familia Theophrastaceae que crece en el occidente de Venezuela y en las Antillas del Caribe. Infusiones de las hojas de esta planta se han utilizado por mucho tiempo en la medicina tradicional herbal.

La composición química de las hojas de *J. frutescens* indican la presencia de flavonoides, alcaloides, saponinas, cumarinas y triterpenos. Estos compuestos, especialmente los flavonoides, tienen propiedades antioxidantes.

Con el objetivo de evaluar los mecanismos de las propiedades antioxidantes y la toxicidad de los extractos de esta planta poco estudiada, los extractos acuosos de sus hojas fueron inducidos a interactuar con eritrocitos humanos y los modelos moleculares de su membrana. Estos últimos consistían en bicapas de dimiristoilfosfatidilcolina (DMPC) y dimiristoilfosfatidiletanolamina (DMPE), representantes de las clases de fosfolípidos situados en las monocapas exterior e interior de la membrana de los eritrocitos, respectivamente.

Observaciones en microscopía electrónica de barrido (SEM), indicaron que los extractos lograron una alteración significativa en la forma de los eritrocitos, induciendo la formación equinocitos. Según la hipótesis del par bicapa, los cambios en la forma indican que los compuestos presentes en el extracto de *J. frutescens* se localizan en la monocapa externa de la membrana de los eritrocitos. Los resultados obtenidos por difracción de rayos X de las bicapas de DMPC y DMPE, confirman esta conclusión.

Referencias

- [1] M. Suwalsky, K. Oyarceb, M. Avello, F. Villena, C. Sotomayor. Chem-Biol Inter, 179, 413–418 (2009).
- [2] M. Sheetz, S. Singer. Proc. Nat. Acad. Sci. USA . 71: 11, 4457-4461(1974).
- [3] Schnee, L. Plantas comunes de Venezuela. Universidad Central de Venezuela (3a. ed.). Caracas, (1984).

Agradecimientos: A Fernando Neira por su asistencia técnica y FONDECYT (proyecto de investigación 1.130.043)

Picrato de Lamivudina, 3TCH.pic: Em busca de novos sítios moleculares, para a modulação de propriedades de estado sólido e farmacêuticas.

J. C. Tenorio^a, J. Ellena^a.

^aInstituto de Física de São Carlos, Universidade de São Paulo, São Carlos, Brasil.

A importância da engenharia de cristais aplicada para o aprimoramento de propriedades farmacológicas de compostos atualmente comercializados na indústria farmacêutica, mediante a síntese de sais/cocristais, é uma vertente que tem ganhado espaço dentro do campo farmacêutico. Parte dos esforços feitos nesta abordagem é a busca por novos sítios moleculares gerados entre um co-formador e, neste caso, um fármaco. Uma vez que a modulação de algumas propriedades físico-químicas destes sais/cocristais é uma consequência das interações supramoleculares, por exemplo, a estabilidade ou a solubilidade entre outras [1]. Neste caso é apresentada a análise cristalográfica por difração de raios X de monocristal de um sal do fármaco lamivudina, 3TC. Um dos antirretrovirais da transcriptase reversa, mais utilizados e comercializados atualmente no mundo para o tratamento do HIV. Trata-se do sal derivado do ácido pícrico, o picrato de lamivudina, 3TCH.pic. Este sal orgânico é uma nova modificação cristalina do 3TC, o qual cristaliza no grupo espacial ortorrômbico $P2_12_12_1$, com um par iônico por unidade assimétrica. Um aspecto característico deste novo sal é a formação de um novo sítio molecular, denominado sítio: Dois doadores/Três aceptores (2D/3A), não reportado dentro das estruturas cristalinas conhecidas do fármaco 3TC até agora [2,3], no qual há a presença de dois centros doadores (Nitrogênios imídico e amínico da citosina) e três centros aceptores (Oxigênios dos grupos fenol e nitro do ácido pícrico) de ligações de hidrogênio. As implicações da estabilidade e recorrência deste sítio molecular, como também, das demais interações intermoleculares envolvidas no empacotamento cristalino são discutidas. Resultados envolvendo outras técnicas suplementares para caracterização de estado sólido desta modificação cristalina também serão apresentados (Raios X de pó, Infravermelho, Raman e Microscopia Térmica “Hotstage”). Este estudo de caracterização cristalográfica e estrutural pretende prever determinadas propriedades (estabilidade estrutural) as quais possam futuramente estar relacionadas com aplicações farmacêuticas para o melhoramento do desempenho do fármaco da lamivudina 3TC.

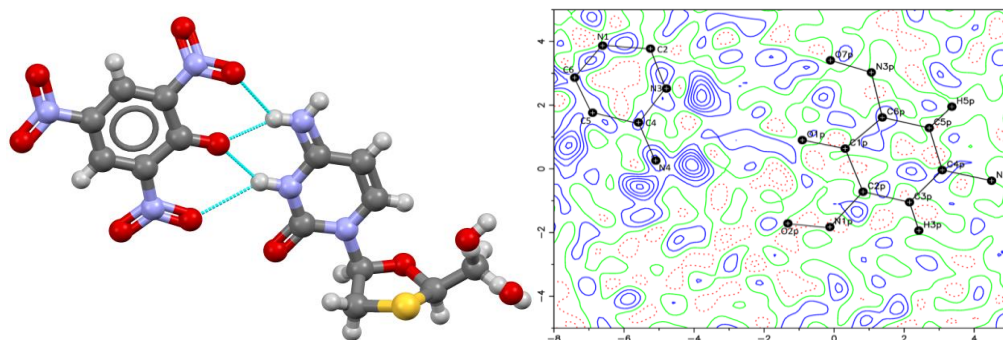


Figura 1: Estrutura do sal 3TCH.pic (esquerda). Mapa de densidade residual por síntese de Fourier diferença (direita) dos fragmentos envolvidos no sítio molecular (2-D/3-A). As linhas sólidas e as tracejadas são contornos positivos e negativos. Os níveis de contorno são intervalos de $0,1 \text{ \AA}^{-3}$.

- [1] Wouters, J., *Pharmaceutical Salts and Co-crystals*; Royal Society of Chemistry, Cambridge (2011).
- [2] Tenorio, J., Ellena, J., *CrystEngComm*, **Advanced Article** (2015).
- [3] da Silva, C., Martins, F., *CrystEngComm*, **15**, 6311 (2013).

Agradecimentos: Fundação de Amparo à Pesquisa do Estado de São Paulo FAPESP

Study of the structural effect of the addition of a nitro group in Copper(II)-dipeptidephenanthroline complexes and its consequence on their cytotoxic activity.

Natalia Alvarez^a, Sebastián Iglesias^a, M. Gabriela Kramer^b, María H. Torre^a, Eduardo Kremer^a, Javier Ellena^c, Antonio J. Costa-Filho^d, Gianella Facchin^a.

^aFacultad de Química, Universidad de la República, Montevideo, Uruguay.

^bInstituto de Higiene, Facultad de Medicina, UdelAR, Montevideo, Uruguay.

^cInstituto de Física de São Carlos, Universidade de São Paulo, São Carlos, SP, Brasil

^dFaculdade de Filosofia, Ciências e Letras de Ribeirão Preto, USP, Ribeirão Preto, SP, Brasil

In the search of new inorganic compounds with antitumor activity a new series of homonuclear copper complexes have been obtained. The compounds present the general formula [Cu(L-dipeptide)(5-NO₂-phen)]·nH₂O, where dipeptide is Ala-Phe, Phe-Ala, Phe-Val and Phe-Phe. They have been characterized by elemental analysis, FT-IR, EPR, electronic spectroscopy and suitable crystals for X-ray diffraction studies were obtained only for the complex with Phe-Ala, being the sixth known structure of a copper complex of 5-nitro-phenanthroline.

Comparative studies of the crystal structure of [Cu(Phe-Ala)(5-NO₂-phen)]·4H₂O with its analogue with phenanthroline were carried out with the solid state module of the Mercury program. The compounds are isomorphic, the introduction of the nitro substituent did not affect the structure of the obtained solid, neither the geometry of the metal center (Figure 1).

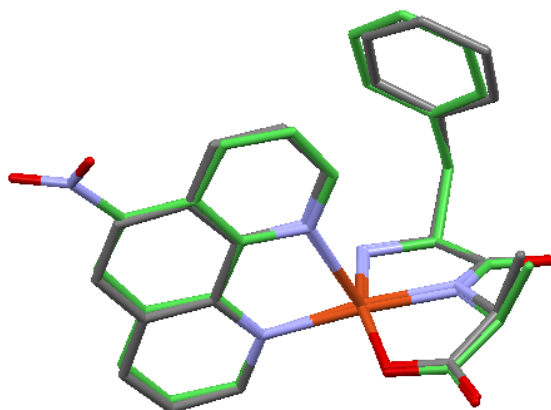


Figure 1: Results of the solid form module comparison tool for the Cu Phe-Ala complex with phenanthroline and 5-nitro-phenanthroline.

The complexes present square-based pyramidal coordination geometry. UV-Vis spectroscopy results suggest that the coordination observed in solid state is maintained in solution. The complexes bind to isolated DNA, as studied by Circular Dichroism.

Biological experiments showed that all the complexes induce cell death in HeLa (human cervical adenocarcinoma) and MDA MB (human metastatic breast adenocarcinoma) cell lines. [Cu(Ala-Phe)(5-NO₂-phen)] presents the lowest IC₅₀ value. [Cu(dipeptide)(5-NO₂-phen)] complexes are less active than their analogs [Cu(dipeptide)(phen)] complexes. The results suggest that the decreased cytotoxic activity is not due to structural variations around the copper center but the presence of the nitro substituent in the phenanthroline ligand which affects its affinity towards DNA and could modify the electronic properties of the complex (such as redox potential) given that the nitro group is electron attractor.

Acknowledgments: CAPES/UdelAR; CNPq; PEDECIBA; CSIC.

Motilidad de Espiroquetas: estudios estructurales del flagelo de *Leptospira*

F. San Martín¹, F. Trajtenberg¹, L. Zarantonelli¹, A. Mechaly¹, N. Morero^{1*}, A. Buschiazzo¹

¹ *Unidad de Cristalografía de Proteínas, Institut Pasteur de Montevideo, Uruguay*

* *Dirección actual: European Molecular Biology Laboratory, Heidelberg, Germany*

La Leptospirosis es una de las zoonosis más extendidas en el mundo, con más de 1.700.000 casos en humanos por año (tasas de mortalidad del 10%, o más en variantes con síndrome pulmonar hemorrágico – estimaciones de OMS, 2012). La enfermedad es causada por *Leptospira*, bacterias espiroquetas alargadas y con forma celular espiralada. A diferencia de la mayoría de las bacterias conocidas, presenta dos flagelos periplasmáticos dispuestos uno en cada polo. La rotación coordinada de los mismos determina el movimiento translacional, siendo esencial para la virulencia de las especies patógenas.

La composición proteica del filamento flagelar de *Leptospira* es más compleja que la de flagelos mejor conocidos como de *E. coli* y *Salmonella spp.* Presenta cuatro isoformas de la proteína FlaB, homólogas a flagelina, que formarían el núcleo del filamento. Esta estructura está rodeada por proteínas adicionales, algunas mejor conocidas como las isoformas 1 y 2 de FlaA (que se postula funcionan de vaina), y otras recientemente descubiertas por nuestro y otros laboratorios: Fcp1 (*Flagellar-coiling protein 1*) y Fcp2. Esenciales para el movimiento translacional, Fcp1 y Fcp2 están involucradas en el super-enrollamiento espontáneo del filamento flagelar.

En este trabajo avanzamos en la caracterización estructural de los componentes flagelares. Recientemente hemos obtenido las estructuras cristalinas de Fcp1 de *L. biflexa* y de Fcp2 de *L. interrogans*, trabajo que estamos extendiendo a las proteínas ortólogas faltantes. Asimismo, estamos optimizando la expresión recombinante de las proteínas FlaA, para su posterior estudio cristalográfico. Las estructuras de estas proteínas adicionales, junto al modelo por homología del núcleo de FlaB nos permitirán avanzar hacia su ajuste en reconstrucciones 3D de filamentos flagelares intactos por crio-microscopía electrónica.

Efecto del extracto de *Pilocarpus goudotianus* sobre eritrocitos humanos y modelos moleculares de membrana celular.

J. Colina^a, M. Suwalsky^a, K. Petit^a, M. Avello^b

^aFacultad de Ciencias Químicas, Universidad de Concepción, Concepción, Chile.

^bFacultad de Farmacia, Universidad de Concepción, Concepción, Chile.

Pilocarpus goudotianus es una planta de la familia Rutaceae que crece en la zona tropical de América, particularmente en Venezuela y Colombia. Las preparaciones a partir de las hojas de esta planta son usadas en la medicina tradicional para tratar diferentes tipos de enfermedades. El análisis fitoquímico del extracto acuoso de las hojas de esta planta indica la presencia de alcaloides y compuestos fenólicos los cuales tienen propiedades tóxicas y antioxidantes.

Con el fin de evaluar los mecanismos de toxicidad y sus propiedades antioxidantes, extractos acuosos de las hojas de *P. goudotianus* fueron inducidos a interactuar con glóbulos rojos humanos, y modelos moleculares de su membrana, estos consistían en bicapas de dimiristoilfosfatidilcolina (DMPC) y dimiristoilfosfatidiletanolamina (DMPE), dos de los fosfolípidos situados en las monocapas exterior e interior de las membranas celulares, en particular la del eritrocito. Se escogieron eritrocitos humanos debido a la relativamente simple constitución de su membrana y la ausencia de orgánulos internos, lo que representa un sistema celular ideal para estudiar interacciones de compuestos químicos con la membrana celular. Este sistema ha sido usado en nuestro laboratorio para determinar la interacción y efecto protector al estrés oxidativo en eritrocitos por extractos acuosos de plantas nativas Chilenas.

La capacidad de los extractos para perturbar la estructura de las bicapas de DMPC y DMPE fue evaluada por difracción de rayos X, cambios en la morfología de los eritrocitos fue observada por microscopía electrónica de barrido (SEM), de acuerdo con la hipótesis del par bicapa las perturbaciones morfológicas que ocurren en los eritrocitos son causadas por la interacción de moléculas con la monocapa externa o interna de su membrana. Las propiedades antioxidantes fueron determinadas a través de ensayos de hemólisis causada por HClO, el cual es un poderoso oxidante biológico que causa daño a bacterias, células tumorales y eritrocitos.

Los resultados de difracción de rayos X muestran que los extractos acuosos de *P. goudotianus* producen perturbaciones estructurales en las bicapas de DMPC, pero no se observaron efectos significativos en las bicapas de DMPE, las observaciones de SEM indican que los extractos inducen alteraciones en la morfología de los eritrocitos humanos, de la forma discoide normal a la de equinocito, estos resultados indican que los compuestos presentes en el extracto de las hojas de *P. goudotianus* se localizan principalmente en la monocapa externa del eritrocito. Los ensayos de hemólisis muestran que los extractos de *P. goudotianus* neutralizan la capacidad de HClO para producir hemólisis, demostrando un efecto protector al daño oxidativo causado por HClO sobre eritrocitos humanos.

Referencias

- [1] M. Suwalsky, P. Vargas, M. Avello, F. Villena, C. Sotomayor. Int Jour of Phar 363, 85-90 (2008).
- [2] M. Suwalsky, P. Orellana, M. Avello, F. Villena. Food and Chemical Toxic. 45 (2007) 130-135
- [3] M. Sheetz, S. Singer. Proc. Nat. Acad. Sci. USA . 71: 11, 4457-4461(1974).
- [4] Amaro J., Massanet G., Pando E., Rodriguez F., Zubia E. Planta Med. 56, 304-306 (1990)

Agradecimientos: A Fernando Neira por su asistencia técnica y FONDECYT (proyecto de investigación 1.130.043)

Structure of full-length human galectin-4

J. K. Rustiguel^a, R. O. S. Soares^a, K. L. Malzbender^b, K. M. Davis^c, S. Meisburger^b, N. Ando^b, M. C. Nonato^a.

^a*Departamento Química e Física, Faculdade de Ciências Farmacêuticas de Ribeirão Preto, Ribeirão Preto, Brasil.*

^b*Department of Chemistry, Princeton University, New Jersey, United States of America.*

Galectins are a multifunctional family of proteins that share characteristics as affinity for beta-galactosides and the presence of at least one Carbohydrate Recognition Domain – CRD [1]. With sixteen members, galectins are grouped in three subtypes, based on the number and organization of their CRDs: proto-type, chimera and tandem repeat [2]. The tandem repeat type is characterized by the presence of two different CRDs (CRD1 at the N-terminal and CRD2 at the C-terminal) connected by a linker peptide. Studies have shown that tandem repeat galectins are more potent to induce the same cell response compared with the proto-type ones [3], probably due the presence of the linker domain [4]. Moreover, differences in the biological function can be consequence of the length and intrinsic features of the linker [4], but its biological role is poorly understood. In general, there are limited studies about structural aspects of tandem repeat galectins that correlate its biological activity and different preferences for carbohydrates. In our work, we propose the first structure for a full-length tandem repeat galectin, the human galectin-4 (hGal-4), using X-ray crystallography, small-angle X-ray scattering (SAXS), molecular modelling, molecular dynamics simulations and thermofluor methodologies. In this context, the isolates CRDs and full-length protein were cloned and obtained by heterologous expression in *E. coli* followed by affinity purification in Ni-NTA resin and size exclusion chromatography. CRD1 and CRD2 have been successfully crystalized by vapor diffusion and both structures have been solved by molecular replacement. The full-length structure was built in MODELLER using CRD1 and CRD2 coordinates and an *ab initio* model for the linker peptide from ROSETTA server. Molecular dynamics simulations were applied to obtain the best-minimized model. The thermofluor and SAXS studies for hGal4 corroborate the final dynamics simulation model. Our results provide an important contribution to the structural knowledge of tandem repeat galectins and can be used as tools for understanding the biological functions that hGal4 plays in pathological processes in colorectal cancer and inflammatory bowel disease [5, 6].

[1] S.H. Barondes, D.N.W. Cooper, M.A. Gitt, H. Leffler. *Journal of Biological Chemistry*, **269**, 20807-20810 (1994).

[2] J. Hirabayashi, K.-i. Kasai. *Glycobiology*, **3**, 297-304 (1993).

[3] Y. Levy, S. Auslender, M. Eisenstein, R.R. Vidavski, D. Ronen, A.D. Bershadsky, Y. Zick. *Glycobiology*, **16**, 463-476 (2006).

[4] S. Di Lella, V. Sundblad, J.P. Cerliani, C.M. Guardia, D.A. Estrin, G.R. Vasta, G.A. Rabinovich. *Biochemistry*, **50**, 7842-7857 (2011).

[5] M.F. Troncoso, M.T. Elola, D.O. Croci, G.A. Rabinovich. *Front Biosci*, **4**, 864-887 (2012).

[6] A.I. Belo, A.M. van der Sar, B. Tefsen, I. van Die. *PLoS One*, **8**, e65957 (2013).

Acknowledgments: Fundação de Amparo à Pesquisa (2010/16153-2 and 2011/21811-1 grants).

Crystallization and preliminary X-ray diffraction analysis of a GH74 xyloglucanase from *Xanthomonas campestris* pv. *campestris*

E. A. de Araújo^a, A. Tomazini Jr^a, M. A. S. Kadowaki^a, M. T. Murakami^b and I. Polikarpov^a

^a Instituto de Física de São Carlos, Universidade de São Paulo, 400, Trabalhador Saocarlense, São Carlos, São Paulo, 13566-590, Brasil.

^b Laboratório Nacional de Biociências, CNPEM, 10000, Giuseppe Máximo Scolfaro, Campinas, São Paulo, 13083-100, Brasil.

Xyloglucanases (Xghs) are important enzymes involved in xyloglucan modification and degradation [1–9]. *Xanthomonas campestris* pv. *campestris* (*Xcc*) is a phytopathogenic bacterium able to synthesize a wide range of extracellular enzymes which hydrolyze different kinds of substrates and a large number of glycosyl hydrolases (GH), but has only one family 74 GH (*Xcc*-Xgh) [10–12].

Analyzing the genomic sequence data of *Xcc* ATCC33913 in the CAZy [13], the uncharacterized gene XCC1752 (GenBank: NP_637119.1) was identified. This gene was annotated as a putative cellulase (81.14 kDa) belonging to GH74. We set out to determine *Xcc*-Xgh three-dimensional structure in hope that its structural characterization will contribute to the catalog of GH74 structures and might provide insights about molecular basis of bacterial xyloglucanases mode of action on xyloglucan polysaccharides.

The *Xcc*-Xgh protein was submitted to several crystallization trials and small crystals were obtained by a sitting-drop method in a condition consisting of 100 mM sodium cacodylate buffer pH 6.5, 200 mM calcium acetate and 18% (w/v) polyethylene glycol 8000, however macroscopic form of the crystals resembled a shower of needles (Fig. 1a). In order to obtain diffraction-quality crystals, the condition of initial crystallization was exhaustively optimized and the best crystals with a typical size of 0.2 mm in the largest dimension were obtained in 100 mM sodium cacodylate buffer pH 6.5, 18% PEG 8000, 200 mM calcium acetate at 291 K and grew in 1 day (Fig. 1b).

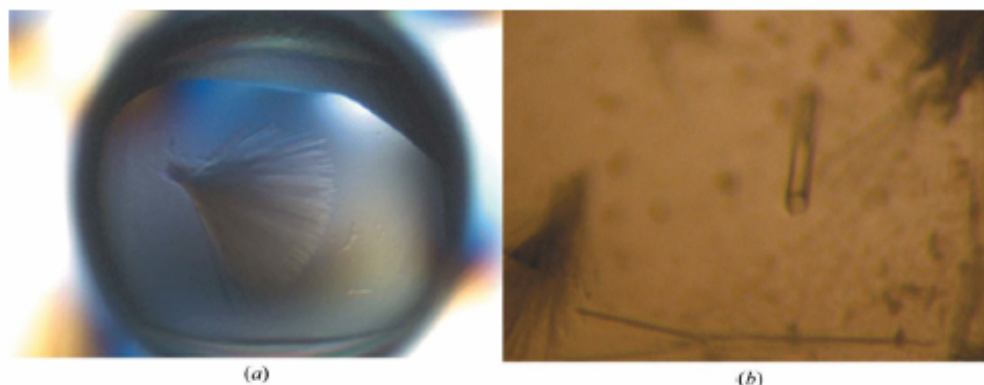


Figure 1: Crystals of *Xcc*-Xgh obtained during initial screening (a) and after optimization of crystallization conditions (b).

Diffraction data set to 2.0 Å resolution was collected at 100 K from a cryo-protected apo-protein crystal. The second diffraction dataset, of the enzyme in complex with glucose, was collected to 2.1 Å resolution. Glucose-soaked crystal has slightly different unit cell dimensions when compared to the non-complexed crystal, suggesting impact of glucose on the crystal lattice. Assuming one molecule per asymmetric unit, the solvent content of the crystals was estimated to be ~50.0% as based on

The abstract was not suitable for template. The text had to be cut

A new binding site for snake venom C-type lectins?

M. C. Nonato^a; R. A. P. de Pádua^a; M. A. Sartim^a; S. V. Sampaio^a

^a Faculdade de Ciências Farmacêuticas de Ribeirão Preto, Universidade de São Paulo, Ribeirão Preto, Brazil

C-type lectins are proteins that bind different glycan molecules by interactions with a calcium atom present in a carbohydrate recognition domain (CRD). Many organisms (plants, bacteria, virus and animals) use these proteins in various biological events like lymphocyte adhesion, erythrocyte agglutination and extracellular matrix organization. The C-type lectin fold is plastic and possible for about 10^{13} different sequences, what promoted its adaptation to diverse functions, similarly to the observed for the immunoglobulin fold (10^{14} - 10^{16} sequences). It is comprised of about 110-130 amino acid residues that folds in two four-stranded beta sheets sandwiched by two alpha helices. Interestingly, C-type lectins present in snake venoms are possible anti-cancer agents since they are toxic to cancer cells and inhibit the adhesion and proliferation of various cancer cell lines.

We have purified a lactose binding C-type lectin from the venom of *Bothrops jararacussu* (BJcuL) to study its structure and binding properties to different sugars. BJcuL crystals were obtained by vapor diffusion and the structure solved by X-ray crystallography to 2.9 Å resolution. BJcuL structure is a decamer formed by a pseudo fivefold axis rotation of a dimer hold by a disulfide bond. (Figure 1). Each monomer binds a calcium atom and possibly another metal at a second and opposed binding site. The decamer possesses a donut shaped structure with 10 calcium ions on the surface available for interactions with carbohydrate molecules.

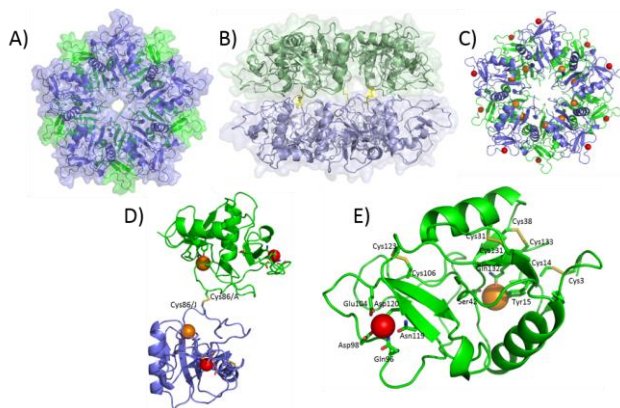


Figure 1. Crystallographic structure of *Bothrops jararacussu* C-type lectin determined at 2.9 Å resolution. Different perspectives of BjCuL decameric structure (A to C). D) Dimer estabilized by a disulfide bond E) Sodium and calcium binding sites found at the monomeric structure.

Binding specificity was evaluated for 20 carbohydrates using differential scanning fluorimetry (DSF) that showed BJcuL interacts with galactose and lactose but less with glucose and sucrose. Surprisingly, high levels of thermostabilization of BJcuL was achieved with the antibiotic aminoglycosides geneticin (G418) and gentamicin in a calcium concentration dependent manner, but not kanamycin. Intriguingly, while lactose and galactose inhibited erythrocyte agglutination by BJcuL, G418 and gentamicin did not affect hemagglutination implying a second site of binding. DSF analysis also suggested the presence of a second binding site for the antibiotics and crystallization of the complexes are in progress in order to understand fully this new binding mechanism of C-type lectin with antibiotics

Acknowledgments: FAPESP: 2011/23236-4 (Nonato, MC); 2014/11266-4 (Padua, RAP); 2015/06290-6 (Sartim, MA); 2011/23236-4 (Sampaio, SV).

The structure of the extended DNA-binding active domains of the E2 bovine papillomavirus type 1 protein

L. M. D. Leroy^a, J. A. Barbosa^b, I. Polikarpov^c, C. B. Pinheiro^a

^a*Departamento de Física, Universidade Federal de Minas Gerais, Belo Horizonte, Brasil.*

^b*Pós-Graduação em Ciências Genômicas e Biotecnologia, Universidade Católica de Brasília, Brasília, Brasil.*

^c*Departamento de Física, Universidade de São Paulo, Brasil.*

Papilloma viruses (PV) are a group of small circular double-stranded DNA viruses that cause tumors (warts, papillomas) in the skin, mucosal epithelia and at others parts of the body ^[1]. The genome of the PV has approximately 7900 base pairs and contains two types of open reading frames (ORFs): the two late transcription ORF's, L1 and L2, and the five early transcription ORF's – E1 and E2 moderate transcription and replication while E5, E6 and E7 modulate transformation in the host cell.

The extended DNA-binding domain of the dominant transcriptional regulator from Bovine Papillomavirus strain 1 (E2) has a modular architecture with an N-terminal activation domain and a C-terminal DNA binding domain ^[2]. It has a dimeric functional form and acts as a transcription activation factor. E2 also plays a direct role in the initiation of replication, interacting with the viral helicase E1 to cooperatively assist binding at the origin of the replication ^[3]. Moreover, E2 can counteract the repressive effects of chromatin on BPV replication ^[4] and interact directly with the cellular replication protein A ^[5].

The crystal structure at 2.0Å of E2 has been solved and refined in the $P3_121$ space group. Structure determination by molecular replacement revealed the structure of a tetramer with two functional dimers (Figure 1) with a previous unobserved loop (between the second and the third β -sheet). The structural refinement ^[6] showed no disulphide bonds between functional dimers, differing from the previously reported crystal structure solved by X-Ray diffraction techniques for a crystal with symmetry described by the $P6_522$ space group ^[7]. This motivated stability analysis and active site studies that allowed us to establish the role played by the Cys340 owing the different crystalline contacts formed.

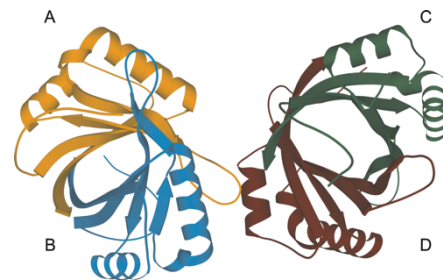


Figure 1: BPV E2 type 1. Each monomer is displayed with a different color, being the functional dimers composed by the pairs: A and B, and D and C.

[1] De Villiers, E. M., Fauquet, C., Broker, T. R., Bernard, H. U., zur Hausen, H., Classification of Papillomaviruses, 324(1), 17-27 (2004)

[2] Hedge, R. S., Grossman, S. R., Laimins, L. A., & Sigler, P. B., Nature, 359(6395), 505-512, (1998)

[3] Ferguson, M. K., Botchan, M. R., Journal of Virology, 70(7), 4193-4199, (1996)

[4] Li, R., Botchan, M. R., Proceedings of the National Academy of Sciences, 91(15), 7051-7055, (1994)

[5] Li, R., Knight, J. D., Jackson, S. P., Tjian, R., Botchan, M. R., Cell, 65(3), 493-505, (1991)

[6] Barbosa, J., Pinheiro, C., Alves, A. C., Alonso, L. G., Prat-Gay, G., & Polikarpov, I., Protein and Peptide Letters, 8(4), 323-326, (2001).

[7] Hedge, R. S., Grossman, S. R., Laimins, L. A., & Sigler, P. B., Nature, 359(6395), 505-512, (1992)

Acknowledgments: FAPEMIG e CNPq.

Solubility analysis of carvedilol salts

O.M.M.Santos^{ab}, J.T.J.Freitas^b, M.B.Araújo^b, A.C.Doriguetto^a

^aInstituto de Química, Universidade Federal de Alfenas, Alfenas, Brasil.

^bFaculdade de Ciências Farmacêuticas, Universidade Federal de Alfenas, Alfenas, Brasil..

More than 80% of the Active Pharmaceutical Ingredients (APIs) are commercialized as tablets and around 40% of them show a low solubility [1]. The reduction in the development of new drugs and their low solubility causes the need to improve the properties of the APIs that have already been commercialized in the market; in fact, the formation of salts is an excellent tool, considering that APIs generally show a low aqueous solubility in their neutral state. Salts are charged multi-component solids. [2]

Carvedilol is an anti-hypertensive API of aqueous low-solubility and it belongs to the beta blockers class. The aim of this work was to compare the solubility of the salts hemi-hydrate phosphate of carvedilol, dihydrate sulphate of carvedilol and mono-hydrate hydrochloride of carvedilol with the raw material commercialized (form II). Their characterization was realized by thermal analyses, infrared spectroscopy and Powder X-Ray Diffraction (PXRD).

The aqueous solubility in equilibrium was determined by using method “shake flask” after 48 hours of stirring at 150 rpm at 25°C in the physiological pH range of (~1 a 7,2) with the following solutions: water, pH 7.2 phosphate buffer, pH 6.8 phosphate buffer, pH 5.8 phosphate buffer, pH 4.5 acetate buffer, pH 3.0 citrate buffer and 0.01 mol.L⁻¹ hydrochloric acid. After this test the pH value was measured and the remaining powder was dried in a desiccator and analyzed by PXRD (CuK α , λ = 1.5418 Å; in a continuous mode, in the angular scanning range included between 3.00 and 35.00 2 θ , with an optical step of 0.02°, with a sampling time of 1.00° 2 θ per minute).

Quantitation was performed by HPLC (Shimadzu, Japan) comparing the areas of the chromatograms of each sample with an analytical curve (5 to 50 mg.L⁻¹) of carvedilol USP (USP Rockville, MD, USA, GOK336) at 240 nm

with a Zorbax Eclipse Plus C8 (4.6 x 50 mm, 5 μ m, Agilent, USA) as stationary phase at 50 ° C. The mobile phase consisted of pH 2.0 potassium phosphate buffer: acetonitrile (69:31 v/v), flow rate of 1.0 mL min⁻¹ and the injection volume of 20 μ L. In Figure 1, it was observed that carvedilol phosphate salt showed a higher solubility than the others salts and the Form II in water and in pH 6.8, being less soluble only in pH 4.5.

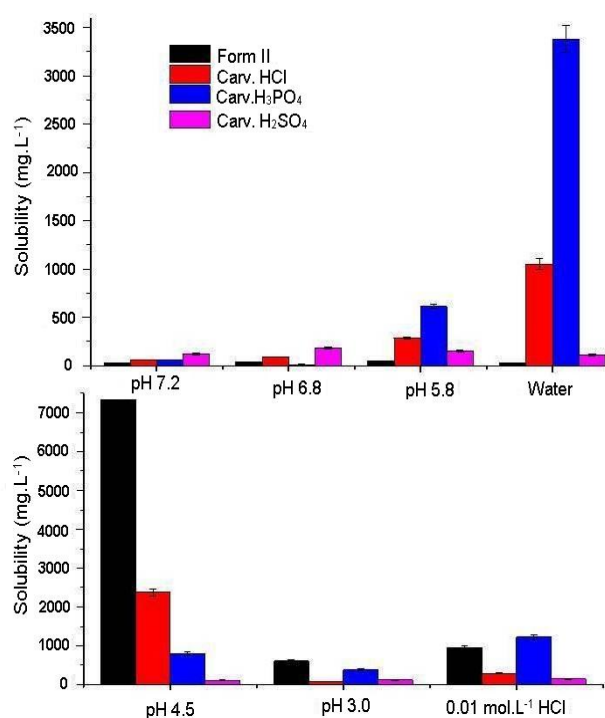


Figure 1: Solubility in equilibrium after 48 hours of carvedilol form II and the phosphate, hydrochloride and sulphate salts.

Dissolution profile of tablets containing such salts must be performed to verify if the release *in vitro* also has advantages over Form II, so this API may be further incorporated into formulations containing carvedilol with improved solubility.

[1] BABU, N. J.; NANGIA, A. *Cryst. Growth Des.*, **v.11**, p.2662- 2679 (2011).

[2] KUMAR, L; AMIN, A.; BANSAL, A.K. *Pharm. Develop. Technol.*, **v.13**, p.345-357 (2008).

Acknowledgments: FAPEMIG; CNPq; Laboratory of Crystallography of UNIFAL-MG.

Structural characterization of Imidazole Alkaloids from *Pilocarpus microphyllus* leaves

A.C. Mafud ^{1*}, J.A. Rocha ², L.M.C. Veras ², J.R.S.A. Leite ², J. de Moraes ³, Y.P. Mascarenhas ¹.

¹ Physics Institute, University of São Paulo, São Carlos, SP, Brazil. ² Federal University of Piauí, Parnaíba, PI, Brazil. ³ FACIG, Guarulhos, SP, Brazil.

Schistosomiasis has been reported as the most pestilent parasitic disease in wide world [1]. The only therapeutic drug for treatment and control disease is the isoquinoline-pyrazino derivative, praziquantel. In this sense, natural products have proven to be an important source of lead compounds to development of new drug candidates. No long ago, epiisopiloturine, an alkaloids extract from *Pilocarpus microphyllus* leaves, has been reported as an active compound against *Schistosoma mansoni* [2,3]. Here, we present the molecular and crystalline structures of the diastereoisomers Isopilosine (ISO) and Epiisopilosine (EPIIS).

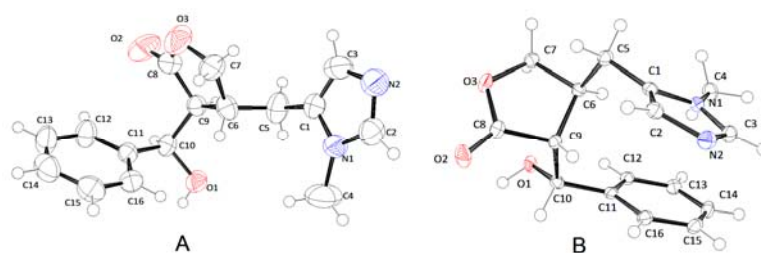


Figure 1: ORTEP-3 view of molecular unit of (A) ISO and (B) EPIIS.

The alkaloids were purified from the biomass generated in the pilocarpine production, and characterized according to [4]. The colorless single crystals were obtained by low evaporation of alcoholic solution, and data were collected in a Bruker APEX II, with Cu α radiation, at room temperature. Both of them were crystallized in a chiral group, and the main data can be found in Table 1. The compounds were tested *in vitro* against *S. mansoni* and, only EPIIS showed anthelmintic activity (to be published). From the Friedel pairs analysis, we confirmed the isomerization of the products. EPIIS is the (3*S*,4*R*)-3-[(*S*)-hydroxy(phenyl) methyl]-4-[(1-methyl-1*H*-imidazol-5-yl)methyl]oxolan-2-one, while ISO is (3*R*,4*S*)-3-[(*S*)-hydroxy(phenyl) methyl]-4-[(1-methyl-1*H*-imidazol-5-yl)methyl]oxolan-2-one. The main difference between these structures is the rings position: while in EPIIS the imidazole and phenyl rings are almost parallel, given rise to a N---H... π contact, and a globular packing; in ISO, the rings are separated and there is no interaction among them. These structural differences may be the reason for their activity behavior, besides the isomerization. Thus, EPIIS can be considerate a lead compound to further studies.

Table 1: Main crystallographic data.

Compound	ISO (CCDC 1417943)	EPIIS (CCDC 957103)
Molecular formula/weight (g/mol)	C ₁₆ H ₁₈ N ₂ O ₃ / 286.32	
Crystal system	Monoclinic	Orthorhombic
Space group	P2 ₁	P2 ₁ 2 ₁ 2 ₁
Cell parameters (Å; °)	a=9.4902(5)	a=6.317(5)
	b=7.9978(4)	b=14.853(5)
	c=10.6633(5)	c=15.083(5)
	β =114.7540(10)	
Cell volume (Å ³)	734.98(6)	1415.2(13)
Z	2	4
Data / restraints / parameters	2884 / 0 / 244	1929 / 1 / 196
Goodness-of-fit on F ²	1.049	1.072
R1 , wR2 [I>2 σ (I)]	0.0334; 0.0810	0.0378 , 0.0936
R1 , wR2 (all data)	0.363; 0.0829	0.0386 , 0.0946

1. Webster BL, Diaw OT, Seye MM, Faye DS, Stothard JR, et al. (2013) Acta Trop 128: 292-302. 2. Veras LM, Guimaraes MA, Campelo YD, Vieira MM, Nascimento C, et al. (2012) Curr Med Chem 19: 2051-2058. 3. Guimaraes MA, de Oliveira RN, Veras LM, Lima DF, Campelo YD, et al. (2015) PLoS Negl Trop Dis 9: e0003656. 4. Veras LM, Cunha VR, Lima FC, Guimaraes MA, Vieira MM, et al. (2013) PLoS One 8: e66702.

Acknowledgments: FAPESP (14/02282-6); CNPq (302674/2010-1); CAPES; FAMa (FAPESP 2009/540354).